9-7-2016 12:00 AM

Innovating Two-Stage Concrete with Improved Rheological, Mechanical and Durability Properties

Manal F. Najjar
The University of Western Ontario

Supervisor
Dr. Moncef Nehdi
The University of Western Ontario

Graduate Program in Civil and Environmental Engineering
A thesis submitted in partial fulfillment of the requirements for the degree in Doctor of Philosophy
© Manal F. Najjar 2016

ABSTRACT

Two-stage concrete (TSC), also known as preplaced aggregate concrete, is a special type of concrete that is produced using a unique procedure which differs from that of conventional concrete. TSC is distinguished by its high coarse aggregate content and exceptional placement technique, whereby aggregates are first pre-placed in the mold then injected with a special grout. The preplacement of aggregates saves substantial energy since only the grout needs mechanical mixing; the grout is self-leveling and needs no vibration and no mechanical compaction. However, TSC applications are still limited despite substantial advancement of modern concrete technology. Therefore, there is a need to explore new possibilities and applications for TSC through adjusting and improving its properties. The objective of this study is to advance the TSC technology through the use of supplementary cementitious materials (SCMs), fibre reinforcement, capturing its sustainability features to develop novel pavements with very high recycled content, and establishing models with predictive capability for its engineering properties.

Therefore, the fresh and hardened properties of grout mixtures incorporating various SCMs, including fly ash (FA), silica fume (SF) and metakaolin (MK) were investigated. An attempt was made to identify the optimum water-to-binder (w/b) ratio and the high-range water-reducing admixture (HRWRA) dosages for grout mixtures that meet the recommended efflux time (i.e. 35-40 ± 2 sec) according to ACI 304.1 (2005). Moreover, the effects of various SCMs at different dosages on the development of TSC mechanical properties were investigated. Likewise, the performance of TSC made with single, binary and ternary binders exposed to different environments conducive to physical and chemical sulfate attack was explored.

The negative influence of fibres on the workability of conventional concrete is eliminated in TSC since the coarse aggregates and fibres are preplaced in the formwork and then injected with a flowable grout. This allows using fibre dosages beyond the practical levels typically adopted in conventionally mixed concrete. Therefore, the mechanical performance of two-stage steel fibre-reinforced concrete (TSSFRC) made with different dosages of steel fibres having various lengths was explored for the first time.

The high coarse aggregate content endows TSC with superior volume stability, making it an ideal contender for pavements and sidewalks, which typically suffer from shrinkage and thermal cracking. In this study, the preplaced material consists of recycled concrete aggregate and scarp tire rubber granules along with scrap tire steel wire fibres, while the grout uses high-volume fly ash. The performance of such a "green" TSC pavement construction technology was explored. Finally, the experimental results were used to create a database which was utilized for developing fuzzy logic (FL) models as a means of predicting the grout flowability (i.e. efflux time and spread flow) and the mechanical properties (i.e. compressive and tensile strength) of a variety of two-stage concrete (TSC) mixtures.

Results indicated that grouts made with water-to-binder ratio (w/b) = 0.45 can achieve the recommended grout flowability for successful TSC production. Moreover, TSC grout properties highly depended on the type and dosage of SCM used. The grout flowability was significantly enhanced as the FA dosage was increased, while the compressive strength was decreased. Partially replacing cement with 10% SF or 10% MK reduced the grout flowability and enhanced its compressive strength. Moreover, the binder composition has a great influence on the TSC mechanical properties. Empirical relationships between the properties of the grout and those of the corresponding TSC were proposed, offering a potential tool for estimating TSC properties based on primary grout properties.

Furthermore, the ease of using a high dosage of pre-placed fibres in TSSFRC allowed achieving exceptional engineering properties for the pre-placed aggregate concrete. Indeed, TSSFRC can easily be produced with 6% steel fibre dosage, which makes it an innovative option and a strong contender in many construction applications.

Fully immersed TSC specimens incorporating FA or MK in sodium sulfate solution exhibited high sulfate resistance. Surprisingly, TSC specimens incorporating SF deteriorated significantly due to thaumasite formation. Under physical sulfate attack exposure, TSC specimens incorporating FA and/or SF incurred severe surface scaling at the evaporative front, while those made with MK exhibited high resistance to surface scaling.

A novel eco-efficient technology for the construction of pavements and sidewalks was proposed. The results demonstrate the feasibility of TSC eco-efficient technology to produce

durable and cost-effective sidewalks and pavements, offering ease of placement and superior sustainability features. Finally, the performance of the developed FL models was evaluated using error and statistical analyses. The results indicate that the FL models can offer a flexible, adaptable and reasonably accurate tool for predicting the TSC grout flowability and mechanical properties.

The findings of this study should provide a leap forward in establishing the TSC technology as a strong contender in many construction applications. It contributes to taking the TSC from a basic technology to a more modern system that benefits from advancements in concrete technology through the use of SCMs, chemical admixtures and fibre reinforcement. In particular, in a new context that values sustainability and "green" construction technology, this study has proven TSC to be exceptional in its ability to use recycled materials without the drawbacks observed in normal concrete technology. These findings should contribute to enhancing the understanding of the TSC behaviour, paving the way for its wider implementation in today's concrete industry.

Keywords: Two-stage; concrete, grout, supplementary cementitious materials, flowability, mechanical properties, durability, steel fibre, sulfate attack, pavements, sidewalks, sustainability, fuzzy logic; model.

CO-AUTHORSHIP STATEMENT

This thesis was prepared according to the integrated-article layout designated by the Faculty of Graduate Studies at Western University, London, Ontario, Canada. All the work stated in this thesis including experimental testing, data analysis, modeling, and writing of draft manuscripts for publication was carried out by the candidate under the close guidance and direct supervision of her thesis advisor. The role of any other co-author (if applicable) was to help in establishing experimental procedures and proof reading of initial drafts of manuscripts. The following publications have been either accepted or submitted to peer-reviewed technical journals and international conferences:

1. **Najjar, M.**, Soliman, A. and Nehdi, M., (2014), "Critical overview of two stage concrete: properties and applications," *Construction and Building Materials*, Vol. 62, pp. 47-58. **Published**

2. **Najjar, M.**, Soliman, A. and Nehdi, M., (2016), "Two-stage concrete made with single, binary and ternary binders," *Materials and Structures*, Vol. 49, No. 1, pp. 317-327. **Published**

3. **Najjar, M.**, Soliman, A. and Nehdi, M., (2015), "Grouts incorporating supplementary cementitious materials for two-stage concrete," *ASCE Journal of Materials in Civil Engineering*. **Submitted**

4. **Najjar, M.**, Soliman, A., Nehdi, M. and Azabi, T., (2016), "Mechanical performance of two-stage steel fibre-reinforced concrete," *Cement and Concrete Composites*. **Submitted**

5. **Najjar, M.**, Soliman, A., Nehdi, M. and Azabi, T.M, (2016), "Durability of two-stage concrete to chemical and physical sulfate attack," *Materials and Structures*. **Submitted**

6. **Najjar, M.**, Soliman, A., Nehdi, M. and Azabi, T., (2016), "Novel eco-efficient pavement construction technology using two-stage concrete," *Construction and Building Materials*. **<u>Submitted</u>**

7. **Najjar, M.**, Nehdi, M., Azabi, T. and Soliman, A., (2016), "Fuzzy inference systems based prediction of engineering properties of two-stage concrete," *Computers and Concrete*. **<u>Submitted</u>**

8. **Najjar, M.F.**, Soliman, A.M., and Nehdi, M.L., (2016) "Sustainable high-volume fly ash grouts for two-stage concrete," *Proceedings of the CSCE Annual Conference: Resilient Infrastructure*, London, Ontario, Canada. **<u>Published</u>**

9. **Najjar, M.F.**, Soliman, A.M., Azabi, T. and Nehdi, M.L., (2016) "Green sidewalks using sustainable two-stage concrete," *Proceedings of the CSCE Annual Conference: Resilient Infrastructure*, London, Ontario, Canada. **<u>Published</u>**

DEDICATION

This thesis is dedicated to:

My Father: Faruk Najjar

My Mother: Nazeha Ben-Daw

My Aunt: Fatoomah Najjar

ACKNOWLEDGMENTS

I sincerely thank my thesis advisor, Dr. Moncef Nehdi for his precious guidance, unconditional support and encouragement through this research. It has been a great opportunity to work under his supervision and gain from his professional knowledge.

I also would like to state my appreciation to Dr. Ahmed Soliman for his valuable comments and his effective contribution to my research.

I am very thankful to Mr. Wilbert Logan and to all the Staff members of the Department of Civil and Environmental Engineering at Western University for their help and support during my study at Western. In addition, I am grateful to the summer-work undergraduate students who helped me during my laboratory works.

I am deeply grateful to my husband, Tareq Azabi for his support, patience and positive attitude that played a vital role towards the completion of my thesis. Also, I would like to express my gratitude to my mother Nazeha and my father Faruk for their sincere encouragement and prayers. I would like to thank my brother Adnan and my lovely children; Mohamed, Fatma-Zahraa and Emadeddin for their sacrifices and warm feelings through the years.

Finally, my personal involvement with the study would not have been possible without the financial support of the Libyan Ministry of Higher Education. Also, several companies including Lafarge and BASF are appreciated for their materials donations.

TABLE OF CONTENTS

LIST OF TABLES

LIST OF FIGURES

NOMENCLATURE

A and B   Fuzzy sets

A/b Aggregate-to-binder ratio

ACI   American concrete institute

AEA   Air-Entraining Admixture

ANOVA   Analysis of variance

Avg.   Average

B_p Minimum water content needed to initiate flow

C_3A Tri-calcium aluminate

$C_3S\bar{S}\bar{C}H_{15}$ Thaumasite

C_4AH_{13} Hydrated calcium aluminate,

$C_4A\bar{S}H_{12-18}$ Monosulfate

$C_6A\bar{S}_3H_{32}$ Ettringite

Ca^{++} Calcium ions

CC   Conventional concrete

CH   Calcium hydroxide

CSH   Calcium silicate hydrate

$C\bar{S}H_2$ Gypsum

D_1 and D_2 Spread flow diameters

D_o Cone base diameter

DSC   Differential scanning calorimetry

E Modulus of elasticity of two-stage concrete

EA   Expanding admixture

EDX	Energy dispersive X-ray
E_p	Deformation coefficient
FA	Fly ash
$f_c^`$	Compressive strength of two-stage concrete
f_t	Tensile strength of two-stage concrete
GGBFS	Ground granulated blast furnace slag
GHG	Greenhouse gas
H_p	Minimum HRWRA dosage to disperse the binder particles
HRWRA	High-range water-reducing admixture
HSFRC	High-strength fibre-reinforced concrete.
HSRC	High sulphate resistant cement
I_{10}	Toughness index at 5.5 δ_1
I_{20}	Toughness index at 10.5 δ_1
I_{30}	Toughness index at 15.5 δ_1
I_5	Toughness index at 3 δ_1
$MAPE$	Mean absolute percentage error
MIP	Mercury intrusion porosimetry
MK	Metakaolin
N	Number of added SCMs
n	Number of data points
Na_2SO_4	Thenardite
$Na_2SO_4 \cdot 10H_2O$	Mirabilite
OPC	Ordinary portland cement

P_{exp}	Experimental values of the properties
P_{pre}	Predicted values of the properties
R	Tire rubber particles
R_{10-20}	Residual strength factors for deflection interval ($5.5\delta_1$- $10.5\delta_1$)
R^2	Absolute fraction of variance
R_{20-30}	Residual strength factors for deflection interval ($10.5\delta_1$- $15.5\delta_1$)
R_{5-10}	Residual strength factors for deflection interval ($3\delta_1$- $5.5\delta_1$)
RCA	Recycled aggregate
RH	Relative humidity
$RMSE$	Root-mean-square error
RP	Rock Powder
R_p	Relative slump
r_{xy}	Correlation coefficient
S	Percentage of added SCMs
s/b	Sand-to-binder ratio
SCMs	Supplementary cementitious materials
SEM	Scanning electron microscopy
SF	Silica fume
SFRC	Steel fibre-reinforced concrete
SH_p	Deformation coefficient
SP	Superplasticizer
STDEV	Standard deviation
T	Temperature

t	Time
TSC	Two-stage concrete
TSSFRC	Two-stage steel fibre-reinforced concrete
UHPFRC	Ultra-high performance fibre-reinforced concrete
UHSC	Ultra high-strength concrete
V_1	Volume of grout at the beginning of the bleeding test
V_w	Volume decanted bleed water
w/b	Water-to-binder ratio
X_{Ct}	Change of mass or length at time (t)
X_i	Initial mass or gauge length before exposure to the sulfate solution
X_t	Mass or the length at time t
z	Output value in a fuzzy subset(s)
z^*	Defuzzified output value
α	Significance Level for Analysis of Variables
α_N	Multiplication of α for the used binder
$\delta 1$	Deflection at the first crack
$\delta 2$	Deflection at the peak load
$\mu_{(X)}$	Membership function
$\mu_{(z)}$	Membership degree of output

1. INTRODUCTION

1.1. TWO-STAGE CONCRETE

Two-Stage Concrete (TSC), also known worldwide under different names such as Colcrete, Prepacked Concrete and Preplaced Aggregate Concrete, is considered as a unique type of concrete that is produced using a special procedure, which differs from that of conventional concrete (ACI 304.1, 2005). In conventional concrete, all concrete ingredients are mixed then placed in the formwork. However, in TSC, coarse aggregates are first placed in the formwork. Subsequently, voids between coarse aggregate particles are filled through injecting special cementitious grout mixtures (Abdelgader and Najjar, 2009). The properties of the used grout and its ability to flow around the pre-place aggregate particles and effectively fill voids have a predominant effect on the TSC properties (Abdel Awal, 1984; Abdelgader and Elgalhud, 2008). Moreover, the TSC technique provides cost benefits since 60% of the material (i.e. coarse aggregate particles) is directly placed into formwork and only 40% (i.e. grout) goes through mixing and pumping procedures (Abdelgader, 1996).

TSC has been successfully used for many years in special applications including underwater construction, placement in areas with closely spaced reinforcement and rehabilitation of existing concrete structures (ACI 304.1, 2005). It is distinguished by its unique placement technique, which offers several technological and sustainability advantages. Preplacing the coarse aggregates in the formwork before injecting grout allows using aggregates that constitute challenges in normal concrete production. For example, the production process of TSC makes it one of the preferable technologies for the construction of nuclear power plants (ACI 304.1, 2005). Since the coarse aggregates are pre-placed, very heavy materials incorporated within aggregates can be used in concrete production without segregation. Moreover, TSC has a high potential for use in mass concrete (e.g. dams) due to the low volume changes and heat of hydration of the TSC compared to that of conventional

concrete (ACI 304.1, 2005; Bayer, 2004). Furthermore, recycled concrete aggregates that normally cause loss of workability and severe pumping problems due to their higher water absorption will not contribute to concrete casting problems in the TSC technology (Morohashi *et al.*, 2013). However, TSC technology has remained elementary and basic, rather targeting the lower end of the construction market.

1.2. RESEARCH NEEDS AND MOTIVTION

The TSC technology has been well established since the early 1950ies; however, its applications are still limited despite major advancements in modern concrete technology. Therefore, there is need to discover new possibilities and applications for TSC through adjusting and improving its properties. The key controlling factor of the mechanical strength and durability of TSC is the quality of the grout used in injecting the preplaced coarse aggregate, along with the rheological properties of the grout which should be conducive to effectively filling the space between preplaced aggregates and reducing the voids volume to a minimum.

Resorting to new generation admixtures can allow producing low water-to-binder ratio (*w/b*) and high-strength grouts with adequate flowability, which should produce higher strength TSC. Moreover, using binary and ternary binders in producing TSC grouts can enhance the interfacial transition zone between the preplaced aggregates and the injected grout matrix. Furthermore, supplementary cementitious materials used in TSC grouts can enhance the durability of TSC to sulfate attack, damage by freezing-thawing cycles, ingress of chloride ions and various other degradation mechanisms, in a similar manner to that well documented in normally placed concrete. However, the use of emerging new admixtures and more sustainable and highly durable binder systems have rarely been explored in TSC. According to (ACI 304.1, 2005) "*Class C fly ash and blast-furnace slag have been employed to a limited extent, but data on grout mixture proportions, properties, and in place experience are lacking. There are no known data on the application of silica fume in grout for Preplaced Aggregate Concrete.*" Therefore, a detailed study is required to investigate enhancing the TSC rheological, mechanical, and durability properties based on recent developments in materials science and technology.

Furthermore, the fibre reinforcement dosage in fibre-reinforced concrete (FRC) is severely hampered by the interference of fibres with placement since the fibres cause serious concrete casting and consolidation problems. Conversely, in TSC, very high dosages of fibres can be premixed dry and preplaced with the coarse aggregates in the mold and later injected with a grout, allowing to possibly reach ductility and toughness levels that are not conceivable using the normal FRC technology. However, there is currently no accessible data in the open literature regarding the mechanical performance of TSC incorporating different steel fibre dosages. In addition, TSC long-term performance under different exposure conditions is still unclear and there are scant data available. Hence, before the wide implementation of TSC in full-scale construction, the durability and long-term properties of TSC under sulfate attack need to be explored under different simulated field-like ageing conditions.

Moreover, incorporating different types of concrete waste by-products such as recycled aggregates and demolished concrete as coarse aggregate in TSC needs to be investigated. This will pave the way for using TSC on site to recycle demolished and waste concrete along with saving natural resources. Furthermore, a major problem with recycle aggregate concrete is the pumping difficulties associated with the slump loss due to absorption of moisture in the hollow aggregate. TSC is not vulnerable to this effect, and thus green TSC is an attractive option that needs detailed investigation.

Most TSC past applications have been limited to mass concrete (e.g. dams), underwater concrete (e.g. bridge piers), and the rehabilitation of existing concrete structures. In order to pave the way for the TSC industry, there is need to discover the possibility of producing new TSC products based on the results obtained from this study.

1.3. SPECIFIC RESEARCH OBJECTIVES

In order to accomplish the above-mentioned research needs, the specific research goals are:
1. Investigating the effect of different binder compositions, supplementary cementitious materials (SCMs), and new generation chemical admixtures on TSC grout properties.
2. Investigating the effects of various SCMs at different addition rates on the development of TSC mechanical properties over time and exploring possible

correlations between the grout properties and the corresponding TSC mechanical properties.

3. Exploring the mechanical performance of two-stage steel fibre-reinforced concrete made with different steel fibres dosages and lengths.

4. Studying the durability of TSC under different sodium sulfate exposure regimes.

5. Developing green sustainable TSC using recycled solid construction waste as coarse aggregate.

6. Building models based on fuzzy logic inference systems (FIS) that are capable of predicting the grout flowability and the mechanical properties of various TSC mixtures made with single, binary and ternary binders.

1.4. STRUCTURE OF THESIS

This dissertation has been prepared according to the integrated-article format predefined by the Faculty of Graduate Studies at Western University, London, Ontario, Canada. It consists of 9 chapters covering the scope of this study: Innovating Two-Stage Concrete with Improved Rheological, Mechanical and Durability Properties. Substantial parts of this thesis have been published, accepted, or submitted for possible publication in peer-reviewed technical journals and conference proceedings.

Chapter 1 provides a brief introduction along with the research motivation, objectives, thesis structure and original contributions of the research.

Chapter 2 reviews the state-of-the-art knowledge on the two-stage concrete technology, including its development history, material specifications, engineering properties and long-term performance. Also, this chapter provides useful information that can assist contractors and engineers in producing TSC.

Chapter 3 explores the effects of using different supplementary cementitious materials (SCMs), including fly ash, silica fume and metakaolin, on the properties of TSC grout mixtures. Moreover, grout mixture proportions that can achieve high-strength TSC were identified.

Chapter 4 presents the mechanical properties of TSC made with various grout mixtures and incorporating single, binary, and ternary binders. Also, empirical relationships between

the properties of the grout and those of the corresponding TSC are proposed, offering a potential tool for estimating TSC properties based on primary grout properties.

Chapter 5 presents a study on the mechanical performance of two-stage steel fibre-reinforced concrete (TSSFRC) incorporating various steel fibre lengths and dosages. Two types of steel fibre with aspect ratio of 44 and 80 (short and long steel fibres) were added at dosages of 1%, 2%, 4% and 6%. The TSSFRC mechanical performance was evaluated based on the mechanical properties, load‑deflection curves and toughness.

Chapter 6 investigates the performance under sulfate exposure of TSC mixtures incorporating different SCMs, including fly ash (FA), silica fume (SF) and metakaolin (MK) as partial replacement for ordinary portland cement (OPC). Two different sodium sulfate exposure conditions were simulated: full immersion (i.e. chemical sulfate attack) and partial immersion combined with cyclic temperature and relative humidity (i.e. physical sulfate attack).

Chapter 7 explores the performance of "green" TSC incorporating recycled concrete aggregates (RCA) and crumb rubber from scrap tires. Mechanical properties of the proposed green TSC including compressive strength, modulus of elasticity, flexural strength and toughness, as well as durability to freezing-thawing cycles were investigated. Moreover, a novel eco-efficient technology for the construction of pavements and sidewalks is proposed.

Chapter 8 presents the development of fuzzy logic (FL) models for predicting the grout flowability and mechanical properties for various TSC mixtures made with single, binary and ternary binders. A database of laboratory work presented in chapters 3, 4 and 5 was utilized to build the FL models.

Chapter 9 includes general and specific conclusions drawn from the research study along with recommendations for further research.

1.5. ORIGINAL CONTRIBUTIONS

To the best of the author's knowledge, there is currently no comprehensive research that investigates enhancing the TSC rheological, mechanical, and durability properties based on recent developments in materials science and technology. Thus, the findings of the research

program provide useful and comprehensive information on the TSC technique, including its mechanical and durability performance. This information contributes to enhancing the understanding of TSC behaviour, paving the way for its wider implementation in today's concrete industry. Moreover, the findings of the present research are a step towards revisiting the TSC technology in order to upgrade it to the state-of-the-art of normally placed concrete, which now experiences the advent of applications of novel admixtures, nano-materials, bio-inspired and self-healing technologies, etc.

The specific original contributions of this research include:

1. Providing a detailed study on the flowability of various TSC grout mixtures made with single, binary and ternary binders. The findings of this study provide practitioners with new guidance to produce more sustainable and more durable high-strength TSC, which can open the door for novel applications of TSC never considered before.

2. Conducting a detailed investigation on the mechanical properties of TSC made with various grout mixtures and incorporating single, binary, and ternary binders. The findings of this investigation filled a considerable knowledge gap in the TSC literature. In addition, empirical correlations between the properties of grouts and the mechanical properties of the corresponding TSC have been proposed, offering a simple tool for designing TSC mixtures incorporating SCMs.

3. Providing, for the first time in the open literature, a detailed study on the mechanical properties of TSSFRC. TSSFRC can easily be produced with 6% steel fibre dosage, which makes it an innovative option and a strong contender in many construction applications.

4. Exploring the performance of TSC made with single, binary and ternary binders exposed to different environments conducive to physical and chemical sulfate attack. The findings should outline the mechanisms of damage of TSC incorporating SCMs under various sulfate exposure regimes and point out to needed future research in this area.

5. Discovering the performance of "green" TSC mixtures incorporating recycled concrete aggregates, scrap tire granules, and tire steel wire fibres along with grouts made with ternary binders incorporating high-volume fly ash. This material was

intended for creating a novel eco-efficient construction technology of sidewalks and pavements. The findings demonstrate the feasibility of TSC eco-efficient technology to produce durable and cost-effective sidewalks and pavements, offering ease of placement and superior sustainability features.

6. Finally, developing fuzzy logic models for predicting the flowability and mechanical properties of TSC, offering an accurate tool for designing TSC mixtures incorporating several types and dosages of SCMs.

1.6. REFERENCES

Abdelgader, H.S. and Elgalhud A.A., (2008), "Effect of grout proportions on strength of two-stage concrete", *Structural Concrete* , Vol. 9, No. 3, pp. 163-170.

Abdelgader, H.S. and Najjar, M.F., (2009), "Advances in concreting methods", *International Conference on Sustainable Built Environment Infrastructures in Developing Countries*, pp. 315-324.

Abdelgader, H.S., (1996), "Effect of quantity of sand on the compressive strength of two-stage concrete", *Magazine of Concrete Research*, Vol. 48, No. 177, pp. 353-360.

Abdul Awal, A.S., (1984), "Manufacture and properties of prepacked aggregate concrete", *Master Thesis, Melbourne University*, Australia, 121 p.

ACI 304, (2005), "Guide for measuring, mixing, transporting, and placing concrete", *American Concrete Institute*, ACI Committee 304, 49 p.

ACI 304.1, (2005), "Guide for the use of preplaced aggregate concrete for structural and mass concrete applications", *American Concrete Institute*, ACI Committee 304.1, 19 p.

Bayer R. (2004). Use of preplaced aggregate concrete for mass concrete applications. *Master Thesis. Middle East Technical University*. Turkey. 160 p.

Morohashi N., Meyer C., and Abdelgader H. S. (2013). "Concrete with recycled aggregate produced by the two-stage method. *CPI-Concrete Plant International*, Vol. 4, 34-41.

Chapter 2

2. LITRATURE REVIEW[(*)]

2.1. INTRODUCTION

Two-stage concrete (TSC) is defined as concrete produced by placing coarse aggregate particles in the designed formwork, then filling the internal gaps with a special grout mixture. TSC is known worldwide under different terms that are listed in **Table 2.1**. These different names of TSC reflect the difference in its production methods. For instance, in the United Kingdom it is known as "Colcrete" as they mix the grout in a colloidal mixer before injecting it into the coarse aggregate.

Table 2.1 – Different names of Two-Stage Concrete

TSC Name	Ref.
Colcrete	(Manohar, 1967; Abdelgader, 1996)
Polcrete	(Abdelgader, 1996; ACI 304.1, 2005)
Naturbeton	(ACI 304.1, 2005)
Arbeton	(ACI 304.1, 2005)
Prepacked concrete	(Baumann, 1948; Abdul Awal, 1984; Tang, 1977)
Preplaced aggregate concrete	(ACI 304.1, 2005)
Grouted aggregate concrete	(Champion and Davies, 1958; ACI 304.1, 2005)
Injected aggregate concrete	(ACI 304.1, 2005)
Rock- filled Concrete	(Huang *et al.*, 2008)

Generally, the TSC grouting process can be done either by gravity or by a pumping process (Abdul Awal, 1984). In the gravity process (i.e. penetration method), the grout is poured on the top surface of the preplaced aggregate and allowed to penetrate through the aggregate body to the bottom of the section under its own weight. However, this method is particularly useful for grouting thin sections with a depth of less than 300 mm [12 in] (Champion and Davis, 1958). In the pumping process, the grout is pumped into the aggregate mass from the bottom through a network of pipes as illustrated in **Figure 2.1**. The minimum

---

[(*)]*A version of this chapter was published in the Construction and Building Materials journal (2014).*

coarse aggregate size plays a major role in selecting the suitable grouting method. For instance, the gravity process can be successfully used for aggregates with a minimum size of 50 mm [2 in], while the pumping method is preferred with lower void content coarse aggregate (i.e. finer aggregates) (Casson and Davies, 1986).
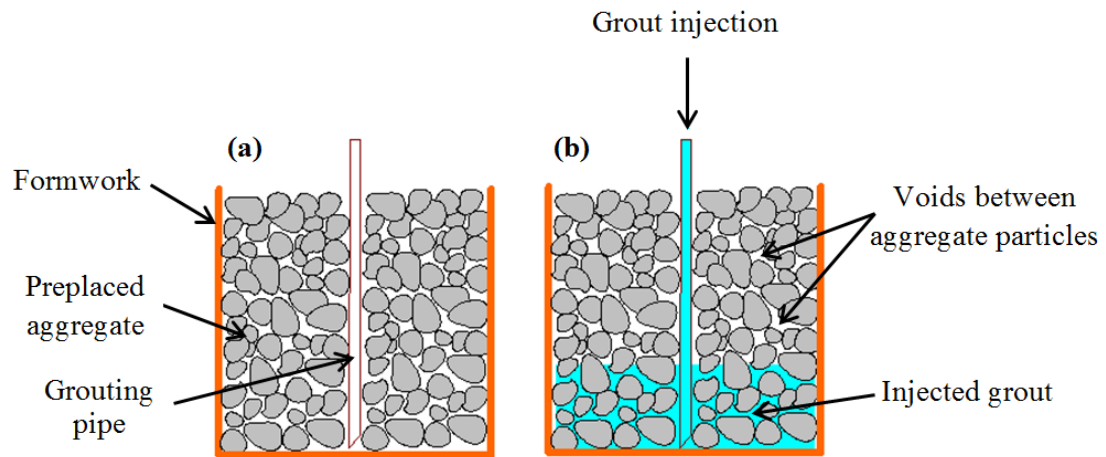
Figure 2.1 – TSC grout pumping process: a) Coarse aggregate placement and, b) Grout pumping through pipes.

TSC differs from conventional concrete in several aspects. First, all ingredients of conventional concrete are mixed together and then placed in the formwork, while in TSC the grout ingredients are mixed separately and then injected into the pre-placed aggregate mass as mentioned earlier. Second, TSC has a higher coarse aggregate content (about 60% of the total volume) than that of conventional concrete (about 40% of the total volume) (Abdelgader, 1996). Hence, TSC can be considered as a skeleton of coarse aggregate particles resting on each other, leaving only internal voids to be filled with grout (Abdelgader, 1996). Conversely, in normal concrete the aggregates are rather dispersed. Therefore, TSC has a specific stress distribution mechanism at which the stresses are transferred through contact areas between aggregate particles (**Figure 2.2**) (O'Malley and Abdelgader, 2009). These stresses can be responsible for the fracture and tearing of aggregate particles away from the grout (Abdelgader and Górski, 2003).

The TSC technique provides a solution for the coarse aggregate segregation problem, especially for heavy weight aggregate concretes, through pre-placing the aggregates in the formwork. Furthermore, TSC does not need compaction, vibration or any other consolidation processes to achieve a dense structure, which in turn reduces its production cost. The formwork used for TSC must be strong and sufficiently tight to resist the lateral pressure induced by the injected grout and to minimize its leakage. Consequently, the cost of TSC formwork is about one-third higher than that used for conventional concrete (US Army Corps of Engineers, 1994). On the other hand, TSC is considered as the most cost-effective technique for underwater concreting compared to other techniques (Abdelgader, 1999). However, the construction of TSC requires special skill and experience that most contractors do not have. Therefore, this chapter provides useful information that can assist contractors and engineers in producing TSC.
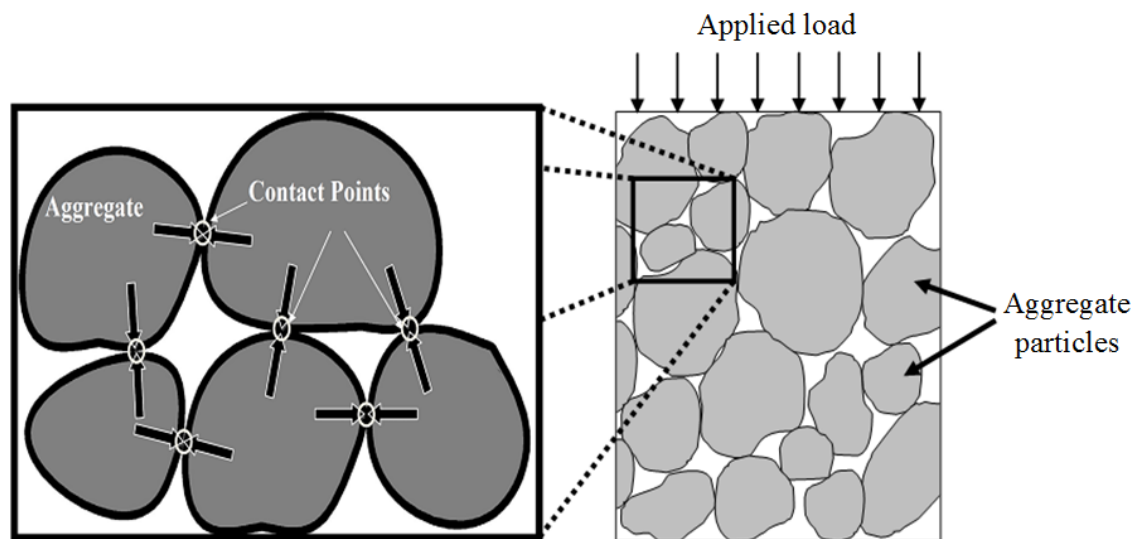
Figure 2.2 – Mechanism of transmission of stresses in TSC.

2.2. HISTORY OF TWO-STAGE CONCRETE APPLICATIONS

In 1930s, TSC was developed after the invention of the high-speed colloidal mill mixer, which made the manufacture of highly stable flowable grout feasible (Reschke, 2000). Initially, TSC was introduced as a repair technique for existing concrete infrastructure such as bridges and tunnel linings. The first use of TSC was in 1939 for the rehabilitation of the Santa Fe railroad tunnel, California (ACI 304.1, 2005). In 1950, Japanese construction

companies bought rights to use TSC in their construction projects (ACI 304.1, 2005). Since then, TSC has been widely used in many construction applications. For example, about 383000 m^3 [13525520 ft^3] of TSC were used to construct the 34 piers of the Mackinac Bridge (ACI 304.1, 2005; Davis and Haltenhoff, 1956).

On the other hand, the production process of TSC makes it one of the preferable technologies for the construction of nuclear power plants since the coarse aggregate is pre-placed. Hence, very heavy minerals incoperated within aggregates (e.g. magnetite, which is a highly effective material in nuclear and biological shields) can be used in concrete production without segregation concerns (ACI 304.1, 2005). Morover, the low volume changes and heat of hydration of the TSC compared to that of conventional concrete increased its potential appliactions in mass concrete in which thermal cracking, shrinkage, and cold joints are major considerations (O'Malley and Abdelgader, 2009).

Recently, a modified TSC was developed and used in several projects in China. This modified TSC was produced by pouring ready-mixed self-compacting concrete instead of grout to fill voids between large rock (i.e. minimum size of 300 mm [12 in]) (Huang *et al*., 2008). Hence, TSC is a technique that is gaining momentum in the construction market. **Table 2.2** summarizes important projects in which TSC was implemented as a major construction material.

Table 2.2 – Examples of TSC conducted projects

Project	Date of Construction	Ref.
Pre-facing of Barker Dam at Nederland in Colorado.	1946	(Davis *et al*. 1948)
Scroll case at Bull Dam Powerhouse.	1951	(ACI 304.1, 2005)
Piers of Mackinac Bridge.	1954-1955	(Davis and Haltenhoff, 1956)
Plugs in gold mine in South Africa	2001-2006	(Littlejohn and Swart, 2006)
Auxiliary dam in China	2006	(Huang *et al*., 2008)

2.3. MATERIALS SPECIFICATIONS

2.3.1. Coarse Aggregate

The engineering properties of TSC depend to a large extent on the properties of the coarse aggregate used. As mentioned early, the applied stresses in TSC are transferred first to the coarse aggregate particles and then to the hardened grout (Abdelgader, 1996). Hence, choosing the coarse aggregate is a key aspect in TSC mixture design. According to ACI 304.1 "Guide for the Use of Preplaced Aggregate Concrete for Structural and Mass Concrete Applications", the coarse aggregate used in TSC should be washed, free of surface dust and fines, and chemically stable in order to achieve a high bond with the injected grout (ACI 304.1, 2005). Moreover, the shape, texture and mineralogy of the coarse aggregate particles significantly affect the developed bond.

Bulky rounded or angular shaped aggregate particles are preferred to flat and elongated particles (O'Malley and Abdelgader, 2009). Flat and elongated particles can cause narrow channels and inhibit the flow of grout, leading to honeycombing and weak zones in the TSC (O'Malley and Abdelgader, 2009). Interestingly, the mechanical strength of the used coarse aggregate did not have a significant influence on the TSC mechanical strength, while its shape, texture, grading and void content had a dominant effect (O'Malley and Abdelgader, 2009). This is probably because very high strength TSC has not yet been produced. Aggregate particles with a rough texture provide a better surface for grout inter-keying, leading to enhanced mechanical interlock, and consequently higher strength than that produced with smooth rounded stone (Manohar, 1967; O'Malley and Abdelgader, 2009).

On the other hand, crushed aggregate entraps large voids between its particles, leading to more grout consumption per concrete volume. Hence, a well graded aggregate is often recommended in order to minimize the void content between aggregates (ACI 304.1, 2005). Generally, this void content will range between 35% and 50% of the total volume for well graded and uniformly sized aggregates. However, combing two coarse aggregates with different grading (e.g. mixing 12 to 38 mm [0.5 to 1.5 in] and 200 to 250 mm [7.9 to 9.8 in]) can reduce the void content to 25% of the total volume (ACI 304.1, 2005). Moreover, mixing crushed aggregate with round aggregate particles was found beneficial in producing an aggregate skeleton with low void content and high contact points, leading to lower grout

consumption and consequently lower cost TSC (O'Malley and Abdelgader, 2009; Abdelgader, 1999). Nevertheless, reducing the void content between coarse aggregate particles can also cause difficulties in the grouting process. Hence, a more flowable grout and higher injection pressure will be required. **Table 2.3** provides different recommended gradings for TSC coarse aggregates.

Table 2.3 – Grading limits for TSC coarse aggregate

Sieve Size mm[*]	Cumulative Percentage Passing			Ref.
	Grading (1)	Grading (2)	Grading (3)	
37.5	95 - 100	----	0.5	(ACI 304.1, 2005; ACI 304, 2005)
25.0	40 - 80	----	----	
19.0	25 - 40	00 - 10	----	
12.5	00 - 10	00 - 02	----	
9.50	00 - 02	00 - 01	----	
150	100	----	----	(Neville and Brooks, 2010)
75.0	67	100	----	
37.5	40	62	97	
19.0	06	04	09	
12.5	01	01	01	

*1mm = 0.039 in

In reinforced concrete structures, the TSC largest coarse aggregate size will depend on the dimensions of the structural member and spacing between reinforcement bars, which is similar to conventional concrete. In TSC mass concrete, there are no specific limitations on the maximum size of the coarse aggregate used, while the smallest aggregate size is controlled by the targeted grout flowability and its penetrability in voids (Abdul Awal, 1984). For instance, the maximum aggregate size used for repairing the Barker Dam in the USA was 114 mm [4.5 in] (Davis *et al*., 1948), whereas a maximum size of 300 mm [12 in] was used in constructing a dam in Switzerland (Baumann, 1948).

The smallest size of coarse aggregate should be at least four times that of the largest size of the used fine aggregate in order to improve grout penetrability through the aggregate skeleton (Orchard, 1973). Moreover, coarse aggregate particles smaller than 20 mm [0.8 in] are eliminated as they could block the grout injection pipes and impede grout flow (Abdelgader and Najjar, 2009). According to Champion and Davis, the recommended

minimum particle size of coarse aggregate is 38 mm [1.5 in] (Champion and Davis, 1958). However, Orchard suggested that the minimum size of coarse aggregate could be 10 mm [0.4 in] (Orchard, 1973). Indeed, the selection of the minimum size of coarse aggregate depends on the grout mixture type and the applied grouting method to produce the TSC. For instance, with a minimum size of coarse aggregate of 300 mm [12 in], the gravity grouting process can be conducted using self-compacting concrete or grout containing coarse sand. On the other hand, with a 20 mm [0.8 in] minimum coarse aggregate size, a special pumping process for grouting should be implemented in order to insure the penetrability of the grout through small voids between aggregates (Abdelgader and Najjar, 2009).

2.3.2. Grout Mixture

The grout used in TSC normally consists of pure or blended Portland cement, well graded sand, water, and chemical admixtures. The ability of grout to flow around the pre-placed aggregates is essential. Therefore, some chemical admixtures are recommended to improve the penetrability of the grout and better control the engineering properties and performance.

2.3.2.1. Fine Aggregate

The used fine aggregate should be hard, dense, and stable (ACI 304.1, 2005). The grading of the fine aggregate plays a significant role in controlling the flowability of the used grout. **Table 2.4** summarizes recommended fine aggregate gradations and sizes for TSC. It was reported that using a well graded fine aggregate increased the stability of the grout and reduced segregation (O'Malley and Abdelgader, 2009). On the other hand, using fine aggregate with a high fineness modulus will increase the water demand, leading to a reduction in compressive strength and an increase of drying shrinkage. It was recommended that the fineness modulus of the used fine aggregate should range from 1.2 to 2.0 (King, 1959).

Table 2.4 – Recommended grading limits of fine aggregate for TSC

Sieve Size		Cumulative Percentage Passing		Ref.
mm	ASTM #	Grading (1)	Grading (2)	
4.75	No.4	----	100	(ACI 304.1, 2005; ACI 304, 2005)
2.36	No.8	100	90 - 100	
1.18	No.16	95 - 100	80 - 90	
0.60	No.30	55 - 80	55 - 70	
0.30	No.50	30 - 55	25 - 50	
0.15	No.100	10 - 30	05 - 30	
0.075	No.200	00 - 10	00 - 10	
Fineness Modulus		1.3-2.1	1.6-2.45	
2.36	No.8	100		(Neville and Brooks, 2010)
1.18	No.16	98		
0.60	No.30	72		
0.30	No.50	34		
0.15	No.100	11		
2.36	No.8	100		(Davis and Haltenhoff, 1956)
1.18	No.16	95-100		
0.60	No.30	55-75		
0.30	No.50	25-45		
0.15	No.100	05-20		
0.075	No.200	00-05		
Fineness Modulus		1.65-2.1		
2.36	No.8	100		(Orchard, 1973)
1.18	No.16	90		
0.60	No.30	60-80		
0.30	No.50	20-50		
0.15	No.100	10-20		
0.075	No.200	00-07		
Fineness Modulus		1.6-2.2		

*1mm = 0.039 in

2.3.2.2. Cementitious Materials

Ordinary Portland cement (OPC) is the commonly used cementitious material for TSC grouts. Supplementary cementitious materials (SCMs) including ground granulated blast furnace slag (GGBFS), and silica fume (SF), and metakaolin (MK) had also been used in TSC. Generally, SCMs contribute to the hardened properties of TSC through enhanced particle packing, pozzolanic activity, or both depending on their chemical and physical properties. Hence, SCMs addition is expected to provide several benefits to TSC such as

reducing its permeability and improving its mechanical properties and durability (Malhotra, 1993). For instance, the effect of using OPC and fly ash on the mechanical properties of TSC was investigated (Abdelgader, 1999). The addition of class F fly ash led to several benefits, including improvement of the grout flowability, extending the grout's handling time, and reducing the water demand and bleeding of the TSC grout. Adding up to 33% of fly ash as partial replacement for OPC was recommended for TSC mass concrete as it reduces the heat of hydration significantly (ACI 304.1, 2005).

On the other hand, the effect of silica fume addition on TSC properties was investigated by O'Malley and Abdelgader (2009). It was reported that silica fume had two conflicting effects on the TSC properties: increasing the mechanical strength and reducing workability. SF acts as a micro filler material for spaces between cement and sand grains due to its very fine particle size. Simultaneously, it is a very reactive pozzolanic material. Hence, it reacts chemically with calcium hydroxide (CH) in the cement paste to form more calcium silicate hydrate (CSH), which is responsible for additional strength gain (Malhotra, 1993). However, SF usually has an adverse effect on the flowability of the grout (O'Malley and Abdelgader, 2009). Therefore, the addition rate of SF to TSC grout should be optimized through conducting different trial batches and using adequate chemical admixtures to achieve higher strength grout with adequate flowability.

Metakaolin (MK), which is classified as a natural pozzolan, has a similar effect to that of silica fume. Other filler materials (e.g. limestone powder) have been used in conventional concrete as it acts as a fine filler material along with improving flowability. Generally, the effect of these filler materials on TSC properties will be affected by their fineness, water demand and compatibility with chemical admixture (Christianto, 2004).

Beside the many benefits that SCMs and other filler materials can import to TSC, using these as partial replacement for cement can reduce the TSC carbon footprint, leading to greener and more environmental friendly TSC construction.

2.3.2.3. Admixtures

Fluidifier admixtures have been used in TSC grout mixtures in order to reduce its mixing water, retard the setting time and provide expansion during the plastic state of the grout.

According to ASTM C937, a TSC grout fluidifier admixture should meet the requirements shown in **Table 2.5** (ASTM C937, 2004). A grout fluidifier commonly consists of a water-reducing admixture, expanding agent, and a chemical buffer (ACI 304.1, 2005; ASTM C937, 2004). The recommended dosage of grout fluidifier is usually 1% by weight of the grouts cementitious materials (ACI 304.1, 2005).

Table 2.5 – Grout fluidifier admixture requirements

Physical Requirements	Limit
Min reduction in mixing water	3%
Expansion after 3 hrs from mixing relative to cement alkali content :	
0.80 or more	7 to 14%
0.40 to 0.79	5 to 12%
0.39 or less	3 to 9%
Max. bleeding after 3 h from mixing	2%
Min increase in water retentively	60%
Min initial setting time	4 hrs
Max. final setting time	24 hrs

Aluminum powder is an expanding agent that chemically reacts with the lime freed by cement hydration to generate hydrogen gas (Goual *et al*., 2006). The generated gas induces slight expansion of the grout before setting. As a result, bleed water pockets that can cumulate under coarse aggregate particles can be removed, leading to enhanced grout coarse aggregate bond (Abdul Awal, 1984).

In 1943, the effect of aluminum powder on TSC compressive strength was investigated for the first time by Menzel (1943). He reported an increase in the TSC compressive strength by the addition of a limited amount of aluminum powder (about 13 g [0.46 oz] per 100 kg [220.4 lb] of cement for dry gravel and 8 g [0.28 oz] for wet gravel). However, adding higher amounts of aluminum powder was found to increase the TSC porosity, consequently reducing its compressive strength (Menzel, 1943). Therefore, the recommended dosage of

aluminum powder in TSC grout should range between 0.01 and 0.02% by weight of cement (Casson and Davies, 1986).

In general, new generations of expanding admixtures contain aluminum powder. Hence, using 1% by weight of cement of these admixtures was found to improve the TSC compressive strength by about 46% (Abdul Awal, 1984), while adding 2% had caused only 20% increase (Abdelgader and Elgalhud, 2008). However, selecting the suitable dosage of an expanding admixture mainly depends on the amount of generated hydrogen gas, while caution should be taken regarding the effect on the TSC compressive strength.

Air-entraining admixtures can also be added to enhance the durability of TSC to freezing/thawing cycles (ASTM C260, 2006). However, the air voids induced by the expanding admixture should be considered in dosing the air-entraining admixture in order to prevent excessive increase of the voids content, which can compromise the TSC mechanical strength.

Water-reducing and retarding admixtures have been used to improve the flowability for TSC grouts (ACI 304.1, 2005). Although, high-range water-reducing admixtures enhance the strength and durability of concrete, there is no accessible data on their effect in TSC. The addition of a superplasticizer increases the grout fluidity even at low water/binder ratio (w/b) and consequently facilitates the effective filling of voids between aggregate particles. However, using an over dosage of a superplasticizer could increase bleeding, thus leading to excessive segregation of the sand in the grout mixture (Tang, 1977). The recommended dosage of superplasticizer for TSC normally ranges between (1.2 to 2% by cement weight) depending on its type (i.e. naphthalene sulphonate acid, poly-carboxylate ester, etc.) (Abdul Awal, 1984; Abdelgader and Elgalhud, 2008; O'Malley and Abdelgader, 2009). Moreover, it was reported that combining a superplasticizer and a viscosity modifying admixture can improve the TSC grout properties significantly. The use of a viscosity modifying admixture along with an adequate dosage of a superplasticizer can ensure high stability and adequate flowability for the grout, allowing the production of TSC grouts with superior bleeding resistance (Christianto, 2004).

2.3.3. Grout Mixture Proportions

The ASTM C938 "Standard Practice for Proportioning Grout Mixtures for Preplaced-Aggregate Concrete" provides procedures for selecting the grout mixture proportions based on the measured flowability and bleeding for different trial grout mixtures (ASTM C938, 2010). The suitable proportions (i.e. water/binder ratio (w/b) and sand/binder ratio (s/b)) are selected to produce a flow of 22 ± 2 sec according to the flow cone test (as will be discussed later). Moreover, bleeding of the grout should be less than 0.5% (ACI 304.1, 2005). The grout mixture proportions of TSC will vary depending on the application and required specifications.

It was reported that a leaner grout mixture having s/b equal to 4 could be used to produce more cost-effective TSC (Abdul Awal, 1984). However, grouts used for underwater TSC applications should be rich mixtures (i.e. s/b = 1 to 2) (Orchard, 1973). A grout mixture with (s/b = 1.0 and w/b = 0.47) exhibited adequate flowability to produce TSC (Tang, 1977). Furthermore, it was reported that the optimum grout proportions for mixtures incorporating fly ash are s/b = 1.33 and w/b = 0.53 (Taylor, 1965). According to ACI 304.1 for beams, columns, and thin concrete sections, the ratio of (s/b) should usually be equal to 1.0, while in massive concrete elements this ratio may be increased up to 1.5 (ACI 304.1, 2005).

Comparing the flowability of different grout mixtures with a s/b ratio ranging from 1.0 to 1.5, it was found that there was little difference in the achieved flowability at similar w/b ratio (Abdul Awal, 1984). Based on economic considerations, an optimum grout mixture with a flow time of 25 s had s/b = 1.5 and w/b = 0.52 without superplasticizer, or w/b = 0.47 with 1.25% superplasticizer by cement weight (Abdul Awal, 1984).

The effect of the grout mixture proportions on the bleeding of grout consisting of OPC, fly ash, sand, and 2% superplasticizer by weight of cement was investigated (Abdelgader, 1999). For a grout mixture with w/b = 0.4 and s/b = 1.5, the bleeding was zero. However, the grout was too thick and it could not penetrate through aggregate voids. At the same w/b, reducing the s/b to 1.0 enhanced the fluidity partially, even with the addition of superplasticizer. On the other hand, increasing the w/b ratio within the range of (0.45-0.55) at s/b =1.5 led to adequate rheological and bleeding properties (Abdelgader, 1999). Therefore,

selecting the *s/b* and *w/b* is extremely important since the amount of sand and water control the rheological and bleeding properties of the TSC grout.

Based on the data discussed above, it is argued that selecting an optimum proportion for a TSC grout mixture is highly affected by the chemical and physical properties of the materials used (i.e. sand, cement, and SCMs). Moreover, the addition of chemical admixtures induces significant changes in the fresh properties of the TSC grout. Therefore, trial grout mixtures should be conducted in order to achieve optimum grout proportions that can meet the requirements of ASTM C938 (2010) and successful full-scale construction.

2.3.4. Grout Flowability Measuring Techniques

Evaluating the grout consistency is very important since it has a direct effect on pumpability and void penetrability (Abdul Awal, 1984). The flow cone method is the most commonly used test for measuring the TSC grout flowability. The flow cone test consists of measuring the time of efflux of 1725 ml [0.06 ft^3] of the grout through a specific cone having a 12.7 mm [0.5 in] discharge tube according to ASTM C939 "Standard Test Method for Flow of Grout for Preplaced-Aggregate Concrete" (ASTM C939, 2010). Previous research has shown that grout with a time of efflux between 20 and 24 s is ideal for TSC (ACI 304.1, 2005; ASTM C939, 2010). However, grout with time of efflux as high as 35 to 40 s is recommended for high-strength concrete (ACI 304.1, 2005).

The other method used is the spread flow test. In this test, a fixed volume of grout (i.e. 250 ml [0.008 ft^3]) is filled into a cylinder then poured from a height of 1 cm [0.4 in] over a scaled plate. The spreading diameter of the grout over the plate is then recorded as an indication of the TSC grout flowability (Abdelgader, 1996). It is believed that using modern rheometers that can characterize the yield value and plastic viscosity of the grout, which could lead to better characterization of the TSC grout rheology.

2.4. CONSTRUCTION PROCEDURE OF TWO-STAGE CONCRETE

Generally, the construction process of TSC includes two main stages: placing the coarse aggregate particles in the formwork, followed by the injection the grout. Detailed steps for the construction process of TSC reinforced elements are outlined below.

Initially, the construction location is prepared and an impermeable strong formwork is erected to prevent grout leakage and resist the lateral pressure induced during the grout pumping. Plywood formwork systems have been used successfully in large TSC projects. However, for underwater pier construction, steel sheet piling is preferred to resist water pressure. In deep-water piers, an adequate internal anchorage for the steel sheet piling should be secured to avoid any deflection during the grouting process (ACI 304.1, 2005; ACI 304, 2005).

Subsequently, the steel reinforcement is placed and arranged according to the design detailing and drawings, followed by coarse aggregate placement. For constructing TSC foundations, the aggregates and reinforcement can be placed in sequence at different layers depending on the construction conditions and the spacing between the reinforcement mesh (ACI 304.1, 2005).

Prior to placing the aggregates, pipes for injecting the grout are fixed in carefully selected locations. These pipes are normally 20 to 30 mm [0.8 to 1.2 in] in diameter for normal structural concrete and up to 40 mm [1.6 in] for massive concrete. These grout insert pipes should be extended vertically about 150 mm [6 in] above the bottom of the aggregate mass to provide adequate space during the first flow of grout. Moreover, pipes may be extended horizontally through the formwork at different elevations, especially in repair works (ACI 304.1, 2005; ACI 304, 2005). For very deep placements (e.g. caissons in deep water), double insert pipes should be used to inject grout at different levels. For example, to inject grout at 30 m [98 ft] depth, two pipes are used. A 25 mm [1 in] pipe to grout the bottom portion (i.e. depth of 15 m [49 ft] and down to 30 m [98 ft]), while the remainder from the surface to a depth of 15 m [49 ft] is injected using a 50 mm [2 in] pipe. The required number of grout insert pipes and their locations depend on the size and shape of the constructed concrete element (US Army Corps of Engineers, 1994). Moreover, the spacing between these pipes relies on the propagation of grout mixtures. ACI 304.1 (2005) provides detailed guidelines on the installation of pipes for uniform distribution of grouts in TSC.

Figure 2.3 illustrates a typical propagation curve of a grout mixture in preplaced coarse aggregate. The propagation curve is the shape of grout flow through the preplaced aggregate particles and it is used to describe the relation between grouting level and the spacing between grouting pipes (Abdelgader, 1995). The shape of the curve depends on several

factors such as the grout mixture density, intensity of mixing, shape and size of the coarse aggregate (Abdelgader, 1995). It was reported that the grout propagation generally has a slope (vertical: horizontal) of 1:4 and 1:6 for dry conditions and under water placements, respectively (ACI 304.1, 2005). An empirical equation (**Eq. 2.1**) for the propagation curve of grout in coarse aggregates was derived (Abdelgader, 1995):

$$y = \frac{\alpha}{(\beta x^2 + 1)\sqrt{\frac{\gamma}{t} - \frac{1}{\beta} + 1}}$$
Eq. 2.1

Where y = grout mixture level in coarse aggregate (m), x = spacing between grout insert pipes (m), α = thickness of stone layer (m), t = time (min), $\beta = (a \times b \times f)$, a = parameter dependent of the mixture fluidity, b = parameter dependent of stone: shape, size, type of grain, surface texture, and coarse aggregate fraction, f = parameter dependent of the environment of construction, $\gamma = (c \times d \times e)$, c = parameter dependent of efficiency of flushing pipe (m³/min), d = parameter dependent of perforation, e = parameter dependent of the type of excavation bottom.
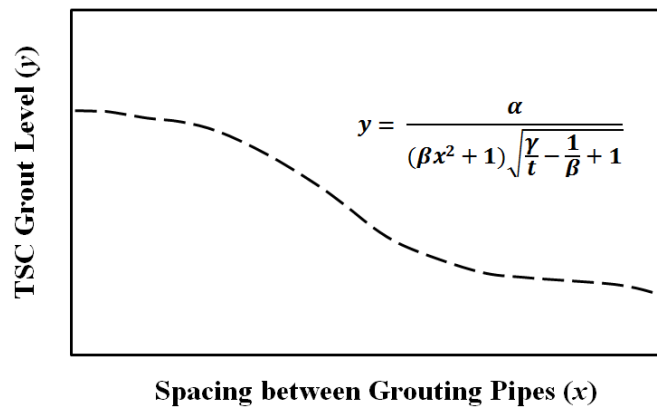
Figure 2.3 – Propagation curve of grout mixture in coarse aggregates for TSC (Abdelgader, 1995).

Placement of the coarse aggregates can be done by hand or mechanically using dumping. If it is necessary to saturate the coarse aggregate after placement in the formwork, water should be injected through the insert pipes rather than by flushing. Flushing water will accumulate fines at the lower aggregate layer, leading to the development of honeycombing,

while injecting the water will uplift any fines to the surface without causing problems (ACI 304, 2005).

The flowability of the used grout should be carefully selected relatively to the dimensions of the constructed concrete element, the coarse aggregate size and the reinforcement detailing. After selection, the grout is injected using a delivery system consisting of a single line from the grout pump directly to the grout insert pipe. This delivery line should have a sufficient diameter to control the grout velocity according to the planned operating rate (i.e. 0.6 to 1.2 m/sec [1.97 to 3.9 ft/sec]) (ACI 304, 2005). Very low velocity will permit segregation and eventual line blockage, while too high velocity will force the grout to cascade over adjacent aggregates rather than penetrating their internal voids (ACI 304, 2005).

Finally, the hardened TSC is cured and finished following similar procedures to that of conventional concrete, taking into consideration that the curing time may be extended to achieve the target compressive strength. Moreover, in case of cold joints, the grout pumping should be stopped before the grout reaches the upper surface of the aggregate (i.e. 300 mm [12 in] under the aggregate surface). Hence, a clean rough exposed aggregate surface for the next grout should be provided (ACI 304.1, 2005).

2.5. PROPERTIES OF TWO-STAGE CONCRETE

2.5.1. Compressive Strength

Compressive strength is generally considered as the key property of concrete. Hence, the compressive strength of TSC has been investigated extensively (Abdul Awal, 1984; Abdelgader, 1996; Bayer, 2004; O'Malley and Abdelgader, 2009). It was concluded that TSC compressive strength is mainly affected by its *w/b* ratio, *s/b* ratio, type of coarse aggregate and its void content, and the compressive strength of the used grout. **Table 2.6** summarizes data of compressive strength of TSC at different ages with respect to the used grout mixture collected from various studies.

Table 2.6 – TSC compressive strength

Grout Mixture Proportions				Compressive Strength (MPa)			Ref.
w/b	*s/b*	Mineral Admixture	Chemical Admixture	Age (Days)			
				28	90	365	
0.38	0.60	----	----	41.10	48.50	NA	(Klein and Crockett, 1953)
0.38	0.67		----	40.30	50.50	NA	
0.44	1.50	----	----	22.20	32.34	NA	(Davis *et al.*, 1955)
0.56	1.68	----	1% EA	22.20	29.72	NA	(Davis and Haltenhoff, 1956)
0.62	2.63			15.50	23.93	NA	
0.52	1.50	----	----	28.90	31.90	39.10	(Abdul Awal, 1984)
0.50			1.25 % SP	29.00	32.00	41.60	
0.47			1% EA	42.30	45.60	54.80	
0.45			1% EA +1.25 % SP	42.50	46.50	50.60	
0.40	1.25	35% FA	2% SP	35.16	NA	NA	(Abdelgader, 1996)
0.45				31.81	NA	NA	
0.50				26.90	NA	NA	
0.55				21.31	NA	NA	
0.40	1.50	35% FA	2% SP	28.35	NA	NA	
0.45				30.71	NA	NA	
0.50				25.57	NA	NA	
0.55				23.94	NA	NA	
0.45	0.00	20% RP	1% SP + 0.2% AEA	10.90	14.90	19.50	(Bayer, 2004)
		25% RP +25% FA		13.70	15.50	28.90	
		50% GGBFS		19.50	23.70	25.70	
		50% FA		10.60	14.90	19.60	

Note: Ordinary Portland Cement (OPC) was used in all mixtures, mineral admixtures were added as partial replacement for OPC.

(FA): Fly Ash, (RP): Rock Powder, (GGBFS): Ground Granulated Blast Furnace Slag. (EA): Expanding Admixture, (SP): Superplasticizer, (AEA): Air – Entraining Admixture.

It can be observed in **Table 2.6** that increasing the *w/b* reduces the TSC compressive strength as expected. However, using very low *w/b* drastically affects the grout flowability, resulting in honeycombed TSC. In conventional concrete, the compressive strength increases as the cement content increases up to an optimum level, beyond which no significant strength is gained (Ezgi, 2010). However, the optimum cement content for TSC depends on the void content of the coarse aggregate used and the required flowability of the grout mixture (Abdelgader, 1999). Although using a high cement dosage will increase the compressive

strength of the grout, it may reduce the TSC compressive strength due to increasing the water demand, consequently lowering grout flowability (Abdelgader, 1999). Hence, the use of water-reducing admixtures is critical for providing high strength TSC.

The *s/b* seems to have insignificant effect on the TSC compressive strength. Conversely, it has great influence on the flowability and stability of the grout mixture. For example, at *s/b* = 1.5 and *w/b* = 0.4, the grout was too thick to penetrate all voids between aggregate particles, leading to honeycombed TSC with lower strength (Abdelgader, 1996). On the other hand, adjusting the *w/b* in the range of 0.45 to 0.55 along with changing the *s/b* ratio induced slight difference in compressive strength as shown in **Figure 2.4** (Abdelgader, 1996).
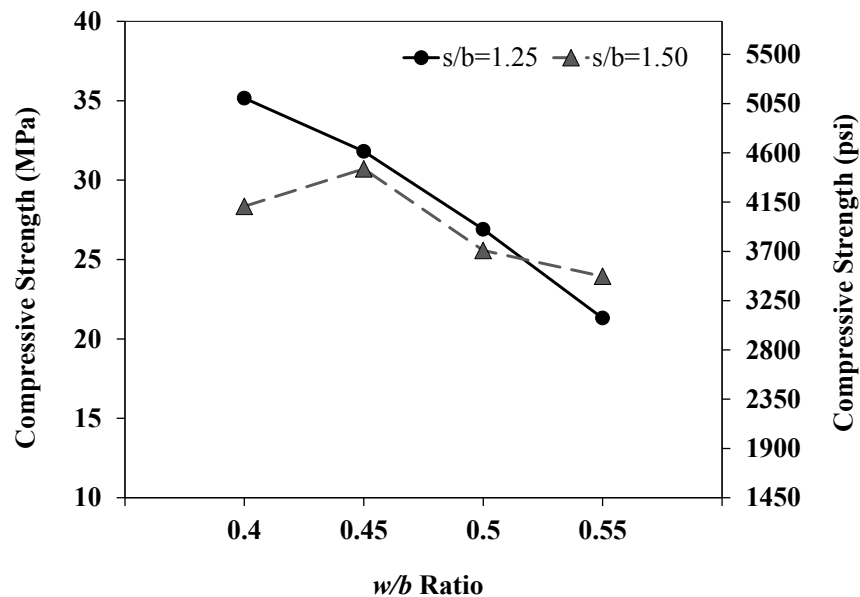
Figure 2.4 – Influence of *s/b* ratio on compressive strength of TSC versus *w/b* ratio (Abdelgader, 1996).

Furthermore, adding a superplasticizer was found to improve the TSC compressive strength. This can be ascribed to the reduction in *w/b* required to achieve adequate flowable grout (Abdul Awal, 1984). Moreover, expanding admixtures are commonly used in TSC to expand the grout before its setting as mentioned earlier. Adding such expanding admixtures significantly increased the TSC compressive strength (Ezgi, 2010). For instance, adding 1%

of expanding admixture increased the TSC compressive strength by about 46% with respect to that of the control TSC mixture without expanding admixture at age of 28 days **(Table 2.6)** (Abdul Awal, 1984). This can be attributed to better bond as a result of removing void spaces between the aggregates as discussed earlier.

The effect of adding mineral admixtures such as rock powder (RP), fly ash, and GGBFS on the TSC compressive strength was investigated by Bayer (2004). It was found that the mixture incorporating 50% GGBFS as partial replacement for cement exhibited the highest compressive strength at 28 days (**Figure 2.5**). Moreover, after one year, the compressive strength of TSC mixtures incorporating mineral admixtures at rates of (20% RP, 25% FA + 25% RP, and 50% FA) was approximately twice that at 28 days (Abdelgader, 1995). This indicates the role of mineral admixture in improving the long- term strength of TSC.
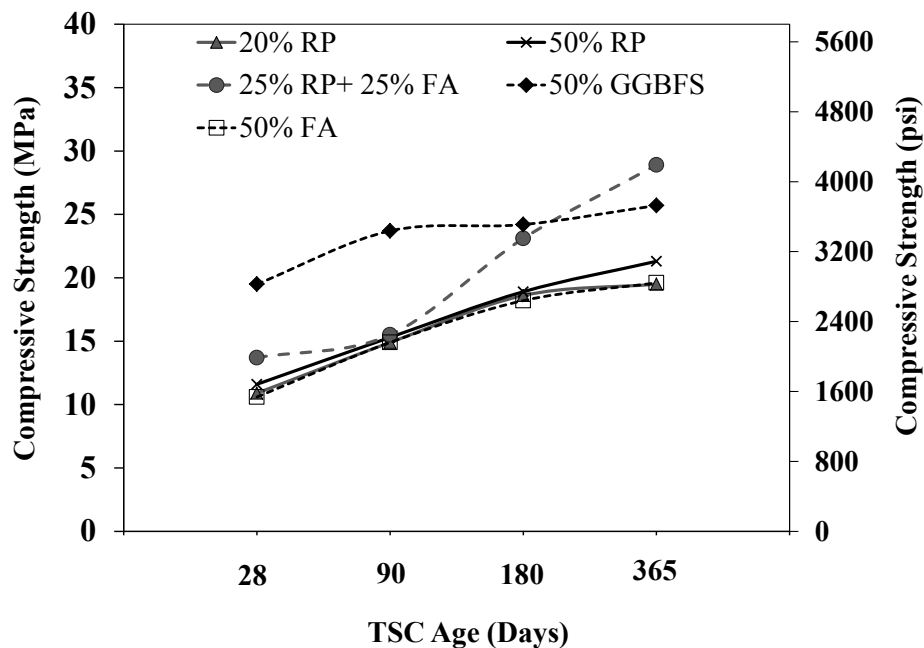
Figure 2.5 – Development of TSC compressive strength with different mineral admixtures (Bayer, 2004).

The effects of the void content and shape of the coarse aggregate on the TSC compressive strength have also been investigated (Abdelgader, 1996; O'Malley and Abdelgader, 2009). TSC mixture incorporating crushed aggregate exhibited higher

compressive strength than that of the mixture incorporating rounded aggregates at the same *w/b* ratio. This can be attributed to the fact that crushed aggregates provide better interlock than that of rounded aggregates (Abdelgader, 1996). Compressive strength of TSC made with recycled concrete aggregate is investigated. It was concluded that natural aggregate used to produce TSC can be partially replaced with recycled coarse and fine aggregate without a major drop in TSC strength, especially for grouts have a high *w/b* ratio (i.e. *w/b* ratios more than 0.45). For low *w/b* ratios, the grout flowability reduces, leading to insufficient penetration of grout through recycled aggregate particles (Morohashi *et al*., 2013).

Figure 2.6 shows a comparison between the compressive strength of grout and the corresponding TSC strength for several mixtures. It can be observed that usually the TSC compressive strength is lower than that of the used grout. Increasing the strength of the grout does not guarantee an improvement of the TSC compressive strength. For instance, mixture #2 had a grout compressive strength higher than that of mixture #1; however, the achieved compressive strength for both TSC mixtures was comparable. Conversely, adding an expanding admixture (i.e. mixture #3) improved the TSC compressive strength despite that the corresponding grout compressive strength was lower (i.e. compared to that of mixtures #1 and 2). This can be explained as follows. In the grout mixture there was no expansion restraint; hence, the generated hydrogen gas will increase voids, leading to lower compressive strength. Conversely, the interlocked aggregate particles in the TSC mixture limit the expansion of the grout and induce a confinement. Moreover, this early expansion removes cumulated water pockets under coarse aggregate particles as discussed earlier (Abdul Awal, 1984).

Thus, the compressive strength of the grout is not a direct indication of the TSC compressive strength. Furthermore, there is no direct proportional relationship between the increase in the grout strength and the corresponding increase in the TSC strength. As shown in **Figure 2.6**, an 80% increase in the grout strength could only cause 60-65% increase in the TSC strength (Abdelgader, 1996, 1999). The bond properties between aggregate particles and the grout have a significant effect on the compressive strength of TSC (Abdul Awal, 1984; Abdelgader, 1996; O'Malley and Abdelgader, 2009) and require dedicated research.
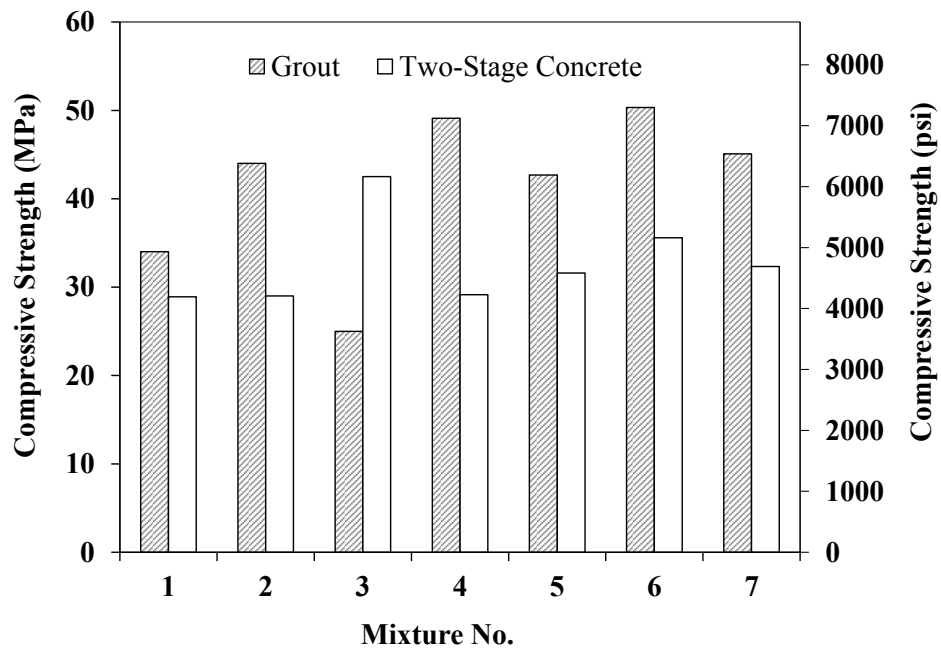
Figure 2.6 – Comparison between compressive strength of grout and TSC in several mixtures (Mixtures 1-3 (Abdul Awal, 1984), Mixtures 4-7 (Abdelgader, 1996)).

To investigate the effects of the production process of TSC on its compressive strength, the compressive strength of TSC and that of conventional concrete with identical mixture proportions were compared. Several researchers found that TSC was weaker than conventional concrete of similar mixture design, while others claimed that it was stronger (Abdul Awal, 1984). **Figure 2.7** displays a comparison between the compressive strength of TSC and that of conventional concrete obtained from two studies (Abdul Awal, 1984; Bayer, 2004). In fact, it is very difficult to compare TSC directly with conventional concrete, not only because of its quite different placement method, but also because of its different mixture proportions. However, an attempt was made in these studies to design normal concrete mixtures having water-to-binder ratio (*w/b*) and aggregate-to-binder ratio (*A/b*) similar to those in TSC mixtures. For mixtures 1-2, the variable parameter was the type of chemical admixtures (Abdul Awal, 1984). While mixtures 3-5, the variable parameter was the type of cementitious materials (Bayer, 2004). It can be observed that the compressive strength of TSC is comparable to that of conventional concrete. However, TSC mixtures incorporating expanding admixtures (e.g. mixture #2) exhibited higher strength than that of the control

conventional mixture. This can be attributed to the absence of expansion restraint in conventional concrete; hence, the generated hydrogen gas increased voids in its matrix, consequently reducing its compressive strength. Conversely, the interlocked aggregate particles in TSC limit the expansion of the grout and induce a confinement. Moreover, the compressive strength of the mixture #5 TSC was higher than that of conventional concrete since the TSC mixture contains 50% Ground Granulated Blast-Furnace Slag (GGBFS) as a mineral admixture, leading to enhance its compressive strength.
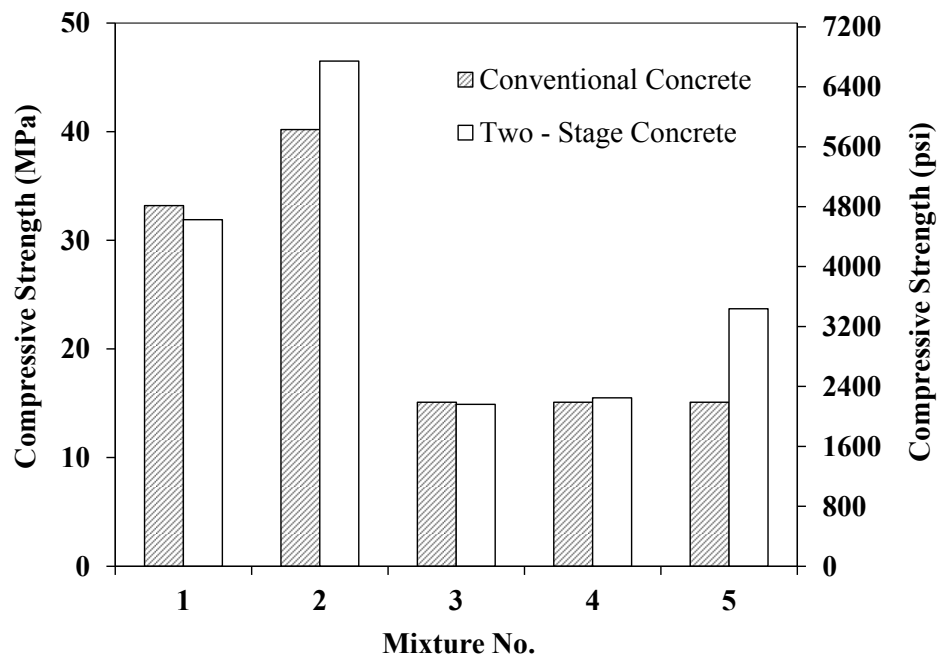
Figure 2.7 – Comparison between compressive strength of conventional concrete and TSC (Mixtures 1-2 (Abdul Awal, 1984), Mixtures 3-5 (Bayer, 2004)).

The relationship between the compressive strength of TSC and the grout mixture proportions (i.e. *w/b* and *s/b*) is illustrated using nonlinear regression analysis. Several equations have been proposed as shown in **Table 2.7**. Some of these formulas depend on the coarse aggregate shape (Abdelgader, 1999), while others are based on the used admixtures (Abdelgader and Elgalhud, 2008).

Table 2.7 – Compressive strength (f_c') as a function of (w/b) ratio and (s/b) ratio

Equation	Ref.
$f_c' = 64.27 - 72.25\,(w/b) - 0.06\,(s/b)^{-1}$ (MPa) For rounded coarse aggregate $f_c' = 62.08 - 71.00(w/b) + 0.52\,(s/b)^{-1}$ (MPa) For crushed coarse aggregate $f_c' = 64.78 - 75.33\,(w/b) + 0.26\,(s/b)^{-1}$ (MPa) For mixed (rounded and crushed) coarse aggregate	(Abdelgader, 1999)
$f_c' = -3.67 + 11.20\,(w/b) + 3.96(w/b)^{-1.79} + 3.7\,(s/b)^{-1}$(MPa) Without admixture $f_c' = 43.90 - 32.55\,(w/b) - 3.27(w/b)^{-1.68} + 2.42\,(s/b)^{-1}$ (MPa) With 2% SP $f_c' = -14.31 - 39.83\,(w/b) + 68.45(w/b)^{0.47} + 2.63\,(s/b)^{-1}$(MPa) With 2% EA $f_c' = -25.70 - 87.70\,(w/b) + 126.75(w/b)^{0.52} + 1.88\,(s/b)^{-1}$(MPa) With 2% SP and 2% EA	(Abdelgader and Elgalhud, 2008)

(EA): Expanding Admixture, (SP): Superplasticizer.

2.5.2. Tensile Strength

The tensile strength of concrete is an important property; especially during early stages when concrete is a vulnerable to volumetric deformation due to moisture and thermal gradients (Nehdi and Soliman, 2011). Such deformations induce stresses that can lead to cracking once they exceeded the concrete tensile strength. In TSC, the splitting tensile strength has commonly been used to represent tensile strength (Abdul Awal, 1984; Abdelgader and Elgalhud, 2008; Abdelgader and Ben-Zeitun, 2005).

Table 2.8 summarizes TSC tensile strength results for different grout mixtures. It can be observed that the tensile strength of TSC increased as the *w/b* was decreased to 0.40. Decreasing the *w/b* ratio below 0.40 led to a honeycombed structure that is partially binding coarse aggregates, consequently reducing the tensile strength (Abdelgader and Elgalhud, 2008). The effect of adding superplasticizer and expanding admixtures on the TSC tensile

strength was also investigated (Abdul Awal, 1984). Results indicated that a significant improvement in tensile strength can be achieved by combining a superplasticizer and an expanding admixture. Moreover, it was found that at constant *w/b* ratio, the effect of different *s/b* ratios on the tensile strength of TSC was negligible as shown in **Figure 2.8** (Abdelgader and Ben-Zeitun, 2005).

Table 2.8 – TSC tensile strength

Grout Mixture Proportions			Tensile Strength (MPa) at 28 days	Ref.
w/b	*s/b*	Chemical Admixture		
0.52		----	3.00	
0.50	1.5	1.25%SP	3.10	(Abdul Awal, 1984)
0.47		1 % EA	3.30	
0.45		1% EA + 1.25 % SP	3.50	
0.40			3.35	
0.45	0.5		3.14	
0.50		----	2.83	
0.55			2.72	(Abdelgader and Ben-Zeitun, 2005)
0.40			3.34	
0.45	1.0		3.02	
0.50		----	2.86	
0.55			2.53	
0.38		2% SP	2.38	
0.38	0.5	2% EA	2.16	
0.38		2% SP + 2% EA	2.54	
0.55		2% SP	2.84	
0.55	0.5	2% EA	2.82	
0.55		2% SP + 2% EA	3.36	(Abdelgader and Elgalhud, 2008)
0.38		2% SP	1.98	
0.38	1.0	2% EA	1.86	
0.38		2% SP + 2% EA	2.06	
0.55		2% SP	2.66	
0.55	1.0	2% EA	2.58	
0.55		2% SP + 2% EA	2.88	

(EA): Expanding Admixture, (SP): Superplasticizer.
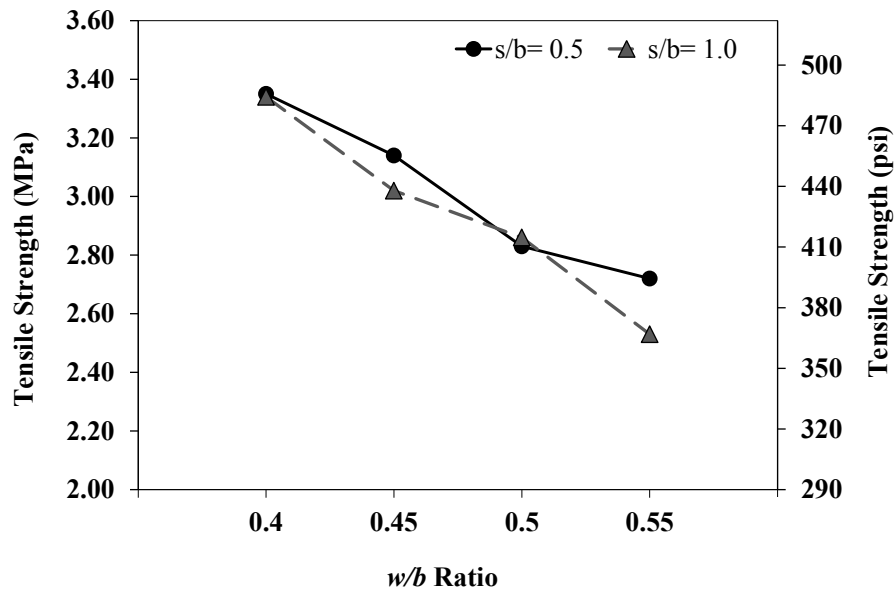
Figure 2.8 – Influence of *s/b* ratio on tensile strength of TSC versus *w/b* ratio (Abdelgader and Ben-Zeitun, 2005).

Generally, TSC exhibits lower tensile strength than that of ordinary concrete with similar mix design (Tang, 1977; Chefdeville, 1963). This was attributed to the weaker interfacial bond between coarse aggregate particles and the grout mixture, leading to splitting failure. Conversely, TSC mixtures incorporating a superplasticizer and an expanding admixture exhibited higher tensile strength than that of the control ordinary concrete (**Figure 2.9)** (Abdul Awal, 1984).
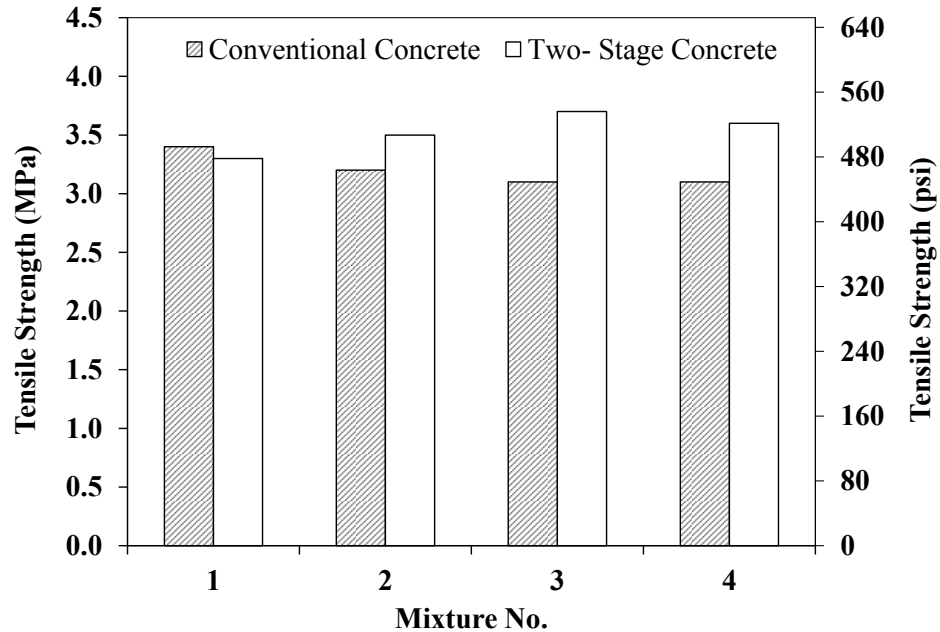
Figure 2.9 – Comparison between tensile strength of conventional concrete and TSC (Abdul Awal, 1984).

According to Abdelgader and Elgalhud (2008), the tensile strength of TSC can be estimated as a function of the *w/b* ratio, *s/b* ratio, and the compressive strength of TSC using equations listed in **Table 2.9** (Abdelgader and Elgalhud, 2008). These equations are based on certain dosages and types of admixtures (i.e. 2% superplasticizer and/or 2% expanding admixture). On the other hand, it was found that the tensile strength of TSC increased as the compressive strength increased, which is similar to conventional concrete. Therefore, more general correlations between the tensile and compressive strengths of TSC have been proposed (**Table 2.10**).

Table 2.9 – Tensile strength (f_t) of TSC as a function of (w/b) ratio, (s/b) ratio, and compressive strength for TSC (f_c') (Abdelgader and Elgalhud, 2008)

Equation	Admixture Type
$f_t = -0.25 + 1.26\,(w/b) + 0.67(w/b)^{-1.29} + 0.51\,(s/b)^{-1}$ (MPa) $f_t = -49.67 - 0.44\,f_c' + 38.63\,(f_c')^{0.15}$ (MPa)	Without admixture
$f_t = -12.75 - 25.27(w/b) + 39.03(w/b)^{0.5} + 0.39\,(s/b)^{-1}$ (MPa) $f_t = 39.97 + 0.36\,f_c' - 32.28\,(f_c')^{0.1}$ (MPa)	2% SP
$f_t = -11.54 - 23.20(w/b) + 36.12(w/b)^{0.52} + 0.48\,(s/b)^{-1}$ (MPa) $f_t = -4.30 - 0.30\,f_c' + 1.28\,(f_c')^{0.658}$ (MPa)	2% EA
$f_t = 9.82 - 7.41\,(w/b) - 1.37\,(w/b)^{-1.39} + 0.42\,(s/b)^{-1}$ (MPa) $f_t = 162.65 + 1.15\,f_c' - 132.28\,(f_c')^{0.108}$ (MPa)	2% SP and 2% EA

(EA): Expanding Admixture, (SP): Superplasticizer.

Table 2.10 – Tensile strength (f_t) as a function of compressive strength (f_c') for TSC

Equation	Ref.
$f_t = 0.677\,f_c^{0.434}$ (MPa) (Splitting Tensile Strength)	(Abdul Awal, 1984)
$f_t = 0.768\,f_c^{0.441}$ (MPa) (Splitting Tensile Strength) $f_t = 0.374\,f_c^{0.540}$ (MPa) (Double-Punch Tensile Strength)	(Abdelgader and Ben-Zeitun, 2005)

2.5.3. Modulus of Elasticity

The modulus of elasticity is a principal property of concrete, which reflects its stiffness and ability to deform elastically. Generally, it is obtained from the stress–strain curve at a certain stress level relative to the ultimate strength (Nehdi and Soliman, 2011). The modulus of elasticity for both TSC and conventional concrete is mainly affected by the compressive strength. However, it was reported that TSC exhibits higher modulus of elasticity than that of conventional concrete even for mixtures with similar compressive strength (Akatsuka and Moriguchi , 1967). This can be ascribed to the fact that TSC is a skeleton of coarse aggregate particles resting on each other. Therefore, loads will transmit through contact points between aggregate particles as illustrated earlier. In addition, the modulus of elasticity of coarse

aggregates is generally higher than that of cement paste (Abdul Awal, 1984). Consequently, the higher elastic modulus of TSC can be considered as a consequence of the modulus of elasticity of the used coarse aggregate (Abdul Awal, 1984; Abdelgader and Górski, 2003). Modulus of elasticity values for several TSC mixtures are summarized in **Table 2.11**. Moreover, the modulus of elasticity of the coarse aggregate usually will not change with time; hence, TSC is expected to have a nearly constant modulus of elasticity (Abdul Awal, 1984; Davis *et al*., 1955).

Several studies reported that changing the *w/b* ratio of the grout mixture had no effect on the TSC modulus of elasticity (Abdul Awal, 1984; Abdelgader and Górski, 2003), while reducing the *s/b* ratio can cause a reduction in modulus (Abdelgader and Górski, 2003; Bayer, 2004). **Figure 2.10** illustrates the effect of *s/b* ratio on modulus of elasticity versus *w/b* for TSC made using crushed basalt as a preplaced aggregate. For instance, at *w/b* = 0.45, increasing the *s/b* from 0.8 to 1.5 increased the modulus of elasticity by about 15% (Abdelgader and Górski, 2003).

Similar to conventional concrete, the modulus of elasticity of TSC was correlated to its compressive strength (Abdelgader and Górski, 2003). **Equations 2.2** to **2.4** have been proposed to estimate the TSC modulus of elasticity (E) according to its compressive strength (f_c'). However, these equations can only be used for a limited range of compressive strength $(22\ MPa\ \leq f_c' \leq 32\ MPa)$ (Abdelgader and Górski, 2003).

$$E = 28.7 + 0.080\ f_c'\ \text{(GPa) (rounded aggregate)} \qquad \textbf{Eq. 2.2}$$

$$E = 33.9 - 0.049\ f_c'\ \text{(GPa) (crushed aggregate)} \qquad \textbf{Eq. 2.3}$$

$$E = 34.9 - 0.090\ f_c'\ \text{(GPa) (mixed: rounded and crushed aggregate)} \qquad \textbf{Eq. 2.4}$$

Table 2.11 – Modulus of elasticity of TSC

Grout Mixture Proportions				Modulus of Elasticity (GPa)			Ref.
				Age (Day)			
w/b	*s/b*	Mineral Admixture	Chemical Admixture	28	90	365	
0.52		----	----	34.60	34.80	36.20	(Abdul Awal, 1984)
0.50		----	1.25%SP	35.7	36.00	39.80	
0.47	1.50	----	1%EA	39.30	39.80	40.30	
0.45		----	1% EA and 1.25 % SP	36.60	37.40	39.10	
0.45		----		34.48	NA	NA	(Abdelgader and Górski, 2003)
0.50	1.50	----	2% SP	34.68	NA	NA	
0.55		----		34.88	NA	NA	
0.45		----		31.88	NA	NA	
0.50	1.00	----	2% SP	32.08	NA	NA	
0.55		----		32.28	NA	NA	
0.45		----		30.00	NA	NA	
0.50	0.80	----	2% SP	30.12	NA	NA	
0.55		----		30.32	NA	NA	
0.45	0.00	20% RP	1% SP and 0.2% AEA	10.15	11.95	13.83	(Bayer, 2004)
		25% RP+25% FA		11.12	13.25	16.75	
		50% GGBFS		12.73	13.94	15.49	
		50% FA		8.96	10.67	12.80	

(FA): Fly Ash, (RP): Rock Powder, (GGBFS): Ground Granulated Blast Furnace Slag. (EA): Expanding Admixture, (SP): Superplasticizer, (AEA): Air – Entraining Admixture.
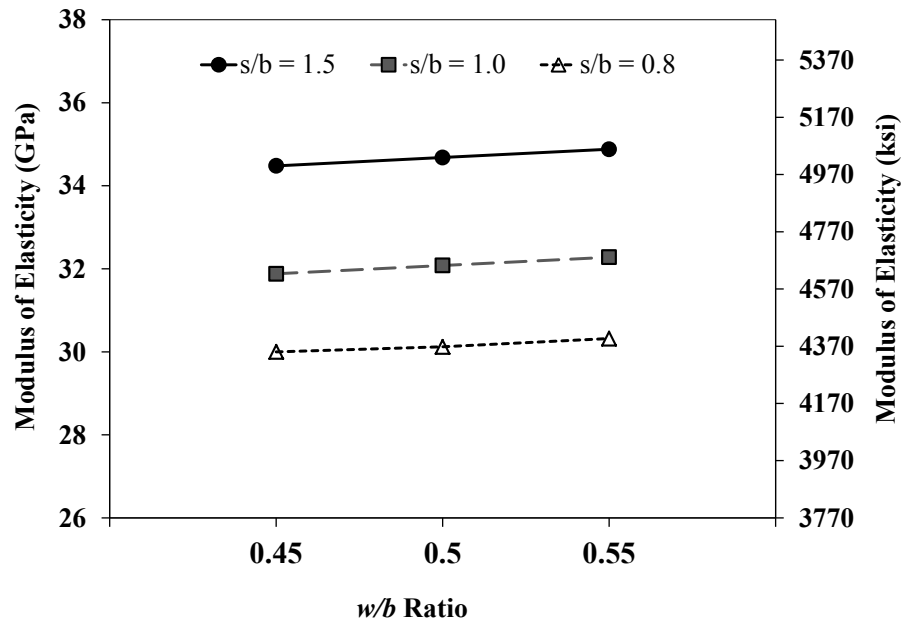
Figure 2.10 – Influence of *s/b* ratio on crushed basalt TSC modulus of elasticity versus *w/b* ratio (Abdelgader and Górski, 2003).

2.5.4. Shrinkage

Shrinkage is generally known as a reduction of the concrete volume with time due to loss of physically adsorbed water from cement paste (Mehta and Monteiro, 2006). There are generally three types of shrinkage including drying shrinkage, autogenous shrinkage, and carbonation shrinkage (Nehdi and Soliman, 2011). The shrinkage of TSC was found to be much lower than that of conventional concrete (ACI 304.1, 2005; Abdelgader and Elgalhud, 2008; Abdelgader and Ben-Zeitun, 2005). This can be explained according to the drying shrinkage equation (**Eq. 2.5**) proposed by Lyse (1959).

$$S_t = S_0 \, (1 - e^{-S_t})\rho \qquad\qquad \textbf{Eq. 2.5}$$

Where S_t = shrinkage after time of drying (t), S_0 = final shrinkage in relation to the percentage of cement paste in the concrete, S = rate of shrinkage depending on the relative humidity of the ambient atmosphere, and ρ = percentage of cement paste in the concrete.

Therefore, since TSC contains less cement paste and more coarse aggregate than conventional concrete, TSC is expected to exhibit lower shrinkage. Experimentally, it was found that the drying shrinkage of TSC was about 330 micro-strains compared to about 600 micro-strains for conventional concrete (Davis, 1960). Adding a superplasticizer and/or an expanding admixture was found to reduce the TSC shrinkage (Abdul Awal, 1984). However, TSC mixtures incorporating superplasticizers have shown lower drying shrinkage than that of TSC made with expanding admixtures. This was attributed to reduction of the water demand induced by the superplasticizers (Abdul Awal, 1984).

2.5.5. Creep

Very limited data on TSC creep are available in the open literature. Three months creep tests for TSC have shown much lower creep values than that of normal concrete (Tang, 1977). It was also reported that the 90 days creep strain in conventional concrete was about 24% higher than that in TSC at the same age (Abdul Awal, 1984). This can be ascribed to the fact that TSC is considered volumetrically more stable than conventional concrete. Indeed, TSC has a higher amount of coarse aggregate and lower amount of cement paste, which is primarily responsible for creep. Hence, it is expected that creep of TSC will be lower since it

is proportional to the cement paste content (Abdul Awal, 1984). Furthermore, creep recovery for TSC, which is defined as the amount of strain that is recovered immediately after removing the load, was investigated (Abdul Awal, 1984). Results showed that TSC has lower creep recovery compared to that of conventional concrete **(Table 2.12)**.

Table 2.12 – Creep recovery of TSC and conventional concrete (CC) [adapted after (Abdul Awal, 1984)]

Concrete Type	(w/b) Ratio	Admixture Type	Compressive Strength (MPa)	Creep (10^{-6})	Creep Recovery (10^{-6})
TSC	0.52	without	31.90	779	61
CC		admixture	33.20	965	97
TSC	0.47	1.25% SP	32.00	688	72
CC			44.80	731	75
TSC	0.50	1% EA	45.60	945	71
CC			38.20	1325	100
TSC	0.45	1% EA +	46.50	719	96
CC		1.25% SP	40.20	947	110

2.5.6. Heat of Hydration

During the hydration process of cementitious materials, significant heat is liberated. The amount of heat will mainly depend on the type of cement (i.e. cement composition and cement fineness), and the concrete mixture proportions (i.e. cement content, SCMs content, and aggregate content) (Chefdeville, 1963). Moreover, the geometry of the concrete member and ambient temperature have a significant influence on the resultant rise of the concrete temperature. In massive concrete, the external surface cools faster than the core, leading to tensile strains and stresses that can cause thermal cracking (ACI 207, 1996). It is recommended that the maximum temperature difference between the concrete core and its exterior surface not to exceed 20°C to avoid the development of thermal cracking (Portland Cement Association, 1997).

TSC has been used in massive concrete structures such as dams owing to its low cement content leading to lower heat of hydration and consequently less thermal cracking. However, there is limited research on the thermal properties of TSC. Changes in massive TSC temperature were monitored in 1-m^3 [35.3 ft^3] specimens (Bayer, 2004). Periodical

temperature measurements were taken every 8 hours until the temperature reached a steady-state. It was found that adding mineral admixtures (i.e. rock powder, fly ash, GGBFS) as partial replacement for cement significantly reduced the temperature differences between the surface and core of TSC specimens (**Table 2.13)**.

Table 2.13 – Peak temperature differences with different mineral admixtures for TSC [adapted after (Bayer, 2004)]

Specimen No.	Mineral Admixture as Partial Replacement for Cement (%)	Peak Temperature Difference (°C)
1	20% Rock Powder	08.5
2	50% Rock Powder	08.0
3	25% Fly Ash and 25% Rock Powder	08.0
4	50% GGBFS	13.0
5	50% Fly Ash	09.5
6	50% Brick Powder	07.0
7	25% Brick Powder and 25% Fly Ash	09.5

2.5.7. TSC Durability

Concrete durability is defined as its ability to resist damaging effects induced by different mechanical and environmental loadings during its service life. The penetration rate for any aggressive substances (e.g. chloride and sulphate ions, carbon dioxide, etc.) into concrete is controlled by the porosity of concrete and its connectivity and the existence of micro-cracks (Mehta, 1988).

According to ACI 304.1 (2005), TSC was very durable when exposed to aggressive environments (ACI 304.1, 2005). Moreover, TSC containing air entraining admixtures showed high frost resistance similar to that of conventional concrete (Tynes and McDonald, 1968). Recently, field investigation of TSC piles of the Tasman Bridge in Australia was conducted after 48 years of service in order to evaluate the TSC long-term durability. Results showed that the TSC technique produced dense and durable concrete in this marine environment. The chloride and sulfate contents based on examining cores from these piles were low at the reinforcement bars depth (Berndt, 2012). Moreover, minimal corrosion of reinforcement was observed during visual inspection. Furthermore, the sulfate concentrations

ranged between 1.3% and 3.8% by weight of cement, which is not an excessive concentration under such severe exposure condition (Berndt, 2012).

2.6. CONCLUDING REMARKS AND RECOMMENDATIONS

The TSC technology has been widely used in many applications over the past 70 years, including repair, massive concrete, underwater concreting, etc. In some of these applications, the TSC was by far the most economical. In others, favorable properties were the principal reason for its use. Based on this review chapter, the following concluding remarks on TSC can be outlined:

- TSC provides cost benefits since 60% of the material (i.e. coarse aggregate particles) is directly placed into the formwork and only 40% (i.e. grout) goes through mixing and pumping procedures.

- TSC has a high aggregate to cement ratio (*A/C*) compared to that of conventional concrete, which can lead to higher volume stability, thus resulting in less cracking.

- The selection of the type and size of the coarse aggregates is a key aspect since these influence the TSC mechanical properties.

- Grout flowability is a paramount factor affecting the TSC engineering properties as it directly controls the inter-aggregate void penetrability.

To the best of the author's knowledge, there is currently scarce data that evaluate the effects of adding different admixtures and/or SCMs (e.g. silica fume, metakaolin, fly ash, and GGBFS) on TSC properties. To gain a better understanding of TSC and the factors controlling its properties, there is need to investigate the following:

- Effect of different binder compositions (e.g. using SCMs) and/or new generation chemical admixtures (e.g. superplasticizers, viscosity modifying admixtures) on TSC grout properties.

- Effect of the coarse aggregate properties on the mechanical properties of TSC. For instance, the use of recycled aggregates with TSC, dense aggregates for TSC radiation shielding, and lightweight aggregate TSC need yet to be explored.

- The durability and long-term performance of TSC under different exposure conditions (e.g. wetting/drying and/or freezing/thawing cycles combined with chloride or sulphate ion environments) need dedicated investigation.

- Moreover, mobilizing the TSC technology in precast applications where it can provide particular advantages still needs dedicated research.

2.7. REFERENCES

Abdelgader, H. S. and Ben-Zeitun, A. E., (2005), "Tensile strength of two-stage concrete measured by double-punch and split tests," *Proceedings of International Conference on Global Construction, Role of Concrete in Nuclear Facilities,* University of Dundee, Scotland, UK, pp. 43-50.

Abdelgader, H. S. and Elgalhud, A. A., (2008), "Effect of grout proportions on strength of two-stage concrete," *Structural Concrete*, Vol. 9, No. 3, pp. 163-170.

Abdelgader, H. S. and Górski, J., (2003), "Stress-strain relations and modulus of elasticity of two-stage concrete," *Journal of Materials in Civil Engineering*, *ASCE*, Vol. 15, No. 4, pp. 329-334.

Abdelgader, H. S. and Najjar, M. F., (2009), "Advances in concreting methods," *Proceedings of International Conference on Sustainable Built Environment Infrastructures in Developing Countries*, Algeria, pp. 315-324.

Abdelgader, H. S., (1996), "Effect of quantity of sand on the compressive strength of two-stage concrete," *Magazine of Concrete Research*, Vol. 48, No. 177, pp. 353-360.

Abdelgader, H. S., (1995), "Polcrete economical method for dams," *Proceedings of the MWA International Conference on Dam Engineering*, Kuala Lumpur, Malaysia, pp. 1-4.

Abdelgader, H. S., (1999), "How to design concrete produced by a two-stage concreting method," *Cement and Concrete Research*, Vol. 29, No. 3, pp. 331-337.

Abdul Awal, A. S., (1984), "Manufacture and properties of pre-packed aggregate concrete," *Master Thesis*, University of Melbourne, Australia, 121 p.

ACI 207, (1996), "Mass concrete," *American Concrete Institute*, Farmington Hills, USA, 42 p.

ACI 304, (2005), "Guide for measuring, mixing, transporting, and placing concrete," *American Concrete Institute*, Farmington Hills, USA, 49 p.

ACI 304.1, (2005), "Guide for the use of preplaced aggregate concrete for structural and mass concrete applications," *American Concrete Institute*, Farmington Hills, USA, 19 p.

Akatsuka, Y. and Moriguchi, H., (1967), "Strengths of prepacked concrete and reinforced prepacked concrete beams," *ACI Journal,* Vol. 64, pp. 204-212.

ASTM C260, (2006), "Standard specification for air-entraining admixtures for concrete," *American Society for Testing and Materials*, West Conshohocken, PA, USA, 3 p.

ASTM C937, (2002), "Standard specification for grout fluidifier for preplaced-aggregate concrete," *American Society for Testing and Materials*, West Conshohocken, PA, USA, 3 p.

ASTM C938, (2010), "Standard practice for proportioning grout mixtures for preplaced-aggregate concrete," *American Society for Testing and Materials*, West Conshohocken, PA, USA, 3 p.

ASTM C939, (2010), "Standard test method for flow of grout for preplaced-aggregate concrete (flow cone method)," *American Society for Testing and Materials*, West Conshohocken, PA, USA, 3 p.

Baumann, P., (1948), "Use of prepacked aggregate concrete in major dam construction," *ACI Journal,* Vol. 45, pp. 229-235.

Bayer, R., (2004), "Use of preplaced aggregate concrete for mass concrete applications," *Master Thesis*, Middle East Technical University, Turkey, 160 p.

Berndt, M., (2012), "Long–term durability of preplaced aggregate concrete piles," *Concrete International*, Vol. 34, No. 12, pp. 36-42.

Casson, R. B. J. and Davies, I. L., (1986), "Performance of concrete backfilling materials for shafts and tunnels in rock formations", *Commission of the European Communities. Directorate- General Science*, Vol. 1, No. EUR 10383EN/1, 91 p.

Champion, S. and Davis, L. T., (1958), "Grouted concrete construction," *Reinforcement Concrete Review*, pp. 569-608.

Chefdeville, M. J., (1963), "Prepacked aggreggate concrete and activated mortar," *Building Research Station. Library Communication LC1190*, 19 p.

Christianto, H. A., (2004), "Effect of chemical and mineral admixtures on the fresh properties of self-compacting mortars," *Master Thesis*, Middle East Technical University, Turkey, 60 p.

Davis, R. E. and Haltenhoff, C. E., (1956), "Mackinac bridge pier construction," *ACI Journal*, Vol. 53, No. 12, pp. 581-595.

Davis, R. E., Jansen, E. C. and Neelands, W. T., (1948), "Restoration of Barker dam," *ACI Journal*, Vol. 44, No. 4, pp. 633-668.

Davis, R. E., Johnson, G. D. and Wendell, G. E., (1955), "Kemano penstock tunnel liner backfilled with prepacked concrete," *ACI Journal*, Vol. 52, No. 11, pp. 287-308.

Davis, R. E., (1960), "Prepacked method of concrete repair," *ACI Journal*, Vol. 57, No. 2, pp. 155-172.

Ezgi, Y., (2010), "Optimizing concrete mixtures with minimum cement content for performance and sustainability," *Master Thesis*, Iowa State University, USA, 121 p.

Goual, M. S., Bali, A., de Barquin, F., Dheilly, R. M. and Quéneudec, M., (2006), "Isothermal moisture properties of clayey cellular concretes elaborated from clayey waste, cement and aluminium powder," *Cement and Concrete Research*, Vol. 36, No. 9, pp. 1768-1776.

Huang, M., An, X., Zhou, H. and Jin, F., (2008), "Rock- filled concrete-development, investigation, and applications," *International Water Power and Dam Construction*, Vol. 60, No. 4, pp. 20-24.

King, J. C., (1959), "Concrete by Intrusion Grouting," Handbook of Heavy Construction. *MC Graw- Hill book*, New York, USA, pp. 1-10.

King, J. C., (1967), "Strength evaluation and quality control of prepacked concrete," *American Concrete Institute, ACI Journal Proc*. Vol. 64, pp. 744.

Klein, A. M. and Crockett, J. H. A., (1953), "Design and construction of a fully vibration-controlled forging hammer foundation", *ACI Journal*, Vol. 49, No. 1, pp. 421-444.

Littlejohn, G. S. and Swart, A. H., (2006), "Design of permanent intruded plugs at south deep gold mine," *The Journal of the South African Institute of Mining and Metallurgy*, Vol. 106, pp. 331-342.

Lyse, I., (1959), "The shrinkage and creep of concrete". *Magazine of Concrete Research*, Vol. 11, No. 33, pp. 143-150.

Malhotra, V. M., (1993), "Fly ash, slag, silica fume, and rice- hush ash in concrete: a review," *Concrete International*, Vol. 15, No. 4, pp. 23-28.

Manohar, S. N., (1967), "The production and application of colcrete," *Indian Concrete Journal*, Vol. 41, No. 7, pp. 262-275.

Mehta, K., (1988), "Durability of concrete exposed to marine environment – A fresh look," *Proceedings of 2nd International Conference on Concrete in Marine Environment, ACI, SP-109*, St. Andrews, Canada, pp. 109:1-30.

Mehta, P. K. and Monteiro, J. M., (2006), "Concrete: microstructure, properties, and materials," *3rd Edition, McGraw-Hill*, New York, USA, 96 p.

Menzel, C. A., (1943), "Some factors influencing the strength of concrete containing admixture of powdered aluminium," *ACI Journal*, Vol. 14, pp. 165-184.

Morohashi, N., Meyer, C. and Abdelgader, H. S., (2013), "Concrete with recycled aggregate produced by the two-stage method," *CPI-Concrete Plant International*, Vol. 4, pp. 34-41

Nehdi, M. L. and Soliman, A. M., (2011), "Early-age properties of concrete: Overview of fundamental concepts and state-of-the art research," *Construction Materials, ICE*, Vol. 164 (CM2), pp. 55-77.

Neville, A. M. and Brooks, J. J., (2010), "Concrete Technology," *2nd Edition, Longman Group,* UK, pp.141-142.

O'Malley, J. and Abdelgader, H. S., (2009), "Investigation into the viability of using two stage (pre-placed aggregate) concrete in an Irish setting," *GSBEIDCO -1st*, Vol. 1, pp. 215-222.

Orchard, D. F., (1973), "Concrete Technology," *3rd Edition*, *Applied Science Publishers Ltd*, London, UK, Vol. 2, p. 409-416.

Portland Cement Association, (1997), "Portland cement, concrete, and heat of hydration," *Portland Cement Association*, Skokie, Illinios, USA, Vol. 18, No. 2, pp. 1-8.

Reschke, A. E., (2000), "The development of colloidal mixer based CRF systems," *Minefill. Brisbane*, Australia, 11 p.

Tang, C. K., (1977), "Properties of prepacked concrete," *Master Thesis*, University of Melbourne, Australia, 218 p.

Taylor, W. H., (1965), "Concrete Technology and Practice," *Angus and Robertson*, Sydney, Australia, pp. 357-358.

Tynes, W. O. and McDonald, J. E., (1968), "Investigation of resistance of preplaced-aggregate concrete to freezing and thawing," *Miscellaneous Paper C-68-6, U.S. Army Waterways Experiment Station*, Vicksburg, Miss. USA, 33 p.

US Army Corps of Engineers, (1994), "Standard practice for concrete for civil works structures," EM 1110-2-2000, 3 p.

3. GROUTS INCORPORATING SUPPLEMENTARY CEMENTITIOUS MATERIALS FOR TWO-STAGE CONCRETE[(*)]

3.1. INTRODUCTION

Two-stage concrete (TSC), also known as preplaced aggregate concrete, is produced by first placing the dry coarse aggregate in the formwork and then filling the inter-particle voids with a flowable grout mixture. It has been successfully used in various applications, such as concrete repair, underwater construction and mass concrete (Najjar *et al.*, 2014). The unique placement technique of TSC offers several technological and sustainability advantages. Preplacing the coarse aggregates in the formwork before injecting grout allows using aggregates that constitute challenges in normal concrete production. For example, very heavy aggregates (e.g. magnetite, which is highly desirable in the construction of nuclear power plants) can be used in concrete production without segregation concerns (ACI 304.1, 2005). Moreover, recycled concrete aggregates that normally cause loss of workability and severe pumping problems due to their higher water absorption will not contribute to concrete casting problems in the TSC technology (Morohashi *et al.,* 2013). Likewise, in TSC, the coarse aggregate, which represents the predominant fraction of the concrete volume, is not mixed in concrete mixers. Not only does this accelerate construction by dramatically reducing the volume of the concrete mixture, but also reduces the energy consumed in concrete mixing and pumping (ACI 304.1, 2005).

The key controlling factor of the mechanical strength and durability of TSC is the quality of the grout used in injecting the preplaced coarse aggregate, along with the rheological properties of the grout, which should be conducive to effectively filling the space between preplaced aggregates and reducing the volume of voids to a minimum (Abdul Awal, 1984; ACI 304.1, 2005). Therefore, grouts used for TSC applications have to meet specific criteria

---

for flowability, stability and mechanical strength as recommended by ACI 304.1. The mixture proportions of TSC grouts are generally selected according to ASTM C938-2010, which mainly depends on the grout flowability.

The most important parameter in the TSC production process is the grout flowability, which is an indicator of the ability of the grout penetrate around the aggregate particles and effectively fill the inter-particle space. The Grout flowability depends mainly on the chemical and physical properties of the used mixture ingredients (i.e. sand, cement, SCMs and admixtures) along with their respective proportions (Abdelgader and Elgalhud, 2008; Najjar *et al.*, 2014). Moreover, the optimum water content, defined as the amount of water at the point where the powder material starts to flow freely, is a significant parameter for controlling TSC grout flowability. Furthermore, the mixing water acts as a dispersing phase for the binder and sand in the grout mixture (Hunger and Brouwers, 2009). For cementitious materials, the useful water is that needed for cement hydration reactions. Any water added in excess of that is used to adjust the cementitious material flowability (Hunger and Brouwers, 2009; Kismi *et al.*, 2011). Consequently, the surface texture and particle shape of the powder (i.e. binder) in a grout mixture will affect its flowability (Khayat *et al.*, 2008).

The use of emerging new admixtures and more sustainable and highly durable binder systems have rarely been explored in TSC. Previous research showed that the addition of fly ash (FA) up to 33% as partial replacement for cement improved the flowability, extended the handling time and reduced the water demand of TSC grout mixtures (ACI 304.1, 2005). Moreover, partially substituting cement by 6% silica fume (SF) was found to improve the TSC grout compressive strength, while adversely affecting its flowability (O'Malley and Abdelgader, 2010). Resorting to new generation admixtures can allow producing low *w/b* high-strength grouts with adequate flowability, which should produce higher strength TSC. Moreover, using binary and ternary binders in producing TSC grouts can enhance the interfacial transition zone between the preplaced aggregates and the injected grout matrix. Furthermore, SCMs used in TSC grouts can enhance the durability of TSC in a similar manner to that well documented in normally placed concrete.

Therefore, this research work aims at quantifying the relationship between SCMs and TSC grout properties. Moreover, the changes in water demand for TSC grout mixtures incorporating different types and dosages of SCMs were investigated. The effect of high-

range water-reducing admixture (HRWRA) addition on the flowability of grout mixtures was also monitored. An attempt was made to identify an optimum *w/b* ratio and HRWRA dosages for further testing of the associated TSC grout mixtures to evaluate their properties. The findings of this study should provide practitioners with new guidance to produce more sustainable and more durable high-strength TSC, which can open the door for novel applications of TSC never considered before.

3.2. EXPERIMENTAL PROGRAM

3.2.1. Materials and Grout Mixture Proportions

Ordinary portland cement (OPC) was used as the main binder for all tested grout mixtures. Three types of SCMs including Fly Ash (FA), Silica Fume (SF), and Metakaolin (MK) were used as partial replacement for OPC. **Table 3.1** summarizes physical and chemical properties of the used materials. In TSC, relatively finer sand having a fineness modulus ranging from 1.2 to 2.0 is desirable since it is used in the grout injection between preplaced aggregates. Using coarse sand can reduce the stability of the grout and increase the segregation. Therefore, silica sand with a fineness modulus of 1.47 and a saturated surface dry specific gravity of 2.65 was used as a fine aggregate. Moreover, **Figure 3.1** shows SEM images illustrating the size and shape difference of the used cementitious materials. Three water-to-binder ratios (*w/b*) of 0.35 (Group A), 0.45 (Group B) and 0.55 (Group C) were tested. A poly-carboxylate HRWRA with a specific gravity of 1.064, a solid content of 34% and pH of 5 was added at different dosages in order to control the grout's flowability. Several TSC grout mixtures were prepared using single, binary, and ternary binders. The SCMs substitution rates were selected based on guidance in the open literature (e.g. Kosmatka *et al.*, 2003). The mixtures proportions of the tested grouts are provided in **Table 3.2**.

Table 3.1 – Chemical analysis and physical properties of OPC, FA, SF, and MK

	OPC	FA	SF	MK
SiO_2 (%)	19.60	43.39	95.30	53.50
Al_2O_3 (%)	4.80	22.08	00.17	42.50
CaO (%)	61.50	15.63	00.49	0.20
Fe_2O_3 (%)	3.30	7.74	00.08	1.90
SO_3 (%)	3.50	1.72	00.24	0.05
Na_2O (%)	0.70	1.01	00.19	0.05
Loss on ignition (%)	1.90	1.17	4.7	0.50
Specific gravity	3.15	2.50	2.20	2.60
Surface area $(m^2/kg)^*$	371	280	19500	15000
Particle size $(\mu m)^*$				
D10	2.47	1.98	0.06	2.0
D50	14.97	14.06	0.17	4.5
D90	40.90	81.68	0.29	25

$^*1\ m^2/kg = 4.882\ ft^2/lb$, $1\mu m = 0.000393$ in.
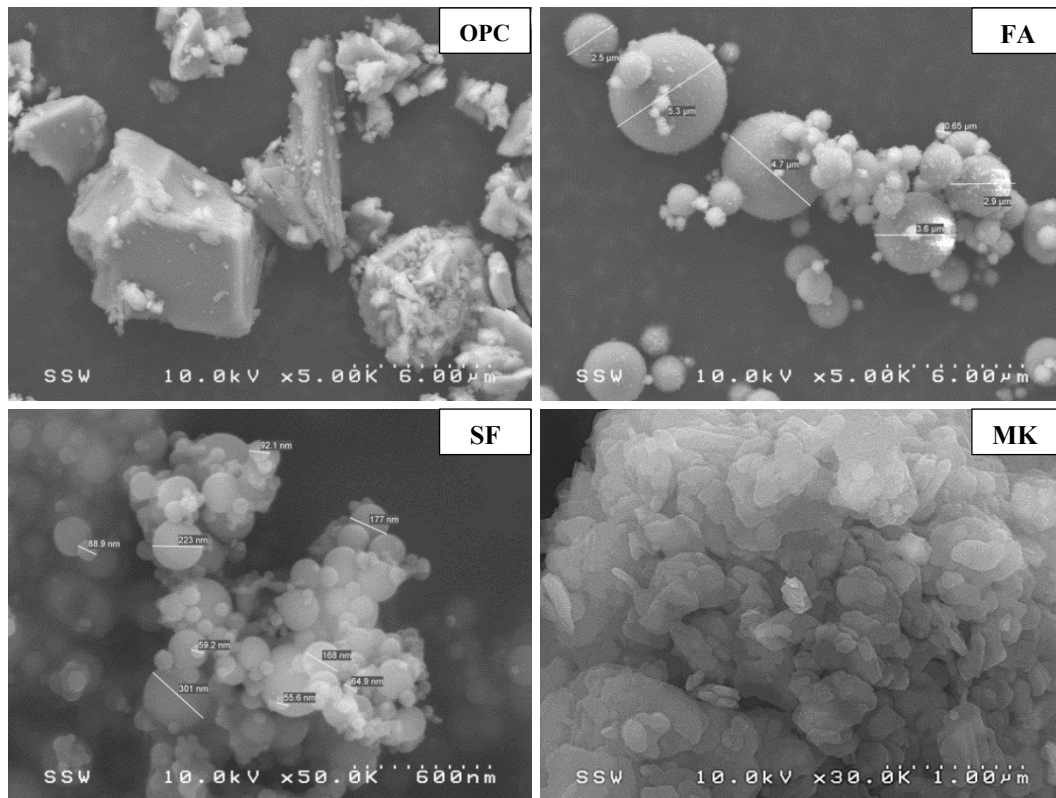
Figure 3.1 – SEM images illustrating the size and shape difference of the used cementitious materials.

Table 3.2 – Grout mixture proportions

Grout Mixture ID	Grout Mixture Notation	Binder (kg/m^3)[*]				Sand (kg/m^3)[*]	Water (kg/m^3)[*]
		OPC	FA	SF	MK		
C-0.35	100OPC	957	--	--	--	957	335
F1-0.35	90OPC-10FA	855	95	--	--	950	332
F3-0.35	70OPC-30FA	654	280	--	--	935	327
F5-0.35	50OPC-50FA	460	460	--	--	921	322
S1-0.35	90OPC-10SF	850	--	94	--	945	331
SF4-0.35	50OPC-10SF-40FA	458	366	92	--	916	321
M1-0.35	90OPC-10MK	856	--	--	95	951	333
MF4-0.35	50OPC-10MK-40FA	461	369	--	92	922	323
C-0.45	100OPC	874	--	--	--	874	393
F1-0.45	90OPC-10FA	781	87	--	--	867	390
F3-0.45	70OPC-30FA	599	257	--	--	855	385
F5-0.45	50OPC-50FA	422	422	--	--	843	379
S1-0.45	90OPC-10SF	777	--	86	--	863	388
SF4-0.45	50OPC-10SF-40FA	420	336	84	--	839	378
M1-0.45	90OPC-10MK	782	--	--	87	868	391
MF4-0.45	50OPC-10MK-40FA	422	338	--	84	844	380
C-0.55	100OPC	803	--	--	--	803	442
F1-0.55	90OPC-10FA	718	80	--	--	798	439
F3-0.55	70OPC-30FA	551	236	--	--	788	433
F5-0.55	50OPC-50FA	389	389	--	--	778	428
S1-0.55	90OPC-10SF	715	--	79	--	795	437
SF4-0.55	50OPC-10SF-40FA	387	310	77	--	774	426
M1-0.55	90OPC-10MK	719	--	--	80	799	439
MF4-0.55	50OPC-10MK-40FA	389	311	--	78	778	428

[*]1 kg/m^3= 0.06247 lb/ft^3

3.2.2. Experimental Procedures

All grout mixtures were prepared as per the guidelines of ASTM C938-2010. Mixing and flowability measurements were conducted at room temperature (T = 23 ± 2°C) [73.4 ± 3.6°F]. Immediately after mixing, the grout flowability was evaluated using a flow cone test according to ASTM C939-2010 (**Figures 3.2**). The flow cone test consists of measuring the time of efflux of 1725 ml [0.06 ft^3] of the grout through a specific cone having a 12.7 mm [0.5 in.] discharge tube.

Figure 3.2 – Flow cone test.

In addition, the spread flow test was conducted to study the effects of SCMs on the point where the grout mixture starts to flow freely, which identifies an optimum water content (Hunger and Brouwers, 2009). The grout is filled in a special conical mould, which is lifted straight upwards in order to allow free flow. From the spread-flow test, two diameters perpendicular to each other (D_1 and D_2) are determined. Then, the relative slump, R_p, which is a measure for the deformability of the mixture, can be calculated using the following equation (**Eq. 3.1**).

$$R_p = \left(\frac{\left(\frac{D_1 + D_2}{2} \right)}{D_o} \right)^2 - 1 \qquad \textbf{Eq. 3.1}$$

Where D_o represents the base diameter of the used cone (i.e. 100 mm [4 in.]). The spread flow test is described in greater detail elsewhere (Hunger and Brouwers, 2009).

Based on the efflux time and the spread flow results of various grout mixtures, an optimum w/b was identified. Thereafter, the optimum HRWRA dosage that meets the required efflux time (i.e. 35-40 ± 2 sec) recommended by ACI 304.1 (2005) was considered for each grout mixture made with the selected w/b. Moreover, the effects of incorporating

various rates and types of SCMs on the properties of selected TSC grouts were investigated based on evaluating the flowability loss, the resistance to bleeding, the setting time and the compressive strength.

In order to monitor the loss in grout flowability, the efflux time for each grout mixture was measured at 0, 30, 60 and 90 minutes from the end of the mixing stage to demonstrate that the grout flowability is suitable for field practical conditions (Nehdi and Martini, 2009a and 2009b). The grouts rested undisturbed between testing at laboratory conditions; i.e. ($T =$ 23 ± 2°C) [73.4 ± 3.6°F] and with a RH of 70%. However, immediately before testing, grouts were stirred in an identical manner before measuring the efflux time. Moreover, the resistance to bleeding of the grout mixtures was also evaluated according to ASTM C940-2010. After 3 h, the grout bleeding is calculated according as per equation (**Eq. 3.2**):

$$\text{Grout bleeding (\%)} = \frac{V_w}{V_1} \times 100 \qquad\qquad \textbf{Eq. 3.2}$$

Where V_1 is the volume of grout at the beginning of test (ml [oz]) and V_w is the volume decanted bleed water (ml [oz]).

The initial and final setting times of the grout mixtures were determined using the Vicat apparatus following the procedure of ASTM C953-2010. The compressive strength development of the TSC grout mixtures was monitored through testing 50 mm [2 in.] cubic specimens at the ages of 7, 28, and 56 days according to ASTM C942-2010. Immediately after demolding, cube test specimens were moved to a moist curing room ($T = 23 \pm 2$°C [73.4 ± 3.6°F] and RH = 98%) until the desired testing ages.

Differential scanning calorimetry (DSC) tests were performed at 7 days on samples taken from selected TSC grout mixtures. Samples were ground to powder with an average particle size of 45 μm. Then, a 30 to 60 mg [0.001 to 0.002 oz.] powder specimen was heated in a helium atmosphere at a constant rate of 10°C [50°F] per minute up to 550°C [1022°F]. The endothermic peak for CH was observed at approximately 440°C [824°F]. The area under the curve was related to the quantity of CH in the sample using a built-in regression equation.

3.3. RESULTS AND DISCUSSION

3.3.1. Effects of SCM Type on Flow Properties of TSC Grouts

Tables 3.3 and **3.4** report the efflux time and spread flow results for all the tested grout mixtures. For mixtures with 0% HRWRA, it can be observed that the efflux time increased as the *w/b* ratio decreased. Moreover, some grout mixtures exhibited very long efflux time (i.e. > 300 sec) or even did not show any measurable flowability. For instance, the grout mixture incorporating 10% SF did not show any flow at a *w/b* = 0.35, while it exhibited a very long efflux time (i.e. > 300 sec) as the *w/b* was increased to 0.45. This is due to the high yield stress and high viscosity of these grouts. However, all the grout mixtures made with *w/b* = 0.55 can flow easily without the need for HRWRA addition. This can be attributed to the lower viscosity of such grouts.

The flowability of the grout mixture is mainly affected by the amount of water used, which depends on the amount of required water to cover binder particles and fill the inter-granular porosity in the mixture. The amount of pore water is influenced by the SCMs type and its replacement rate (Kismi *et al.*, 2011). This can be explained using a graphical analysis of the spread flow results. All measured relative slump, R_p, values are plotted versus the respective *w/b* ratio at 0% HRWRA (**Figures 3.3** and **3.4**). A linear relation can be computed for each mixture via linear regression using the following equation (**Eq. 3.3**):

$$ ^w\!/_b = E_p R_p + B_p $$

<div align="right">**Eq. 3.3**</div>

Where the value B_p is the intersection of this linear function with the ordinates axis at R_p = 0, which depicts the minimum water content needed to initiate flow (Okamura and Ouchi, 2003; Khayat *et al.* 2008); E_p is the deformation coefficient, which indicates the sensitivity to the water needed for a specified flowability.

Table 3.3 – Grout efflux time results

Grout Mixture ID	Grout Efflux Time (sec)				
Group A	HRWRA Dosage (%)				
	0.6	1.0	1.2	1.6	2.0
C-0.35	>300.0	164.0	130.0	115.0	114.0
F1-0.35	299.0	117.0	114.0	110.0	109.0
F3-0.35	153.0	103.0	66.0	59.0	57.0
F5-0.35	80.0	52.0	46.0	44.0	43.0
S1-0.35	>300.0	>300.0	>300.0	215.0	193.0
SF4-0.35	>300.0	>300.0	240.0	170.0	98.0
M1-0.35	>300.0	>300.0	>300.0	247.0	218.0
MF4-0.35	>300.0	>300.0	262.0	186.0	103.0
Group B	HRWRA Dosage (%)				
	0.0	0.2	0.4	0.6	0.8
C-0.45	>300.0	91.0	39.0	38.0	--
F1-0.45	312.0	43.0	35.0	34.0	--
F3-0.45	90.0	34.0	24.0	22.0	--
F5-0.45	39.0	25.0	22.0	19.0	--
S1-0.45	>300.0	95.0	60.5	44.0	41.0
SF4-0.45	60.0	39.0	23.5	23.0	--
M1-0.45	>300.0	>300.0	99.0	64.0	42.0
MF4-0.45	130.0	56.0	38.0	29.0	--
Group C	HRWRA Dosage (%)				
	0.0	0.1	0.2	--	--
C-0.55	35.0	25.0	16.0	--	--
F1-0.55	24.0	21.0	15.0	--	--
F3-0.55	18.0	16.0	14.0	--	--
F5-0.55	15.5	14.0	13.0	--	--
S1-0.55	130.0	62.0	35.0	--	--
SF4-0.55	34.0	22.0	14.0	--	--
M1-0.55	145.0	70.0	39.0	--	--
MF4-0.55	40.0	27.0	17.0	--	--

Table 3.4 – Grout spread flow results

Grout Mixture ID	Grout Spread Flow (cm)[*]				
Group A	HRWRA Dosage %				
	0.6	1.0	1.2	1.6	2.0
C-0.35	13.0	20.5	25.5	28.5	30.0
F1-0.35	17.4	23.0	27.5	29.0	31.0
F3-0.35	27.4	26.5	31.5	31.5	32.0
F5-0.35	28.0	30.5	32.0	34.0	33.0
S1-0.35	12.0	18.0	22.0	27.0	30.0
SF4-0.35	14.0	20.0	24.0	29.0	32.0
M1-0.35	11.0	16.0	21.0	26.0	26.3
MF4-0.35	13.0	19.0	23.0	28.0	31.5
Group B	HRWRA Dosage (%)				
	0.0	0.2	0.4	0.6	0.8
C-0.45	12.0	18.0	24.5	30.0	--
F1-0.45	13.0	23.5	28.5	36.0	--
F3-0.45	16.0	25.0	30.0	37.0	--
F5-0.45	19.0	28.0	35.0	39.0	--
S1-0.45	11.0	17.5	24.0	31.0	33.0
SF4-0.45	17.0	23.0	34.0	37.0	--
M1-0.45	11.0	12.0	19.5	26.0	33.5
MF4-0.45	15.0	17.5	28.0	36.0	--
Group C	HRWRA Dosage (%)				
	0.0	0.1	0.2	--	--
C-0.55	18.0	22.0	24.0	--	--
F1-0.55	19.0	23.0	24.5	--	--
F3-0.55	22.0	28.5	30.0	--	--
F5-0.55	27.0	29.0	31.0	--	--
S1-0.55	13.0	19.0	21.0	--	--
SF4-0.55	16.0	21.0	23.0	--	--
M1-0.55	12.0	18.0	20.0	--	--
MF4-0.55	15.0	20.0	22.0	--	--

[*] 1 cm = 0.3937 in.
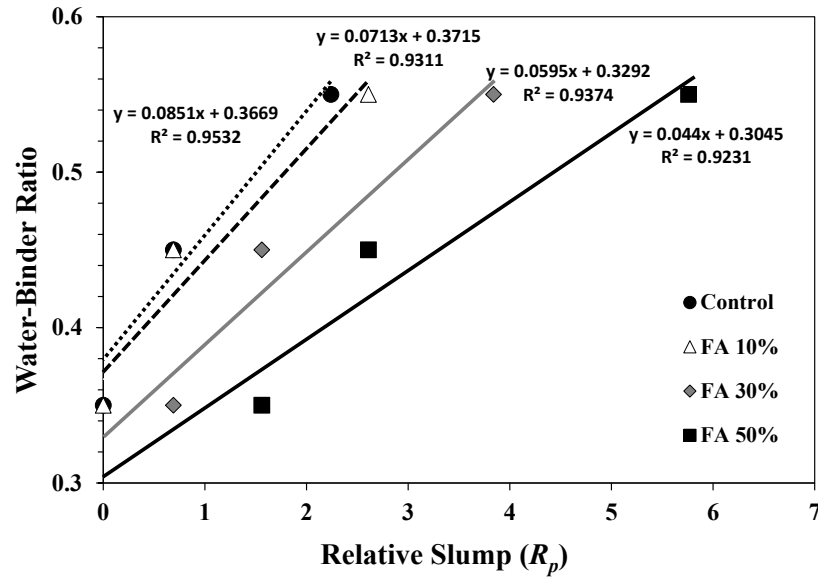
Figure 3.3 – Relative slump flow based on the spread flow test as a function of the water/binder ratio for grout mixtures (C, F1, F3 and F5).
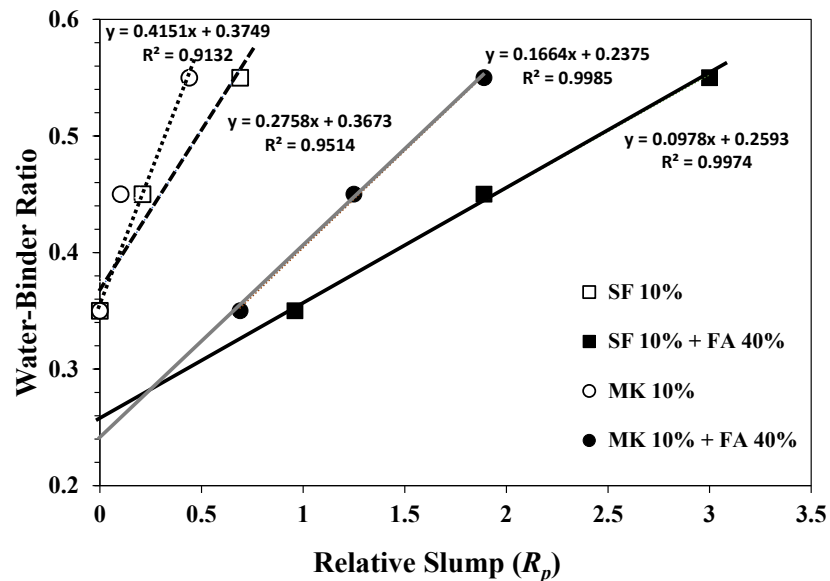
Figure 3.4 – Relative slump flow based on the spread flow test as a function of the water/binder ratio for grout mixtures (S1, SF4, M1 and MF4).

For grout mixtures incorporating 30% FA and 50% FA, the B_p value was about 0.33 and 0.30, respectively, as shown in (**Figure 3.3**). It can be observed that the higher the FA partial replacement level for OPC, the lower was the water content required to initiate flow. This is

attributed to the spherical shape and smooth surface texture of the FA (Khayat *et al.* 2008). However, the B_p value was about 0.37 for both grout mixtures S1 and M1 (**Figure 3.4**), which means that a grout mixed with a *w/b* lower than this value will not cause those mixtures to flow. As the *w/b* exceeded 0.37, the S1 and M1 mixtures started to flow. The high value of B_p for the S1 and M1 grout mixtures is mainly due to the high surface area of SF and MK, leading to increasing water demand in these grouts (e.g. Khayat *et al.* 2008).

Generally, all grout mixtures made with a *w/b* = 0.35 were unlikely to flow at 0% HRWRA. This can be attributed to the high yield stress and high viscosity of these grout mixtures due to their relatively low free water content. Significant water gets adsorbed on the surface of binder particles and trapped between them as they form flocs, and this is more stringent at higher binder content and higher binder surface area (Mehta, 2004). As a result, solid particles become connected by capillary forces since the water content is lower than the required pore water volume (Kismi *et al.*, 2011). Thus, lubrication between particles gets diminished and grouts will not flow under their own weight (Wong and Kwan, 2008). This was true for mixtures incorporating different dosages of FA despite that FA is generally perceived as conducive to better workability. At low *w/b* and due to the low density of FA, increasing the mass replacement of cement by FA increased the water requirement due to higher surface area of particles, thus compromising flowability (Sahmaran *et al.*, 2006).

Conversely, all the grout mixtures made with *w/b* = 0.55 had sufficient flow (i.e. grouts can flow easily under their own weight) without the need for HRWRA addition. This can be attributed to the fact that increasing the *w/b* ratio results in an increase of the free water volume in the grout mixture (i.e. excess water), which acts as a lubricating agent between the solid particles, hence leading to higher grout flowability (Kismi *et al.*, 2011). Therefore, the grout efflux time decreased as the free water volume increased. However, the binder type and its dosage had a significant effect on the water demand, and thus on the flowability of the grout mixtures, even at high *w/b* (Khayat *et al.*, 2008). For example, the grout mixtures F1-0.55, F3-0.55 and F5-0.55 exhibited 31.4%, 48.6% and 55.7% shorter efflux time compared to that of the control grout mixture (C-0.55), respectively. Moreover, the spread flow for these mixtures was higher than that of the control grout mixture (C-0.55) by 5.6%, 22% and 50%, respectively. This in agreement with the spread flow results since the value of B_p decreased as the percentage of FA increased (**Figure 3.3**). This can be attributed to the fact

that FA can reduce frictional forces among particles due to its spherical particles (so called ball bearing effect) as illustrated in **Figure 3.1**, leading to lubricating effect, thus facilitating mobility (Yung *et al*., 2013). Moreover, FA can be adsorbed on the surface of oppositely charged cement particles, preventing flocculation and enhancing particle dispersion, which consequently enhances flowability through freeing additional water (Kismi *et al.*, 2011).

On the other hand, partially replacing OPC using SF or MK significantly increased the grout efflux time. For instance, at *w/b* = 0.55, grout mixtures incorporating 10% MK as partial replacement for OPC exhibited an efflux time around 4 times that of the control grout mixture (100% OPC). Moreover, the 10% MK grout mixture exhibited about 33.3% lower spread flow and consequently higher B_p compared to that of the control grout mixture (**Figure 3.4**). This can be attributed to the high water demand of the high surface area MK (Razak and Wong, 2001). Similar trend was exhibited by grout mixtures incorporating SF.

However, ternary grout mixtures involving a combination of OPC+FA+SF or OPC+FA+MK exhibited shorter grout efflux time and higher spread flow compared to that of binary grout mixtures made with OPC+SF or OPC+MK. For instance, the grout mixture MF4-0.55 achieved a 72.4% shorter efflux time than that of the M1-0.55 mixture. This is confirmed through the analysis of spread flow results (i.e. minimum water demand (B_p)) for mixtures incorporating 10% MK or 10% MK+40% FA. The addition of 40% FA to the mixture incorporating 10% MK decreased the water demand from 0.375 to 0.237 (**Figure 3.4**) (i.e. about 37% reduction). This can be ascribed to the lubricant effect induced by the addition of 40% FA as discussed earlier and the enhanced particle packing density of the ternary binder blend whereby smaller particles fit in between coarser particles, leading to a lower inter-particle space and lower water demand.

3.3.2. Effect of HRWRA Dosage on Flow Properties of TSC Grout

Adding adequate dosages of HRWRA into cementitious grouts has a great effect on the grout's flowability as illustrated in **Table 3.3**. The higher the HRWRA dosage, the shorter the efflux time of the grout mixture. For instance, increasing the HRWRA dosage from 0% to 0.4% shortened the efflux time of the grout mixture SF4-0.45 by about 61%. The poly-carboxylate admixture prevents the binder-water agglomeration and the formation of flocs through the steric repulsion mechanism. Moreover, it has unique poly-ethylene oxide side

chains, which move in water and steer the binder grains to disperse evenly into the grout mixture (Safiuddin, 2008). Hence, the addition of the HRWRA reduced the inter-particle friction (i.e. flow resistance) between solid particles, and hence improved the grout's efflux time. Moreover, the HRWRA dosage required for the grout mixture to flow under its self-weight will depend on the type and dosage of SCM. For example, at similar SCM content, the grout mixtures F1-0.45 (made with FA) and M1-0.45 (made with MK) needed about 0.4% and 0.8% HRWRA dosage to meet the targeted efflux time (i.e. 35-40±2 sec), respectively. This is expected since FA has a spherical particular size conducive to lowering friction and smaller surface area per unit weight than that of MK. In contrast, for the same SCM type, mixtures F1-0.45 and F5-0.45 (both made with FA) needed about 0.2% and 0.0% to achieve the recommended efflux time for high strength TSC, respectively. At the same *w/b* of 0.45, mixture F5-0.45 achieved better flow since it has 50% FA particle replacement for OPC, while mixture F1-0.45 only has 10% FA replacement for OPC.

The spread flow of the grouts depends primarily on the degree of dispersion of the binder particles, which largely depends on the HRWRA dosage (e.g. Khayat *et al.*, 2008). The higher the HRWRA dosage, the greater the spread flow diameter. Therefore, the effect of the HRWRA on the spread flow was analyzed graphically, similar to the effect of the *w/b*. All measured R_p values were plotted versus the respective HRWRA dosage and a linear relation were computed for each mixture through linear regression as per the following equation (**Eq. 3.4**):

$$HRWRA\ (\%) = SH_p\,R_p + H_p \qquad\qquad \textbf{Eq. 3.4}$$

Where H_p is the intersection of this linear function with the ordinates axis at $R_p = 0$, which is considered as the minimum HRWRA dosage to disperse the powder particles (Okamura and Ouchi, 2003), SH_p is the deformation coefficient, which indicates the required HRWRA dosage to increase the unit dispersing effect. An example of an analyzed spread-flow test for mixtures with *w/b* = 0.45 is illustrated in **Figures 3.5** and **3.6**.
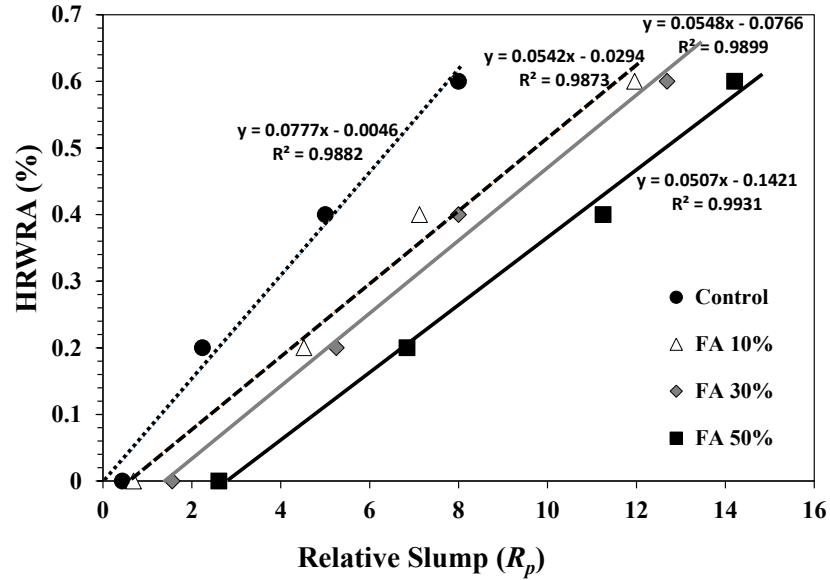
Figure 3.5 – Relative slump flow based on the spread flow test as a function of the HRWRA dosage for grout mixtures (C, F1, F3 and F5).
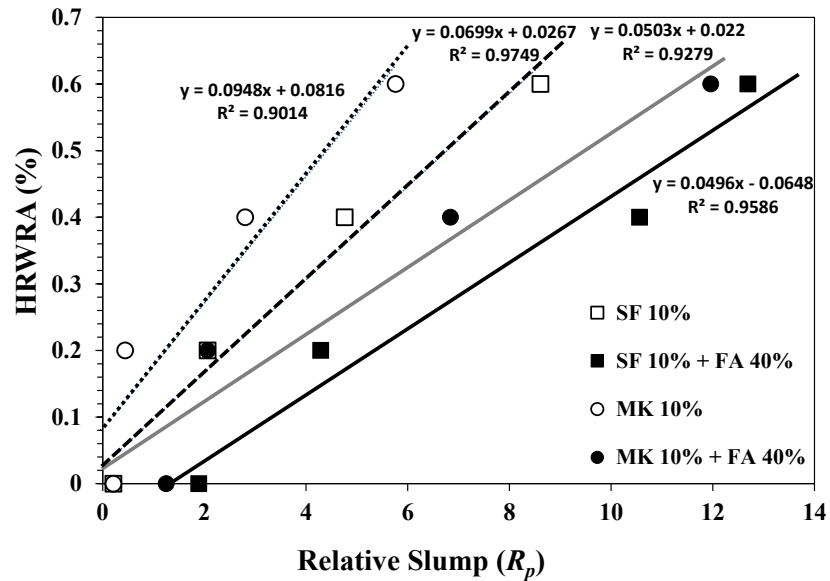
Figure 3.6 – Relative slump flow based on the spread flow test as a function of the HRWRA dosage for grout mixtures (S1, SF4, M1 and MF4).

As shown in **Figure 3.5**, the H_p values for mixtures C-0.45, F1-0.45, F3-0.45 and F5-0.45 were less than zero. This implies that all tested grout mixtures with a $w/b = 0.45$ can initiate flow behavior without the need for HRWRA addition. This is due to the fact that such

mixtures have excess water, which acts as a dispersing phase for the binder, leading to initiating the flow without the need for HRWRA. However, using HRWRA is still needed to achieve the targeted flowability for effective TSC production. Moreover, the binder type has a significant effect on the grout spread flow. A shown in **Figure 3.6**, mixtures S1-0.45 and M1-0.45 required a higher HRWRA dosage than that of the mixtures SF4-0.45 and MF4-0.45. For instance, the H_p value for mixture M1-0.45 decreased from 0.081% to 0.022% as 40% FA was added to the mixture, owing to the lubricating effect induced by FA discussed earlier.

Based on the experimental results discussed above and outlined in **Tables 3.3** and **3.4**, it can be argued that all grout mixtures made with a *w/b* ratio = 0.45 could achieve the efflux time of 35-40 ± 2 sec recommended for successful TSC production. Mixtures having a *w/b* = 0.35 need difficult efflux time tailoring and even at 2.0% HRWRA dosage, their efflux time remained too high. Conversely, those made with a *w/b* = 0.55 can face stability problems via bleeding and separation of the solid-liquid phases. Therefore, in the remainder of this study, grout mixtures with *w/b* = 0.45 with an optimum HRWRA dosage were selected for further investigation as shown in **Table 3.5**.

Table 3.5 – Optimum *w/b* and HRWRA dosage for TSC grout mixtures

Grout Mixture ID	Optimum *w/b* Ratio	Optimum HRWRA Dosage (%)
C	0.45	0.40
F1	0.45	0.40
F3	0.45	0.20
F5	0.45	0.00
S1	0.45	0.80
SF4	0.45	0.20
M1	0.45	0.80
MF4	0.45	0.40

3.3.3. Properties of TSC Grouts

3.3.3.1. Loss of Grout Flowability

Table 3.6 reports the efflux time results for the selected grout mixture, which was measured at 0, 30, 60 and 90 minutes from the end of the mixing stage. It was found that the binder type and HRWRA dosage had a significant influence on the grout's flowability loss. For example, after 90 minutes and with a 0.4% HRWRA dosage, flowability loss for grout mixtures F1 and MF4 were 22% and 38% lower than that of the control mixture C, respectively. It can be observed that the addition of FA decreased the flowability loss. This can partly be attributed to the lubricant effect induced by FA, as discussed earlier. Moreover, FA addition prolonged the grout setting time and consequently led to lower flowability loss with time (Li *et al*., 2004).

Conversely, similar rate of flowability loss was observed for grout mixtures S1 and M1 with incorporating similar HRWRA dosage (i.e. 0.8%). The addition of SF or MK, which are both characterized by a high specific area as reported in **Table 3.1**, increased the water demand and consequently reduced the flowability as observed elsewhere for instance by (Khatib and Clay, 2004; Sakir *et al.*, 2011). However, partially replacing cement with FA into these mixtures to get ternary binders, which also allowed to decrease the HRWRA for the same flow behavior, resulted in mixed results in terms of flowability loss. This can be ascribed to two compensating effects: the lubricant effect induced by fly ash through its spherical shape and reduction of cement hydration through cement dilution (Yung *et al*., 2013), and the increase in water demand due to the higher surface area of fly ash combined with the use of lower HRWRA dosage, which tends to decrease the effectiveness of the admixtures in inhibiting binder agglomeration/fluctuation, thus leading to a higher flowability loss (Safiuddin, 2008).

3.3.3.2. Bleeding (stability)

Bleeding occurs due to the settlement of heavier solid particles suspended in water under their own weight (Tan *et al.*, 2004). As shown in **Table 3.6**, the binder type and HRWRA dosage have significantly affected the resistance to bleeding of the tested grout mixtures. Increasing the FA cement replacement rate was found to increase the mixture bleeding. For

example, increasing the FA content from 10% to 50% increased the bleeding from 0.40% to 1.26%. Generally, fly ash will reduce the amount of bleeding due to the reduction in water demand (Gebler, 1986). However, an exception to this condition is when the fly ash, especially class F, is added without reducing the water content (Thomas, 2007). Therefore, the high bleeding of FA mixtures in this study can be attributed to the increase in the free water content since a constant water content was used in the mixture design. However, the grout mixtures incorporating 10% SF and 10% MK exhibited very low bleeding. This can be ascribed to their very fine particles and high surface area, leading to a reduction in the amount of free water in the grout mixture. Also, the physical filler effect of these very fine materials (i.e. SF and MK) will reduce bleeding due to blocking up pores between cement particles (Khayat *et al.*, 1997, Hsing, 1997, Khatib and Clay, 2004). For ternary binder grout mixtures, FA addition offset the reduction in bleeding induced by SF and MK. For example, the bleeding of mixtures SF4 and MF4 were 8.5 and 3.3 times that of the grout mixtures S1 and M1, respectively.

Table 3.6 – Fresh Properties of TSC grouts

Grout Mixture ID	Bleeding %	Initial Setting Time (h)	Final Setting Time (h)	Grout Efflux Time (sec)[*]			
				0 (min)	30 (min)	60 (min)	90 (min)
C	0.25	5.5	10.0	39	47	51	59
F1	0.40	6.0	10.5	35	43	46	49
F3	1.13	6.0	11.0	34	44	50	61
F5	1.20	7.5	12.5	39	42	46	50
S1	0.13	5.5	10.5	41	46	48	51
SF4	1.10	5.5	10.0	39	46	49	54
M1	0.15	5.0	10.0	42	47	50	52
MF4	1.12	6.0	11.0	38	42	47	50

[*]Grout efflux time results were measured at 0, 30, 60, and 90 minutes from the end of the mixing stage.

3.3.3.3. Setting Time

The initial and final setting times of TSC grouts provide an idea about the window of time for injecting the grout through the preplaced aggregate particles before its hardening (Tan *et*

al., 2004). As shown in **Table 3.6**, the setting time was influenced by the binder type and HRWRA dosage. The initial setting time for mixture F3 was extended by about 10% compared to that of the control mixture C. Conversely, the grout mixture F5 showed a longer initial setting time. This can be attributed to the high percentage of FA (i.e. high cement dilution effect), leading to slower hydration reactions (Chabil *et al.*, 2014). The grout mixtures incorporating 10 % SF and 10% MK as partial replacement for OPC exhibited similar or slightly shorter initial setting time than that of the control grout mixture C, respectively. This can be ascribed to the very high surface area of SF and MK, which provide locations for nucleation and growth of cement hydration reactions, which can shorten the setting time, in addition to more rapid development of pozzolanic reactions compared to the coarser fly ash (Tan *et al.*, 2004). On the other hand, there was no discernable change in the setting time of grout mixtures made with a ternary OPC+FA+SF binder compared with that of the control mixture C due to the conflicting effects of 10% SF and 40% FA.

3.3.3.4. *Compressive Strength*

The compressive strength results for TSC grout mixtures at different ages (7, 28, and 56 days) are presented in **Table 3.7**. Results indicate that increasing the replacement rate of OPC by FA reduced the compressive strength measured at those dates. For example, at the age of 7 days, the grout mixtures incorporating 30% and 50% FA as partial replacement for OPC achieved 79% and 62 % of the compressive strength of the control grout mixture without FA. This can be attributed to the fact that calcium ions (Ca^{++}) adsorb on the surface of FA particles at early ages, causing a depression of the calcium concentration in the pore solution, thus delaying the calcium hydroxide (CH) and calcium silicate hydrate (CSH) nucleation and crystallization. Consequently, such grouts gain mechanical strength much slower at early ages (Bouzoubaâ *et al.*, 2004). This was confirmed by DSC results as shown in **Figure 3.7**. For example, the CH content at 7 days of specimens containing 30% and 50% fly ash was 48% and 56% lower than that of the control specimen without fly ash, respectively. Conversely, the partial substitution of OPC by 10% SF or 10% MK resulted in an increase in compressive strength by about 30 % and 54 % at 7 days, respectively, compared to that of the control C mixture. This is can be ascribed to the high pozzolanic activity induced by SF and MK (Razak and Wong, 2001; O'Malley and Abdelgader, 2009). The combination of fly ash with either 10% SF or 10% MK caused an increase in

compressive strength compared with grouts incorporating FA alone. Increasing the FA replacement rate led to more rapid compressive strength gain compared to that of the control mixture. For example, at 56 days, the rate of strength development of the F5 mixture was about 1.35 times that of the control mixture. However, 10% replacement of cement by SF or MK demonstrated lower strength gaining rate at later ages. For example, the gaining strength rate of mixtures S1 and M1 at 56 days was 0.5 and 0.38 times that of the control grout mixture.

Table 3.7 – Compressive strength of TSC grouts

Grout Mixture ID	Compressive strength of grout at days					
	7		28		56	
	(MPa)*	COV (%)	(MPa)*	COV (%)	(MPa)*	COV (%)
C	33.8	1.3	50.4	1.0	54.3	0.6
F1	31.5	1.2	48.0	1.0	53.8	1.1
F3	27.1	2.0	38.5	1.1	46.2	0.8
F5	21.0	1.7	28.0	1.3	38.2	1.2
S1	43.8	1.2	52.2	1.0	57.0	0.6
SF4	27.0	1.7	38.0	0.8	46.2	0.8
M1	52.1	0.9	61.9	0.7	64.1	0.5
MF4	29.0	1.0	41.0	1.1	49.0	1.5

* 1 MPa = 145.038 psi
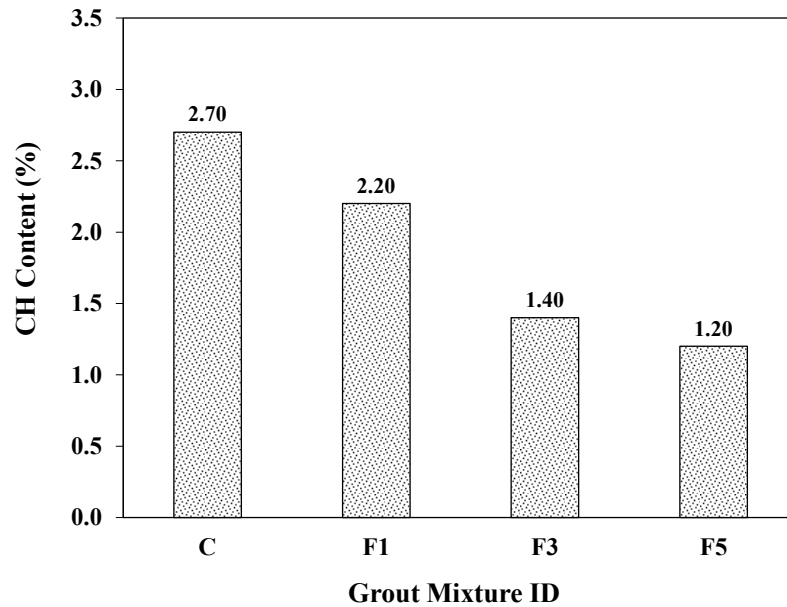
Figure 3.7 – CH content at 7 days of specimens from various TSC grout mixtures (C, F1, F3 and F5).

3.4. CONCLUSIONS

In this study, the flowability of grouts made with single, binary and ternary binders incorporating various supplementary cementitious materials and having different *w/b* ratios was investigated using the flow cone method and the spread flow test. The following concluding remarks can be drawn from this experimental work:

- Grouts made with *w/b* = 0.45 and 0.55 can achieve the target flowability for TSC grouts specified in pertinent standards, while those made with *w/b* =0.35 were too thick to use in TSC production despite the use of poly-carboxylate admixtures.

- The *w/b* ratio = 0.45 was perceived as optimum to produce grouts having an efflux time of 35-40 $\pm$ 2 sec. The optimum dosage of HRWRA varies depending on the type of SCM used for partial replacement of OPC and its dosage.

- The partial replacement of OPC with FA improved the TSC grout's flowability, increased its bleeding and reduced its compressive strength up to 56 days.

- Partial substitution of OPC by 10% SF or 10% MK achieved a reduction in flowability, while enhancing the resistance to bleeding and the compressive strength of the TSC grout.

- Ternary binders incorporating OPC, FA and SF or MK produced grouts that exhibited acceptable flowability, adequate bleeding resistance and compressive strength.

- Research is needed to produce TSC with superior mechanical properties, durability, and enhanced sustainability performance. The TSC technology is expected to shift from basic concrete technology to novel techniques that involve new generation admixtures, SCMs and to incorporate innovations that already made their way to normal concrete technology.

3.5. REFERENCES

Abdelgader, H.S., (1996), "Effect of quantity of sand on the compressive strength of two-stage concrete," *Magazine of Concrete Research*, Vol. 48, No. 177, pp. 353-360.

Abdelgader, H. S. and Elgalhud, A. A., (2008), "Effect of grout proportions on strength of two-stage concrete," *Structural Concrete*, Vol. 9, No. 3, pp. 163-170.

Abdul Awal, A. S., (1984), "Manufacture and properties of pre-packed aggregate concrete," *Master Thesis*, University of Melbourne, Australia, 121 p.

ACI 304.1, (2005), "Guide for the use of preplaced aggregate concrete for structural and mass concrete applications," *American Concrete Institute*, Farmington Hills, USA, 19 p.

Al-Martini, S. and Nehdi, M., (2009), "Coupled effects of time and high temperature on rheological properties of cement pastes incorporating various chemical admixtures," *ASCE Journal of Materials in Civil Engineering*, Vol. 21, No. 8 pp. 392-401.

ASTM C938, (2010), "Standard practice for proportioning grout mixtures for preplaced-aggregate concrete," *American Society for Testing and Materials*, West Conshohocken, PA, USA, 3 p.

ASTM C939, (2010), "Standard test method for flow of grout for preplaced-aggregate concrete (flow cone method)," *American Society for Testing and Materials*, West Conshohocken, PA, USA, 3 p.

ASTM C940, (2010), "Standard test method for expansion and bleeding of freshly mixed grouts for preplaced- aggregate concrete in the Laboratory)," *American Society for Testing and Materials*, West Conshohocken, PA, USA, Vol. 4.02.

ASTM C942, (2010), "Standard test method for flow of grout for compressive strength of grouts for preplaced-aggregate concrete in the laboratory)," *American Society for Testing and Materials*, West Conshohocken, PA, USA, Vol. 4.02.

ASTM C953, (2010), "Standard test method for time of setting of grouts for preplaced-aggregate concrete in the laboratory," *American Society for Testing and Materials, ASTM International*, 2 p.

Bouzoubaâ, N., Bilodeau, A., Sivasundaram, V., Fournier, B. and Golden, D. (2004) "Development of Ternary Blends for High-Performance Concrete," *ACI Materials Journal*, Vol. 101, pp. 19-29

Chabil, F., Brunetaud, X. and Al-Mukhtar, M., (2014), "Optimization of HRWRA content using flow time measurements," *Journal of Zhejiang University- Science A*, 10 p.

Erdoğdu, Şakir, Caner Arslantürk, and Şirin Kurbetci. (2011). "Influence of fly ash and silica fume on the consistency retention and compressive strength of concrete subjected to prolonged agitating," *Construction and Building Materials*, Vol. 25, No. 3, pp. 1277-1281.

Hsing Huang, W., (1997), "Properties of cement-fly ash grout admixed with bentonite, silica fume, or organic fiber," *Cement and Concrete Research*, Vol. 27, No. 3, pp. 395-406.

Hunger, M. and Brouwers, H. J. H., (2009), "Flow analysis of water–powder mixtures: application to specific surface area and shape factor," *Cement and Concrete Composites*, Vol. 31, No. 1, pp. 39-59.

Khatib, J. and Caly, R., (2004), "Absorption characteristics of metakaolin concrete," *Cement and Concrete Research*, Vol. 34, No. 1, pp. 19-29.

Khayat, K., Vachon, M. and Lanctôt, M., (1997), "Use of blended silica fume cement in commercial concrete mixtures," *ACI Materials Journal*, Vol. 94, No. 3, pp. 183-192.

Khayat, K., Yahia, A. and Sayed, M., (2008) "Effect of supplementary cementitious materials on rheological properties, bleeding, and strength of structural grout," *ACI Materials Journal*, Vol. 105, No. 6, pp. 585-593.

Kismi, M., Claude Saint, J. and Mounanga, P., (2011), "Minimizing water dosage of superplasticized mortars and concretes for a given consistency," *Construction and Building Materials*, Vol. 28, No. 1, pp. 747-758.

Li, Y., Zhou, S., Yin, J. and Gao, Y., (2004), "The effect of fly ash on the fluidity of cement paste, mortar, and concrete," *Proc., Int. Workshop on Sustainable Development and Concrete Technology, Beijing, China*, Center for Transportation Research and Education, Iowa State University, Ames, Iowa, USA, pp. 339-345.

Mehta, P. K., (2004), "High-performance, high-volume fly ash concrete for sustainable development," *Proc., Int. Workshop on Sustainable Development and Concrete Technology, Beijing, China*, Center for Transportation Research and Education, Iowa State University, Ames, Iowa, USA, pp. 3-14.

Molhotra, V. M., (1993), "Fly ash, slag, silica fume, and rice- hush ash in concrete: a review," *Concrete International*, Vol. 15, No. 4, pp. 23-28.

Morohashi, N., Meyer, C. and Abdelgader, H. S., (2013), "Concrete with recycled aggregate produced by the two-stage method," *CPI-Concrete Plant International*, Vol. 4, pp. 34-41.

Najjar, M., Soliman, A. and Nehdi, M., (2014), "Critical overview of two stage concrete: properties and applications," *Construction and Building Materials*, Vol. 62, pp. 47-58.

Nehdi, M. and Al-Martini, S., (2009), "Coupled effects of high temperature, prolonged mixing time and chemical admixtures on rheology of fresh concrete," *ACI Materials Journal*, Vol. 106, No. 3, pp. 231-240.

O'Malley, J. and Abdelgader, H., (2010), "Investigation into viability of using two stage (pre-placed aggregate) concrete in an Irish setting," *Frontiers of Architecture and Civil Engineering in China*, Vol. 4, No. 1, pp. 127-132.

Okamura, H. and Ouchi, M. (2003). "Self-compacting concrete." *Journal of Advanced Concrete Technology*, Vol. 1, No. 1, pp. 5-15.

Razak, H. and Wong, H., (2001), "Effect of incorporating metakaolin on fresh and hardened properties of concrete," *Special Publication*, Vol. 200, pp.309-324.

Safiuddin, M., (2008), "Development of self-consolidating high performance concrete incorporating rice husk ash," *Master Thesis*, University of Waterloo, Canada, 326 p.

Sahmaran, M., Christianto, H.A. and Yaman, Ö., (2006), "The effect of chemical admixtures and mineral additives on the properties of self-consolidating mortars," *Cement and Concrete Composites*, Vol. 28, No. 5, pp. 432-440.

Tan, O., Zaimoglu, A., Hinislioglu, S. and Altun, S., (2005), "Taguchi approach for optimization of the bleeding on cement-based grouts," *Tunneling and Underground Space Technology*, Vol. 20, pp. 167-173.

Wong, H. H. C. and Kwan, A. K. H. (2008), "Rheology of cement paste: role of excess water to solid surface area ratio," *Journal of Materials in Civil Engineering*, Vol. 20, No. 2, pp. 189–197.

Yung, H., Ten, W., Chung, C. and Yo, C., (2013), "Study of the material properties of fly ash added to oyster cement mortar," *Construction and Building Materials*, Vol. 41, No. 1, pp. 532-537.

4. TWO-STAGE CONCRETE MADE WITH SINGLE, BINARY AND TERNARY BINDERS[(*)]

4.1. INTRODUCTION

Two-stage concrete (TSC) is a special type of concrete produced using a unique procedure which differs from that of conventional concrete. In TSC, coarse aggregate particles are first placed in the formwork. Subsequently, voids between the aggregate particles are injected with a highly flowable grout mixture. TSC is considered as a skeleton of coarse aggregate, which represents about 60% of its total volume (Abdelgader, 1996). Therefore, TSC has a specific stress distribution mechanism whereby stresses are transferred through contact areas between aggregate particles (O'Malley and Abdelgader, 2009). Such stresses can be responsible for the fracture and/or tearing of aggregate particles from the grout (Abdelgader and Górski, 2003).

The grout used in TSC normally consists of ordinary portland cement (OPC), well graded sand, water and chemical admixtures. With the advent of supplementary cementitious materials (SCMs), blended binders have been used in some TSC mixtures. Partially replacing OPC with about 33% class F fly ash was recommended in order to improve the grout flowability, decrease its water demand and achieve lower heat of hydration (ACI 304.1, 2005; Bayer, 2004).

Moreover, using silica fume (SF) as partial replacement for OPC was found to induce two conflicting effects on TSC properties: reducing the grout's workability and increasing the TSC strength (O'Malley and Abdelgader, 2009). Silica fume acts as a microfiller for voids between cement and sand grains and increases the water demand due to its very high surface area, thus leading to lower workability of TSC grouts (O'Malley and Abdelgader, 2009). Simultaneously, SF is highly reactive with calcium hydroxide (CH), forming

---

additional calcium silicate hydrate (CSH), which is the primary mechanical strength producing hydration product (Molhotra, 1993). Likewise, metakaolin (MK) has comparable effects to that of the SF. Yet, no information is available in the open literature regarding its behavior in TSC.

The mechanical properties of TSC have been investigated (Abdelgader, 1996; O'Malley and Abdelgader, 2009; Bayer, 2004; Abdul Awal, 1984). TSC's mechanical properties are mainly affected by its water-to-cement ratio (w/b), sand-to-cement ratio (s/b), and properties of the coarse aggregate. It was argued that using SCMs could enhance the mechanical properties and durability of TSC (Molhotra, 1993). However, the effects of the binder type on the mechanical properties of TSC have not yet been duly explored in the open literature. For instance, no relationship between the SCM addition rate and the TSC mechanical properties has yet been established. Therefore, the present study investigates the effects of various SCMs at different addition rates on the development of TSC mechanical properties over time and explores possible correlations between the grout properties and the corresponding TSC mechanical properties.

4.2. RESEARCH SIGNIFICANCE

SCMs typically enhance the hardened properties of concrete through improved particle packing density and pozzolanic activity. Moreover, partial replacement of OPC with SCM often has economic and environmental benefits, including saving energy, reducing concrete's carbon footprint, and beneficiation of industrial waste. Substantial research has investigated the mechanical properties of conventional concrete incorporating SCMs. However, only scarce research has explored the mechanical properties of TSC made with SCMs. The present chapter attempts to fill this knowledge gap. In addition, empirical correlations between the properties of grouts and the mechanical properties of the corresponding TSC have been proposed, offering a simple tool for designing TSC mixtures incorporating SCMs.

4.3. EXPERIMENTAL PROGRAM

4.3.1. Materials and Grout Mixture Proportions

CSA A3001-08 GU cement (noted herein OPC) was used in all the grouts. Three types of SCMs including class F fly ash (FA), silica fume (SF), and metakaolin (MK) were used as

partial replacement for OPC. Physical and chemical properties of the used materials are listed in **Table 4.1**. Crushed limestone coarse aggregate with a maximum nominal size of 40 mm, a saturated surface dry specific gravity of 2.65 and water absorption of 1.63 % was used. Silica sand with a fineness modulus of 1.47 and a saturated surface dry specific gravity of 2.65 was used as a fine aggregate. To control the flowability of the grout mixtures, a poly-carboxylate high-range water-reducing admixture (HRWRA) was employed.

Table 4.1 – Chemical analysis and physical properties of OPC, FA, SF, and MK

	OPC	FA	SF	MK
SiO_2 (%)	19.60	43.39	95.30	53.50
Al_2O_3 (%)	4.80	22.08	00.17	42.50
CaO (%)	61.50	15.63	00.49	0.20
Fe_2O_3 (%)	3.30	7.74	00.08	1.90
SO_3 (%)	3.50	1.72	00.24	0.05
Na_2O (%)	0.70	1.01	00.19	0.05
Loss on ignition (%)	1.90	1.17	4.7	0.50
Specific gravity	3.15	2.50	2.20	2.60
Surface area (m^2/kg)	371	280	19500	15000

Several grout mixtures were prepared using single, binary, and ternary binders. The proportions of SCMs in the tested grout mixtures are shown in **Table 4.2**. All grout mixtures had the same sand-to-binder ratio (s/b = 1.0) and water-to-binder ratio (w/b = 0.45). Several trial grout mixtures for each type of binder were conducted in order to identify the optimum HRWRA dosage that meets the recommended efflux time of grout (i.e. 35-40 ± 2 sec) for high strength TSC according to ACI 304.1 (ACI 304.1, 2005). **Table 4.3** illustrates the optimum HRWRA dosage for the tested grout mixtures.

Table 4.2 – TSC grout mixture proportions

Grout Mixture No.	Grout Mixture Notation	Binder (kg/m^3)				Sand (kg/m^3)	Water (kg/m^3)
		OPC	FA	SF	MK		
C	100OPC	874	--	--	--	874	393
F1	90OPC-10FA	781	87	--	--	867	390
F2	80OPC-20FA	689	172	--	--	861	387
F3	70OPC-30FA	599	257	--	--	855	385
F4	60OPC-40FA	509	340	--	--	849	382
F5	50OPC-50FA	422	422	--	--	843	379
S1	90OPC-10SF	777	--	86	--	863	388
SF3	60OPC-10SF-30FA	507	254	85	--	845	380
SF4	50OPC-10SF-40FA	420	336	84	--	839	378
M1	90OPC-10MK	782	--	--	87	868	391
MF3	60OPC-10MK-30FA	510	255	--	85	850	383
MF4	50OPC-10MK-40FA	422	338	--	84	844	380

Table 4.3 – Adjustment of grout flowability (Flow Cone Method)

Grout Mixture Number	Grout Efflux Time (sec)					Optimum HRWRA dosage (%)
	HRWRA dosage					
	0.0%	0.2%	0.4%	0.6%	0.8%	
C	>300.0	91.0	39.0	38.0	--	0.40
F1	>300.0	43.0	35.0	34.0	--	0.40
F2	180.0	38.0	29.0	25.0	--	0.20
F3	90.0	34.0	24.0	22.0	--	0.20
F4	53.0	29.5	23.0	20.0	--	0.15
F5	39.0	25.0	22.0	19.0	--	0.00
S1	>300.0	95.0	60.5	44.0	41.0	0.80
SF3	100.0	42.5	27.0	26.0	--	0.25
SF4	60.0	39.0	23.5	23.0	--	0.20
M1	>300.0	>300.0	99.0	64.0	42.0	0.80
MF3	260.0	180.0	39.0	37.5	--	0.40
MF4	130.0	56.0	38.0	29.0	--	0.40

4.3.2. Experimental Procedures

The grout mixture was mixed for 6 minutes using a high-speed mixer according to ASTM C938 (Standard Practice for Proportioning Grout Mixtures for Preplaced-Aggregate Concrete) (ASTM C938, 2010). Immediately after mixing, the grout's efflux time was measured according to ASTM C939 (Standard Test Method for Flow of Grout for Preplaced-

Aggregate Concrete - Flow Cone Method) (ASTM C938, 2010). Moreover, the amount of accumulated bleeding water at the surface of the fresh grout was evaluated as per the guidelines of ASTM C940 (Standard Test Method for Expansion and Bleeding of Freshly Mixed Grouts for Preplaced- Aggregate Concrete in the Laboratory) (ASTM C940, 2010). The mixing and flowability measurements were conducted at room temperature (23±2°C) [73.4±3.6°F]. The compressive strength of the grout was tested on 50 mm [2 in] cubic specimens at ages of 7, 28, and 56 days according to ASTM C 942 (Standard Test Method for Compressive Strength of Grouts for Preplaced-Aggregate Concrete in the Laboratory) (ASTM C942, 2010). Immediately after demolding, specimens were moved to a moist curing room (T = 25°C [77°F] and RH = 98%) until the testing age.

Furthermore, 21 TSC cylindrical specimens (150 mm × 300 mm [3 in. × 6 in.]) were prepared for each mixture. The molds were first filled with coarse aggregates and then the grout was injected into the voids (**Figure 4.1**). Specimens were covered with wet burlap to prevent surface drying. After 24 h, specimens were demolded and cured in the moist room described above. At each testing age (i.e. 7, 28 and 56 days), the compressive and split tensile strengths of TSC were evaluated according to ASTM C943 (Standard Practice for Making Test Cylinders and Prisms for Determining Strength and Density of Pre-placed-Aggregate Concrete in the Laboratory) (ASTM C943, 2010) and ASTM C496/C496M (Standard Test Method for Splitting Tensile Strength of Cylindrical Concrete Specimens) (ASTM C496/C496M, 2011), respectively. Moreover, the static modulus of elasticity of TSC at 28 days was measured as per the procedure of ASTM C469/C469M (Standard Test Method for Static Modulus of Elasticity and Poisson's Ratio of Concrete in Compression) (ASTM C469/C469M, 2010). **Table 4.4** shows the coefficient of variance (COV) for the various tests conducted.

Differential scanning calorimetry (DSC) tests were performed on samples taken from selected TSC mixtures at 7 days. Samples were ground to powder with an average particle size of 45 μm. Then, a 30 to 60 mg [0.001 to 0.002 oz.] powder specimen was heated in a helium atmosphere at a constant rate of 10°C [50°F] per minute up to 550°C [1022°F]. The endothermic peak for CH was observed at approximately 440°C [824°F]. The area under the curve was related to the quantity of CH in the sample using the regression equation obtained from calibration graphs built in the apparatus. Moreover, samples from selected TSC

mixtures were examined under scanning electron microscopy coupled with energy dispersive X-ray analysis (SEM/EDX) using a Hitachi S-4500 Field Emission SEM.

Stage (1)   **Stage (2)**
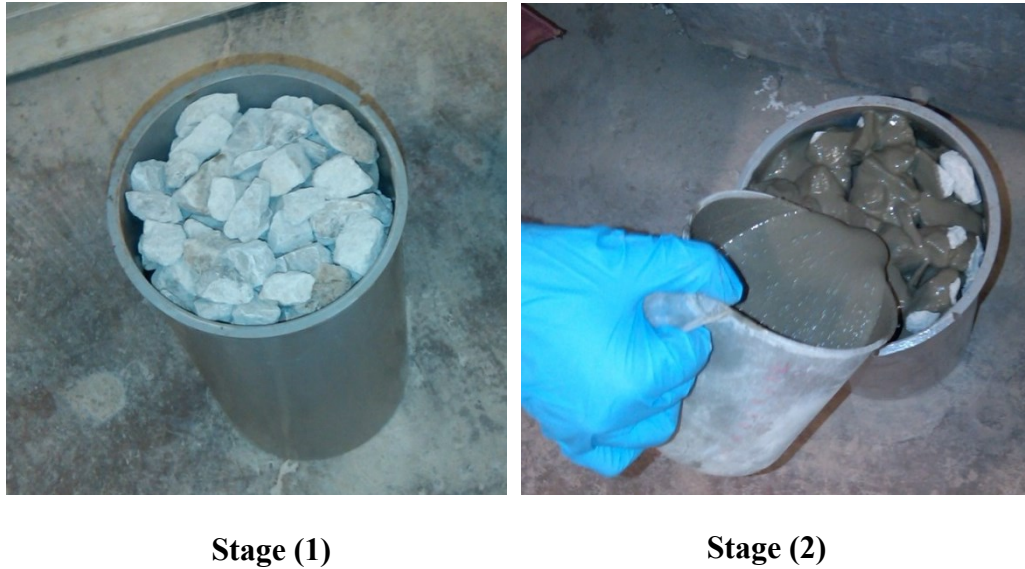
Figure 4.1 – TSC production stages.

Table 4.4 – Coefficient of variance for various tests

Mixture ID	Coefficient of variance for various tests (%)									
	Compressive strength of grout at days			Compressive strength of TSC at days			Splitting tensile strength of TSC at days			Modulus of elasticity at 28 days
	7	28	56	7	28	56	7	28	56	
C	1.28	0.97	0.60	1.44	1.19	1.07	1.05	0.80	0.98	1.19
F1	1.19	1.03	1.06	1.53	1.02	1.24	1.55	1.63	0.96	1.36
F2	1.29	1.25	0.90	2.69	2.14	1.74	2.26	1.78	1.40	1.59
F3	1.98	1.12	0.81	2.54	2.41	1.76	2.04	1.54	1.38	1.25
F4	1.57	1.55	1.04	2.70	2.57	1.39	1.89	1.63	1.15	2.13
F5	1.69	1.34	1.19	4.14	2.52	3.06	1.63	1.96	1.05	1.46
S1	1.16	0.98	0.62	0.90	1.10	1.17	1.18	1.41	2.04	1.29
SF3	1.25	0.86	0.61	2.48	1.13	1.25	1.32	0.89	1.20	1.01
SF4	1.68	0.77	0.81	2.40	1.42	1.39	2.04	0.95	1.33	1.49
M1	0.87	0.70	0.46	1.02	0.94	1.06	1.31	1.27	1.81	1.39
MF3	1.30	0.90	0.87	2.35	1.23	1.41	2.21	1.53	1.38	1.22
MF4	1.02	1.11	0.88	1.48	1.15	1.87	1.60	1.84	1.34	1.71

4.4. RESULTS AND DISCUSSION

The engineering properties of TSC are highly affected by the composition and properties of the used grout, including its flowability, stability and mechanical strength. In particular, the grout flowability is of paramount importance since it directly affects the penetrability of voids between aggregate particles, and consequently the mechanical strength of TSC (Abdul Awal, 1984). Therefore, the flowability of all used grouts was adjusted to similar efflux time in order to minimize variability in its effect on the TSC mechanical properties.

4.4.1. Grout Efflux Time

Several grout trial batches were conducted with different HRWRA dosages to achieve the required efflux time (i.e. 35 to 40 $\pm$ 2 sec) (**Table 4.3**). Results showed that the efflux time decreased significantly as the FA addition rate was increased. For example, the grout mixture incorporating 50% FA as partial replacement for OPC achieved the target flowability without need for HRWRA addition. This is because FA reduces frictional forces among particles owing to the spherical shape of its particles which have smooth vitreous surfaces, leading to a lubricant ball-bearing effect, thus facilitating mobility (Yung Wang *et al*., 2013). In addition, FA can be adsorbed on oppositely charged cement particles surfaces, preventing flocculation and enhancing particle dispersion, which consequently enhances flowability with more free water (Kismi *et al*., 2011).

Conversely, partially replacing OPC with 10% SF or 10% MK increased the grout's efflux time. For instance, at 0.6% HRWRA, grout mixtures S1 and M1 exhibited 16% and 68% longer efflux time, respectively compared to that of the C mixture. This can be ascribed to the high water demand induced by the very fine particles of SF and MK (Khayat *et al*., 1997; Razak and Wong, 2001). However, ternary grout mixtures involving a combination of OPC + FA + SF or MK exhibited better flowability compared to that of binary grout mixtures without FA (i.e. S1 and M1). For instance, at 0.6% HRWRA, the grout mixture SF3 achieved a 41% shorter efflux time than that of the S1 mixture. This can be attributed to the lubricant effect induced by FA addition as mentioned earlier.

4.4.2. Grout Bleeding Resistance

Bleeding of the grout is considered as an important property affecting the performance of TSC. It is defined as the segregation of water on the grout's surface before its setting time (Hsing Huang, 1997). Grout bleeding occurs due to the settlement of suspended materials in the mixing water (i.e. binder, fine aggregate) under its own weight due to gravity. The total amount of bleeding (i.e. sedimentation) depends on the mixture proportions of the grout (i.e. free water content) and properties of fine materials (i.e. including binder and sand), which will affect the cohesion of the mixture (Tan *et al.*, 2005). The higher the grout cohesion, the lower is the bleeding (Bruce *et al.*, 1997). As shown in **Figure 4.2**, increasing the FA dosage resulted in higher bleeding. Higher FA content tends to increase the free water as it reduces the water demand and the grout cohesion (Hasan, 2012). The reduction in water demand can be attributed to the particle shape of FA as mention previously along with its "particle packing effect". OPC and FA generally have comparable particle size range (i.e. 1 to 45 μm). Hence, both can be considered as excellent filler. However, due to the lower density and higher volume per unit mass of FA, it is a more efficient void-filler than OPC (Mehta, 2004).
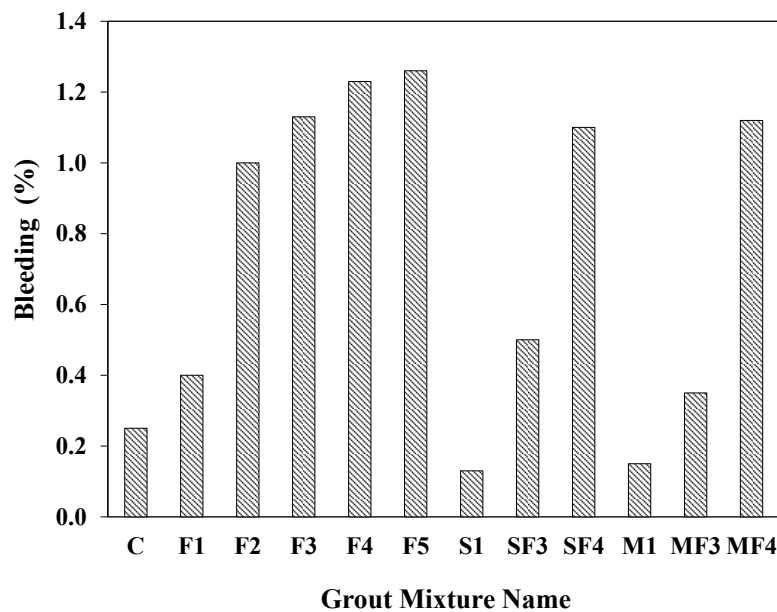
Figure 4.2 – Bleeding of grout mixtures.

Conversely, using SF or MK as partial replacement for OPC significantly minimized the grout's bleeding. This can be attributed to the high fineness of SF and MK compared to that of OPC and FA, which in turn increases the contact area between particles and the amount of adsorbed water (Khayat *et al*., 1997; Hsing Huang, 1997; Khatib and Caly, 2004). Moreover, the physical microfiller effect provided by such ultrafine materials reduced bleeding by blocking pores between cement particles (Khayat *et al*., 1997). Interestingly, adding FA to grout mixtures incorporating SF or MK increased bleeding. For example, the bleeding for mixtures SF3 and MF3 was 3.8 and 2.3 times that of grout mixtures S1 and M1, respectively. This can be considered as a result of FA addition as it decreased the water demand, leading to more free water.

4.4.3. Effect of Grout on TSC Compressive Strength

Table 4.5 reports compressive strength results at different ages for the tested grouts and corresponding TSC mixtures at optimum HRWRA dosage. Generally, the grouts and TSC mixtures exhibited comparable compressive strength trend with respect to the type of binder. Moreover, the higher the FA partial replacement level for OPC, the greater was the reduction in compressive strength. For example, increasing the FA rate in the grout from 10% to 50% resulted in about 43.4% greater reduction in the 7-days compressive strength of TSC compared to that of the control TSC. This is because grouts incorporating FA gain strength slowly due to slower hydration reactions at early-age (Bouzoubaâ *et al*., 2004). At very early age, calcium ions (Ca^{++}) adsorb on the surface of FA particles, leading to a depression of the calcium concentration in the pore solution and consequently delaying the CH and CSH nucleation and crystallization. This was confirmed by DSC results as shown in **Figure 4.3**. For example, the CH content of specimens containing 30% and 50% fly ash at 7 days was 48% and 56% lower than that of the control mixture, respectively. Moreover, the reduction of the calcium concentration will result in a lower calcium/silica ratio, leading to slower pozzolanic reaction (Zhang *et al*., 2008; Narmluk and Nawa, 2011; Sarker, 2013).

Conversely, adding SF or MK to mixtures incorporating OPC improved compressive strength. This can be attributed to its high pozzolanic activity (Snelson *et al*., 2008; Weng *et al*., 1997). This was also confirmed by DSC results; the measured CH contents at 7 days for the grout samples taken from TSC mixtures with S1 and M1 grouts were 26% and 50% lower

than that of the control mixture (C), respectively. In addition, the presence of such fine materials strengthens the microstructure through enhanced particle packing density.

Further replacing 30% and 40% of OPC by FA in those TSC mixtures incorporating 10% SF or MK reduced compressive strength, yet strength values were still higher than those of mixtures incorporating FA alone. According to the DSC results, the CH content was much lower in such mixtures (**Figure 4.3**) due to a delay of cement hydration reactions induced by FA (Weng *et al*., 1997; Snelson *et al*., 2008). For example, adding 30% FA to TSC mixtures made with 10% SF or 10% MK reduced compressive strength at 7 days by about 46.9% and 34.9%, respectively compared to those of mixtures with SF or MK alone.

At later ages (i.e. more than 7 days), mixtures incorporating 10% SF or MK achieved higher compressive strength than that of the control mixture. However, mixtures incorporating FA exhibited higher strength gaining rate, thus exceeding that of the control mixture. For instance, the TSC mixture with 20% FA had strength gaining rate was 1.7 and 2.4 times that of the control mixture at 28 and 56 days, respectively. Hence, mixtures with FA are expected to achieve comparable compressive strength to that of the control at later age owing to more rapid strength gaining rate sustained over a longer period of time than that of mixtures made with pure OPC (Hwang *et al*., 2004; Chindaprasirt *et al*., 2005).

However, the compressive strength level will depend on the ability of the grout to resist bleeding (Abdul Awal, 1984). The settlement of grout ingredients generally occurs at the underside of aggregates, leading to the formation of voids. These voids create weak aggregate-grout interfacial zones in TSC, hindering the grout bond to coarse aggregates (Abdul Awal, 1984). Moreover, TSC grouts incorporating FA (F3 and F6) produced voids (i.e. large capillary pores), which are considered as a source of weakness in concrete (**Figures 4.4(a)** and **4.4(b)**). These voids formed due to excess water that remained as free water in the TSC grout structure. The volume of capillary voids increased with the increase of free water and depended on the degree of binder hydration (O'Malley and Abdelgader, 2009). Conversely, TSC mixture M1 with lower amount of free water created less voids compared to other TSC mixtures (F6 and F3), thus achieving higher TSC compressive strength (**Figure 4.4(c)**).

Table 4.5 – Mechanical properties of TSC versus binder type

Grout Mixture Number	Compressive strength of grout (MPa) at days			Compressive strength of TSC (MPa) at days			Tensile strength of TSC (MPa) at days			Elastic modulus at 28 days (GPa)
	7	28	56	7	28	56	7	28	56	
C	33.8	50.4	54.3	25.9	31.5	33.3	3.40	3.70	3.80	38.3
F1	31.5	48.0	53.8	23.2	29.0	36.7	3.20	3.50	3.70	37.4
F2	28.9	40.7	47.9	16.9	23.2	28.5	2.60	3.00	3.50	35.9
F3	27.1	38.5	46.2	14.0	18.9	25.8	2.50	2.80	3.30	34.5
F4	23.8	32.1	41.5	13.2	17.7	21.2	2.40	2.65	3.10	34.1
F5	21.0	28.0	38.2	12.0	14.1	18.5	2.30	2.60	2.80	33.6
S1	43.8	52.2	57.0	32.8	34.1	38.9	3.60	3.80	4.06	39.5
SF3	30.0	41.4	48.1	17.4	26.1	29.9	2.70	3.30	3.60	37.0
SF4	27.0	38.0	46.2	15.6	25.0	25.6	2.50	3.10	3.24	36.0
M1	52.1	61.9	64.1	35.0	40.0	43.0	3.80	3.90	4.02	41.0
MF3	34.9	48.1	58.4	22.8	30.4	36.2	3.02	3.50	3.60	37.3
MF4	29.0	41.0	49.0	19.9	28.5	31.5	2.85	3.20	3.40	36.0
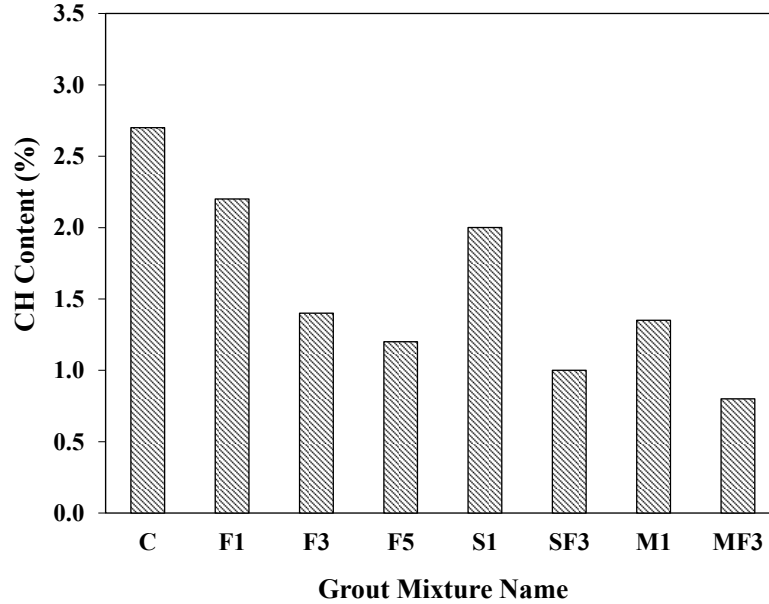
Figure 4.3 – CH contents for TSC mixtures (C, F1, F3, F5, S1, SF3, M1, and MF3) at 7 days.
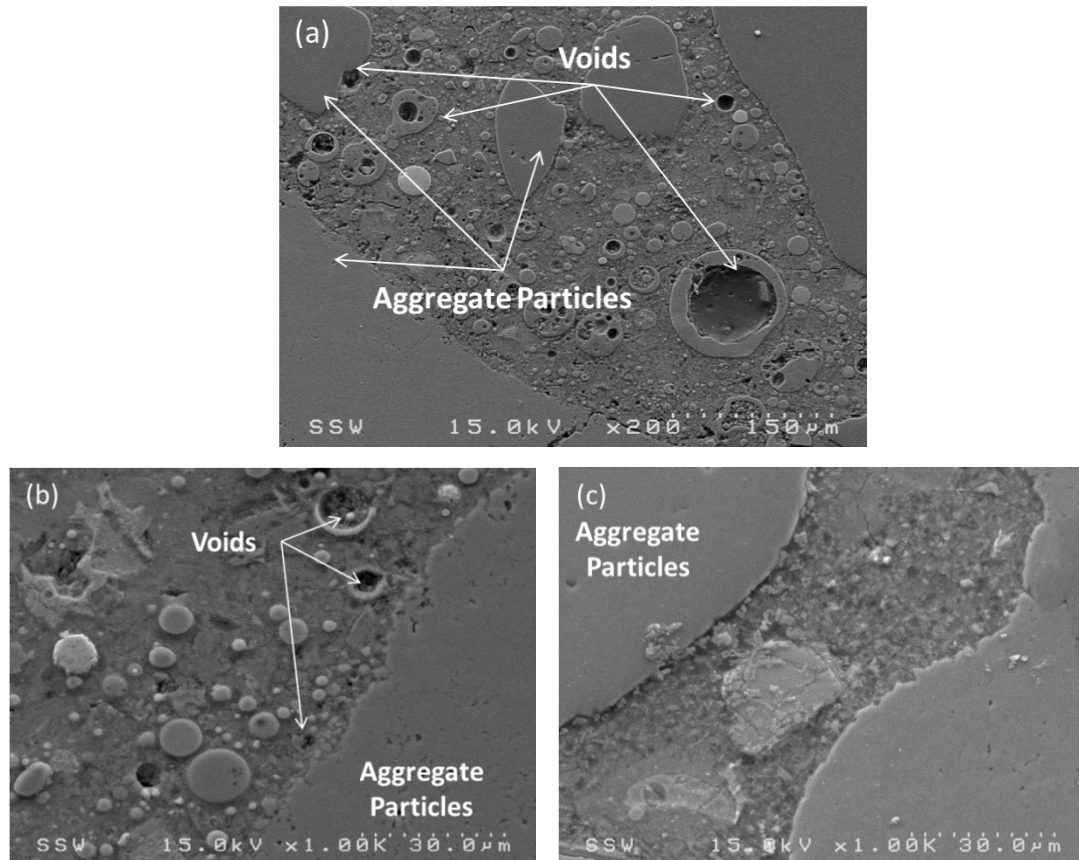
Figure 4.4 – SEM of specimens from different TSC mixtures: (a) F6; (b) F3; (c) M1.

4.4.4. Relationship between Compressive Strength of Grout and Corresponding Two-Stage Concrete

The relation between the compressive strength of grout and that of the corresponding TSC is not yet well defined in the open literature. Therefore, an attempt has been made herein to fill this knowledge gap. Previous studies reported that increasing the grout's compressive strength will lead to higher TSC compressive strength (Abdelgader, 1996; 1999). However, increasing in the grout's strength did not always ensure similar improvement in the TSC compressive strength. For instance, 80% increase in the grout strength resulted only in about 65% increase in the TSC strength (Abdelgader, 1996, 1999). For crushed aggregates, Abdelgader proposed the following empirical equation (**Eq. 4.1**) for the relationship between the grout and TSC compressive strength at 28 days (Abdelgader, 1999):

$$f_c^{`} = 6.70 + 0.42 \times f_g^{1.07} \qquad\qquad \textbf{Eq. 4.1}$$

Where $f_c^{`}$ is the 28 days TSC compressive strength (MPa), and f_g is the grout's 28 days compressive strength (MPa). In the present study, **Eq. 4.1** was modified to account for the addition of SCMs through a new parameter, β as shown in **Eq. 4.2**.

$$f_c^{`} = 6.70 + 0.42 \times f_g^{1.07-\beta} \qquad\qquad \textbf{Eq. 4.2}$$

The constant β is a function of the percentage of added SCMs (S), type of binder (α) and number of added SCMs (N) as expressed in **Eq. 4.3**.

$$\beta = N \times \left[\left(\left(0.035 + \frac{S}{1000} \right) \times \frac{1}{\alpha_N} \right) - \left(\frac{S^3 + S^2 + 100\,S}{(S+1) \times 10^5} \right) \right] \qquad \textbf{Eq. 4.3}$$

Where α_N is the multiplication of α for the used binder (the values of α obtained from regression analysis for each type of binder are: OPC: 1, FA: 0.5, SF: 3.5, MK: 4.5).

The proposed modified equation was assessed statistically based on the root-mean-square error (*RMSE*), absolute fraction of variance (R^2) and correlation coefficient (r_{xy}) between model and experimental results. *RMSE*, R^2, and r_{xy} values were 1.63 MPa, 0.996 and 0.973, respectively, which indicates that the modified equation could reasonably capture the relation between the grout and TSC compressive strength. However, further study is needed to account for the effects of different aggregates on the proposed relationship.

4.4.5. TSC Tensile Strength

The splitting tensile strength is commonly used to evaluate the tensile strength of TSC (Abdul Awal, 1984; Abdelgader and Ben-Zeitun, 2005; Abdelgader and Elgalhud, 2008). As shown in **Table 4.5**, the TSC tensile strength followed similar trend to that of the compressive strength. The splitting tensile strength at 7 days was low, especially for mixtures incorporating FA, and then its rate of development increased with time. For instance, the 7-days tensile strength for the mixture incorporating 20% FA was 24% lower than that of the control mixture, while its tensile strength development rate was 1.75 and 2.9 times that of the control mixture at 28 and 56 days, respectively.

Generally, the higher the TSC compressive strength, the greater the TSC tensile strength was, in agreement with previous studies (Abdul Awal, 1984; Abdelgader and Ben-Zeitun, 2005). Several empirical equations have been proposed to describe the correlation between the compressive and tensile strengths of TSC. In this study, the equation proposed by Abdelgader and Ben-Zeitun (**Eq. 4.4**) (Abdelgader and Ben-Zeitun, 2005) was adapted.

$$f_t = 0.768 \, f_c^{`0.441}$$
<div align="right">**Eq. 4.4**</div>

Where, f_t is the TSC's tensile strength and $f_c^`$ is its compressive strength in MPa. As shown in (**Figure 4.5**), a good fitting of experimental data using **Eq. 4.4** was achieved. The residual between the experimental and predicted TSC tensile strength was only ± 0.2 MPa. In addition, the *RMSE*, R^2, and r_{xy} values were 0.105 MPa, 0.999 and 0.979, respectively, which indicates that **Eq. 4.4** can successfully predict the tensile strength of TSC made with different binders.
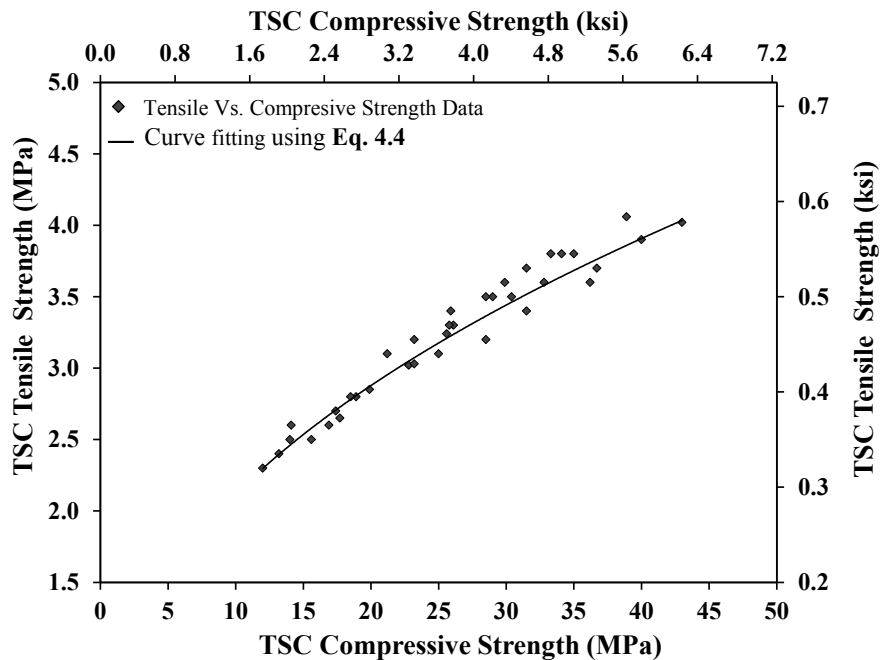
Figure 4.5 – Relationship between compressive and tensile strength of TSC.

4.4.6. TSC Modulus of Elasticity

Modulus of elasticity values at 28 days for TSC mixtures made with various binders are presented in **Table 4.5**. It can be observed that similarly to compressive and tensile strength, the TSC modulus of elasticity is affected by the binder type. For example, TSC mixtures incorporating 50% FA achieved a modulus of elasticity 12% lower than that of the control mixture. However, TSC mixtures made with 10% SF or 10% MK achieved modulus of elasticity values 3% and 7% higher than that of the control, respectively. The relationship between the TSC modulus of elasticity and its compressive strength differs from that of conventional concrete. It was reported that TSC exhibits higher modulus of elasticity than that of conventional concrete with comparable compressive strength (Abdul Awal, 1984). This can be ascribed to the fact that TSC has higher coarse aggregate (about 60% of the total volume) than that of conventional concrete (about 40% of the total volume). Thus, TSC has a skeleton of coarse aggregate particles resting on each other and the stresses are transferred through their contact points (Abdul Awal, 1984; Abdelgader, 1996; Abdelgader and Górski, 2003). An empirical relationship between the elastic modulus of TSC and its compressive strength was proposed in this study using nonlinear regression analysis as given in **Eq. 4.5 (Figure 4.6)**.

$$E = 19.53 \, f_c^{`0.195}$$ **Eq. 4.5**

Where, E is the modulus of elasticity for TSC (GPa) and $f_c^{`}$ is its compressive (MPa). The *RMSE*, R^2, and r_{xy} values were 0.67 MPa, 0.999 and 0.950, respectively, indicating satisfactory predictive ability of the proposed equation. Moreover, the modulus of elasticity of TSC can be estimated based on the compressive strength of the grout (i.e. **Eq. 4.6**, which is derived by substituting **Eq. 4.2** in **Eq. 4.5**).

$$E = 19.53 \left(6.70 + 0.42 \times f_g^{1.07-\beta} \right)^{0.195}$$ **Eq. 4.6**
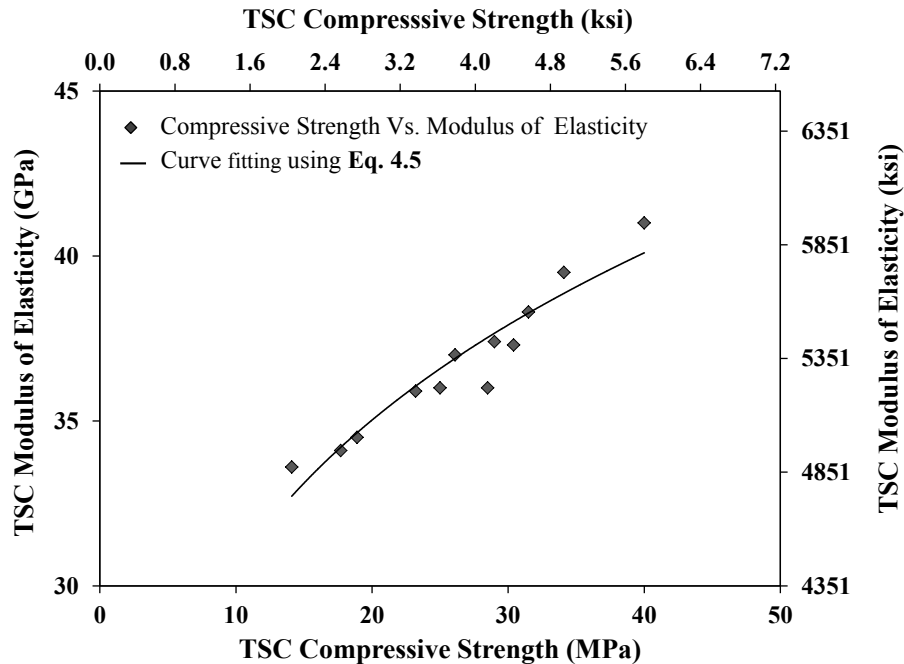
Figure 4.6 – Relationship between compressive strength and modulus of elasticity of TSC.

4.5. CONCLUSIONS

In this study, the rheological and mechanical properties of two-stage concrete made with single, binary and ternary binders were explored. The following conclusions can be drawn:

- Partial replacement of OPC with FA improved the grout's flowability while reducing its resistance to bleeding.

- Partial replacement of OPC with SF or MK increased the grout's bleeding resistance and mechanical properties, while reducing its flowability. However, flowability can be adjusted using a proper dosage of HRWRA.

- An empirical equation for predicting the compressive strength of TSC based on the corresponding grout's compressive strength and considering the binder type was proposed.

- There was no significant effect of the binder type on the relation between the compressive and tensile strengths of TSC.

- An empirical relationship between the modulus of elasticity of TSC and its compressive strength was proposed in the present study. This equation can be extended to estimate the modulus of elasticity of TSC based on the grout's compressive strength as outlined in **Eq. 4.6**.

However, it should be mentioned that the proposed model highlighted the existence of a relationship between the properties of TSC and its grout formulation and binder type. Such a relationship cannot be extrapolated beyond the domain of the data used in this study. It can, however, be extended beyond the current experimental domain and include other experimental variables should sufficient data needed for such an extension become available in the future.

4.6. REFERENCES

Abdelgader, H. S., (1996), "Effect of quantity of sand on the compressive strength of two-stage concrete," *Magazine of Concrete Research*, Vol. 48, No. 177, pp. 353-360.

Abdelgader, H. S., (1999), "How to design concrete produced by a two-stage concreting method," *Cement and Concrete Research*, Vol. 29, No. 3, pp. 331-337.

Abdelgader, H. S. and Ben-Zeitun, A. E., (2005), "Tensile strength of two-stage concrete measured by double-punch and split tests," *Proceedings of International Conference on Global Construction, Role of Concrete in Nuclear Facilities,* University of Dundee, Scotland, UK, pp. 43-50.

Abdelgader, H. S. and Elgalhud, A. A., (2008), "Effect of grout proportions on strength of two-stage concrete," *Structural Concrete*, Vol. 9, No. 3, pp. 163-170.

Abdelgader, H. S. and Górski, J., (2003), "Stress-strain relations and modulus of elasticity of two-stage concrete," *Journal of Materials in Civil Engineering*, *ASCE*, Vol. 15, No. 4, pp. 329-334.

Abdul Awal, A. S., (1984), "Manufacture and properties of pre-packed aggregate concrete," *Master Thesis*, University of Melbourne, Australia, 121 p.

ACI 304.1, (2005), "Guide for the use of preplaced aggregate concrete for structural and mass concrete applications," *American Concrete Institute*, Farmington Hills, USA, 19 p.

ASTM C938, (2010), "Standard practice for proportioning grout mixtures for preplaced-aggregate concrete," *American Society for Testing and Materials*, West Conshohocken, PA, USA, 3 p.

ASTM C939, (2010), "Standard test method for flow of grout for preplaced-aggregate concrete (flow cone method)," *American Society for Testing and Materials*, West Conshohocken, PA, USA, 3 p.

ASTM C469/C469M, (2010), "Standard test method for static modulus of elasticity and Poisson's ratio of concrete in compression)," *American Society for Testing and Materials*, West Conshohocken, PA, USA, Vol. 4.02.

ASTM C940, (2010), "Standard test method for expansion and bleeding of freshly mixed grouts for preplaced- aggregate concrete in the Laboratory)," *American Society for Testing and Materials*, West Conshohocken, PA, USA, Vol. 4.02.

ASTM C942, (2010), "Standard test method for flow of grout for compressive strength of grouts for preplaced-aggregate concrete in the laboratory)," *American Society for Testing and Materials*, West Conshohocken, PA, USA, Vol. 4.02.

ASTM C943, (2010), "Standard practice for making test cylinders and prisms for determining strength and density of pre-placed-aggregate concrete in the laboratory)," *American Society for Testing and Materials*, West Conshohocken, PA, USA, Vol. 4.02.

ASTM C496/C496M, (2011), "Standard test method for splitting tensile strength of cylindrical concrete specimens)," *American Society for Testing and Materials*, West Conshohocken, PA, USA, Vol. 4.02.

Bayer, R., (2004), "Use of preplaced aggregate concrete for mass concrete applications," *Master Thesis*, Middle East Technical University, Turkey, 160 p.

Bouzoubaâ, N., Bilodeau, A., Sivasundaram, V., Fournier, B. and Golden, D. (2004), "Development of Ternary Blends for High-Performance Concrete," *ACI Materials Journal*, Vol. 101, pp. 19-29.

Bruce, D. A., Littlejohn, G. S. and Naudts, A., (1997), "Grouting materials for ground treatments: A practitioner's guide. In Geotechnical Special Publication; Grouting: Compaction, Remediation and Testing, C. Vipulanandan (Ed.)," *ASCE*, New York, Vol. 66, pp. 306-334.

Chindaprasirt, P., Jaturapitakkul, C. and Sinsiri, T., (2005), "Effect of fly ash fineness on compressive strength and pore size of blended cement paste," *Cement and Concrete Composites*, Vol. 27, No. 4, pp. 425-428.

Hasan, H. A., (2012), "Effect of fly ash on geotechnical properties of expansive soil," *Journal of Engineering and Development*, Vol. 16, No. 2, pp. 306-316.

Hsing Huang, W., (1997), "Properties of cement-fly ash grout admixed with bentonite, silica fume, or organic fiber," *Cement and Concrete Research*, Vol. 27, No. 3, pp. 395-406.

Hwang, K., Noguchi, T. and Tomosawa, F., (2004), "Prediction model of compressive strength development of fly ash concrete," *Cement and Concrete Composites*, Vol. 34, No. 12, pp. 2269-2276.

Khatib, J. and Caly, R., (2004), "Absorption characteristics of metakaolin concrete," *Cement and Concrete Research*, Vol. 34, No. 1, pp. 19-29.

Khayat, K., Vachon, M. and Lanctôt, M., (1997), "Use of blended silica fume cement in commercial concrete mixtures," *ACI Materials Journal*, Vol. 94, No. 3, pp. 183-192.

Kismi, M., Claude Saint, J. and Mounanga, P., (2011), "Minimizing water dosage of superplasticized mortars and concretes for a given consistency," *Construction and Building Materials*, Vol. 28, No. 1, pp. 747-758.

Mehta, P. K., (2004), "High-performance, high-volume fly ash concrete for sustainable development," *International workshop on sustainable development and concrete technology*, Beijing, China.

Molhotra, V. M., (1993), "Fly ash, slag, silica fume, and rice- hush ash in concrete: a review," *Concrete International*, Vol. 15, No. 4, pp. 23-28.

Narmluk, M. and Nawa, T., (2011), "Effect of fly ash on the kinetics of Portland cement hydration at different curing temperatures," *Cement and Concrete Research*, Vol. 41, No. 6, pp. 579-589.

O'Malley, J. and Abdelgader, H. S., (2009), "Investigation into the viability of using two stage (pre-placed aggregate) concrete in an Irish setting," *GSBEIDCO -1st*, Vol. 1, pp. 215-222.

Razak, H. and Wong, H., (2001), "Effect of incorporating metakaolin on fresh and hardened properties of concrete," *Special Publication*, Vol. 200, pp.309-324.

Sarker, P. K., (2013), "Early-age tensile strength and calcium hydroxide content of concrete containing low-calcium fly ash," *Australian Journal of Structural Engineering*, Vol. 14, No. 3, pp. 206-216.

Snelson, D., Wild, S. and O'Farrell, M., (2008), "Heat of hydration of Portland Cement–Metakaolin–Fly ash (PC–MK–PFA) blends," *Cement and Concrete Research*, Vol. 38, No. 6, pp. 832-840.

Tan, O., Zaimoglu, A., Hinislioglu, S. and Altun, S., (2005), "Taguchi approach for optimization of the bleeding on cement-based grouts," *Tunneling and Underground Space Technology*, Vol. 20, pp. 167-173.

Weng, J. K., Langan, B. W. and Ward, M. A., (1997), "Pozzolanic reaction in Portland cement, silica fume, and fly ash mixtures," *Canadian Journal of Civil Engineering*, Vol. 24, No. 5, pp. 754-760.

Yung Wang, H., Ten Kuo, W., Chung Lin, C. and Yo, C., (2013), "Study of the material properties of fly ash added to oyster cement mortar," *Construction and Building Materials*, Vol. 41, No. 1, pp. 532-537.

Zhang, M. H., Swaddiwudhipong, S., Tay, K. Y. and Tam, C. T., (2008), "Effect of silica fume on cement hydration and temperature rise of concrete in tropical environment," *The IES Journal Part A: Civil & Structural Engineering*, Vol. 1, No. 2, pp. 154-162.

<div align="right">

Chapter 5

</div>

5. MECHANICAL PERFORMANCE OF TWO-STAGE STEEL FIBRE-REINFORCED CONCRETE[(*)]

5.1. INTRODUCTION

Two-stage concrete (TSC), also called preplaced aggregate concrete, is a special type of concrete fabricated using a different casting method than that of conventional concrete. In TSC, the volume of coarse aggregate is first placed in the formwork. Subsequently, voids between aggregates are filled with a flowable grout. Since 1939, TSC has been successfully used in various applications, such as in underwater construction, mass concrete and concrete repair (Najjar *et al.*, 2014). Over the last few decades, several researchers investigated the mechanical properties of TSC (Abdul Awal, 1984; Abdelgader, 1996; O'Malley and Abdelgader, 2010; Abdelgader *et al.*, 2013; Coo and Pheeraphan, 2015). It was argued that the mechanical properties of TSC are mainly affected by the coarse aggregate properties and the mixture proportions of the grout (i.e. water/binder ratio (*w/b*) and sand/binder ratio (*s/b*)). However, up to now, there has been no data accessible in the open literature on two-stage concrete reinforced with fibres.

Steel fibres have been used for several decades in many concrete applications such as in pavements, bridge decks, tunnel linings and various precast elements (Holschemacher *et al.*, 2010; Mohamed *et al.*, 2014). It is well established that the addition of steel fibres in concrete can minimize crack forming, reduce crack width and limit its propagation via a crack bridging mechanism. Moreover, steel fibres increase the fracture toughness of concrete owing to the energy required to debond and pull-out the fibres from the cementitious matrix (Köksal, *et al.*, 2008).

Generally, the engineering properties of steel fibre-reinforced concrete (SFRC) depend on several variables, including the fibre dosage, shape, length and aspect ratio, along with the

properties of the cementitious matrix (Mohamed, *et al.*, 2014). It was reported that using steel fibre dosages up to 1% had a minimal effect on the compressive strength of SRFC, while it significantly improved its splitting and flexural strength (Şahin and Köksal, 2011). However, the addition of high steel fibre dosages (more than 3%) can adversely affect the compressive and tensile strengths of concrete (Ikraiam *et al.*, 2009; Yoo, *et al.*, 2013). This can be ascribed to the fact that at high steel fibre dosage, the workability of concrete decreases dramatically due to the fibre-balling effect (Yang, 2011). As a result, internal voids increase in the concrete, leading to a reduction in mechanical properties (Ikraiam *et al.*, 2009; Sahoo *et al*, 2015). Therefore, the ACI 544.1 (2002) (Report on Fibre-Reinforced Concrete) limited the maximum practical steel fibre dosage in conventional concrete produced by normal mixing and placing procedures to 1.5 to 2%.

In the present study, the mechanical performance of two-stage steel fibre-reinforced concrete (TSSFRC) made with different steel fibres dosages and lengths was explored for the first time. It is anticipated that great enhancement in TSSFRC mechanical strength and toughness associated with savings through its highly effective placement technique can pave the way for its wider implementation in modern civil construction applications.

5.2. EXPERIMENTAL PROGRAM

5.2.1. Materials and Grout Mixture Proportions

Ordinary portland cement (OPC) with a specific gravity of 3.15 and a surface area of 371 m^2/kg [1811 ft^2/lb] was used in this investigation. Silica sand having a fineness modulus of 1.47 and a saturated surface dry specific gravity of 2.65 was used as fine aggregate. It is to be noted that fine sand is desirable in TSC since it is used in the grout injected between preplaced coarse aggregates. The grout mixture with sand-to-binder ratio (*s/b* = 1.0) and water-to-binder ratio (*w/b* = 0.45) was used in the production of TSSFRC. The grout mixture composition was as follows: cement content = 874 (kg/m^3), sand content = 874 (kg/m^3) and water content = 393 (kg/m^3). To improve grout flowability, a high-range water-reducing admixture (HRWRA) was added. Several trial grout mixtures were conducted in order to identify the adequate HRWRA dosage to achieve the efflux time of 35-40 ± 2 sec recommended by the ACI 304.1 (2005) (Guide for the Use of Preplaced Aggregate Concrete for Structural and Mass Concrete Applications). The optimum HRWRA dosage was 0.4% by

the weight of cement. The efflux time of the used grout mixture was 39 sec, while its bleeding was 0.25%. Crushed limestone coarse aggregate with a maximum nominal size of 40 mm [1.57 in.], a saturated surface dry specific gravity of 2.65 and a water absorption of 1.63% was used as preplaced coarse aggregate. Two types of cold-drawn hooked-end steel fibres were used and their properties are given in **Table 5.1**. The steel fibre dosages (i.e. volume fractions) used in TSC were 1%, 2%, 4% and 6%.

Table 5.1 – Properties of hooked-ends steel fibres

Steel Fibre Type	Length (mm)*	Diameter (mm)*	Aspect ratio	Specific gravity	Tensile strength (MPa)*
Short (S)	33	0.75	80	7.85	1100
Long (L)	60	0.75	44	7.85	1100

* 1 in. = 25.4 mm, 1 ksi = 6.894 MPa

5.2.2. Experimental Procedures

TSSFRC cylindrical specimens (150 mm × 300 mm [6 in. × 12 in.]) and prisms (150 mm × 150 mm × 550 mm [6 in. × 6 in. × 22 in.]) were prepared. First, coarse aggregates and steel fibres were premixed and preplaced in the molds (**Figure 5.1**). A grout was subsequently injected to fill in the space around the coarse aggregates and fibres. All TSSFRC specimens were demolded after one day and moist cured at 20 °C [68 °F] and 95% RH until the age of 28 days. The compressive strength and splitting tensile strength were evaluated on TSSFRC cylinders according to ASTM C943 (Standard Practice for Making Test Cylinders and Prisms for Determining Strength and Density of Preplaced-Aggregate Concrete in the Laboratory) (ASTM C943, 2010) and ASTM C496 (Standard Test Method for Splitting Tensile Strength of Cylindrical Concrete Specimens) (ASTM C496/C496M, 2011), respectively. The flexural performance of TSSFRC prisms was assessed using a three-point bending test as per the guidelines of ASTM C1609 (Standard Test Method for Flexural Performance of Fibre-Reinforced Concrete-Using Beam with Third-Point Loading) (ASTM C1609/C1609M, 2012). The test was conducted using a closed loop deflection-controlled testing at a loading rate of 0.1 mm/min [0.004 in/min] (**Figure 5.2**). Toughness was calculated as the area under

the load-deflection curve up to a deflection of 3 mm [0.11 in.] in accordance with ASTM C1609. Moreover, the flexural toughness indices, which are defined as the ratio between the absorbed energy up to a given deflection to that at the first crack, were evaluated based on ASTM C1018 (Standard Test Method for Flexural Toughness and First-Crack Strength of Fibre-Reinforced Concrete-Using Beam with Third-Point Loading) (ASTM C1018, 1997). The standard toughness indices I_5, I_{10}, I_{20} and I_{30} are defined for deflections of $3\delta_1$, $5.5\delta_1$, $10.5\delta_1$ and $15.5\delta_1$, respectively, where δ_1 is the deflection at the first crack. Values of 5, 10, 20, and 30 for I_5, I_{10}, I_{20} and I_{30} correspond to a linear elastic material behaviour up to the first crack and perfectly plastic behaviour thereafter. Furthermore, the residual strength factors, which provide data on the level of strength retained after first crack formation as a percentage of the first-crack strength for different deflection intervals were calculated based on ASTM C1018 as per the following equations:

$$R_{5-10} = 20 \times (I_{10} - I_5) \qquad \textbf{Eq. 5.1}$$
$$R_{10-20} = 10 \times (I_{20} - I_{10}) \qquad \textbf{Eq. 5.2}$$
$$R_{20-30} = 10 \times (I_{30} - I_{20}) \qquad \textbf{Eq. 5.3}$$

Moreover, analysis of variance (ANOVA) was used to analyze the experimental data. To investigate whether an experimental variable (e.g. fibre dosage or fibre length) is statistically significant, an F value is determined as the ratio of the mean squared error between treatments (e.g. different steel fibre dosages) to that of within treatments (due to using replicates rather than testing only one specimen). This value is then compared to a standard (critical) F value of an F-distribution density function obtained from statistical tables based on the significance level ($\alpha = 0.05$) and the degrees of freedom of error determined from the number of treatments and observations in an experiment. Exceeding the critical value of an F-distribution density function reflects that the tested variable affects the mean of the results (Montgomery, 2013).

Figure 5.1 – Preplacing coarse aggregates and steel fibres.

Figure 5.2 – Flexure test setup.

5.3. RESULTS AND DISCUSSION

5.3.1. Compressive Strength

Table 5.2 presents the compressive strength results for the various TSSFRC mixtures incorporating different steel fibre dosages at 28 days. Results indicate that the compressive strength of TSSFRC increased as the steel fibre dosage increased. ANOVA at a significance level $\alpha = 0.05$ (**Table 5.3**) confirmed that the variation in the fibre dosage had a significant effect on the mean of the total compressive strength results. The calculated F value of 276.03 for the total compressive strength results was significantly larger than the corresponding critical F value of 5.19 ($F_{0.05, 4, 5}$). According to Montgomery (2013), exceeding the critical value of F-distribution density function reflects that the tested variable affects the mean of the results.

Table 5.2 – Compressive and tensile strength of TSSFRC specimens

TSSFRC Mixture ID	Steel Fibre Type	Steel Fibre Dosage (%)	Compressive Strength		Tensile Strength	
			$(MPa)^*$	COV (%)	$(MPa)^*$	COV (%)
M0	--	0	31.5	4.1	3.7	4.4
MS1		1	35.9	3.9	4.8	3.4
MS2		2	37.3	3.9	5.9	3.7
MS4	Short	4	40.8	3.0	6.7	1.6
MS6		6	46.9	1.9	7.7	2.1
ML1		1	36.2	1.0	5.0	5.9
ML2		2	38.4	1.7	6.2	2.6
ML4	Long	4	41.3	3.1	7.3	2.2
ML6		6	47.9	1.8	8.2	1.7

* 1 ksi = 6.894 MPa

Table 5.3 – Analysis of variance (ANOVA)

Mechanical Properties of TSSFRC	Effect of Fibre Dosage		Effect of Fibre Length			
			at Fibre Dosages (1% and 2%)		at Fibre Dosages (4% and 6%)	
	F	$F_{(0.05,4,5)}$	F	$F_{(0.05,1,6)}$	F	$F_{(0.05,1,6)}$
Compressive Strength	276.03	5.19	0.01	5.99	0.09	5.99
Tensile Strength	76.17	5.19	0.38	5.99	3.30	5.99
Flexural Strength	8.85	5.19	3.26	5.99	7.12	5.99
Toughness	16.93	5.19	0.36	5.99	6.55	5.99

Based on the results in **Table 5.2**, the MS1 and MS2 mixtures (made with 1% and 2% short steel fibres, respectively) achieved around 14% and 18% higher compressive strength than that of the control specimens without steel fibres (M0). The steel fibre dosage in conventional SFRC is usually limited to 2% due to workability consideration and to maintain a homogeneous distribution of steel fibres (Ikraiam *et al.*, 2009; Yoo, *et al.*, 2013). Hence, higher steel fibre dosage (i.e. more than 2%) tends to induce voids, causing weaknesses and flaws where micro-cracks initiate, consequently reducing compressive strength (Aydin, 2013). Conversely, the TSSFRC production method mitigates such problems since the coarse aggregates and fibres are preplaced before injecting the grout. It is interesting therefore that high steel fibres dosages up to 6% achieved higher compressive strength values in TSC. For instance, the MS4 and MS6 mixtures (incorporating 4% and 6% short steel fibres, respectively) achieved around 9% and 26% higher compressive strength than that of the MS2 mixture (incorporating 2% steel fibres). This can be ascribed to the fact that increasing the steel fibre dosage improved the resistance to crack formation and propagation, leading to higher compressive strength (Farnam *et al.*, 2010; Yang, 2011; Yoo, *et al.*, 2013).

However, the steel fibre length only had a minor effect on the compressive strength of TSSFRC, even at high fibre dosage. For instance, at a steel fibre dosage of 6%, the difference in compressive strength of TSSFRC mixtures made with short (i.e. 33 mm [1.3in.]) and long (i.e. 60 mm [2.4 in.]) steel fibres (i.e. MS6 and ML6) was about 2%. This was emphasized by ANOVA, which showed that the variation in fibre length had an insignificant effect on the mean of the total compressive strength results (**Table 5.3**). For example, the calculated F value of 0.09 for the total compressive strength at fibre dosages of 4% and 6% was lower

than the corresponding critical F value of 5.99 ($F_{0.05,\ 1,\ 6}$). Yet, in normal SFRC, the fibre length can significantly affect its compressive strength. At high steel fibre dosage (i.e. more than 2%), long fibres generally tend to ball in the concrete mixture, causing workability problems and associated reduction in compressive strength (Singh *et al.*, 2014). Conversely, such problems do not occur in TSSFRC since the fibres are premixed and preplaced in the mold with the coarse aggregates before injection of the grout.

5.3.2. Splitting Tensile Strength

The 28-day splitting tensile strength test results of TSSFRC mixtures incorporating different dosages of steel fibres having various lengths are presented in **Table 5.2**. It can be observed that the splitting tensile strength increased with increasing steel fibre dosage. This observation was confirmed by ANOVA since the F value of 76.17 was significantly larger than the corresponding critical F value of 5.19 ($F_{0.05,\ 4,\ 5}$) (**Table 5.3**). For instance, an increase in the splitting tensile strength of about 30% and 60% was observed for the MS1 and MS2 mixtures compared with that of the control fibreless mixture (M0), respectively. Generally, the tensile strength of concrete increases with the increase of the number of fibres that are aligned along the tensile force (Lee and Kim, 2010). Therefore, the orientation of the fibres within the cementitious matrix with respect to the tensile load greatly dominates its tensile strength. In conventional SFRC, the fibre distribution and orientation are affected by the concrete workability and the direction of concrete placing (Barnett *et al.*, 2010; Zofka *et al.*, 2014).

Increasing the steel fibre dosage beyond 2% tends to exhibit inadequate workability of SFRC along with a risk of fibre balling and improper distribution, which can result in a reduction of tensile strength (Boulekbache *et al.*, 2010). Conversely, for the TSSFRC mixtures having high steel fibre dosage (i.e. more than 2%), fibres are randomly distributed in the preplaced aggregate matrix, resulting in multiple fibres crossing any failure plane. Thus, higher fibre dosage results in higher tensile strength (Lee and Kim, 2010; Manoharan and Anandan, 2014). For example, the MS4 and MS6 mixtures achieved around 14% and 31% increase in splitting tensile strength compared with that of the MS2 mixture, respectively. Moreover, the splitting tensile strength of the TSSFRC specimens incorporating 6% fibre dosage was around double that of the control mixture (M0). This is attributed to the

role of steel fibres in intersecting, blocking and arresting crack propagation (Song and Hwang, 2004).

The fibre length had minor effects on the splitting tensile strength of TSSFRC. For example, the tensile strength of the ML2 mixture (made with 2% of long steel fibres (i.e.60 mm)) was only 5% higher than that of the MS2 mixture (made with 2% of short steel fibres (i.e. 33 mm)). Moreover, ANOVA confirmed that the variation in the fibre length had an insignificant effect on the mean of the tensile strength results. The calculated F value of 0.38 for the TSSFRC tensile strength results at fibre dosages of 1% and 2% was lower than the corresponding critical F value of 5.99 ($F_{0.05,\ 1,\ 6}$) (**Table 5.3**).

However, the slight increase in tensile strength for TSSFRC mixtures with long fibre can be attributed to the fact that TSC had relatively large internal voids around the aggregates due to bleeding of the grout mixture (Najjar *et al*., 2016). Therefore, these voids can adversely affect the fibre-matrix bond, especially in the case of short steel fibres, leading to a reduction in tensile strength. Long steel fibre have greater macro-crack bridging ability and bonded length than that of a short fibre, which can result in enhanced tensile strength (Brouwers *et al.*, 2014).

5.3.3. Flexural Strength and Load-Deflection Behaviour

The flexural strength test results of TSSFRC specimens made with different dosages of steel fibres having various lengths are reported in **Table 5.4**. Similar to conventional concrete, the addition of steel fibres modified the failure mode of the tested specimens from brittle to ductile. As expected, the flexural strength of TSSFRC improved significantly with the addition of steel fibres. For example, the MS1 and MS2 mixtures achieved about 22% and 41% higher flexural strength than that of the fibreless control mixture (M0). This has also been confirmed by statistical analysis (**Table 5.3**). For instance, ANOVA for the flexural strength results had F value of 8.85, which is larger than the corresponding critical F value of 5.19 ($F_{0.05,\ 4,\ 5}$). This means that the variation in the fibre dosage had a significant effect on the mean of the total flexural strength results.

Table 5.4 – Flexural test results of TSSFRC specimens

TSSFRC Mixture ID	Flexural Strength at First Crack			Flexural strength at Peak Load		Residual Strength (MPa)[*]	
	(MPa)[*]	COV (%)	δ1 (mm)[*]	(MPa)[*]	δ2 (mm)[*]	at δ of L/600 (0.75 mm)[*]	at δ of L/150 (3 mm)[*]
M0	3.7	6.8	0.049	3.7	0.049	--	--
MS1	4.5	2.8	0.049	4.5	0.049	2.1	1.3
MS2	5.2	4.2	0.040	5.2	0.040	3.8	1.1
MS4	5.3	3.6	0.057	6.6	0.279	5.6	3.2
MS6	7.2	1.9	0.048	9.2	0.316	8.6	5.4
ML1	4.0	3.1	0.041	4.0	0.041	1.8	1.4
ML2	4.5	3.8	0.035	4.8	0.279	3.7	2.4
ML4	7.4	1.9	0.057	9.5	0.345	8.2	5.1
ML6	8.4	2.0	0.051	12.7	0.518	12.4	7.6

* 1 in. = 25.4 mm, 1 ksi = 6.894 MPa

Generally, the flexural strength of normal SFRC is significantly affected by the fibre dosage, length, shape and orientation, along with the characteristics of the cementitious matrix. It was found that the flexural strength increases as the fibres get more oriented in the direction of the tensile flexural stresses (Boulekbache *et al.*, 2010). In conventional SFRC, the orientation and distribution of fibres are affected by the fibre dosage and the matrix workability, as well as the direction of concrete casting (Zofka *et al.*, 2014). High fibre dosage (e.g. more than 2%) can cause fibres to intermingle, leading to their improper distribution (Barnett *et al.*, 2010; Zofka *et al.*, 2014). Increasing the workability of SFRC can overcome this problem. However, high workable SFRC can suffer from bleeding and/or segregation of fibres and aggregates, with consequent reduction in flexural performance (Barnett *et al.*, 2010). On the other hand, during casting of SFRC, fibres tend to align perpendicular to the direction of concrete flow, leading to preferential improvement of flexural strength in one direction (Zofka *et al.*, 2014). Conversely, in TSSFRC mixtures, fibres can have closer to random distribution and will disperse more uniformly, even at high fibre dosages, allowing significant improvement in flexural strength at high fibre dosages not conceivable in normal concrete mixing method. For instance, the ML4 and ML6 mixtures showed 64% and 87% increase in flexural strength compared with that of the ML2 mixture, respectively. **Table 5.5** presents a comparison of the increase in the compressive and flexural strengths for various types of concrete versus TSSFRC. It was observed that TSSFRC achieved superior increase in the flexural strength compared with that of the SFRC and

HSFRC (i.e. high-strength fibre-reinforced concrete) (Barr *et al.*, 1996; Berhe, 2014). Interestingly, TSSFRC mixture incorporating 6% steel fibres having length of 60 mm exhibited about 9% higher increase in the flexure strength compared with that of the UHPFRC (i.e. ultra-high performance fibre-reinforced concrete) incorporating 6% steel fibres having length of 16 mm (Abbas *et al.*, 2015).

Table 5.5 – Increase in the compressive and flexural strengths for various types of concrete incorporating high steel fibre dosages compared with their plain concrete

Concrete Type	Steel Fibre Length (mm)[*]	Steel Fibre Dosage (Vol. %)	Increase in Compressive Strength (%)	Increase in Flexural Strength (%)
SFRC (Barr *et al.*, 1996)	40	2	5	8
		3	7	17
HSFRC[a] (Berhe, 2014)	19	2	19	27
		4	8	32
UHPFRC[b] (Abbas *et al.*, 2015)	16	3	9	112
		6	13	223
UHPFRC[b] (Kazemi and Lubell, 2012)	13	4	18	82
		5	25	132
TSSFRC	33	2	18	41
		4	30	78
		6	49	149
	60	2	22	30
		4	31	157
		6	52	243

[*] 1 in. = 25.4 mm.
[a] HSFRC refers to high-strength fibre-reinforced concrete.
[b] UHPFRC refers to ultra-high performance fibre-reinforced concrete.

Figures 5.3 and **5.4** illustrate the load-deflection curves for TSSFRC specimens incorporating different dosages of short and long steel fibres, respectively. The initial stiffness of the load-deflection curves was generally comparable, while peak load increased with increasing steel fibre dosage. At low steel fibre dosage (i.e. 1%), TSSFRC specimens exhibited sudden increase in deflection coupled with a reduction in load capacity. For example, at the first crack, the defection of the MS1 specimens increased suddenly from 0.049 mm to 0.558 mm, while the corresponding load dropped from 33.8 kN to 18.4 kN. This can be attributed to rapid crack opening once the crack formed due to insufficient number of fibres bridging the crack (Magnusson, 2006). Moreover, the TSSFRC specimens incorporating 1% and 2% steel fibre dosage showed a deflection-softening behaviour after

first crack followed by a progressive load reduction as crack width increased. However, increasing the steel fibre dosage led to improvements in the post-peak flexural behaviour. It was observed that the TSSFRC specimens incorporating 4% and 6% steel fibre dosage exhibited a deflection–hardening behaviour due to the higher load-carrying capacity generated after the first cracking (**Figures 5.3** and **5.4**). At the high steel fibre dosages of 4% and 6%, fibres bridging micro-cracks can prevent their early development into principle cracks. Thus, multiple simultaneous cracks can be initiated, resulting in more favourable crack distribution (Magnusson, 2006). Since TSSFRC tends to have a random fibre orientation, at high steel fibre dosage, the crack path becomes more tortuous. Thus, much higher energy is required to de-bond and pull-out the fibres (Ostertag and Yi, 2007).
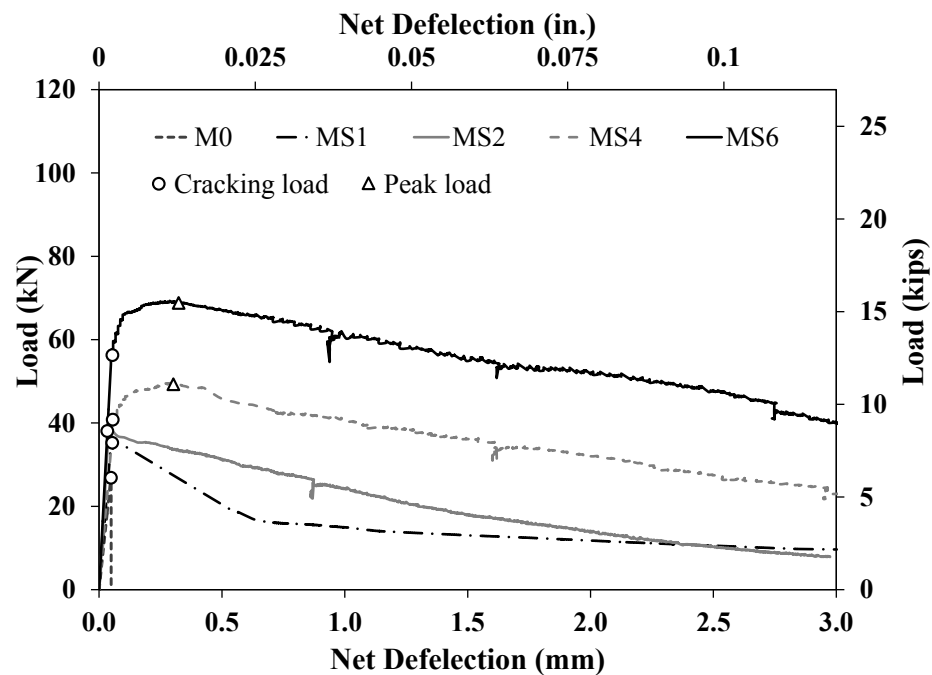
Figure 5.3 – Load-deflection curves for TSSFRC specimens incorporating different dosages of short steel fibres.
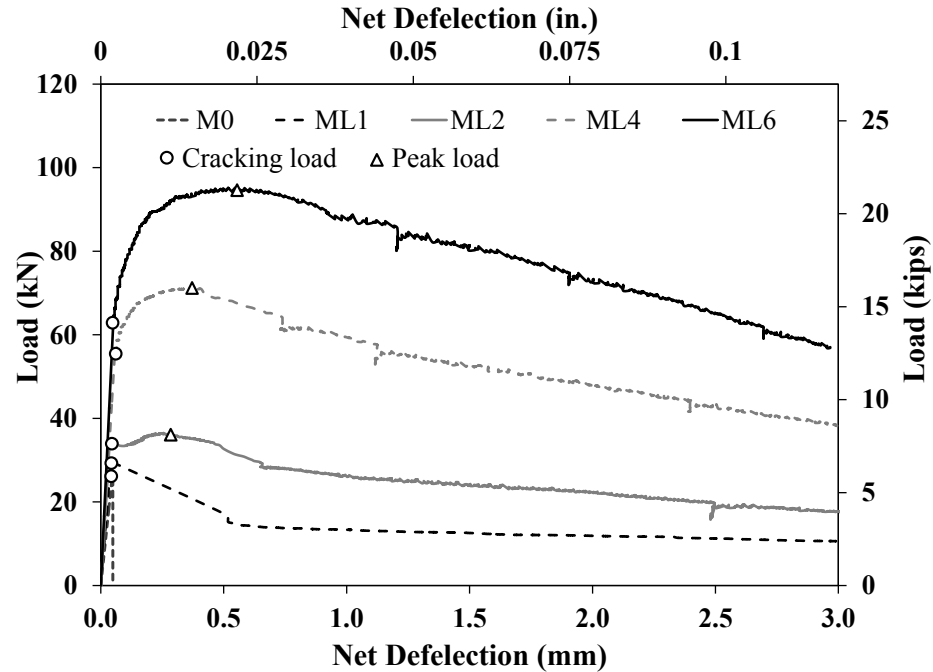
Figure 5.4 – Load-deflection curves for TSSFRC specimens incorporating different dosages of long steel fibres.

Based on the ANOVA results in **Table 5.3**, the variation in the fibre length did not significantly affect the mean of the total flexural strength results at fibre dosages of 1% and 2%. For example, the calculated F value of 3.26 was less than the corresponding critical F value ($F_{0.05, 1, 6}$). Conversely, at steel fibre dosages of 4% and 6%, ANOVA for the flexural strength results had F value of 7.12, which is larger than the critical F value ($F_{0.05, 1, 6}$). This means the variation in the fibre length significantly affect the mean of flexural strength results at 4% and 6% fibre dosages.

At low fibre dosage (i.e. 1%), TSSFRC with short steel fibres (i.e. 33 mm) exhibited higher resistance to the initiation of the first crack than that of TSSFRC incorporating longer fibres (i.e. 60 mm). For example, the flexural strength of the MS1 mixture at first crack was 13% higher than that of the ML1 mixture (**Table 5.4**). This can be attributed to the greater number of short steel fibres in the MS1 mixture compared to that of the ML1 mixture, resulting in better crack bridging ability. On the other hand, for the ML1 mixture, long steel fibres had larger inter-fibre spacing, thus weakening its flexural performance (Abbas *et al.*, 2015).

Moreover, the TSSFRC MS2 mixture incorporating 2% of short steel fibres exhibited 16% increase in flexural strength compared with that of the ML2 TSSFRC mixture having a similar dosage of the longer fibre. However, the ML2 mixture showed better post-crack behaviour than that of the MS2 mixture (**Figures. 5.3 and 5.4**). After the first crack, the short fibres require less energy to be pulled out, leading to more sudden increase in deflection coupled with a reduction in load capacity. Conversely, longer steel fibres have an average greater embedment length, resulting in greater resistance to pull-out. **Figure 5.5(a)** illustrates typical fibre pull-out for the TSSFRC specimens made with short steel fibres, while **Figure 5.5(b)** shows the crack bridging mechanism in TSSFRC specimens incorporating the longer steel fibres.
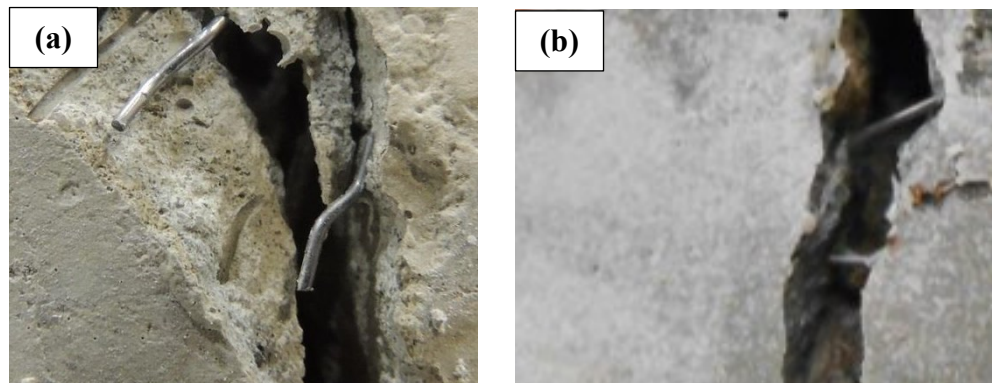
Figure 5.5 – Cracking patterns of TSSFRC specimens showing: (a) short steel fibres pull-out, and (b) crack bridging by long steel fibres.

On the other hand, specimens from mixtures ML4 (4% long fibre) and ML6 (6% long fibre) exhibited 39% and 16% lower flexural strength than that of specimens from mixtures MS4 and MS6, incorporating corresponding dosages of the short fibre, respectively. The long steel fibres allowed achieving enhanced post-crack behaviour compared to that of the short fibres. For example, specimens from the TSSFRC mixtures MS4 and ML4 exhibited substantial strain hardening and peak loads of 49.5 kN and 71.1 kN, respectively. The residual load for ML4 specimens at a corresponding deflection of 0.75 mm was 45% higher than that of the MS4 specimens since the long steel fibres had longer embedment length, leading to higher resistance to fibre pull-out. Furthermore, at high fibre dosages, fibres

become closer to each other, and thus more effective in restraining the growth of micro-cracks (Mohamed, *et al.*, 2014; Abbas *et al.*, 2015).

5.3.4. Toughness

The toughness test results of specimens made from the various TSSFRC mixtures incorporating different dosages of steel fibres having different lengths is presented in **Table 5.6**. As expected, toughness values increased with increasing steel fibre dosage. This was emphasized by ANOVA, which showed that the variation in fibre dosage had a significant effect on the mean of total toughness results (**Table 5.3**). The *F* value of 16.93 was significantly higher than the corresponding critical *F* value of 5.19 ($F_{0.05, 4, 5}$). For example, specimens from mixture ML2 (2% long fibre) achieved about 77% higher toughness than that of specimens from mixture ML1 (1% long fibre). Moreover, specimens from mixtures ML4 and ML6 achieved 2 and 3 times higher toughness than that of specimens from mixture ML2, respectively. Generally, higher steel fibre dosage leads to increased energy for fibre pull-out, consequently, enhancing toughness (Köksal, *et al.*, 2008).

Furthermore, the toughness of TSSFRC was significantly affected by the fibre length. According to the statistical analysis in **Table 5.3**, the variation in the fibre length did not significantly affect the mean of the total toughness results at 1% and 2% fibre dosage as the calculated *F* value of 0.36 was less than the corresponding critical *F* value ($F_{0.05, 1, 6}$). Conversely, at fibre dosage of 3% and 4%, ANOVA for the toughness results had *F* value of 6.55, which is larger than the critical *F* value ($F_{0.05, 1, 6}$). This means the variation in the fibre length significantly affect the mean of the toughness results at 4% and 6% fibre dosages.

At a relatively low fibre dosage of 1%, specimens from mixture MS1 (1% short fibre (i.e. 33 mm)) reached 8% higher toughness than that of specimens from mixture ML1 (1% long fibre (i.e. 60 mm)). This can be attributed to that the greater number of fibres in MS1 specimens, which achieved better ability of crack bridging (Brouwers *et al.*, 2014). Conversely, at higher steel fibre dosage (i.e. 4% and 6%), specimens from the TSSFRC mixtures incorporating longer fibres exhibited higher toughness compared to that of specimens from mixtures incorporating similar dosage of the shorter fibre. In conventional SFRC, high dosage of long fibres can affect the relative mobility of coarse aggregates due to dimensional compatibility between fibres and aggregates (Figueiredo and Ceccato, 2015).

Moreover, the greater the size of aggregate particles, the more fibre balling and interaction occurs, consequently reducing toughness (Sahmaran *et al.*, 2009). However, in TSSRC, the longer fibre could bridge cracks more effectively at high fibre dosage since fibre balling and interaction are absent. Moreover, TSSFRC incorporating long fibres combined with relatively large aggregate particle size (i.e. 40 mm [1.57 in.] crushed limestone aggregate) could achieve higher fracture toughness due to increased resistance to crack propagating (Chen and Juanyu, 2004). For instance, the toughness of specimens from mixture ML4 (4% long fibre) was 1.5 times that of specimens from mixture MS4 (4% short fibre). This can be ascribed to significant improvements in post-peak behaviour of TSSFRC specimens imparted by the longer steel fibres as explained earlier.

5.3.5. Flexural Toughness Indices

Flexural toughness indices are commonly used to evaluate the flexural toughness of concrete. The higher the value of flexural toughness indices, the higher is the flexural toughness of concrete (Appa and Sreenivasa, 2009; Zhang *et al.*, 2014). The toughness indices values (I_5, I_{10}, I_{20}, and I_{30}) for the control fibreless specimens were equal to 1.0 since these specimens failed once they reached their ultimate flexural strength. Indeed, they possess no significant post-carking toughness (Yap *et al.*, 2014). **Figures 5.6** and **5.7** illustrate the variation in flexural toughness indices for tested specimens from the various TSSFRC mixtures incorporating different dosages of short and long steel fibres, respectively. It can be observed that the steel fibre dosage had a paramount effect on the flexural toughness indices. For example, the value of I_{20} for specimens from mixture ML2 (2% long fibre) was 34% higher than that of ML1 (1% long fibre) specimens. As the first crack was initiated, additional energy was required to pull-out the steel fibres from the cementitious matrix for crack propagation to proceed further. Increasing the steel fibre dosage is known to enhance the post-cracking behaviour (Yap *et al.*, 2014). It was reported that maximum toughness indices values for conventional SFRC were achieved when the steel fibre content was 2%, while those values dropped down after the steel fibre dosage exceeded 2% (Zhang *et al.*, 2014). In contrast, in TSSFRC, an increase of 12% and 24% in the I_{20} value was observed for the ML4 (4% fibre) and ML6 (6% fibre) specimens compared with that of ML2 (2% fibre) specimens, respectively.
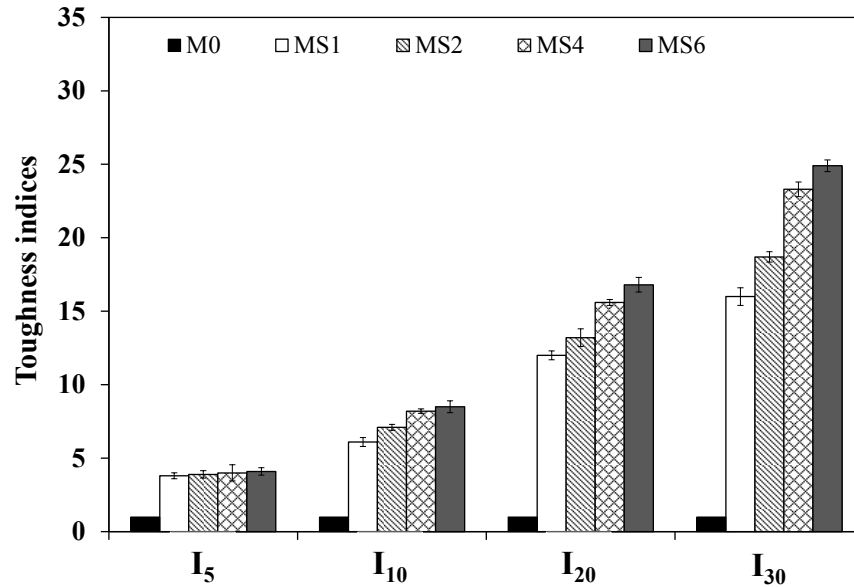
**Figure 5.6 – Toughness indices for TSSFRC specimens incorporating different dosages
of short steel fibres.**
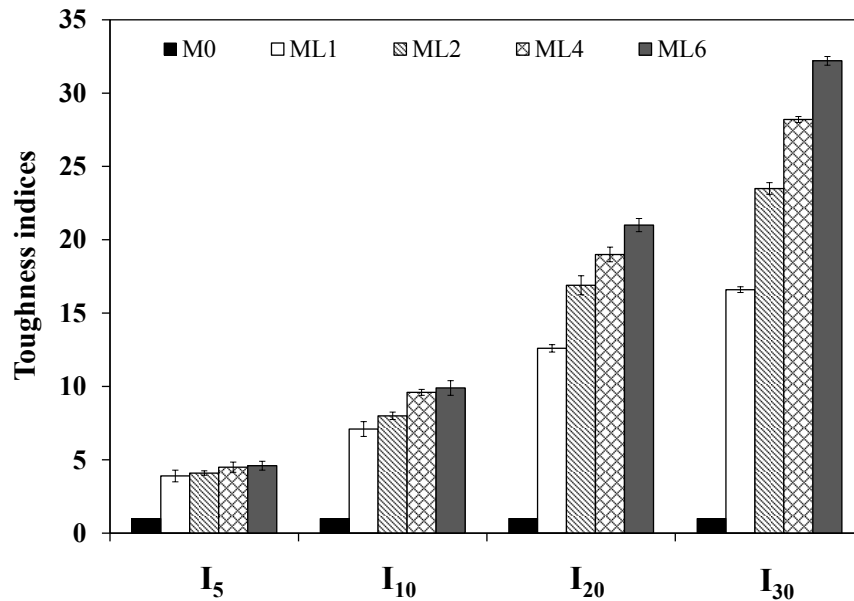
**Figure 5.7 – Toughness indices for TSSFRC specimens incorporating different dosages
of long steel fibres.**

Furthermore, it was found that TSSFRC specimens incorporating the long steel fibre (i.e.
60 mm) had greater toughness indices than that of specimens made with similar dosage of the
short fibre (i.e. 33 mm). For instance, the I_5, I_{10} and I_{20} values for ML2 specimens were 5%,

13% and 28% higher than that of MS2 specimens, respectively. Moreover, ML6 specimens achieved the highest values of toughness indices. This is can be ascribed to the relatively high dosage of long steel fibres, which imparted superior post-cracking behaviour owing to its longer embedment length, consequently leading to greater energy of fibre pull-out, and thus improved flexural toughness (Abbas *et al.*, 2015).

5.3.6. Residual Flexural Strength Factor

The residual strength factor of tested specimens made from the various TSSFRC mixtures incorporating various dosages of long and short steel fibres are presented in **Table 5.6** and further illustrated in **Figures 5.8** and **5.9**. It can be observed that the residual strength factors increased as the steel fibre dosage increased. For example, the R_{10-20} value for MS2 specimens was 3% higher than that for MS1 specimens. Increasing the short steel fibre dosage from 1 to 2%, 4% and 6% resulted in 3% 26% and 41% higher residual strength factor (R_{10-20}), respectively. This can be attributed to the fact that TSSFRC specimens incorporating higher steel fibre dosage (i.e. more than 2%) required higher energy for fibre pull-out, thus exhibiting higher residual strength after first crack initiation (Yap *et al.*, 2014). Furthermore, it was observed that TSSFRC specimens incorporating longer steel fibres (i.e. 60 mm) sustained higher post-cracking load than that of specimens incorporating short fibres (i.e. 33 mm). For example, the R_{20-30} for the ML2 specimens was 22% higher than that for MS2 specimens. Moreover, the R_{20-30} for ML6 specimens was 40% greater than that for the MS6 specimens. This can be attributed to the high toughness indices of TSSFRC specimens incorporating 6% of the long fibre as discussed earlier.

Table 5.6 – Fracture toughness and residual strength of TSSFRC specimens

TSSFRC Mixture ID	Toughness		Toughness Indices				Residual Strength Factors		
	(J)	COV%	I_5	I_{10}	I_{20}	I_{30}	R_{5-10}	R_{10-20}	R_{20-30}
M0	0.9	3.5	1.0	1.0	1.0	1.0	0.0	0.0	0.0
MS1	45.6	5.5	3.8	6.1	12.0	16.0	46.0	59.0	40.0
MS2	59.4	3.3	3.9	7.1	13.2	18.7	65.0	61.0	54.5
MS4	107.4	3.0	4.0	8.2	15.6	23.3	84.0	74.5	77.0
MS6	167.2	1.8	4.1	8.5	16.8	24.9	88.0	83.0	81.0
ML1	42.3	2.8	3.9	7.1	12.6	16.6	65.0	54.5	40.5
ML2	75.0	1.9	4.1	8.0	16.9	23.5	77.0	89.0	66.5
ML4	160.4	1.2	4.5	9.6	19.0	28.2	103.0	94.0	93.0
ML6	231.8	1.6	4.6	9.9	21.0	32.2	106.0	109.5	113.5

* 1 ft. lbs. = 1.356 J
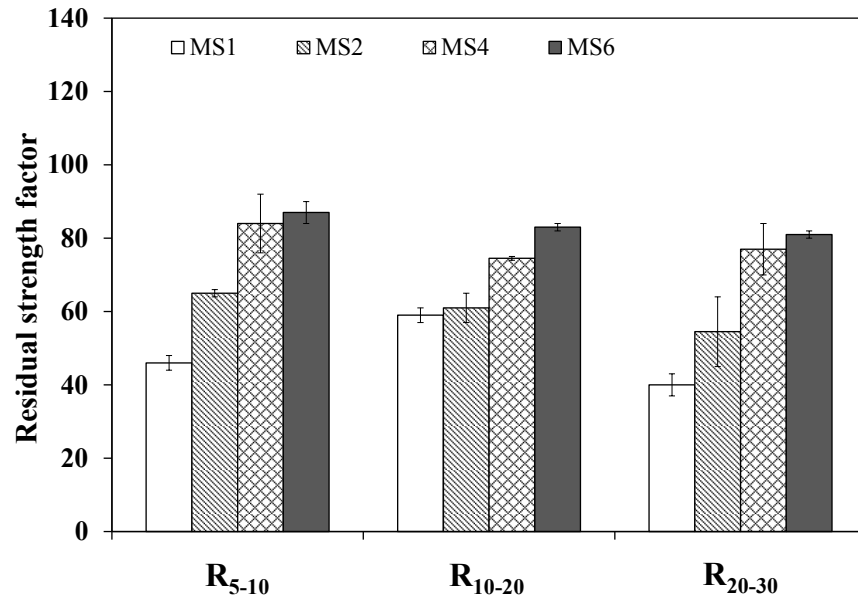
Figure 5.8 – Residual strength factors for TSSFRC specimens incorporating different dosages of short steel fibres.
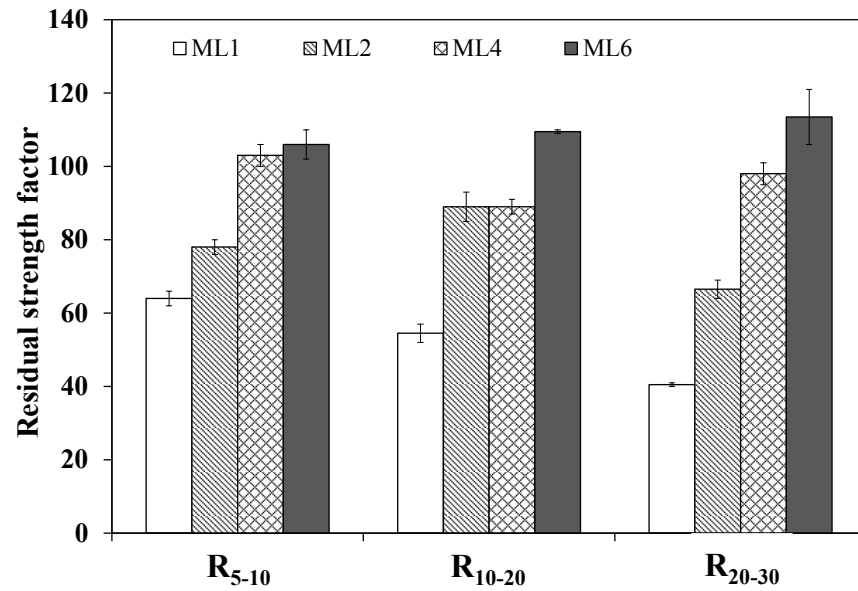
Figure 5.9 – Residual strength factors for TSSFRC specimens incorporating different dosages of long steel fibres.

5.4. CONCLUSIONS

The present study investigates the mechanical properties of two-stage steel fibre-reinforced concrete (TSSFRC), which so far has not been explored in the open literature. TSSFRC is made by first placing previously dry-mixed coarse aggregates and steel fibres in a mold or formwork, and then injecting the internal voids with a grout having adequate flow properties. The conclusions emanating from this experimental study can be summarized as follows:

- The compressive and tensile strengths of TSSFRC increased with increasing steel fibre dosage. In particular, a high steel fibre dosage (6%) achieved significant improvement in TSSFRC compressive and tensile strengths. Conversely, the steel fibre length had only a slight effect on the compressive and tensile strengths of TSSFRC.

- The flexural strength and post-crack behaviour of TSSFRC were greatly enhanced by steel fibre addition. Higher steel fibre length also had significant influence on the flexural strength and post-crack behaviour. TSSFRC specimens incorporating 6% of the long steel fibre achieved best post-crack behaviour.

- The addition of steel fibres greatly enhanced the flexural toughness and residual strength of TSSFRC. Highest values of toughness indices were obtained for TSSFRC specimens having 6% of steel fibre dosage.

- In conventional steel fibre-reinforced concrete, optimal mechanical performance is usually reached at a fibre dosage of around 2% since greater dosages tend to cause serious concrete consolidation problems emanating from fibre intermingling and interaction. Conversely, TSSFRC can be produced with 6% of long steel fibres and even higher dosages, thus allowing to achieve superior mechanical performance.

5.5. REFERENCES

Abbas, S., Soliman, A. and Nehdi, M., (2015), "Exploring mechanical and durability properties of ultra-high performance concrete incorporating various steel fibre lengths and dosages," *Construction and Building Materials*, Vol. 75, pp. 429-441.

Abdelgader, H. S., (1996), "Effect of quantity of sand on the compressive strength of two-stage concrete," *Magazine of Concrete Research*, Vol. 48, No. 177, pp. 353-360.

Abdelgader, H., Saud, A. and El-Baden, A., (2013), "Flexural strength of two-stage concrete," *Proceedings of the Third International Conference on Sustainable Construction Materials and Technologies (SCMT3)*, Kyoto, Japan.

Abdul Awal, A. S., (1984), "Manufacture and properties of pre-packed aggregate concrete," *Master Thesis*, University of Melbourne, Australia, 121 p.

ACI 304.1, (2005), "Guide for the use of preplaced aggregate concrete for structural and mass concrete applications," *American Concrete Institute*, Farmington Hills, Michigan, USA, 19 p.

ACI 544.1R, (2002), "Reports on fibre reinforced concrete," *American Concrete Institute*, Farmington Hills, Michigan, USA, 66 p.

Appa Rao, G. and Sreenivasa Rao, A., (2009), "Toughness indices of steel fibre reinforced concrete under mode II loading," *Materials and Structures/Materiaux et Construction*, Vol. 42, pp. 1173-1184.

ASTM C1018, (1997), "Standard test method for flexural toughness and first-crack strength of fibre-reinforced concrete (using beam with third-point loading)," A*merican Society for Testing and Materials*, West Conshohocken, PA, USA.

ASTM C1609/C1609M, (2012), "Standard test method for flexural performance of fibre-reinforced concrete (using beam with third-point loading," A*merican Society for Testing and Materials*, West Conshohocken, PA, USA, 9p.

ASTM C496/C496M, (2011), "Standard test method for splitting tensile strength of cylindrical concrete specimens," A*merican Society for Testing and Materials*, West Conshohocken, PA, USA.

ASTM C943, (2010), "Standard practice for making test cylinders and prisms for determining strength and density of pre-placed-aggregate concrete in the laboratory," A*merican Society for Testing and Materials*, West Conshohocken, PA, USA.

Aydin, S., (2013), "Effects of fiber strength on fracture characteristics of normal and high strength concrete," *Periodica Polytechnica Civil Engineering*, Vol. 57, No. 2, pp. 191-200.

Barnett, S.J., Lataste, J., Parry, T., Millard, S.G. and Soutsos, M.N., (2010), "Assessment of fibre orientation in ultra-high performance fibre reinforced concrete and its effect on flexural strength," *Materials and Structures*, Vol. 43. No. 7, pp. 1009-1023.

Barr, B., Gettu, R., Al-Oraimi, S.K. and Bryars, L.S., (1996), "Toughness measurement-The need to think again," *Cement and Concrete Composites*, Vol. 18, No. 4, pp. 281-297.

Berhe, A., (2014), "Follow high strength steel fiber reinforced flow-able or SCC concrete with variable fiber by volume fractions for thin plate and shell structures," *PhD thesis*, University of Nevada, Las Vegas, Nevada, USA.

Boulekbache, B., Hamrat, M., Chemrouk, M. and Amziane, S., (2010) "Flowability of fibre-reinforced concrete and its effect on the mechanical properties of the material," *Construction and Building Materials*, Vol. 24, No. 9, pp. 1664-1671.

C.P. Ostertag, C.P. and Yi, CK., (2007), "Crack/Fiber interaction and crack growth resistance behavior in microfiber reinforced mortar specimens," *Materials and Structures*, Vol. 40, No. 7, pp. 679-691.

Chen, B. and Juanyu, L., (2004), "Effect of aggregate on the fracture behavior of high strength concrete," *Construction and Building Materials*, Vol. 18, No. 8, pp. 585-590.

Coo, M. and Pheeraphan, T., (2015), "Effect of sand, fly ash, and coarse aggregate gradation on preplaced aggregate concrete studied through factorial design," *Construction and Building Materials*, Vol. 93, pp. 812-821

Farnam, Y., Moosavi, M., Shekarchi, M., Babanajad, S.K. and Bagherzadeh, A., (2010), "Behaviour of slurry infiltrated fibre concrete (SIFCON) under triaxial compression," *Cement and Concrete Research*, Vol. 40, No. 11, pp. 1571-1581.

Figueiredo, A.D. and Ceccato, M.R., (2015), "Workability analysis of steel fiber reinforced concrete using slump and Ve-Be test," *Materials Research*, Vol. 18, No. 6, pp. 1284-1290.

Holschemacher, K., Mueller, T. and Ribakov, Y., (2010), "Effect of steel fibres on mechanical properties of high-strength concrete," *Materials and Design*, Vol. 31, No. 5, pp. 2604-2615.

Ikraiam, F., Abd El-Latif, A., Abd ELazziz, A. and Ali, J., (2009), "Effect of steel fibre addition on mechanical properties ond γ-ray attenuation for ordinary concrete used pn El-Gabal El-Akhdar area in Libya for radiation shielding purposes," *Arab Journal of Nuclear Science and Applications*, Vol. 42, pp. 287-295.

Kazemi, S. and Lubell, A.S., (2012), "Influence of specimen size and fiber content on mechanical properties of ultra-high-performance fiber-reinforced concrete," *ACI Material Journal*, Vol. 109, No. 6, pp. 675-684.

Köksal, F., Altun, F., Yiğit, İ. and Şahin, Y., (2008), "Combined effect of silica fume and steel fibre on the mechanical properties of high strength concretes," *Construction and Building Materials*, Vol. 22, No. 80, pp. 1874-1880.

Lee, C. and Kim, H., (2010), "Orientation factor and number of fibers at failure plane in ring-type steel fiber reinforced concrete," *Cement and Concrete Research*, Vol. 40, pp. 810-819.

Magnusson, J., (2006), "Fibre reinforced concrete beams subjected to air blast loading," *Int. Journal of Nordic Concrete Research*, Vol. 35, pp. 18-34.

Manoharan, S.V. and Anandan, S., (2014), "Steel fibre reinforcing characteristics on the size reduction of fly ash based concrete," *Advances in Civil Engineering*, Vol. 2014, pp. 1-11.

Mohamed, N., Soliman, A. and Nehdi, M., (2014), "Full-scale pipes using dry-cast steel fibre-reinforced concrete," *Construction and Building Materials*, Vol. 72, pp. 411-422.

Montgomery, D.C., (2013), "Design and analysis of experiments," 8_{th} Edition, *Wiley Subscription Services, Inc*.

Najjar, M., Soliman, A. and Nehdi, M., (2014), "Critical overview of two stage concrete: properties and applications," *Construction and Building Materials*, Vol. 62, pp. 47-58.

Najjar, M., Soliman, A. and Nehdi, M., (2016), "Two-stage concrete made with single, binary and ternary binders," *Materials and Structures*, Vol. 49, No. 1, pp. 317-327.

O'Malley, J. and Abdelgader, H., (2010), "Investigation into viability of using two stage (pre-placed aggregate) concrete in an Irish setting," *Frontiers of Architecture and Civil Engineering in China*, Vol. 4, No. 1, pp. 127-132.

Şahin Y. and Köksal, F., (2011), "The influences of matrix and steel fibre tensile strengths on the fracture energy of high-strength concrete," *Construction and Building Materials*, Vol. 25, No. 4, pp. 1801-1806.

Sahmaran, M., Lachemi, M., Hossain, K.M.A., Ranade, R. and Li, V.C., (2009), "Influence of aggregate type and size on ductility and mechanical properties of engineered cementitious composites," *ACI Material Journal*, Vol. 106, No. 3, pp. 308-316.

Sahoo, D., Solanki, A. and Kumar, A., (2015), "Influence of steel and polypropylene fibres on flexural behavior of Rc beams," *Journal of Materials in Civil Engineering*, Vol. 27, No. 8, pp. 1-9.

Singh, M.P., Singh, S.P. and Singh, A.P., (2014), "Experimental study on the strength characteristics and water permeability of hybrid steel fibre reinforced concrete," *International Scholarly Research Notices*, Vol. 2014, pp. 1-10.

Song, P.S. and Hwang, S., (2004), "Mechanical properties of high-strength steel fibre reinforced concrete," *Construction and Building Materials*, Vol. 18, No. 9, pp. 669-673.

Yang, K., (2011), "Tests on concrete reinforced with hybrid or monolithic steel and polyvinyl alcohol fibres," *ACI Materials Journal*, Vol. 108, No. 6, pp. 664-672.

Yap, S., Bu, C., Alengaram, U., Mo, K. and Jumaat, M., (2014), "Flexural toughness characteristics of steel-polypropylene hybrid fibre-reinforced oil palm shell concrete," *Materials and Design*, Vol. 57, pp. 652-659.

Yoo, D., Joo, H. and Young, S., (2013), "Effect of fibre content on mechanical and fracture properties of ultra high performance fibre reinforced cementitious composites," *Composite Structures*, Vol. 106, pp. 742-753.

Yu, R., Spiesz, P. and Brouwers, H.J.H, (2014), "Static properties and impact resistance of a green ultra-high performance hybrid fibre reinforced concrete (UHPHFRC): experiments and modeling," *Construction and Building Materials*, Vol., 68, pp. 158-171.

Zhang, P., Zhao, Y., Li, Q., Wang, P. and Zhang, T., (2014), "Flexural toughness of steel fibre reinforced high performance concrete containing nano-Sio_2 and fly ash," *The Scientific World Journal*, Vol. 2014, pp. 1-11.

Zofka, A., Paliukaite, M., Vaitkus, A., Maliszewska, D., Josen, R. and Bernier, A., (2014), "Laboratory study on the influence of casting on properties of UBPFRC specimens," *Journal of Civil Engineering and Management*, Vol. 20, No. 3, pp. 380-388.

Chapter 6

6. DURABILITY OF TWO-STAGE CONCRETE TO CHEMICAL AND PHYSICAL SULFATE ATTACK[(*)]

6.1. INTRODUCTION

The deterioration of concrete due to sulfate attack is a complex process that has been widely investigated over several decades. Various damage mechanisms including expansion, cracking, spalling, and loss of strength can manifest in concrete sulfate attack. It has been argued that sulfate attack on concrete can be categorized into chemical and physical phenomena, depending on the sulfate exposure regime. The exposure condition could be through full immersion in a sulfate solution, cyclic wetting and drying in a sulfate rich media, or partial immersion under cyclic temperature and relative humidity.

Chemical sulfate attack arises from various chemical reactions between sulfate ions migrating into the concrete and cement hydration products, leading to alteration of the composition of the cementitious matrix. For example, sulfate ions can react with calcium hydroxide (CH) to form gypsum (C$\bar{\text{S}}$H$_2$). Moreover, secondary ettringite (C$_6$A$\bar{\text{S}}_3$H$_{32}$) can be produced through the reaction of hydrated calcium aluminate (C$_4$AH$_{13}$), monosulfate (C$_4$A$\bar{\text{S}}$H$_{12-18}$) or tri-calcium aluminate (C$_3$A) with the gypsum formed during the first reaction (Mehta, 2000; Skalny *et al*., 2002). Formation of gypsum and ettringite is usually combined with an increase in volume of the reactant materials by about 1.2 to 2.2 times, thus leading to expansion and cracking (Hooton, 1993). Furthermore, in the presence of sulfate and carbonate ions, abundant moisture and low temperature, thaumasite (C$_3$S$\bar{\text{S}}\bar{\text{C}}H_{15}$) can form with decomposition of the calcium silicate hydrate (CSH) phases, resulting in strength loss of concrete (Skalny *et al*., 2002; Skaropoulou *et al*., 2009; Nielsen *et al*., 2014).

On the other hand, concrete can be vulnerable to physical sulfate attack. This process usually occurs at the concrete surface in contact with the sulfate solution under varying

---

temperature and relative humidity conditions (Haynes *et al.*, 2008). Physical sulfate attack is generally a result of the cyclic conversion of sulfate salts from hydrated to un-hydrated forms, which is combined with a volume increase. For example, the conversion of sodium sulfate from its un-hydrated phase (i.e. thenardite Na_2SO_4) to the hydrous form (i.e. mirabilite Na_2SO_4-$10H_2O$) is combined with an increase in volume of about 314% (Haynes *et al.*, 2008; Scherer, 2004; Bassuoni and Nehdi, 2009).

The extent of damage to concrete due to chemical sulfate attack typically depends on the composition of the binder used, the concrete mixture design (especially *w/b* ratio) and the severity of exposure. It is well documented that using SCMs such as fly ash, silica fume and natural pozzolans enhanced the durability of conventional concrete fully immersed in sulfate solutions (e.g. Mehta, 1992; Mangat and Khatib, 1993; Skalny *et al.*, 2002). However, under physical sulfate attack, the extent of damage mainly relates to the pore structure of the cementitious matrix and its tensile strength. The higher the volume of micro-pores connected with large pores, the more severe will be the damage due to salt crystallization (Nehdi *et al.*, 2014; Haynes and Bassuoni, 2011). Hence, while SCMs enhance the durability of concrete to chemical sulphate attack, it may reduce its resistance to physical sulphate attack. Indeed, SCMs tend to refine porosity, leading to higher capillary rise in concrete, and thus can cause more severe surface scaling (Nehdi *et al.*, 2014).

Two-stage concrete, also known as pre-placed aggregate concrete, has been successfully used for many years in various applications, such as underwater construction and in the rehabilitation of various concrete structures (ACI 304.1, 2005; Najjar *et al.*, 2014). TSC is cast differently from normal concrete. Coarse aggregates are first preplaced, and then injected with a mixture of cement, water, fine sand and possibly chemical admixtures, commonly termed "grout" in TSC practice. Due to the particular effects of this unique casting process on the end product, the durability of TSC needs special focus, even for those aspects that are well established for normal concrete technology. However, data on TSC durability is still scarce.

According to the ACI 304.1 (2005) (Guide for the Use of Preplaced Aggregate Concrete for Structural and Mass Concrete Applications), TSC was very durable when exposed to aggressive environments. Recently, a field investigation on the TSC piles of the Tasman

Bridge in Australia was conducted after 48 years of service. By examining core samples extracted from these piles, it was revealed that the sulfate concentrations at the reinforcement bar level ranged from 1.3% to 3.8% by cement mass. Such values were considered very low for such a long exposure to a severe environment (Berndt, 2012). However, the effect of SCMs on the durability of TSC exposed to various sulfate regimes is still largely unexplored and lacks dedicated research. There is only scant related data in the open literature.

Therefore, to fill this knowledge gap, the present study explores the performance of TSC made with single, binary and ternary binders exposed to different environments conducive to physical and chemical sulfate attack. The findings should outline the mechanisms of damage of TSC incorporating SCMs under various sulfate exposure regimes and point out to needed future research in this area.

6.2. EXPERIMENTAL PROGRAM

6.2.1. Materials and Concrete Mixture Proportions

Control TSC mixtures were prepared using both ordinary portland cement (OPC) and high sulphate resistant cement (HSRC). Three types of SCMs including fly ash (FA), silica fume (SF), and metakaolin (MK) were added as partial replacement for OPC in binary and ternary binders. Physical and chemical properties of the used binders are listed in **Table 6.1**. Crushed limestone coarse aggregate with a maximum nominal size of 40 mm, a saturated surface dry specific gravity of 2.65 and a water absorption of 1.63% was used. Silica sand with a fineness modulus of 1.47 and a saturated surface dry specific gravity of 2.65 was used as fine aggregate. A poly-carboxylate high-range water-reducing admixture (HRWRA) was used to adjust the flowability of the grout mixtures within the recommended efflux time (i.e. 35-40 ± 2 sec) according to ACI 304.1 (2005). All grout mixtures had the same sand-to-binder ratio (s/b = 1.0) and water-to-binder ratio (w/b = 0.45). Several trial grout mixtures for each type of binder were conducted in order to identify the optimum HRWRA dosage that meets the recommended efflux time of grout (i.e. 35-40 ± 2 sec) for high strength TSC according to ACI 304.1 (2005). The mixture composition for all used TSC grouts is shown in **Table 6.2**.

Table 6.1 – Chemical analysis and physical properties of OPC, HSRC, FA, SF, and MK

	OPC	HSRC	FA	SF	MK
SiO_2 (%)	19.60	22.0	43.39	95.30	53.50
Al_2O_3 (%)	4.80	4.10	22.08	00.17	42.50
CaO (%)	61.50	64.90	15.63	00.49	0.20
Fe_2O_3 (%)	3.30	4.40	7.74	00.08	1.90
SO_3 (%)	3.50	2.25	1.72	00.24	0.05
Na_2O (%)	0.70	--	1.01	00.19	0.05
Loss on ignition (%)	1.90	0.7	1.17	4.7	0.50
Specific gravity	3.15	3.12	2.50	2.20	2.60
Surface area (m^2/kg)	371	380	280	19500	15000

Table 6.2 – TSC grout mixture proportions

TSC grout Mixture	Binder Proportions (%)	Binder (kg/m^3)					Sand (kg/m^3)	Water (kg/m^3)
		OPC	HSRC	FA	SF	MK		
C	100OPC	874	--	--	--	--	874	393
SR	100HSRC	--	871	--	--	--	871	392
F3	70OPC-30FA	599	--	257	--	--	855	385
F5	50OPC-50FA	422	--	422	--	--	843	379
S1	90OPC-10SF	777	--	--	86	--	863	388
SF4	50OPC-10SF-40FA	420	--	336	84	--	839	378
M1	90OPC-10MK	782	--	--	--	87	868	391
MF4	50OPC-10MK-40FA	422	--	338	--	84	844	380

6.2.2. Experimental Procedures

Different TSC specimens were prepared for each mixture. Initially, all molds were filled with the limestone coarse aggregate and then the specific grout was injected, similar to the procedures adopted in previous TSC studies (e.g. Abdelgader *et al.*, 2010; O'Malley and Abdelgader, 2010). Specimens were covered with wet burlap immediately after casting to prevent surface drying. After 24 hours, specimens were demolded and cured in a moist curing room (temperature (T) = 25 °C [77 °F] and relative humidity (RH) = 98%) for 56 days.

For the chemical sulfate exposure, 150 mm × 300 mm [6 in. × 12 in.] cylindrical specimens and 100 mm × 100 mm × 285 mm [4 in. × 4 in. × 11.2 in.] prisms were prepared as shown in **Figure 6.1**. After 56 days of curing, the TSC specimens were fully immersed

into tanks filled with a solution of 5% sodium sulfate (Na$_2$SO$_4$) for 12 months at room temperature (22 °C [71.6 °F]) (**Figure 6.2**). The sulfate solution was renewed every three months. Before exposure, the initial mass, length and compressive strength of specimens at 56 days were recorded in order to monitor any changes over the investigation period (**Figure 6.3**). The change of mass and length for each specimen were calculated according to **Eq. 6.1**:

$$XC_t = \left(\frac{X_i - X_t}{X_i}\right) \times 100 \qquad \textbf{Eq. 6.1}$$

Where, XC_t (%) is the change of mass or length at time t; X_t is the mass or the length at time t (g, mm) and X_i is the initial mass or gauge length before exposure to the 5% Na$_2$SO$_4$ solution (g, 250 mm [9.84 in.]).

For the physical sulfate exposure, 150 mm × 300 mm [6 in. × 12 in.] cylindrical specimens were prepared and partially immersed in a 5% Na$_2$SO$_4$ solution inside an environmental chamber for 6 months (**Figure 6.4**). During this period, cyclic temperature and relative humidity were applied. Each cycle consisted of one week at T = 20 °C [68 °F] and RH = 80%, followed by one week at T = 40 °C [104 °F] and RH = 35% according to a previous study by Nehdi *et al.* (2014). The sulfate solution was renewed each month. The initial mass and compressive strength of the TSC cylindrical specimens at 56 days were evaluated before sulfate exposure in order to capture any changes at the end of the physical sulfate exposure. The mass loss for each specimen was also calculated using **Eq. 6.1**.

Figure 6.1 – TSC specimens before the exposure to chemical sulfate attack.

Figure 6.2 – TSC specimens are fully immersed into tanks filled with a solution of 5% sodium sulfate (chemical sulfate exposure).

Figure 6.3 – Determining the change of mass and length for TSC specimens after chemical sulfate attack.

Figure 6.4 – TSC specimens are partially immersed in a solution of 5% sodium sulfate inside an environmental (physical sulfate exposure).

Before exposure to sulfates, small pieces were retrieved from selected TSC specimens to evaluate the pore size distribution using Mercury Intrusion Porosimetry (MIP) at the age of 56 days. The MIP measurements were performed using a Micromeritics AutoPore IV 9500 Series porosimeter within a pressure range of up to 414 MPa [60,000 psi]. The assumed surface tension of mercury was 0.484 N/m [2.76×10^{-3} lb/in.] at 25°C [77°F] according to ASTM D4404 (Standard Test Method for Determination of Pore Volume and Pore Volume Distribution of Soil and Rock by Mercury Intrusion Porosimetry). Moreover, scanning electron microscopy (SEM) with energy dispersive X-ray (EDX) analyses were conducted on thin sections and small pieces retrieved from selected TSC specimens in order to identify any sulfate reaction phases over the investigation period. Furthermore, X-ray diffraction analyses were carried out on samples taken from the TSC specimens. Co-Kα radiation with a

wavelength of 1.7902 Å was conducted at a voltage of 45 kV. The scanning speed was 10°/min at a current of 160 mA.

6.3. EXPRIMENTAL RESULTS AND DISCUSSION

6.3.1. Chemical Sulfate Exposure

6.3.1.1. Visual Examination

Figure 6.5 shows various TSC specimens after 12 months of full immersion in the 5% Na_2SO_4 solution. It can be observed that all TSC specimens remained visually intact, except the S1 specimens incorporating 10% SF. For these specimens, deterioration started to appear after 9 months of chemical sulfate exposure. Cracks covered with a whitish soft material were observed. After 12 months of immersion, severe loss of cementitious matrix-aggregate bond at the top and bottom edges of the S1 specimens was observed. Moreover, broken chunks from the S1 specimens exhibited the formation of a whitish substance around the aggregate particles.

6.3.1.2. Expansion Results

Table 6.3 presents the expansion results for the TSC specimens after 12 months of full immersion in the 5% Na_2SO_4 solution. It can be observed that expansion results varied depending on the cement type as well as the type and dosage of SCMs. The control TSC mixture (C) made with 100% OPC yielded an expansion of about 0.23%, which is greater than the maximum allowable expansion limit (i.e. 0.1%) recommended by ACI 201.2R (2008) (Guide to Durable Concrete). However, the TSC mixture (SR) made with 100% HSRC showed an expansion of about 91% lower than that of the C mixture. This expected behavior can be attributed to the lower tri-calcium aluminate (C_3A) content of HSRC, leading to less ettringite formation (e.g. Skalny *et al.*, 2002).
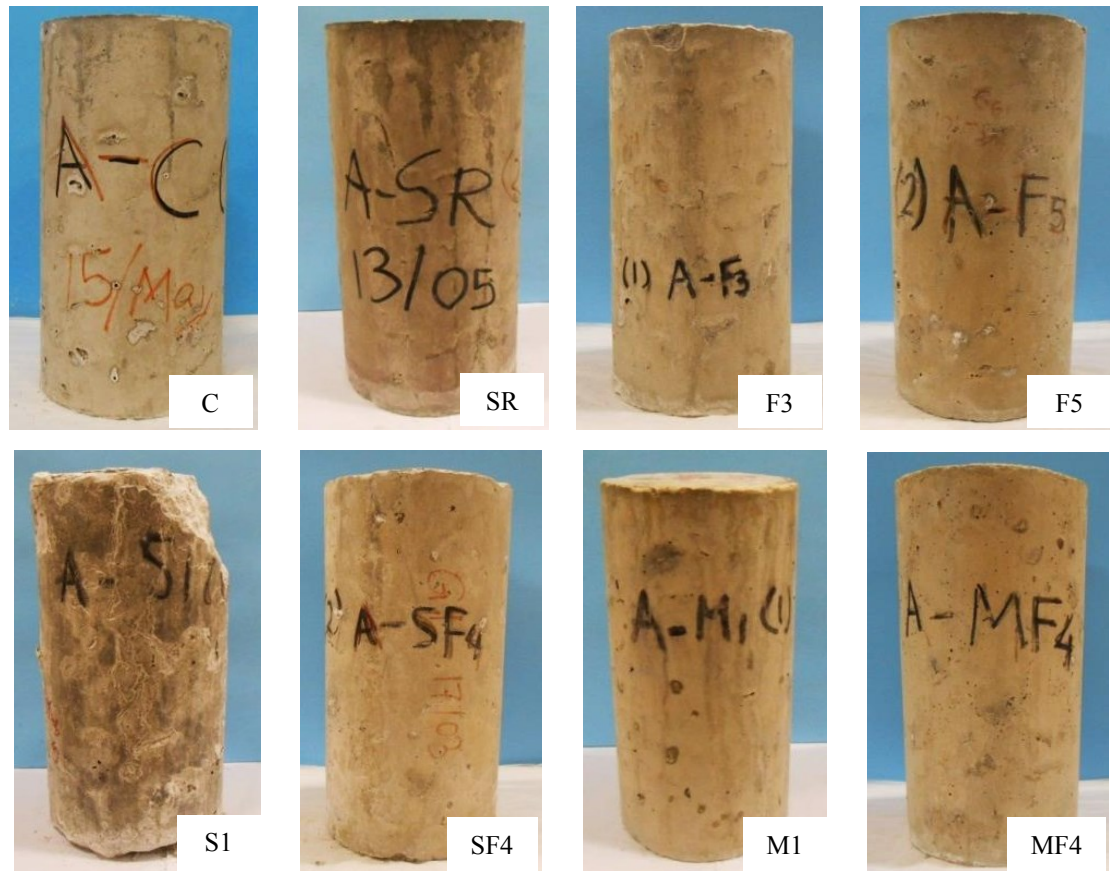
Figure 6.5 – Specimens from various TSC mixtures after 12 months of full immersion in sodium sulfate solution.

Table 6.3 – Results of TSC specimens exposed to different sulfate exposure conditions

TSC Mixture	Chemical sulfate exposure (12 months)						Physical sulfate exposure (6 months)			
	Expansion		Mass change		Change in f_c'		Mass change		Change in f_c'	
	(%)	COV (%)	(%)	COV (%)	(%)	COV (%)	(%)	COV (%)	(%)	COV (%)
C	0.23	9.53	0.34	9.93	12.90	2.95	-0.38	7.62	16.50	4.00
SR	0.02	9.02	0.22	8.01	32.10	1.05	-1.39	3.06	3.80	8.97
F3	0.05	3.26	0.22	7.38	34.70	1.00	-1.12	4.52	4.30	6.86
F5	0.01	8.18	0.19	8.58	47.00	0.89	-4.08	2.28	5.10	6.73
S1	0.13	4.83	-0.37	4.84	-59.90	0.80	-20.17	3.83	-84.60	1.79
SF4	0.12	2.97	0.52	4.71	2.30	8.48	-6.52	7.68	-42.40	4.30
M1	0.04	5.11	0.21	7.76	18.60	1.58	-0.49	7.06	5.10	6.17
MF4	0.02	6.11	0.24	6.98	21.60	1.52	-1.77	5.18	9.50	5.06

TSC mixtures incorporating SCMs as partial replacement for OPC exhibited lower expansion results in comparison with that of the control mixture (C). For example, the TSC

mixtures F3 and F5 made with binary binders (70% OPC-30% FA and 50% OPC-50% FA, respectively) exhibited 78% and 96% lower expansion than that of the C mixture, respectively. Moreover, TSC mixtures SF4 and MF4 made with ternary binders (50% OPC-10% SF-40% FA and 50% OPC-10% MK-40% FA, respectively) exhibited about 61% and 91% lower expansion than that of the C mixture, respectively.

It was reported that the concrete made with 100% OPC can be vulnerable to chemical sulfate attack due to its relatively high C_3A content (e.g. Skalny et al., 2002). Despite the relatively high expansion of the control TSC specimens, no cracks appeared. This can be attributed to the fact that the control TSC had relatively large internal voids which can accommodate some of the pressure of sulfate attack reaction products (Najjar *et al.*, 2014). **Figure 6.6(a)** confirms the existence of such large voids around aggregate particles in the C specimens before chemical sulfate exposure. These voids could relieve the internal pressures induced by the increase in volume of sulfate attack products, thus avoiding concrete damage by expansion stresses. Moreover, SEM image from the control specimen (**Fig. 6.6(b)**) illustrates gypsum produced from chemical sulfate attack.
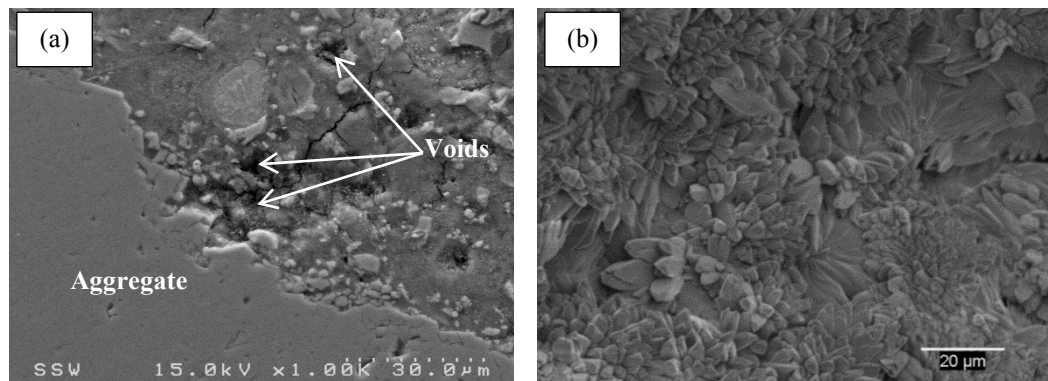
Figure 6.6 – (a) SEM of thin section from control TSC specimen before sodium sulfate exposure. (b) SEM of chunk from control specimen after chemical sulfate exposure showing gypsum.

Generally, the partial replacement of OPC by SCMs minimizes the expansion induced by chemical sulfate attack. This is due to reduction of the C_3A content in the binder (dilution effect), along with the consumption of calcium hydroxide (CH) in pozzolanic reactions (Skalny *et al.*, 2002) and an overall reduced permeability, thus limiting the intrusion of

sulfates in the cementitious matrix. Moreover, it was reported that the SO_3/Al_2O_3 molar ratio in concrete mixtures significantly influences the expansion due to ettringite formation. It was found that there is a SO_3/Al_2O_3 range for which expansion can occur. At very low Al_2O_3 content, ettringite does not typically form. Conversely, at high Al_2O_3 levels, monosulfoaluminate forms rather than ettringite, consequently reducing expansion (Ramlochan *et al.*, 2003). In other words, the higher the Al_2O_3 level, the lower will be the resulting expansion. This highlights the benefits of adding SCMs that contain high Al_2O_3 contents, such as fly ash and metakaolin, leading to better resistance to chemical sulfate attack (Nguyen *et al.*, 2013).

6.3.1.3. *Mass Change*

Table 6.3 reports mass changes for specimens made from various TSC mixtures incorporating different SCMs after 12 months of exposure to chemical sulfate attack. The TSC mixture made with HSRC exhibited 36% lower mass gain compared to that of the C mixture. Moreover, partially replacing OPC with FA or MK led to an increase in the mass of TSC specimens after immersion in sodium sulfate solutions. However, the TSC mixture incorporating 10% SF as partial replacement for OPC exhibited unexpected mass loss. Ternary binder TSC mixtures (SF4 and MF4) gained mass after exposure.

For the C mixture, the mass gain can be ascribed to the reaction between cement hydration products and the sulfate ions which ingress into the specimen. Consequently, expansive products (i.e. gypsum and ettringite) have formed and filled concrete pores, leading to an increase in the specimen mass. This was also observed for instance by Basista and Weglewski (2008) and Bassuoni and Nehdi (2009). The relatively lower mass gain of the SR specimens compared to that of the C specimens can be attributed to the limited formation of ettringite as mentioned earlier.

Conversely, the increase in mass of TSC specimens incorporating SCMs can be attributed to the progress of pozzolanic reactions during exposure. For example, SEM images (**Figure 6.7**) for F5 specimens, before and after exposure to the 5% Na_2SO_4 solution, illustrate that the microstructure became denser around fly ash particles after sulfate exposure. Moreover, it was reported that the Na_2SO_4 solution can be an effective activator for pozzolanic reactions in concrete containing FA, leading to higher mass gain and better resistance to chemical sulfate attack (Liu *et al.*, 2012). Indeed, SEM image (**Figure 6.8**) for

M1 specimens, after exposure to the 5% Na_2SO_4 solution, indicates denser microstructure and the absence of chemical sulfate attack products, which confirms the high resistance of the M1 mixture (90% OPC-10% MK) to chemical sulfate attack.
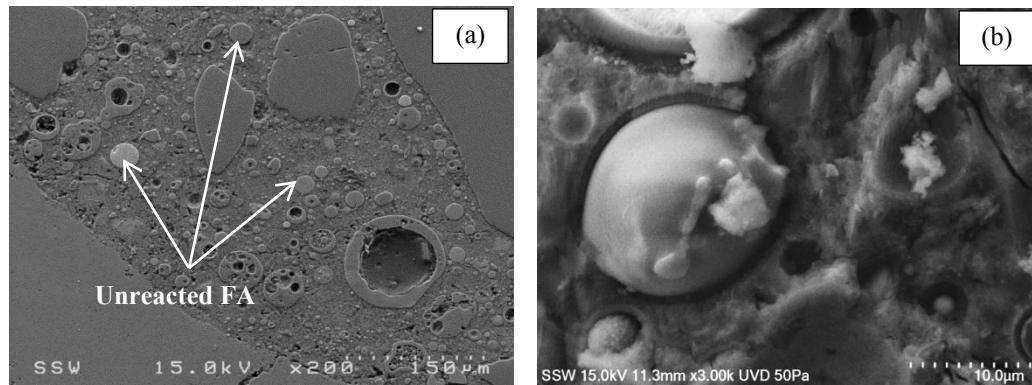
Figure 6.7 – (a) SEM of thin section from F5 specimen before chemical sodium sulfate exposure showing unreacted FA particles, and (b) SEM of chunk from F5 specimen after chemical sulfate exposure showing progress of pozzolanic reaction.
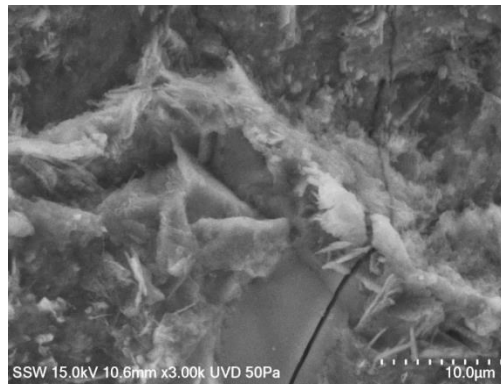
Figure 6.8 – SEM of chunk from M1 specimen after 12 months of full immersion in sodium sulfate solution showing denser microstructure.

Moreover, SEM images and EDX analysis for S1 specimens (**Figure 6.9**) confirmed the formation of thaumasite, which caused severe mass loss in the S1 specimens containing 10% silica fume. In the presence of sufficient sulfate ions, abundant moisture and relatively cool temperatures, concrete incorporating a source of carbonates (the limestone coarse aggregates in the present case) can be vulnerable to thaumasite formation (e.g. Crammond, 2002; Ramezanianpour, 2012). The possibility of thaumasite formation increases in the case of

TSC, which has 50% more coarse aggregate content than that of conventional concrete (Abdelgater, 1996). It was previously reported that thaumasite precipitated only in cementitious systems where the aluminum (Al) has been consumed to form ettringite and the SO_3/Al_2O_3 molar ratio exceeded 3 (Crammond, 2002; Schmidt *et al*., 2008). As shown in **Figure 6.10**, the amount of aluminate (Al_2O_3) in the S1 specimens (10% SF) was less than that in specimens from the TSC mixtures incorporating other SCMs, resulting in a high SO_3/Al_2O_3 and thus the possibility of thaumasite formation. It was also concluded that binders with higher Al_2O_3 content (e.g. TSC mixtures incorporating FA or/and MK) have higher resistance to thaumasite formation since it requires a higher content of sulfates (Juel *et al*., 2003) for thaumasite formation.
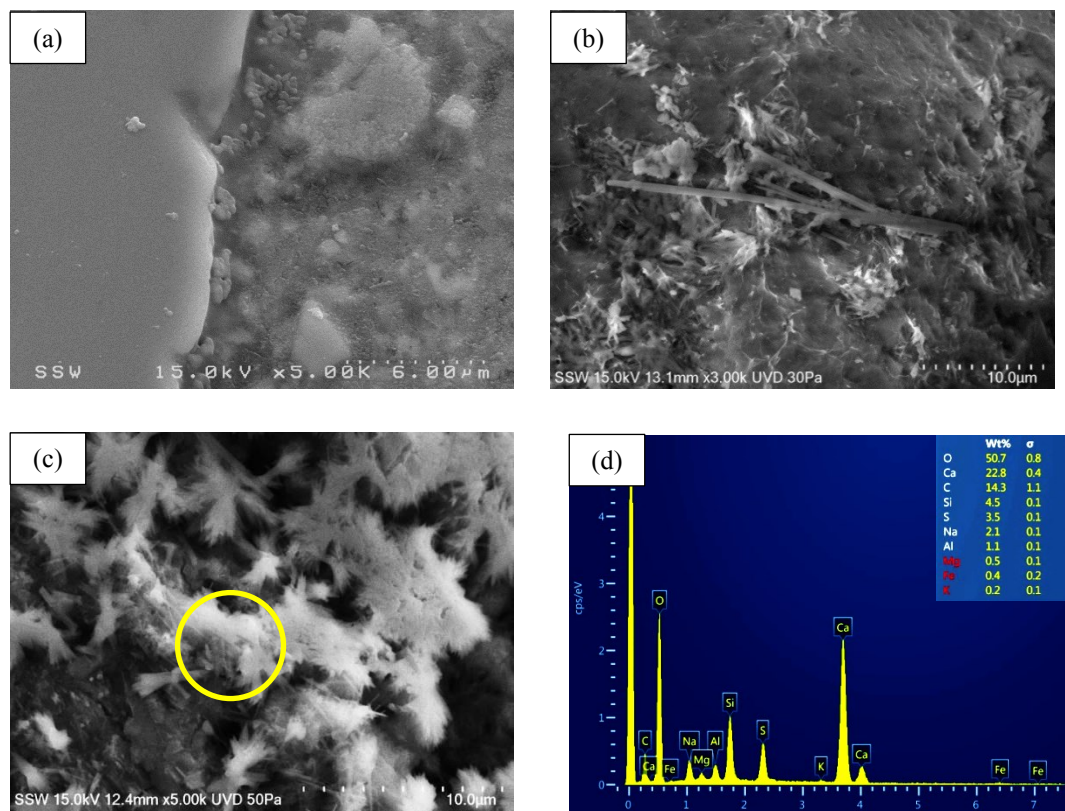
Figure 6.9 – (a) SEM of thin section from S1 specimen before chemical sodium sulfate exposure showing dense aggregate-grout interfacial zone, (b) SEM image of chunk from S1 specimen illustrating ettringite mixed with thaumasite, (c) SEM image of chunk from S1 specimen illustrating large amount of thaumasite formed on aggregate surface, (d) EDX analysis of circled area in (c) showing components of thaumasite.
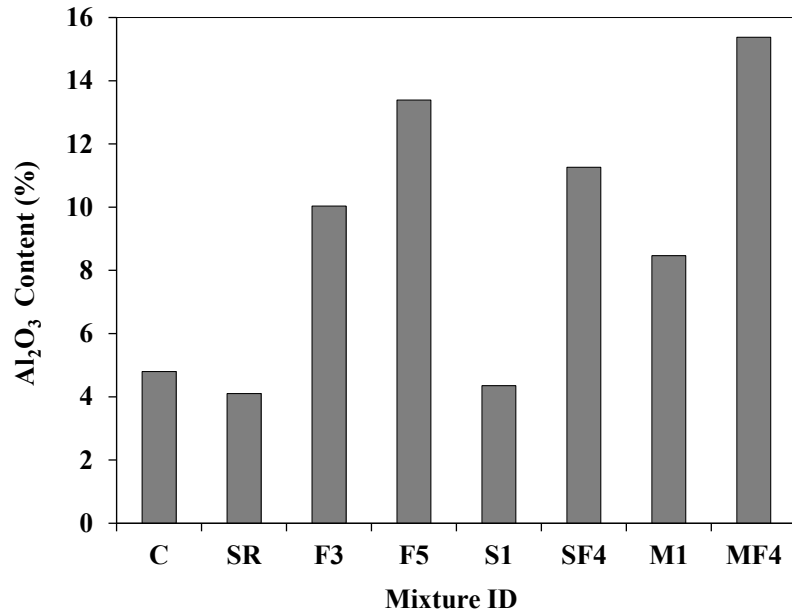
Figure 6.10 – Al$_2$O$_3$ content (%) in the binders used in the various TSC mixtures.

Furthermore, it can be observed that there is a potential for thaumasite formation in specimens from the C and SR mixtures since their Al$_2$O$_3$ content is small, similar to that of S1 specimens (**Figure 6.10**). XRD analysis of powder samples from C specimens confirmed the formation of thaumasite as well as ettringite and gypsum (**Figure 6.11**). However, C specimens did not exhibit distinctive visual features of thaumasite damage. This can be attributed to the competition between ettringite and thaumasite formation (consuming sulfates) and the fact that the control TSC (C) contains larger internal voids near the aggregate particles induced by grout bleeding as discussed earlier, resulting in less dense aggregate-grout interfacial transition zone, capable of accommodating pressures from growing sulfate attack products. Conversely, S1 specimens exhibited denser aggregate-grout interfacial zone due to its higher resistance to bleeding (Najjar *et al.*, 2016). Thus, S1 specimens have undergone extensive thaumasite formation on the aggregate surfaces (e.g. **Figure 6.9(c)**) compared with that of the control TSC specimens, leading to an accelerated damage from thaumasite sulfate attack.
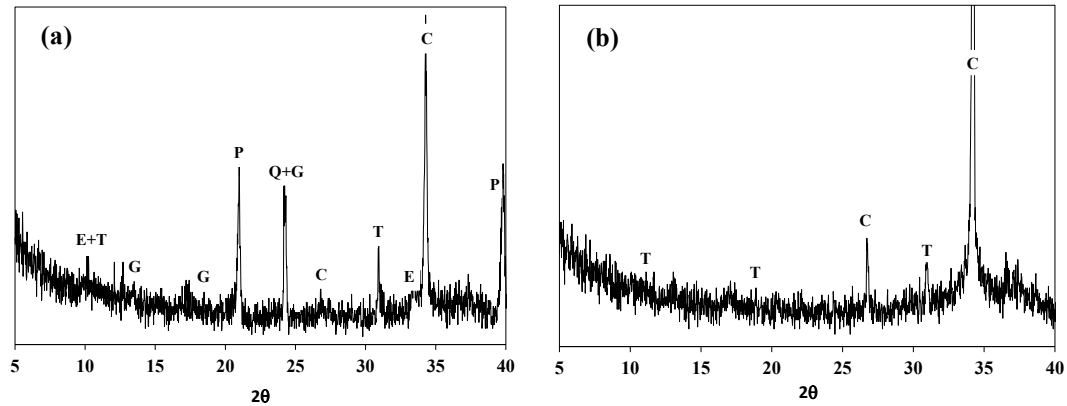
Figure 6.11 – XRD of powder sample from (a) control TSC specimen, (b) S1 specimen after 12 months of exposure to chemical sodium sulfate attack. (E = Ettringite, T = Thaumasite, G = Gypsun, Q = Quartz C = Calcite P = Portlandite).

6.3.1.4. *Compressive Strength Change*

Compressive strength results for TSC mixtures before and after chemical sulfate exposure are presented in **Figure 6.12**. The TSC specimens continued gaining compressive strength after sulfate exposure, except for S1 specimens, which exhibited severe compressive strength loss. Binary binder TSC specimens incorporating 50% FA achieved the highest compressive strength gain during sulfate exposure compared to that of the other TSC mixtures.

In general, the compressive strength increases as hydration reactions of the cementitious matrix progress and fill voids with hydration products (e.g. Bassuoni and Nehdi, 2009). For example, after 12 months of chemical sulfate exposure, F5 specimens gained about 47% higher compressive strength compared to its value before exposure. This can be attributed to the progress of pozzolanic reactions of FA during the exposure time, leading to a gain in mechanical strength (Torii *et al*., 1995).
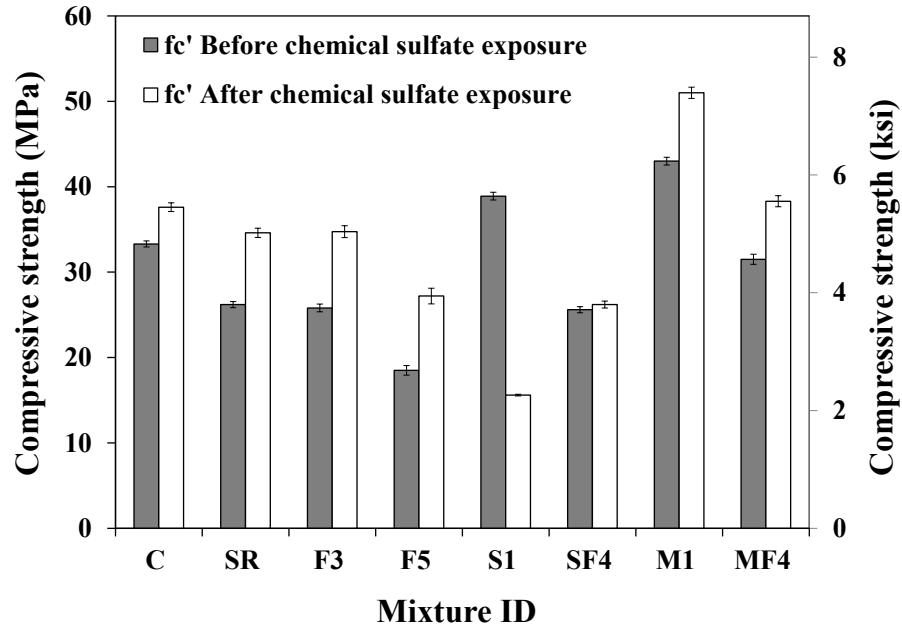
Figure 6.12 – Change in compressive strength (f_c') for specimens from various TSC mixtures after 12 months of full immersion in sodium sulfate solution.

The surprising severe strength loss of the S1 specimens is mainly related to the thaumasite formation, which caused significant deterioration. In thaumasite sulfate attack, CSH phases are destructed, leading to loss of cohesion and strength (Nielsen *et al*., 2014). This was confirmed in the present study by SEM imaging (**Figure 6.9(c)**), which demonstrated abundant formation of thaumasite around the limestone coarse aggregate surfaces.

6.3.2. Physical Sulfate Exposure

6.3.2.1. Visual Examination

During the first week of exposure (i.e. T = 20 °C [68 °F] and RH = 80%), white efflorescence appeared on the evaporative surfaces of the TSC specimens. This efflorescence formed due to the disposition of soluble sodium sulfate salt (i.e. mirabilite formation), which moved up by capillary action towards the drying concrete surface (Liu *et al*., 2012). The TSC specimens which exhibited more efflorescence were from the F5 and SF4 mixtures (**Figure 6.13**). In the second week of exposure (i.e. T = 40 °C [104 °F] and RH = 35%), the environmental condition was conducive to thenardite formation. Cyclic conversion of sodium

sulfate from thenardite to mirabilite can result in crystals growth from a highly supersaturated sodium sulfate solution. Consequently, disruptive pressures in the concrete pores can be generated, leading to surface scaling (Nehdi *et al*., 2014).
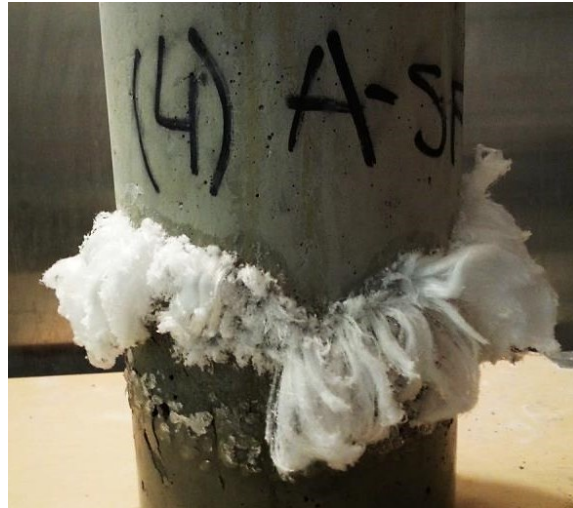
Figure 6.13 – Efflorescence formed on SF4 specimen after the first week of physical sodium sulfate exposure at temperature of 20 °C [68 °F] and RH of 80%.

Table 6.4 presents visual inspection based on the external concrete surface scaling for TSC specimens over the physical sulfate exposure period. After one month, surface scaling started to appear on F5 and SF4 specimens. Conversely, S1, F3 and SR specimens exhibited surface scaling only after two months of exposure. C and M1 specimens achieved better resistance to surface scaling during the entire exposure period.

Figure 6.14 illustrates surface scaling on various TSC specimens after 6 months of physical sulfate attack. It can be observed that the immersed portion of S1 specimens exhibited severe deterioration typical of chemical sulfate attack. **Figure 6.15** shows a comparison between the bottom surfaces of C, F5 and S1 specimens after 6 months of sulfate exposure. A significant loss of cementitious matrix-aggregate bond was observed in S1 specimens, with a whitish soft substance covering the aggregate particles at the immersed portion of these specimens. This is expected since the submerged part of specimens mimics the chemical sulfate exposure discussed earlier.

Table 6.4 – Surface scaling visual rating for TSC specimens after exposure to physical sulfate attack

TSC Specimen	Exposure period (months)					
	1	2	3	4	5	6
C	0	0	0	0	1	1
SR	0	1	2	2	3	4
F3	0	0	1	2	2	3
F5	1	2	2	3	3	4
S1	0	1	2	3	4	5
SF4	1	2	2	3	4	4
M1	0	0	0	0	1	1
MF4	0	1	1	2	2	3

0: No scaling; 1: Very slight scaling (3 mm depth, no coarse aggregate visible); 2: Slight to moderate scaling; 3: Moderate scaling (some coarse aggregate visible); 4: Moderate to severe scaling; 5: Severe scaling (coarse aggregate visible over entire surface)
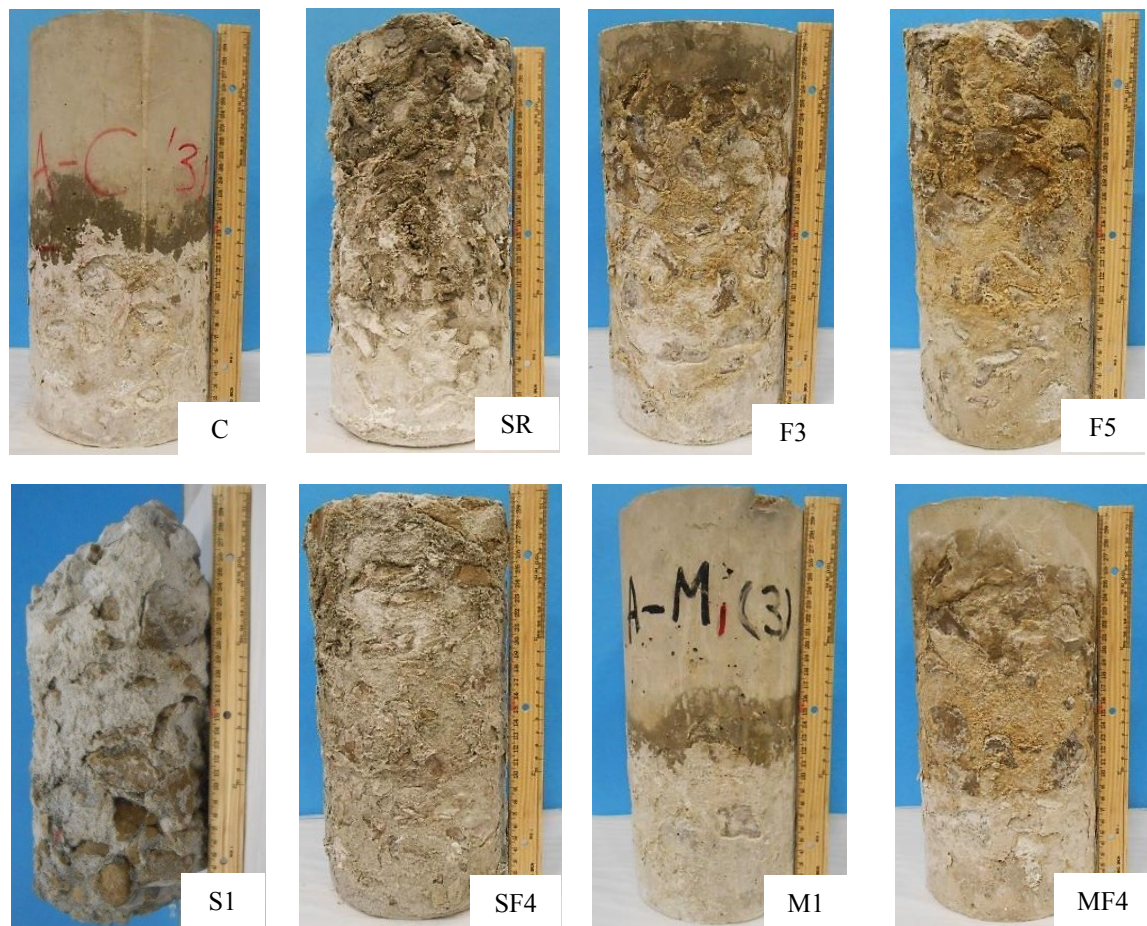
Figure 6.14 – Specimens from various TSC mixtures after 6 months of physical sodium sulfate exposure.

Figure 6.15 – Comparison between bottom surface of C, F5 and S1 specimens after 6 months of physical sodium sulfate exposure.

6.3.2.2. Mass Change

All TSC specimens exhibited mass loss after 6 months of exposure to physical sulfate attack as shown in **Table 6.3**. The extent of mass loss was primarily influenced by the type of binder used and SCMs type and dosage. The maximum mass loss was observed in the S1 specimens, followed by that of SF4 and F5 specimens, while C and M1 specimens showed lower mass loss. In physical sulfate attack, the mass loss of concrete can occur due to supersaturation of sodium sulfate in the evaporative front of specimens, leading to high stresses within surface pores and consequently surface scaling (Liu *et al*., 2012; Nehdi *et al*., 2014). Examining the drying surface of TSC specimens above the solution level using SEM and XRD analysis showed extensive thenardite formation within pores (**Figure 6.16**), which is responsible for the observed surface scaling.

Moreover, mass loss of concrete specimens due to physical sulfate attack is mainly affected by its pore size distribution (Liu *et al*., 2012). **Figure 6.17** illustrates MIP results at 56 days for specimens retrieved from the various TSC mixtures before sulfate exposure. Capillary pores, which have sizes ranging from 0.1 μm to 100 μm, are responsible for transporting sulfate solutions toward the drying portion of concrete specimens (Nguyen, 2011; Wittmann *et al*., 2014; Ma *et al*., 2015). **Figure 6.18** illustrates the volume of capillary pores for each mixture. It can be observed that F5 and SF4 specimens had 35% higher capillary pore volume than that of the control C specimen. This can explain the high surface scaling due to physical salt attack exhibited by these specimens.
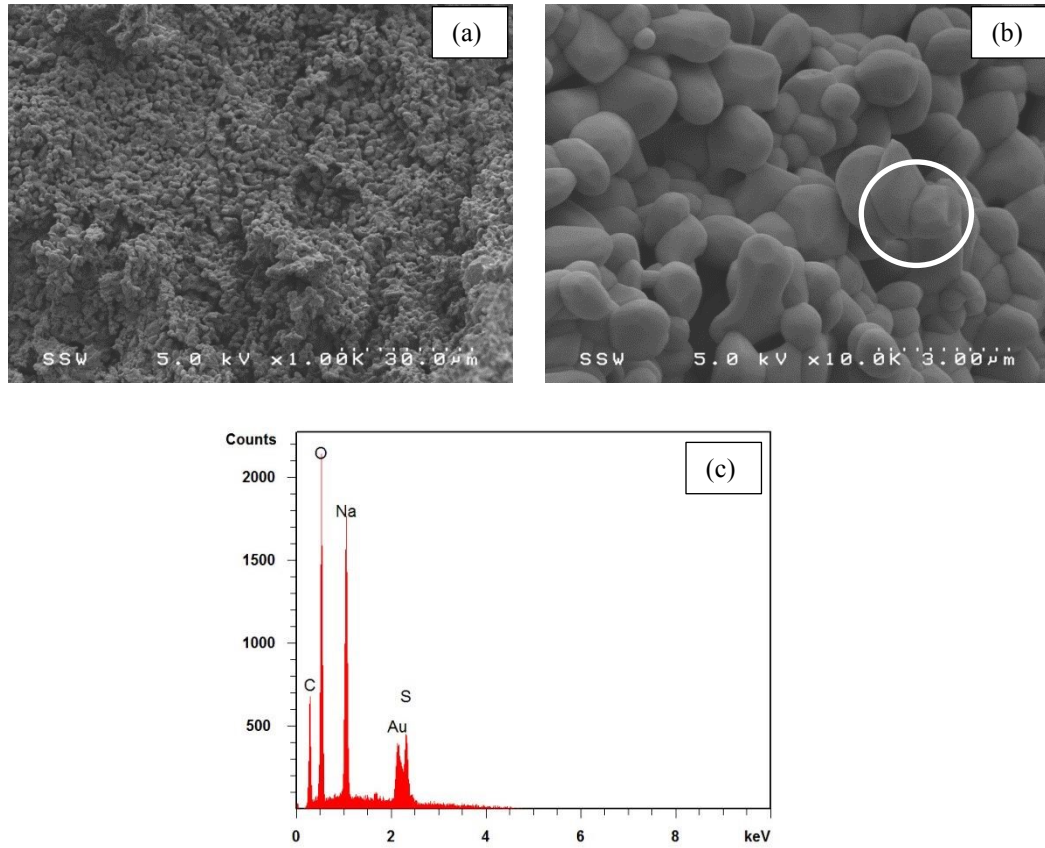
Figure 6.16 – Illustration of thenardite at magnification of (a) 1000 x and (b) 10000× , and (c) XRD analysis of circled area in (b) showing components of Na$_2$SO$_4$ (thenardite).
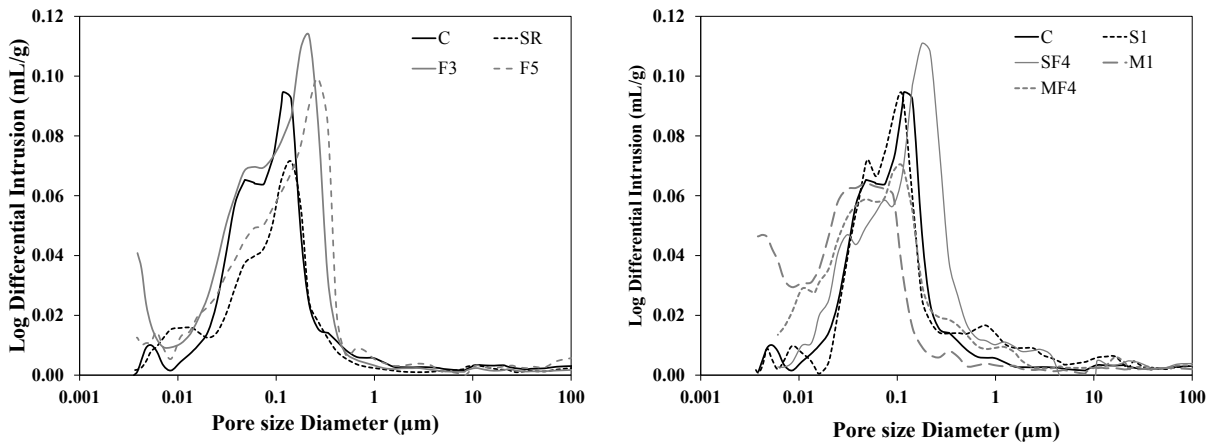
Figure 6.17 – MIP results of specimens from various TSC mixtures before sodium sulfate exposure.
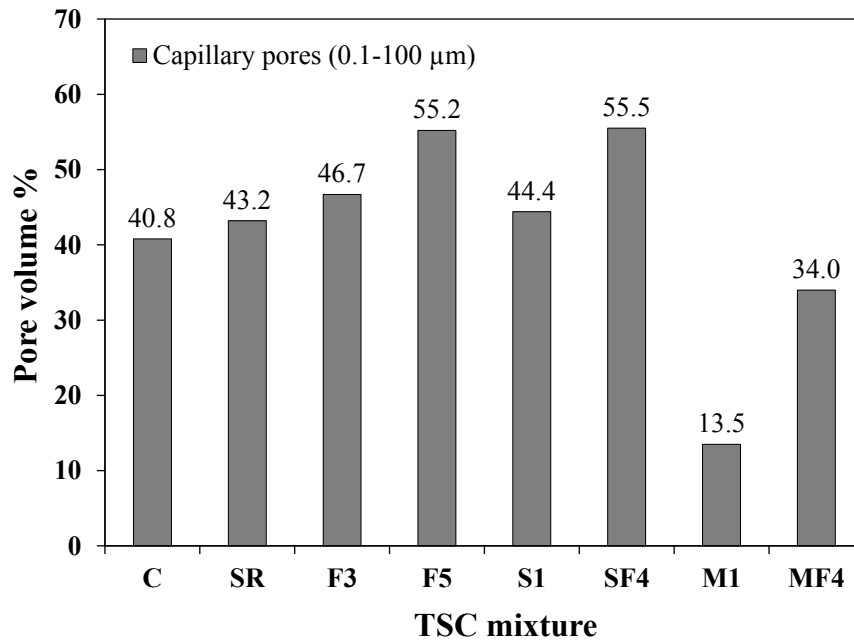
Figure 6.18 – Capillary pore volume (0.1 μm to 100 μm) of specimens from various TSC mixtures before exposure to sodium sulfate attack.

The TSC specimens incorporating 10% SF as partial replacement for OPC incurred excessive surface scaling and internal damage. This can be attributed to its relatively finer pore structure and higher capillary rise. Consequently, higher sulfate crystallization pressures can be generated, leading to extensive cracking as reported elsewhere (e.g. Aye and Oguchi, 2011). **Figure 6.19** illustrates SEM of micro-cracks at the aggregate-cementitious matrix interfacial zone for S1 specimens along with EDX analyses showing thenardite formation.

Conversely, the M1 specimens showed slight surface scaling and little mass loss. This can be attributed to the low volume of capillary pores (i.e. 13.5%) in M1 specimens compared with that in specimens from the other mixtures (**Figures 6.17** and **6.18**). Yet, M1 specimens had very fine pores (i.e. less than 0.1 μm). While fine pores have proven detrimental in physical sulfate attack (e.g. Nehdi *et al*., 2014), this may have reduced capillary action for M1 specimen due to the overall low pore volume (e.g. Khatib and Roger, 2004; Gesoğlu *et al*., 2014). Also, metakaolin may provide higher resistance to the formation of efflorescence due to observed densification of the concrete microstructure (Siddique and Klaus, 2009; Weng *et al*., 2013). Silica fume did not play this role probably due to the

observed higher pore volume. The relatively better performance of TSC specimens incorporating metakaolin under physical sulfate attack exposure in the present study warrants further investigation to determine whether this is a prevalent feature and to elucidate its true mechanisms.
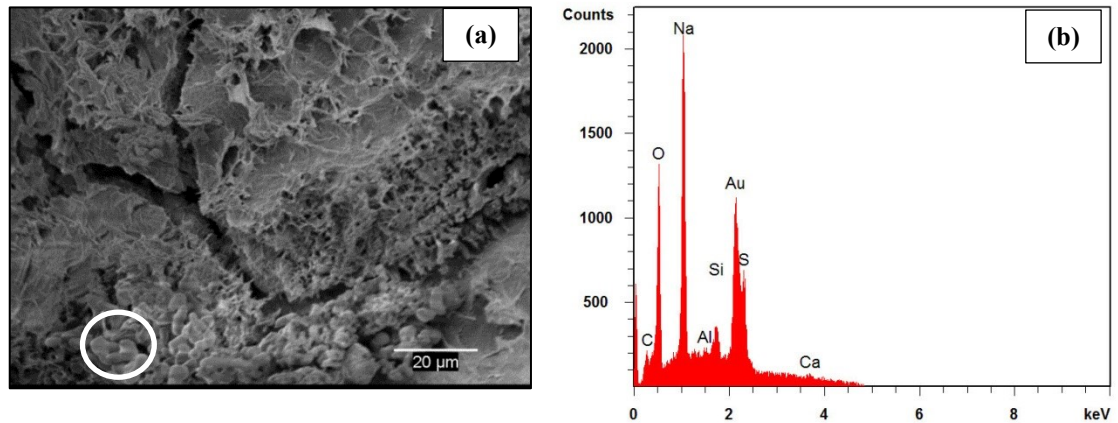
Figure 6.19 – (a): SEM image of micro-cracks at aggregate-cementitious matrix interface for S1 specimen exposed to physical sodium sulfate attack, and (b) XRD analysis of circled area in (a) showing components of Na$_2$SO$_4$ (thenardite).

6.3.2.3. *Compressive Strength Change*

Compressive strength results of specimens from various TSC mixtures tested before and after 6 months of exposure to physical sulfate attack are presented in **Figure 6.20**. It can be observed that changes in concrete compressive strength depended mainly on the binder type. For example, the control C mixture showed the highest compressive strength gain after exposure compared with the other mixtures. This can be attributed to its least surface scaling and surface damage (**Table 6.3**). It is to be noted that the higher expansion of the submerged part of C specimens did not cause cracking and damage at 6 months of exposure. TSC specimens including SR, F3, F5, M1 and MF4 showed slight strength gain although some of these specimens (i.e. SR and F5) incurred great surface scaling, as shown in **Figure 6.14**. Surface scaling by physical sulfate attack will not immediately induce significant reduction in compressive strength since the concrete core was not yet degraded (Nehdi *et al*., 2014). Longer exposure can eventually compromise compressive strength.
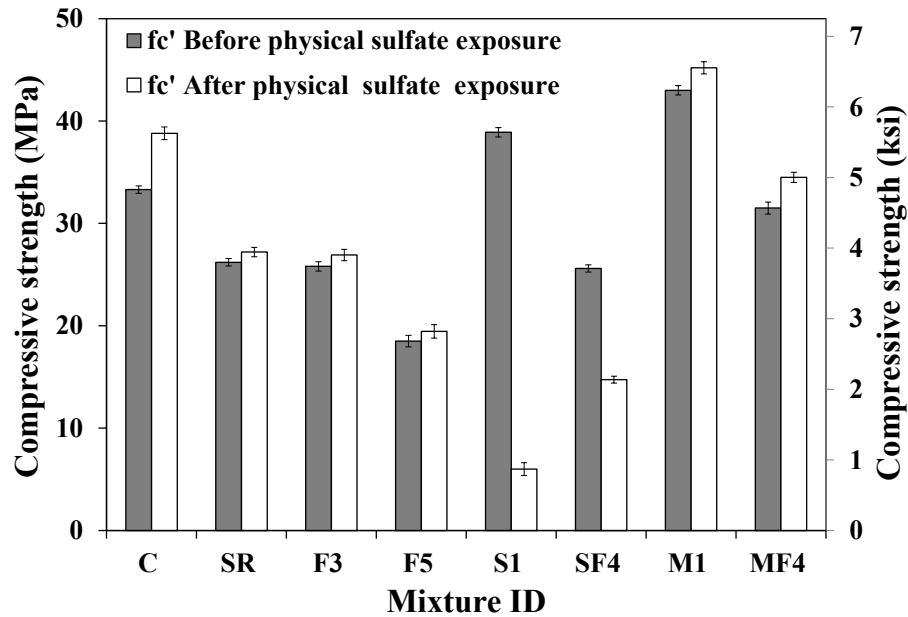
Figure 6.20 – Change in compressive strength (f_c') for specimens from various TSC mixtures after 6 months of physical sodium sulfate attack.

However, SF4 specimens suffered loss in compressive strength. This can be ascribed to the fact that the SF4 specimens had the highest volume of fine capillary pores, as shown in **Figure 6.18**. Therefore, sulfate salt crystallization could generate higher disruptive pressures, leading to concrete damage.

As shown in **Figure 6.20**, S1 specimens incurred the most severe compressive strength loss amongst all specimens. SEM image analysis (**Figure 6.19(a)**) illustrates micro-cracks at the aggregate-cementitious matrix interface in S1 specimens above the solution level due to crystallization of sodium sulfate. Concomitantly, the immersed portion of S1 specimens suffered significant loss of bond between the aggregates and the cementitious matrix due to the formation of thaumasite as illustrated previously in **Figures 6.9** and **6.15**. Therefore, S1 specimens were extensively damaged due to synergistic effects in a dual attack consisting of salt crystallization and chemical sulfate attack.

The conflicting performance of TSC under chemical sulfate attack, where SCMs are highly beneficial, and physical sulfate attack, where SCMs have proven problematic, puts the designer at odds as to what compromise is needed between the two problems. For example, the TSC mixtures incorporating FA showed good resistance to chemical sulfate attack, while

such mixtures exhibited severe surface scaling under physical sulfate exposure. Suleiman *et al*. (2014) have shown that some protective coatings applied at the evaporative front of the concrete subjected to dual sulfate attack can help resisting the distress from physical salt attack, allowing to focus on the submerged part of the concrete element exposed to chemical sulfate attack. However, a concerted research effort is still needed in this area to mitigate performance problems and the potential related litigation similar to that which cropped up over the past two decades.

6.4. CONCLUSIONS

The present study aimed at exploring the durability of TSC exposed to environments conducive to chemical and physical sodium sulfate attack. In both exposure regimes, the effects of using SCMs on TSC were investigated. The following conclusions can be drawn from the experimental study:

- TSC specimens incorporating FA as partial replacement for OPC achieved adequate resistance to chemical sulfate attack. However, under physical sulfate exposure, such specimens exhibited significant surface scaling.

- Under chemical sulfate exposure, TSC specimens incorporating 10% SF as partial replacement for OPC incurred severe damage as a result of thaumasite formation in the presence of limestone coarse aggregates. Moreover, such specimens were entirely destroyed after 6 months of physical sulfate exposure. The drying portion of these specimens was physically damaged by salt crystallization, while the immersed portion concomitantly suffered chemical attacked through thaumasite formation.

- The TSC mixture incorporating 10% MK as partial replacement for OPC exhibited excellent resistance to both chemical and physical sulfate attacks. It also achieved a compressive strength gain after chemical and physical sulfate exposures.

- TSC specimens made with a ternary binder (SF4 and MF4 mixtures) achieved adequate chemical sulfate resistance. Under physical sulfate exposure, the MF4 specimens exhibited better resistance to surface scaling compared with that of the SF4 specimens. This is ascribed to the fact that the SF4 specimens had higher volume of capillary pores (i.e. higher capillary rise), leading to increased surface scaling by physical salt attack.

- The apparently conflicting effects of SCMs on the resistance of concrete to chemical and physical attacks warrant concerted future research effort to permit the designer striking a balance for concrete exposed to environments conducive to both damage mechanisms.

- The unexpected severe thaumasite formation in TSC incorporating 10% SF in the presence of limestone aggregates requires further attention since silica fume is generally perceived as a performance enhancer with regards to the durability of concrete.

- The positive performance of TSC incorporating metakaolin in both chemical and physical sulfate exposures needs dedicated investigation to determine whether this is a prevalent feature and to elucidate the true mechanisms controlling this behavior.

6.5. REFERENCES

Abdelgader, H. S., (1996), "Effect of quantity of sand on the compressive strength of two-stage concrete," *Magazine of Concrete Research*, Vol. 48, No. 177, pp. 353-360.

Abdelgader, H. S., Najjar, M. F. and Azabi, T. M., (2010),"Study of underwater concrete using two-stage (pre-placed aggregate) concrete in Libya," *Journal of Structural Concrete*, Vol. 11, No. 3, pp.161-165.

ACI 201.2R, (2008), "Guide to durable concrete," *American Concrete Institute*, Farmington Hills, USA.

ACI 304.1, (2005), "Guide for the use of preplaced aggregate concrete for structural and mass concrete applications," *American Concrete Institute*, Farnington Hills, USA

ASTM C1012, (2015), "Standard test method for length change of hydraulic-cement mortars exposed to sulfate solution," *American Society for Testing and Materials*, West Conshohocken, PA.

ASTM D4404, (2010), "Standard test method for determination of pore volume and pore volume distribution of soil and rock by mercury intrusion porosimetry," *American Society for Testing and Materials*, West Conshohocken, PA.

Aye, T. and Oguchi, C. T., (2011), "Resistance of plain and blended cement mortars exposed to severe sulfate attacks," *Construction and Building Materials*, Vol. 25, No. 6, pp. 2988-2996.

Basista, M. and Weglewski, W., (2008), "Micromechanical modeling of sulphate corrosion in concrete: influence of ettringite forming reaction," *Theoretical and Applied Mechanics*, Vol. 35, No.1-3, pp. 29-52.

Bassuoni, M. T. and Nehdi, M. L., (2009), "Durability of self-consolidating concrete to different exposure regimes of sodium sulphate attack," *Materials and Structures*, Vol. 42, No. 8, pp. 1039-1057.

Berndt, M., (2012), "Long–term durability of preplaced aggregate concrete piles," *Concrete International, ACI*, Vol. 34, No. 12, pp. 36-42.

Crammond, N., (2002), "The occurrence of thaumasite in modern construction – a review," *Cement and Concrete Composites*, Vol. 24, No. 3, pp. 393-402.

Gesoğlu, M., Güneyisi, E., Özturan, T. and Mermerdaş, K., (2014), "Permeability properties of concretes with high reactivity metakaolin and calcined impure kaolin," *Materials and Structures*, Vol. 47, No. 4, pp.709-728.

Haynes, H. and Bassuoni, M. T., (2011), "Physical salt attack on concrete," *Concrete International, ACI*, Vol. 33, No. 11, pp. 38-42

Haynes, H., O'Neill, R., Neff, M. and Mehta, P. K., (2008), "Salt weathering distress on concrete exposed to sodium sulphate environment," *ACI Materials Journal*, Vol. 105, No. 1, pp. 35-43.

Hooton, R. D., (1993), "Influence of silica fume replacement of cement on physical properties and resistance to sulfate attack, freezing and thawing, and alkali-silica reactivity", *ACI Materials Journal*, Vol. 90, No. 2, pp. 143–151.

Juel, I., Herfort, D., Gollop, R., Konnerup-Madsen, J., Jakobsen, H. and Skibsted, J., (2003), "A thermodynamic model for predicting the stability of thaumasite", *Cement and Concrete Composites*, Vol. 25, pp. 867-872.

Khatib, J. M. and Clay, R. M., (2004), "Absorption characteristics of metakaolin concrete," *Cement and Concrete Research*, Vol. 34, No. 1, pp. 19-29.

Liu, Z., Deng, D., De Schutter, G. and Yu, Z., (2012), "Chemical sulfate attack performance of partially exposed cement and cement plus fly ash paste," *Construction and Building Materials*, Vol. 28, No. 1, pp. 230-237.

Ma, H., Tang, S. and Li, Z., (2015), "New pore structure assessment methods for cement paste," *Journal of Materials in Civil Engineering*, ASCE, Vol. 27, No. 2, A4014002.

Mangat, P. S. and Khatib, J. M., (1993), "Influence of fly ash, silica fume, and slag on sulfate resistance of concrete", *ACI Materials Journal*, Vol. 92, No. 5, pp. 542-552.

Mehta, P. K., (1992), "Sulfate attack on concrete – a critical review," in J. Skalny (ed.), *Material Science of Concrete,* American Ceramic Society, Westerville, OH, pp. 105–130.

Mehta, P. K., (2000), "Sulfate attack on concrete: separating myths from reality", *Concrete International*, Vol. 22, No. 8, pp. 57-61.

Najjar, F. M., Soliman, A. M. and Nehdi, M. L., (2016), "Two-stage concrete made with single, binary and ternary binders," *Materials and Structures*, Vol. 49, No. 1, pp. 317-327.

Najjar, M., Soliman, A. and Nehdi, M., (2014), "Critical overview of two stage concrete: properties and applications," *Construction and Building Materials*, Vol. 62, pp. 47-58.

Nehdi, M. L., Suleiman, A. R. and Soliman, A. M., (2014), "Investigation of concrete exposed to dual sulphate attack," *Cement and Concrete Research*, Vol. 64, pp. 42-53.

Nehdi, M. and Hayek, M., (2005), "Behavior of blended cement mortars exposed to sulfate solutions cycling in relative humidity," *Cement and Concrete Research*, Vol.35, No. 4, pp. 731-742.

Nguyen, H. T., (2011), "water and heat transfer in cement based materials," *PhD thesis*, University of Tromso, Tromso, Norway.

Nguyen, V., Leklou, N., Aubert, J. and Mounanga, P., (2013), "The effect of natural pozzolan on delayed ettringite formation of the heat-cured mortars," *Construction and Building Materials*, Vol. 48, pp. 479-484.

Nielsen, P., Nicolai, S., Darimont, A. and Kestemont, X., (2014), "Influence of cement and aggregate type on thaumasite formation in concrete," *Cement & Concrete Composites*, Vol. 4, No. 53, pp. 115-126.

O'Malley, J. and Abdelgader, H. S., (2010), "Investigation into the viability of using two stage (pre-placed aggregate) concrete in an Irish setting," *Frontiers of architecture and civil engineering in china*, Vol. 4, No. 1, pp.127-132.

Ramezanianpour, A. M., (2012), "Sulfate resistance and properties of portland-limestone cements," *PhD thesis*, University of Toronto, Toronto, ON, Canada.

Ramlochan, T., Zacarias P., Thomas, M. D. A. and Hooton, R. D., (2003), "The effect of pozzolans and slag on the expansion of mortars cured at elevated temperature: part I: expansion behaviour," *Cement and Concrete Research*, Vol. 33, No. 6, pp. 807-814.

Scherer, G. W., (2004), "stress from crystallization of salt," *Cement and Concrete Research*, Vol. 34, No. 9, pp. 1613-1624.

Schmidt, T., Lothenbach, B., Romer, M., Scrivener, K., Rentsch, D. and Figi R., (2008), "A thermodynamic and experimental study of the conditions of thaumasite formation," *Cement and Concrete Research*, Vol.38, No. 3, pp. 337-349.

Siddique, R. and Klaus, J., (2009), "Influence of metakaolin on the properties of mortar and concrete: a review," *Applied Clay Science*, Vol. 43, No. 3, pp. 392-400.

Skalny, J., Marchand, J. and Odler, I., (2002), "Sulfate attack on concrete," *Spon Press*, New York; 217p.

Skaropoulou, A., Tsivilis, S., Kakali, G., Sharp, J. H. and Swamy, R. N., (2009), "Thaumasite form of sulfate attack in limestone cement mortars: a study on long term efficiency of mineral admixtures," *Construction and Building Materials*, Vol. 23, No. 6, pp. 2338-2345.

Suleiman, A.R., Soliman A.M. and Nehdi, M.L., (2014), "Effect of surface treatment materials on durability of concrete exposed to physical sulfate attack," *Construction and Building Materials*, Vol. 73, pp. 674-681.

Torii, K., Taniguchi, K. and Kawamura, M., (1995), "Sulfate resistance of high fly ash content concrete," *Cement and Concrete Research*, Vol. 25, No. 4, pp. 759-768.

Weng, T. L.n Lin, W. T. and Cheng, A., (2013), "Effect of metakaolin on strength and efflorescence quantity of cement-based composites," *Scientific World Journal*, pp. 1-11.

Wittmann, F. H., Wittmann, A. D. A. and Wang, P. G., (2014), "Capillary absorption of integral water repellent and surface impregnated concrete," *Restoration of Buildings and Monuments*, Vol. 20, No. 4, pp. 281-290.

<div align="right">

Chapter 7

</div>

7. NOVEL ECO-EFFICIENT PAVEMENT CONSTRUCTION TECHNOLOGY USING TWO-STAGE CONCRETE[(*)]

7.1. INTRODUCTION

The construction of roadways and sidewalks is energy and resource-intensive, releasing large amounts of emissions and depleting natural resources. In year 2014, the United States alone had constructed about 6.6 million kilometers of public roads, most of which are made of asphalt concrete, with growing use of portland cement concrete. There are approximately 18 billion tons of asphalt on American roads, and roughly 3,500 asphalt concrete mixing sites, producing about 350 million tons of asphalt pavement material per year across the USA. In the United States and Canada, most sidewalks consist of a poured concrete ribbon. Both asphalt and portland cement concrete take a fall on the environment due to depleting virgin aggregates and minerals, use of hydrocarbons, and emissions of greenhouse gas (GHG).

There has been ongoing debate on the environmental footprint of asphalt and portland cement road construction. For instance, Stripple (2001) and the Athena Institute (Meli, 2006) compared flexible and rigid pavements in terms of energy consumption and GHG emissions using the process-based Life Cycle Analysis approach. Stripple found that the energy and GHG emissions for rigid pavements in Sweden were 30% and 29% higher, respectively, than that for flexible pavements when material, construction, and maintenance phases were considered. Conversely, the Athena Institute indicated that the energy use and GHG emissions for flexible pavements in Canada were 40% and 6.8% higher, respectively, than that for rigid pavements.

There is currently clear need for sustainable pavement and sidewalk construction technology that outperforms both conventional techniques. In particular, beneficiating solid wastes in pavement construction can enhance its environmental footprint. For instance, it has

---

[(*)]*A version of this chapter was submitted to the Cement and Concrete Research Journal (2016).*

been estimated that in North America about 175 million tons of construction and demolition wastes and about 4.7 million tons of waste tires are generated annually (US EPA, 2009; Kim *et al.*, 2011; Yeheyis *et al.*, 2013).

According to the Canadian Infrastructure Report Card (2016), 28% of the total sidewalks in Canada are in need of replacement. A primary damage mechanism for sidewalks and pavements in North America is surface scaling and cracking induced by freezing and thawing cycles (Hossack *et al*, 2014). It was reported that premature failure of concrete sidewalks can occur only five years after construction due to severe winter weather (Rajani and Zhan, 1997). As reported by the Roads Construction Standard Specifications (2015), concrete sidewalks shall comply with the CSA A23.1 (2014) (Concrete Materials and Methods of Concrete Construction/Test Methods and Standard Practices for Concrete) requirements for class C2 exposure (i.e. non-structurally reinforced concrete exposed to chlorides with or without freeze-thaw conditions). Moreover, concrete mixtures for paving should be designed to meet the desired flexure strength along with adequate durability as recommended by ACI 330 (2008) (Guide for Design and Construction of Concrete Parking Lots).

Concrete incorporating scrap tire granules can offer a sustainable alternative for the construction of sidewalks where mechanical strength is not of utmost priority. Furthermore, previous study (e.g. Siddique and Naik, 2004) found that the resistance to freezing-thawing cycles of concrete was improved with the addition of rubber particles. This was attributed to the air-void system within the rubberized concrete matrix. Rubber particles are also considered as high-strain capacity materials, able to increase the ductility and toughness of concrete (Topçu, 1995). Moreover, rubber particles can act as crack arresters to control the initiation and propagation of cracks (Turatsinze *et al.*, 2005). However, the compressive strength and workability of concrete are negatively affected by the addition of rubber particles, especially at high dosages (Taha *et al.*, 2008) since rubber particles can form an interlocking structure resisting the normal flow of concrete, thus resulting in poor workability (Turatsinze and Garros, 2008).

Two-Stage Concrete (TSC) is a special type of concrete produced by preplacing coarse aggregate particles in the formwork, followed by grout injection (Najjar *et al.*, 2014). This unique production technique can overcome workability problems induced by the use of

recycled concrete aggregates (RCA) and tire rubber addition. A main hurdle in using RCA in concrete is its high absorption rate, which compromises workability. However, in TSC, the aggregates are preplaced and the effect of RCA on workability is therefore eliminated. Moreover, TSC has 50% more coarse aggregate content than that of conventional concrete (Abdelgater, 1996). Thus, it is endowed with superior resistance against shrinkage and thermal cracking, which are of paramount importance for flat concrete construction work such as pavements and sidewalks.

Most of TSC past applications have been limited to mass concrete (e.g. dams), underwater concrete such (e.g. bridge piers), and the rehabilitation of existing concrete structures. An exciting potential application of TSC is the construction of sidewalks and pavements with high volume recycled materials. The TSC technique provides cost benefits since 60% of the material (i.e. coarse aggregate particles) is directly preplaced into the formwork and only 40% (i.e. grout) goes through mixing and pumping procedures.

Accordingly, TSC made with RCA and tire rubber granules as partial or full replacement for virgin coarse aggregates, along with tire steel wire fibre reinforcement and a sustainable grout incorporating high volume fly ash and/or other recycled by-products as binders, can offer an exceptional eco-efficient alternative for the construction of economical and sustainable pavements and sidewalks. Thus, the present chapter explores this potential. The effects of incorporating RCA, tire rubber granules and tire steel wire fibres on the mechanical performance and freeze-thaw resistance of green TSC are investigated. The findings can pave the way for a novel technology for the construction of more economical, sustainable and eco-efficient sidewalks and pavements with adequate mechanical strength and superior durability.

7.2. EXPERIMENTAL PROGRAM

7.2.1. Materials and Grout Mixture Proportions

For grout mixtures, CSA A3001 GU cement (noted herein OPC) was used as the main binder. Two types of supplementary cementitious materials (SCMs) including class F fly ash (FA) and high reactivity metakaolin (MK) were added as partial replacement for OPC. **Table 7.1** shows physical and chemical properties for the used binders. Silica sand with a fineness modulus of 1.47 and a saturated surface dry specific gravity of 2.65 was used as a fine

aggregate. TSC grout mixtures with a water-to-binder ratio (*w/b*) of 0.45 and sand-to-binder ratio (*s/b*) of 1 were prepared using a single binder (i.e. grout made with 100% OPC (C)) and a ternary binder (grout made with 50% OPC, 10% MK and 40% FA (MF)). For ternary grout mixtures, the SCM substitution rates were selected to produce sustainable grouts with acceptable mechanical strength based on previous study (Najjar *et al.*, 2016). A poly-carboxylate high-range water-reducing admixture (HRWRA) with a specific gravity of 1.06 and a solid content of 34% was used to adjust the flowability of the grouts according to ACI 304.1 (2005) requirements (i.e. efflux time = 35-40 ± 2 sec). **Table 7.2** presents the grout mixture proportions.

Table 7.1 – Chemical analysis and physical properties of OPC, FA and MK

	OPC	FA	MK
SiO_2 (%)	19.60	43.39	53.50
Al_2O_3 (%)	4.80	22.08	42.50
CaO (%)	61.50	15.63	0.20
Fe_2O_3 (%)	3.30	7.74	1.90
SO_3 (%)	3.50	1.72	0.05
Na_2O (%)	0.70	1.01	0.05
Loss on ignition (%)	1.90	1.17	0.50
Specific gravity	3.15	2.50	2.60
Surface area $(m^2/kg)^*$	371	280	15000

*1 m^2/kg = 4.882 ft^2/lb

Table 7.2 – Grout mixture proportions

Grout Mixture No.	Binder $(kg/m^3)^*$			Sand $(kg/m^3)^*$	Water $(kg/m^3)^*$	HRWRA dosage (%)
	OPC	FA	MK			
C	874	--	--	874	393	0.40
MF	422	338	84	844	380	0.35

* 1 kg/m^3= 0.06247 lb/ft^3

RCA having particle size ranging between 19-38 mm [0.75-1.5 in.], a saturated dry specific gravity of 2.6 and a water absorption of 2.0% was used to produce the green TSC. Moreover, tire rubber particles with an average particle size of 20 mm [0.8 in.] were used as 40% partial replacement for the recycled concrete aggregate. The rubber replacement rate was selected according to a previous study by Jackson (2014), which limited the rubber replacement rate to 40% to avoid excessive reduction in concrete compressive strength. Recycled tire steel wires having a mean diameter of 0.2 mm [0.008 in.], a length ranging between 3 mm and 22 mm [0.11 in. and 0.87 in.] and a tensile strength of 2000 MPa [290 ksi] were incorporated in the green TSC. The volume fraction of the recycled tire wires was 1% according to recommendations by Xie *et al.* (2015). **Figure 7.1** exhibits the used recycled materials to produce the eco-efficient TSC mixtures. A summary of the various TSC mixtures is provided in **Table 7.3**.

| Recycled concrete | Tire rubber particles | Recycled tire wire |

Figure 7.1 – Illustration of ingredients used in producing various TSC mixtures.

Table 7.3 – TSC mixtures

TSC mixture ID	Grout mixture ID*	Coarse aggregate (%)		Recycled tire wires (% by concrete volume)
		Recycled aggregate (RCA)	Tire rubber particles (R)	
CRCA		100	0	0
CR0	C	60	40	0
CR1		60	40	1
MFRCA		100	0	0
MFR0	MF	60	40	0
MFR1		60	40	1

* Grout mixture proportions are presented in **Table 7.2**.

7.2.2. Experimental Procedures

Three types of TSC specimens including cylinders (150 mm × 300 mm [6 in. × 12 in.]), prisms (150 mm × 150 mm × 550 mm [6 in. × 6 in. × 22 in.]) and panels (500 mm × 500 mm × 75 mm [20 in. × 20 in. × 3 in.]) were prepared for each green TSC mixture. Initially, aggregates were placed in the mold as shown in **Figure 7.2** then injected by a grout. After casting, the specimens were covered with wet burlap to prevent surface drying. At age of 24 hr, TSC specimens were demolded and cured in a moist room at temperature (T) of 25°C [77°F] and relative humidity (RH) of 98% until testing age.

Figure 7.2 – Preplacing recycled materials to produce sustainable TSC.

After 28 days, the compressive strength and the static modulus of elasticity of TSC were evaluated on cylindrical specimens according to ASTM C943 (Standard Practice for Making Test Cylinders and Prisms for Determining Strength and Density of Pre-placed-Aggregate Concrete in the Laboratory) and ASTM C469 (Standard Test Method for Static Modulus of Elasticity and Poisson's Ratio of Concrete in Compression), respectively. The flexural strength and toughness of TSC prisms were determined using a three-point bending test as per ASTM C1609 (Standard Test Method for Flexural Performance of Fibre-Reinforced Concrete-Using Beam with Third-Point Loading). The test was conducted using a closed loop deflection-controlled testing with a loading rate of 0.1 mm/min [0.004 in/min].

Furthermore, toughness was calculated as the area under the load-deflection curve up to a deflection of 3 mm [0.11 in.] in accordance with ASTM C1609.

The resistance to freezing-thawing cycles of TSC was assessed conforming to ASTM C666 (Standard Test Method for Resistance of Concrete to Rapid Freezing and Thawing). TSC prisms (275 mm × 75 mm × 75 mm [11 in. × 3 in. × 3 in.]), obtained by cutting TSC panels, were used in this test. After 28 days of moist curing, TSC specimens were exposed to nominal freezing-thawing cycles that consisted of alternately lowering the temperature of specimens from 4 to -18°C [40 to 0°F] and raising it from -18 to 4°C [0 to 40°F] over a period of 4 hours. Visual inspection and mass loss for all TSC specimens were observed after 300 cycles of freeze-thaw.

7.3. RESULTS AND DISCUSSION

7.3.1. Compressive Strength

The compressive strength test results of TSC mixtures are presented in **Table 7.4**. As expected, the compressive strength decreased when tire rubber particles were added. For example, the TSC specimens (CR0) incorporating 40% of recycled tire rubber particles exhibited 41% reduction in compressive strength compared to that of the control CRCA specimens (i.e. made with 100% RCA). This can be ascribed to: 1) reduction of load-carrying capacity as the amount of strong coarse aggregate was replaced; 2) the weak adhesion between rubber particles and the concrete matrix; 3) cracks that occurred around rubber particles due to the elastic and thermal mismatch between the rubber particles and the surrounding grout matrix (Nehdi and Khan, 2001; Zheng *et al.*, 2008; Onuaguluchi and Panesar, 2014).

However, the addition of 1% of recycled tire wires improved the compressive strength behaviour of TSC. For instance, TSC specimens (CR1) incorporating 40% rubber and 1% recycled tire wires achieved about 30% higher compressive strength than that of the CR0 specimens. This is due to the role of recycled tire wires in resisting crack formation and crack propagation in the longitudinal direction (Farnam *et al.*, 2010; Graeff *et al.*, 2012).

Moreover, the TSC specimens incorporating the MF grout mixture (i.e. grout made with 50% OPC, 10% MK and 40% FA) exhibited a reduction in compressive strength compared

with that of the TSC specimens incorporating the C grout mixture (i.e. grout made with 100% OPC). For example, the MFRCA specimens (i.e. made with MF grout mixture and 100% RCA) exhibited around 5% lower compressive strength than that of the CRCA specimens. Also, the MFR0 specimens (i.e. incorporating 40% recycled tire rubber particles) and the MFR1 specimens (i.e. incorporating 40% recycled tire rubber particles and 1% recycled tire wires) showed about 28% and 24% reduction in compressive strength compared with that of the CR0 and CR1 specimens, respectively. This can be attributed to the high level of FA partial replacement (i.e. 40%) for OPC in such a grout mixture. It is well known that grouts incorporating FA gain strength slowly at the age of 28 days due to the slower rate of hydration reactions of FA at early-age (Bouzoubaâ *et al.*, 2004). However, incorporating 10% MK in such a grout mixture slightly offset this reduction in compressive strength due to its high pozzolanic activity (Najjar *et al.*, 2016).

Table 7.4 – Mechanical properties of TSC mixtures

TSC mixture ID	Compressive Strength		Modulus of Elasticity		Flexural Strength		Toughness	
	(MPa)*	COV %	(GPa)*	COV %	(MPa)*	COV %	(J)*	COV %
CRCA	26.5	5.3	29.8	3.4	2.8	7.1	0.5	2.2
CR0	15.6	3.2	19.0	5.7	2.2	9.8	8.8	7.2
CR1	20.3	5.6	22.6	4.0	2.8	8.4	30.5	9.6
MFRCA	25.1	6.8	25.2	3.6	1.6	5.5	0.3	8.1
MFR0	11.3	7.6	16.7	4.3	1.4	7.1	8.4	3.1
MFR1	15.4	4.7	19.0	4.7	2.2	3.8	38.5	6.1

* 1 ksi = 6.894 MPa = 0.006894 GPa; 1 ft. lbs. = 1.356 J

7.3.2. Modulus of Elasticity

The modulus of elasticity results of the TSC mixtures incorporating recycled materials are reported in **Table 7.4**. As expected, incorporating recycled tire rubber particles in TSC significantly reduced the modulus of elasticity. For example, the CR0 specimens exhibited 36% lower modulus of elasticity than that of the CRCA specimens. This is ascribed to the very low elastic modulus of the added rubber particles, which affects the overall concrete modulus of elasticity (Turatsinze *et al.*, 2005; Onuaguluchi and Panesar, 2014). However, the

TSC specimens (CR1) incorporating 1% of recycled tire wires achieved about 19% higher elastic modulus compared to that of the CR0 specimens. As mentioned earlier, recycled tire wires resist crack formation and arrest crack propagation, leading to improved stiffness and higher modulus of elasticity.

Similar to compressive strength, the modulus of elasticity of TSC mixtures was affected by the binder type. For example, the MFR0 and MFR1 specimens showed about 17% and 16% reduction in modulus of elasticity compared to that of the CR0 and CR1 specimens, respectively. The modulus of elasticity for TSC is mainly affected by its compressive strength (Najjar *et al.*, 2014). As discussed above, incorporating a high dosage of FA in the grout mixture can reduce the 28-day TSC compressive strength due to the slower hydration reactions of FA at early-age; thus, weakening the modulus of elasticity (Bouzoubaâ *et al.*, 2004).

7.3.3. Flexural Strength

The flexural strength results of TSC specimens incorporating waste materials are presented in **Table 7.4**. Interestingly, incorporating tire rubber particles and/or recycled tire wires changed the failure mode of TSC specimens from brittle (i.e. broken into two pieces) to somewhat ductile. Moreover, the CR0 specimens achieved flexural strength 21% less than that of the CRCA specimens. This is attributed to the weak interfacial transition zone between rubber particles and the grout matrix, leading to initiation and propagation of cracks around the perimeter of the rubber particles (Najim and Hall, 2010; Xie *et al.*, 2015). However, the addition of recycled tire steel wire fibre counterbalanced the negative effects of incorporating tire rubber particles owing to the crack bridging mechanism imparted by the fibres. Therefore, the CR1 specimens achieved similar flexural strength to that of the CRCA specimens.

Figures 7.3 and **7.4** present the load-deflection curves for different TSC mixtures. It can be observed that the CR0 specimens exhibited sudden increase in deflection accompanied by a reduction in the load capacity after the first crack. However, such specimens showed an ability to withstand post failure loads and underwent significant displacement. This is ascribed to the fact that once the micro-cracks encounter rubber particles, the latter will act as crack arresters owing to their ability to sustain large elastic deformation (Toutanji, 1996;

Twumasi-Boakye, 2014). In addition, it was found that the CR1 specimens achieved better improvement in post-crack flexural behaviour than that of the CR0 specimens. This is due to the stress bridging across cracks induced by steel wire fibres, leading to enhanced post-crack flexural behaviour (Graeff *et al.*, 2012).
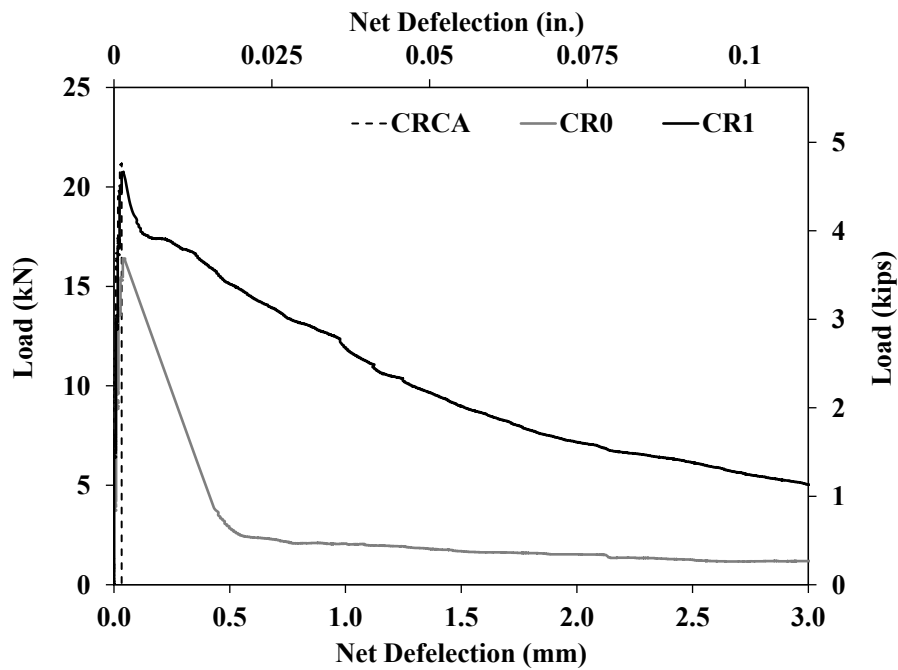
Figure 7.3 – Load-deflection curves for TSC specimens made with the C grout mixture.
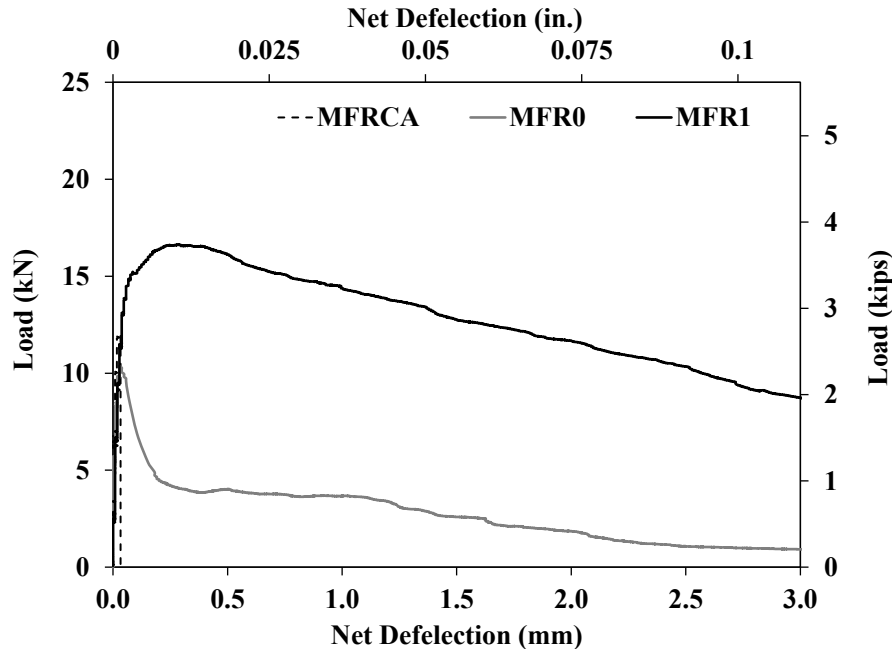
Figure 7.4 – Load-deflection curves for TSC specimens made with the MF grout mixture.

Furthermore, TSC specimens incorporating the MF grout mixture revealed a reduction in flexural strength compared to that of TSC made with the C grout mixture. For example, the MFRCA specimens displayed around 42% lower flexural strength than that of the CRCA specimens. In addition, the MFR0 and MFR1 specimens indicated about 36% and 21% reduction in compressive strength compared with that of the CR0 and CR1 specimens, respectively. This can be attributed to the fact that the grout mixture with high FA dosage (i.e. 40 %) resulted in higher bleeding, which significantly affected the flexural strength of TSC (Hasan, 2012; Najjar *et al.*, 2016). Grouts with high bleeding induce internal voids around aggregate particles and weaken the bond between the aggregates and the surrounding grout matrix; thus, reducing the TSC flexural strength (Abdul Awal, 1984, Najjar *et al.*, 2014). However, the addition of recycled tire wires enhanced the flexural strength of the TSC specimens made with the MF grout mixture owing to their crack bridging mechanism. For instance, the MFR1 specimens achieved about 1.4 times higher flexural strength compared to that of the MFRCA specimens.

7.3.4. Toughness

The toughness test results of the various TSC specimens are presented in **Table 7.4**. The results indicated that the incorporation of recycled tire rubber particles and/or recycled tire wires improved the toughness. For example, the CR0 and CR1 specimens achieved 16 and 56 times higher toughness than that of the control TSC made with 100% RCA (CRCA), respectively. Moreover, the toughness of TSC specimens made with the MF grout mixture was significantly enhanced. For instance, the MFR0 and MFR1 specimens achieved 28 and 128 times higher toughness than that of the MFRCA specimens, respectively. Generally, replacing coarse aggregates by tire rubber particles enhanced the ability of TSC to absorb energy owing to their elastic properties (Toutanji, 1996). Moreover, the addition of recycled tire wires increased the required energy for crack growth, resulting in enhanced toughness of TSC (Graeff *et al.*, 2012).

7.3.5. Resistance to Freezing-Thawing Cycles

The resistance to freezing-thawing cycles of the various TSC mixtures was appraised based on visual inspection and mass loss of TSC specimens subjected to 300 freezing-thawing cycles (**Figures 7.5**-7.7). It was observed that the TSC CRCA specimens made with RCA unveiled surface cracking and loss off concrete portions. The mass loss for CRCA specimens was about 22%. Moreover, the TSC specimens made with the MF grout mixture displayed similar damage features to that of TSC specimens made with the C grout mixture. For instance, the mass loss of MFRCA specimens was around 24%. The mass loss was due to internal stresses associated with ice formation, resulting in surface scaling and cracking of the concrete (Kosmatka, *et al.*, 2003).

Conversely, eco-efficient TSC specimens made with RCA and tire rubber particles were intact upon exposure to freezing-thawing cycles with negligible mass loss. This is attributed to the ability of tire rubber particles to induce entrained air via their non-polar rough surface. Entrained air voids act as stress relief sites, leading to enhanced freeze-thaw durability of TSC (Richardson *et al.*, 2015). Furthermore, the rubber particles can relieve stress build-up induced by ice formation by acting as mini-expansion joints within the concrete (Kaloush *et al.*, 2005). Moreover, the addition of recycled tire wires helped resist the development of cracks induced by freeze-thaw cycles (Sun *et al.,* 1999; Graeff *et al.,* 2012). Thus, CR1 and

MFR1 specimens achieved the best freeze-thaw resistance owing to combined effects of rubber particles and recycled tire wires.
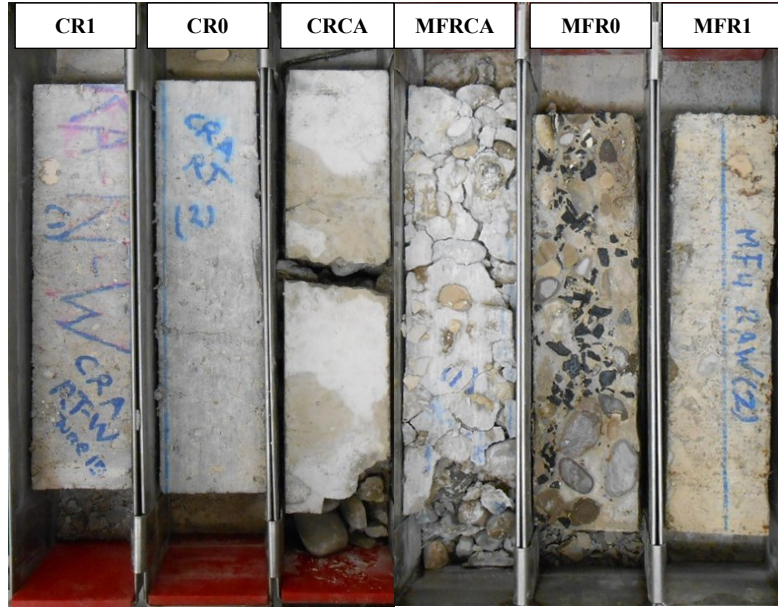
Figure 7.5 – Illustration of various green TSC specimens after 300 freeze-thaw cycles.
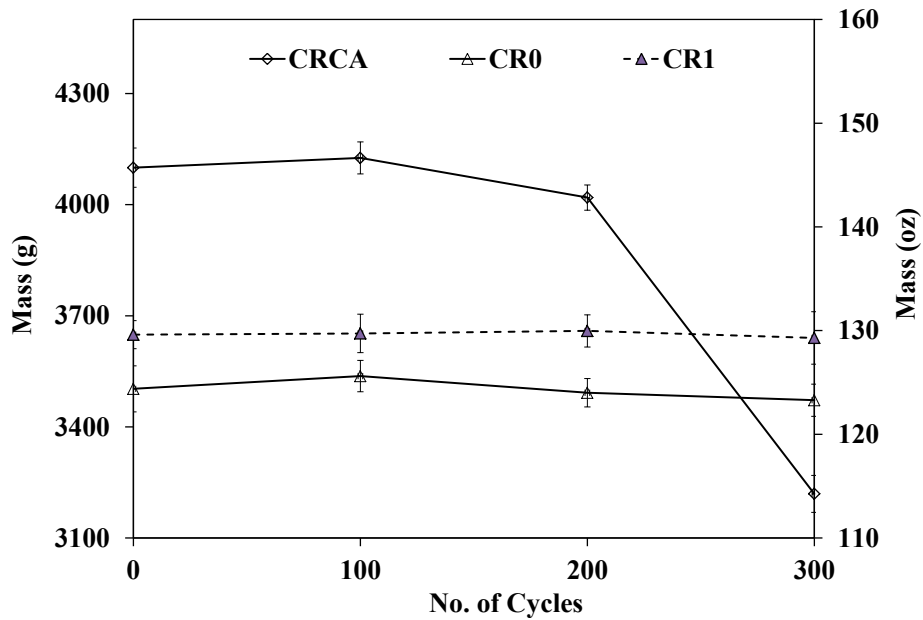
Figure 7.6 – Mass change of TSC specimens made with the C grout mixture versus number of freeze-thaw cycles.
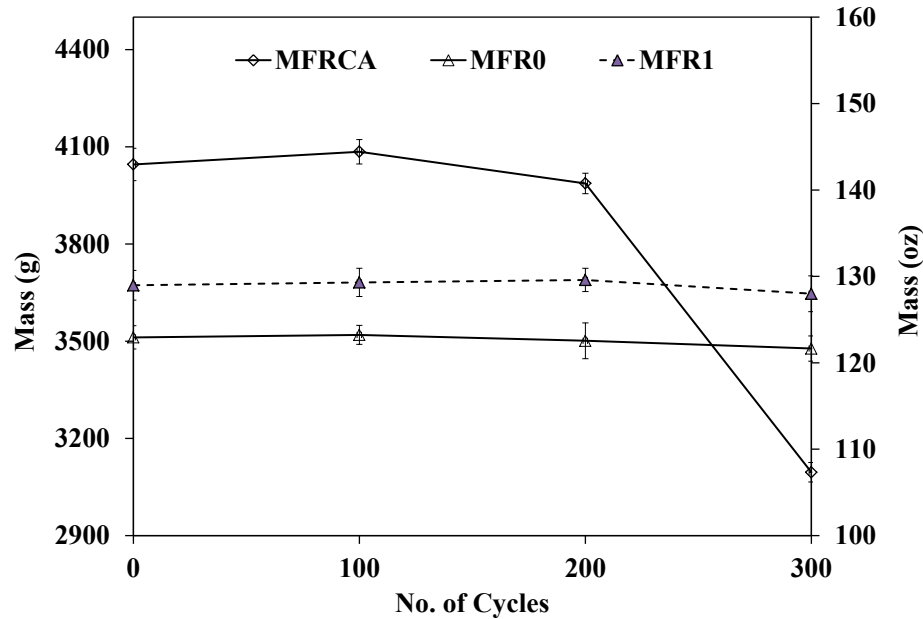
Figure 7.7 – Mass change of TSC specimens made with the MF grout mixture versus number of freeze-thaw cycles.

7.4. STATISTICAL ANALYSIS

Analysis of variance (ANOVA) was used to examine the statistical significance of different experimental variables (e.g. incorporating tire rubber particles, recycled tire wire fibre, and binder type). The *F* value was determined for each variable as the ratio of the mean squared error between treatments to that of within treatments (due to using replicates rather than testing only one specimen). This value is then compared to a standard (critical) *F* value of an *F*-distribution density function obtained from statistical tables based on the significance level ($\alpha = 0.05$) and the degrees of freedom of error determined from the number of treatments and observations in an experiment. Exceeding the critical value of an *F*-distribution density function reflects that the tested variable affects the mean of the results (Montgomery, 2013). **Table 7.5** presents ANOVA results at a significance level of $\alpha = 0.05$ to examine the effects of tire rubber granules and the binder type on the properties of TSC mixtures.

Table 7.5 – Analysis of variance (ANOVA) at a significance level of $\alpha = 0.05$

Properties of Green TSC	Effect of Incorporating Tire Rubber Wastes		Effect of Binder Type	
	F	$F_{(0.05,2,6)}$	F	$F_{(0.05,1,10)}$
Compressive Strength	76.21	5.14	1.12	4.96
Modulus of Elasticity	90.63	5.14	1.35	4.96
Flexural Strength	7.00	5.14	14.63	4.96
Toughness	238.86	5.14	0.07	4.96
Mass Loss after 300 of Freeze-Thaw Cycles	3857.82	5.14	0.01	4.96

The ANOVA Results indicate that incorporating tire rubber wastes as partial replacement for RCA had a significant effect on the mean of the compressive strength, modulus of elasticity, flexural strength, toughness and durability to freeze-thaw cycles of TSC. For example, the calculated F value of 76.21 for the total results of compressive strength was larger than the corresponding critical F value of 5.14 ($F_{0.05, 2, 6}$) (**Table 7.5**). This means that incorporating tire rubber wastes had a significant effect on the mean of the total compressive strength results. Moreover, the variation of the binder type had insignificant effect on the mean of compressive strength, modulus of elasticity, toughness and freeze-thaw durability of TSC. For example, ANOVA for the toughness results had F value of 0.07, which is less than the critical F value of 4.96 ($F_{0.05, 1, 10}$). However, the variation in the binder type revealed a considerable effect of the flexural strength results as the F value of 14.63 was significantly greater than the critical F value of 4.96 ($F_{0.05, 1, 10}$).

7.5. CONCLUSIONS

This study explored the performance of TSC mixtures incorporating recycled concrete aggregates, scrap tire granules, and tire steel wire fibres along with grouts made with ternary binders incorporating high volume fly ash. This material is intended for creating a novel eco-efficient construction technology of sidewalks and pavements, which requires minimal materials mixing and minimal placement effort. Based on the experimental results, the following conclusions can be drawn:

- TSC mixtures made with recycled concrete aggregates performed poorly under freeze-thaw cycles. Hence, it is may not be suitable for pavement construction in cold climates.

- Incorporating tire rubber particles significantly decreased the mechanical properties of TSC, while enhancing its toughness and resistance to freezing-thawing cycles.

- The addition of fibres made from recycled tire wire in TSC allowed overcoming the negative effects on the mechanical properties induced by tire rubber particles. Moreover, the toughness and freeze-thaw resistance were significantly enhanced.

- Using fly ash and metakaolin in a ternary binder for green TSC resulted in a reduction in mechanical properties at 28 days, while the freeze-thaw resistance was comparable to that of TSC made with a 100% OPC single binder.

- Further research is needed to refine TSC formulations for pavement construction, particularly with regards to using various binder combinations in the grout and developing various strength classes for structural pavement design requirements.

- The novel TSC technology proposed for pavement and sidewalk construction is promising. The aggregates are preplaced and not involved in materials mixing. A self-leveling grout is injected with no need for mechanical vibration or compaction effort. This offers substantial labor and energy savings. The preplaced aggregates consist of recycled concrete aggregate and scarp tire granules, thus saving virgin aggregates. The preplacement technique eliminates the well-known negative effects of RCA and tire rubber on concrete workability. The grout can be formulated to consist of high-volume recycled by-products such as fly ash and slag. Using fibres from recycled tire wire, which are preplaced with the aggregates, imparts further performance benefits. The TSC incorporates 50% more coarse aggregate than that of normal concrete. Not only does this offer cost savings, but also superior volume stability through high resistance to shrinkage and thermal cracking. In a nutshell, an eco-efficient technology for making durable, sustainable and more economical pavements and sidewalks seems to be possible using the proposed green TSC method.

7.6. REFERENCES

Abdul Awal, A. S., (1984), "Manufacture and properties of pre-packed aggregate concrete," *Master Thesis*, University of Melbourne, Australia, 121 p.

ACI 304.1, (2005), "Guide for the use of preplaced aggregate concrete for structural and mass concrete applications," *American Concrete Institute*, Farmington Hills, USA, 19 p.

ACI 330, (2008), "Guide for the design and construction of concrete parking lots," *American Concrete Institute*, Farnington Hills, USA.

Association, C. C., Association, C. P. W., Engineering, C. S, C., and Municipalities, F. C. M., (2016), "Canadian infrastructure report card: informing the future," *The Canadian Construction Association (CCA), the Canadian Public Works Association (CPWA), the Canadian Society for Civil Engineering (CSCE) and the Federation of Canadian Municipalities (FCM)*, 164 p.

ASTM C1609/C1609M, (2012), "Standard test method for flexural performance of fibre-reinforced concrete (using beam with third-point loading," A*merican Society for Testing and Materials*, West Conshohocken, PA, USA, 9 p.

ASTM C496/C496M, (2011), "Standard test method for splitting tensile strength of cylindrical concrete specimens," A*merican Society for Testing and Materials*, West Conshohocken, PA, USA.

ASTM C666 / C666M-15, (2015), "Standard test method for resistance of concrete to rapid freezing and thawing," *American Society for Testing and Materials*, West Conshohocken, PA, USA.

ASTM C943, (2010), "Standard practice for making test cylinders and prisms for determining strength and density of pre-placed-aggregate concrete in the laboratory," A*merican Society for Testing and Materials*, West Conshohocken, PA, USA.

Bouzoubaâ, N., Bilodeau, A., Sivasundaram, V., Fournier, B. and Golden, D. (2004) "Development of Ternary Blends for High-Performance Concrete," *ACI Materials Journal*, Vol. 101, pp. 19-29.

CSA A23.1, (2014), "Concrete materials and methods of concrete construction/test methods and standard practices for concrete," *Canadian Standard Association*.

Farnam, Y., Moosavi, M., Shekarchi, M., Babanajad, S.K. and Bagherzadeh, A., (2010), "Behaviour of slurry infiltrated fibre concrete (SIFCON) under triaxial compression," *Cement and Concrete Research*, Vol. 40, No. 11, pp. 1571-1581.

Graeff, A. G., Pilakoutas, K., Neocleous, K. and Peres, M.V., (2012), "Fatigue resistance and cracking mechanism of concrete pavements reinforced with recycled steel fibres recovered from post-consumer tyres," *Engineering Structures*, Vol. 45, pp. 385-395.

Hasan, H. A., (2012), "Effect of fly ash on geotechnical properties of expansive soil," *Journal of Engineering and Development*, Vol. 16, No. 2, pp. 306-316.

Hossack, A., Michael, D. A. Thomas, B. L., Blair, B. and Delagrave, A., (2014), "Performance of Portland limestone cement concrete pavements," *Concrete International*, Vol. 36, No. 1, pp. 40-45.

Jackson, C., States, J., Bewick, B. and Naito, C., (2014), "Assessment of crumb rubber concrete for flexural structural members," *Journal of Materials in Civil Engineering*, Vol. 26, No. 10, pp. 1-8.

Kaloush, K., Way, G. and Zhu, H., (2005), "Properties of crumb rubber concrete," *Journal of the Transportation Research Board*, Washington, D.C., Vol. 1914, pp. 8-14.

Kim, K. S., Yoon, Y. W. and Yoon, G. L., (2011), "Pullout behavior of cell-type tires in reinforced soil structures," *KSCE Journal of Civil Engineering*, Vol. 15, No. 7, pp. 1209-1217.

Kosmatka, S. H., Kerkhoff, B. and Panarese, W. C., (2003), "Design and control of concrete mixtures," *14th edition, Portland Cement Association*, Skokie, Illinois, USA.

Meli, J., (2006), "A life cycle perspective on concrete and asphalt roadways: embodied primary energy and global warming potential," *Athena Institute*, Ottawa, Ontario, Canada.

Montgomery, D.C., (2013), "Design and analysis of experiments," 8_{th} Edition, *Wiley Subscription Services, Inc*.

Najim, K. B. and Hall, M. R., (2010), "A review of the fresh/hardened properties and applications for plain- (PRC) and self-compacting rubberised concrete (SCRC)," *Construction and Building Materials*, Vol. 24, No. 11, pp. 2043-2051.

Najjar, M., Soliman, A. and Nehdi, M., (2016), "Two-stage concrete made with single, binary and ternary binders," *Materials and Structures*, Vol. 49, No. 1, pp. 317-327.

Najjar, M., Soliman, A. and Nehdi, M., (2014), "Critical overview of two stage concrete: properties and applications," *Construction and Building Materials*, Vol. 62, pp. 47-58.

Nehdi, M. and Khan, A., (2001), "Cementitious composites containing recycled tire rubber: an overview of engineering properties and potential applications," *Cement, Concrete, and Aggregates*, Vol. 23, No. 1, pp. 3-10.

Onuaguluchi, O. and Panesar, D. K., (2014), "Hardened properties of concrete mixtures containing pre-coated crumb rubber and silica fume," *Journal of Cleaner Production*, Vol. 82, pp. 125-131.

Rajani, B. and Zhan, C., (1997), "Performance of concrete sidewalks: field studies," *Canadian Journal of Civil Engineering*, Vol. 24, No. 2, pp. 303-312.

Richardson, A., Coventry, K. and Diaz, E., (2015), "Rubber crumb used in concrete to provide freeze-thaw protection," *Proceedings of Euro-Elecs:Latin American and European Conference on Sustainable Buildings and Communities*, Guimarães, Portugal, pp. 21-23.

Siddique, R. and Naik, T. R., (2004), "Properties of concrete containing scrap -tire rubber – an overview," *Waste Management*, Vol. 24, pp. 563-569.

Stripple, H., (2001), "Life cycle assessment of road: a pilot study for inventory analysis," *Report No. B1210E. 2ⁿᵈ ed*. Sweden National Road Administration, Sweden.

Sun, W., Zhang, Y. M., Yan, H. D. and Mu, R., (1999), "Damage and damage resistance of high strength concrete under the action of load and freeze-thaw cycles," *Cement and Concrete Research*, Vol. 29, No. 9, pp. 1519-1523.

Taha, M. M., El-Dieb, A. S., El-Wahab, M. A. and Abdel-Hameed, M. E, (2008), "Mechanical, fracture, and microstructural investigations of rubber concrete," *Journal of Materials in Civil Engineering*, Vol. 20, No. 10, pp. 640-649.

The City of Calgary, (2015), "Roads construction 2015 standard specifications," *Transportation Department, the City of Calgary, ROADS Construction Division*, Calgary, Alberta, Canada, 391 p.

Topçu, I. B., "1995", "The properties of rubberized concretes," *Cement and Concrete Research*, Vol. 25, No. 2, pp. 304-310.

Toutanji, H. A., (1996), "The use of rubber tire particles in concrete to replace mineral aggregates," *Cement and Concrete Composites*, Vol. 18, No. 2, pp. 135-139.

Turatsinze, A. and Garros, M., (2008), "On the modulus of elasticity and strain capacity of self-compacting concrete incorporating rubber aggregates," *Resources, Conservation & Recycling*, Vol. 52, No. 10, pp. 1209-1215.

Turatsinze, A., Bonnet, S. and Granju, J., (2005), "Mechanical characterisation of cement-based mortar incorporating rubber aggregates from recycled worn tyres," *Building and Environment*, Vol. 40, No. 2, pp. 221-226.

Twumasi-Boakye, Richard., (2014), "Ground tire rubber as a component material in concrete mixtures for paving concrete," *M.S. Thesis, ProQuest Dissertations Publishing*, The Florida State University, Florida, USA, 115 p.

U.S.EPA., (2009), "Estimating 2003 building related construction and demolition material amounts," *U.S. Environmental Protection Agency*, Washington DC, U.S.A, 60 p.

Xie, J., Guo, Y., Liu, L. and Xie, Z., (2015), "Compressive and flexural behaviours of a new steel-fibre-reinforced recycled aggregate concrete with crumb rubber," *Construction and Building Materials*, Vol. 79, pp. 263-272.

Yeheyis, M., Hewage, K., Alam, M. S., Eskicioglu, C. and Sadiq, R., (2013), "An overview of construction and demolition waste management in Canada: a lifecycle analysis approach to sustainability," *Clean Technologies and Environmental Policy*, Vol. 15, No. 1, pp. 81-91.

Zheng, L., Sharon Huo, X. and Yuan, Y., (2008), "Strength, modulus of elasticity, and brittleness index of rubberized concrete," *Journal of Materials in Civil Engineering*, Vol. 20, No. 11, pp. 692-699.

Chapter 8

8. FUZZY INFERENCE SYSTEMS BASED PREDICTION OF ENGINEERING PROPERTIES OF TWO-STAGE CONCRETE[(*)]

8.1. INTRODUCTION

Two-stage concrete (TSC), also known as preplaced aggregate concrete, has been successfully used for many years in numerous applications such as underwater construction and the rehabilitation of concrete structures (ACI 304.1, 2005; Najjar *et al.*, 2014). It is cast differently from conventional concrete. Coarse aggregates are first preplaced and then injected with a mixture of cement, water, fine sand, and possibly chemical admixtures, commonly termed "grout" in TSC practice (Abdul Awal, 1984). The properties of the grout used and its ability to flow around the preplaced aggregate particles and effectively fill voids have a governing effect on the mechanical properties and durability of the final product (Abdelgader, 1996; ACI 304.1, 2005).

Grout flowability is primarily dependent on the chemical and physical properties of the ingredients used in the mixture (i.e. sand, cement, supplementary cementitious materials (SCMs), and admixtures) along with their respective proportions (Abdelgader and Elgalhud, 2008; O'Malley and Abdelgader, 2010; Najjar *et al.*, 2014; Coo and Pheeraphan, 2015). It has been argued that using SCMs could enhance the mechanical properties and durability of TSC (ACI 304.1, 2005). However, limited research has been devoted to the investigation of the effects of SCMs on the grout flowability and the mechanical properties of TSC. A recent study has involved the examination of the mechanical properties of TSC incorporating a variety of SCMs. It was found that the type of SCM and the binder composition have a significant influence on the mechanical properties of TSC (Najjar *et al.*, 2016).

Over the last few decades, considerable research has been directed to generating models for predicting the properties of various types of concrete (Kute and Kale, 2013). However, only very few researchers have attempted to propose equations that are essentially based on

---

nonlinear regression analysis for predicting the flowability and mechanical properties of TSC. For example, nonlinear regression analysis was used as a means of establishing the relationship between the compressive strength of TSC and the mixture proportions of the grout (i.e. water-to-binder ratio (*w/b*) and sand-to-binder ratio (*s/b*)) (Abdelgader, 1999; Abdelgader and Elgalhud, 2008). Some of the proposed formulas are dependent on the shape of the coarse aggregate (Abdelgader, 1999), while others are based on the admixtures used (Abdelgader and Elgalhud, 2008). Empirical correlations between the grout properties and mechanical properties of the corresponding TSC have also been suggested (Najjar *et al.*, 2016).

A number of modeling methods based on fuzzy logic systems (FLS) have recently been employed for a variety of civil engineering applications (Kute and Kale, 2013). The primary advantage of fuzzy logic (FL) models is their ability to describe knowledge in a descriptive human-like manner in the form of simple rules based on the use of linguistic variables (Demir, 2005). For instance, an FL model can be effectively used for estimating the properties of concrete without the necessity for performing costly experimental investigations (Feng *et al.*, 2009). However, there has been so far no attempt to develop FL models for estimating the flowability and mechanical properties of TSC in the open literature. The goal of this study is therefore to create FL models that can estimate the flowability and mechanical properties of TSC and serve as accurate predictive tools for designing TSC mixtures in which a variety of types and dosages of SCMs can be incorporated.

8.2. OVERVIEW OF FUZZY LOGIC MODELS

Fuzzy set theory was introduced for the first time in 1965 by Zadeh, who developed fuzzy logic as an alternative to Aristotelian logic, in which only two possibilities are defined: true and false (Zadeh, 1965). FL corresponds to a natural way of thinking, in which verbally expressed rules are applied to address vagueness. This type of logic also encompasses the concept of any object belonging partially to different subsets of the universal set, rather than belonging entirely to only a single set. Partial belonging to a set can be described numerically by a membership function, which assumes values between 0 (completely false) and 1 (completely true) (Topçu and Sarıdemir, 2008; Da Silva and Stemberk, 2013). The ability to deal with imprecise and vague information makes FL reasoning a robust and flexible tool for use in a number of engineering applications (Nehdi and Bassuoni, 2009). However, FL was

reported to be very complex and hence requires more time for execution when applied on high dimensional data. Moreover, FL performs poorly when applied on database of small size (Anifowose *et al.*, 2013).

Fuzzy inference systems (FIS) are modeling tools that can address ambiguity in complex systems. In general, a FIS has four basic components: fuzzification, a fuzzy rule base, a fuzzy output engine, and defuzzification (Ross, 2010). The purpose of fuzzification is to map the crisp input to values from 0 to 1 using a set of input membership functions (Subaşı *et al.*, 2013). Fuzzy membership functions have different forms; however, the linear forms (i.e., triangular shapes) are suitable for most practical applications (Nehdi and Bassuoni, 2009).

In a fuzzy rule base, all possible fuzzy relations between the input and output data are expressed as IF‑THEN statements, which convey human knowledge and expertise (Ross, 2010). Fuzzy rules can be written in the following form (Sivanandam *et al.*, 2007):

***IF** (input₁ is membership function₁) **and/or** (input₂ is membership function₂) **and/or**......**THEN** (outputₙ is membership functionₙ)*

Language connectives such as "logical and" or "logical or," which are similar to the operations of "intersection" and "union," respectively, are commonly used in compounded rules (Nehdi and Bassuoni, 2009). For example, the fuzzy intersection of two fuzzy sets A and B in a universe of discourse X can be expressed in terms of membership functions μ(x), as follows:

$$\mu(x) = min[\mu_A(x), \mu_B(x)] = \mu_A(x) \cap \mu_B(x) \qquad \text{Eq. 8.1}$$

where x is an input element of the universe X; $\mu_A(x)$ and $\mu_B(x)$ are the degrees of membership in fuzzy sets (*A*) and (*B*), respectively; and "min" stands for a minimization operator.

In a fuzzy inference engine, all fuzzy rules in the fuzzy rule base are collected in order to generate an overall conclusion arising from the individual consequences of each rule. The Mamdani inference method is the methodology most commonly applied in the research reported in the literature. It was proposed by Mamdani (1975) as an attempt to control a steam engine by synthesizing a set of linguistic control rules obtained from experienced human operators (Nehdi and Bassuoni, 2009; Subaşı *et al.*, 2013). In this method, the consequences of individual rules are truncated by minimization (min) or scaled by product

operators. In both cases, all consequences are then aggregated by a maximization (max) operator in order to obtain the final conclusion (Ross, 2010; Sivanandam *et al*., 2007).

In defuzzification, the fuzzy output from the fuzzy interference engine is converted to a number (Bassuoni and Nehdi, 2008; Subaşı *et al*., 2013). The centroid method is the approach most widely employed for the defuzzification of fuzzy output sets. The centroid defuzzification technique can be expressed as follows:

$$z^* = \int \frac{\mu(z)zdz}{\mu(z)dz}$$
<div align="right">**Eq. 8.2**</div>

Where, z^* is the defuzzified output value, z is the output value in a fuzzy subset (*s*), and $\mu(z)$ is the corresponding degree of membership of the output in the same fuzzy subsets. Extensive details about FL methods, the associated mathematical background, and the application of these methods are beyond the scope of the study presented in this chapter and have been published previously by Ross (2010). Examples of fuzzy logic models use in the realm of concrete research can be found in (Bedirhanoglu., 2015; Tsai *et al*., 2015; Zhang, 2015).

8.3. EXPERIMENTAL PROGRAM

8.3.1. Materials and Grout Mixture Proportions

Ordinary portland cement (OPC) was used as the main binder for all tested grout mixtures. Three types of SCMs including fly ash (FA), silica fume (SF), and metakaolin (MK) were used as partial replacement for OPC. **Table 8.1** summarizes physical and chemical properties of the used materials. Silica sand with a fineness modulus of 1.47 and a saturated surface specific gravity of 2.65 was used as the fine aggregate. All grout mixtures had the same sand-to-binder ratio (*s/b* = 1.0), which is the commonly accepted practice. Three water-to-binder ratios (*w/b*) of 0.35, 0.45 and 0.55 were tested. A poly-carboxylate high-range water-reducing admixture (HRWRA) with a specific gravity of 1.064, a solid content of 34% and pH of 5 was added at different dosages. Several TSC grout mixtures were prepared using single, binary, and ternary binders corresponding with different HRWRA dosages. The mixture proportions of the tested grouts are provided in **Table 8.2**. Crushed limestone coarse aggregate with a maximum nominal size of 40 mm, a saturated surface dry specific gravity of 2.65, and a water absorption of 1.63% was used for the production of the various TSC

mixtures. Two types of cold-drawn hooked-end steel fibres were employed; their properties are listed in **Table 8.3**. The steel fibre dosages (i.e. volume fractions) used in the TSC were 1%, 2%, 4%, and 6%, which covers the practical dosage range.

Table 8.1 – Chemical analysis and physical properties of OPC, FA, SF, and MK

	OPC	FA	SF	MK
SiO_2 (%)	19.60	43.39	95.30	53.50
Al_2O_3 (%)	4.80	22.08	00.17	42.50
CaO (%)	61.50	15.63	00.49	0.20
Fe_2O_3 (%)	3.30	7.74	00.08	1.90
SO_3 (%)	3.50	1.72	00.24	0.05
Na_2O (%)	0.70	1.01	00.19	0.05
Loss on ignition (%)	1.90	1.17	4.7	0.50
Specific gravity	3.15	2.50	2.20	2.60
Surface area (m^2/kg)*	371	280	19500	15000

*1 m^2/kg = 4.882 ft^2/lb

Table 8.2 – Grout mixture proportions

Grout Mixture No.	Grout Mixture Notation	Binder (kg/m³)*				Sand (kg/m³)*	Water (kg/m³)*
		OPC	FA	SF	MK		
C-0.35	100OPC	957	--	--	--	957	335
F1-0.35	90OPC-10FA	855	95	--	--	950	332
F3-0.35	70OPC-30FA	654	280	--	--	935	327
F5-0.35	50OPC-50FA	460	460	--	--	921	322
S1-0.35	90OPC-10SF	850	--	94	--	945	331
SF4-0.35	50OPC-10SF-40FA	458	366	92	--	916	321
M1-0.35	90OPC-10MK	856	--	--	95	951	333
MF4-0.35	50OPC-10MK-40FA	461	369	--	92	922	323
C-0.45	100OPC	874	--	--	--	874	393
F1-0.45	90OPC-10FA	781	87	--	--	867	390
F3-0.45	70OPC-30FA	599	257	--	--	855	385
F5-0.45	50OPC-50FA	422	422	--	--	843	379
S1-0.45	90OPC-10SF	777	--	86	--	863	388
SF4-0.45	50OPC-10SF-40FA	420	336	84	--	839	378
M1-0.45	90OPC-10MK	782	--	--	87	868	391
MF4-0.45	50OPC-10MK-40FA	422	338	--	84	844	380
C-0.55	100OPC	803	--	--	--	803	442
F1-0.55	90OPC-10FA	718	80	--	--	798	439
F3-0.55	70OPC-30FA	551	236	--	--	788	433
F5-0.55	50OPC-50FA	389	389	--	--	778	428
S1-0.55	90OPC-10SF	715	--	79	--	795	437
SF4-0.55	50OPC-10SF-40FA	387	310	77	--	774	426
M1-0.55	90OPC-10MK	719	--	--	80	799	439
MF4-0.55	50OPC-10MK-40FA	389	311	--	78	778	428

*1 kg/m³= 0.06247 lb/ft³

Table 8.3 – Properties of hooked-end steel fibres

Steel Fibre Type	Length (mm)[*]	Diameter (mm)[*]	Aspect ratio	Specific gravity	Tensile strength (MPa)[*]
Short (S)	33	0.75	80	7.85	1100
Long (L)	60	0.75	44	7.85	1100

* 1 in. = 25.4 mm, 1 ksi = 6.894 MPa

8.3.2. Experimental Procedures

All grout mixtures were prepared as per the guidelines of ASTM C938 (Standard Practice for Proportioning Grout Mixtures for Preplaced-Aggregate Concrete). Mixing and flowability measurements were conducted at room temperature ($T = 23°C \pm 2°C$) [73.4°F ± 3.6°F]. Immediately following the mixing, grout flowability was evaluated using a flow cone test according to ASTM C939 (Standard Test Method for Flow of Grout for Preplaced-Aggregate Concrete - Flow Cone Method). The flow cone test entails measuring the time required for the efflux of 1725 ml [0.06 ft^3] of the grout through a specific cone that has a 12.7 mm [0.5-in.] discharge tube. A spread flow test was also conducted in order to study the effects of SCMs on the point at which the grout mixture begins to flow freely, which identifies the optimum water content (Hunger and Brouwers, 2009). The grout is placed into a special conical mold, which is lifted straight upwards in order to allow free flow.

Based on the efflux time and spread flow results for the various grout mixtures, it was found that all grout mixtures made with a *w/b* ratio = 0.45 could achieve the efflux time of 35-40 ± 2 sec recommended by ACI 304.1 (2005) for successful TSC production. The optimum HRWRA dosage that meets the efflux time recommendations was considered for each grout mixture made with the selected *w/b* ratio. The compressive strength of the selected grouts was tested on 50 mm [2 in.] cubic specimens at ages of 7, 28, and 56 days according to ASTM C 942 (Standard Test Method for Compressive Strength of Grouts for Preplaced-Aggregate Concrete in the Laboratory).

Thereafter, the effects of incorporating various rates and types of SCMs on the mechanical properties of the TSC mixtures made with the selected grouts were investigated. The mechanical performance of two-stage steel fibre-reinforced concrete (TSSFRC)

incorporating different steel fibre dosages and lengths was also explored. Cylindrical TSC and TSSFRC specimens (150mm × 300mm [6-in. × 12-in.]) were prepared. For the TSC specimens, all molds were filled with the coarse limestone aggregate, and the specific grout was then injected in a manner similar to the procedure adopted in previous TSC studies (e.g., Abdelgader *et al*., 2010; O'Malley and Abdelgader, 2010). For the TSSFRC specimens, the coarse aggregates and steel fibres were premixed and preplaced in the molds. A grout made with 100% OPC was subsequently injected to fill in the space around the coarse aggregates and fibres. Specimens were covered with wet burlap immediately after casting in order to prevent surface drying. After 24h, specimens were demolded and cured in a moist curing room (temperature (T) = 25°C [77°F] and relative humidity (RH) = 98%) until the desired testing ages. At each testing age (i.e. 7, 28 and 56 days), the compressive and splitting tensile strengths of the TSC specimens were evaluated according to ASTM 943 (Standard Practice for Making Test Cylinders and Prisms for Determining Strength and Density of Preplaced-Aggregate Concrete in the Laboratory) and ASTM C496/C496M (Standard Test Method for Splitting Tensile Strength of Cylindrical Concrete Specimens), respectively.

The results obtained from this experimental program were used to build a database for the development of FL models for predicting the grout efflux time, grout spread flow, grout compressive strength, TSC compressive strength, and TSC tensile strength.

8.4. FUZZY LOGIC MODELS

8.4.1. Database

In this study, two FL models were created with the goal of predicting the grout flowability and mechanical properties of TSC. FL model I was developed for calculating the expected efflux time and the spread flow of a wide range of TSC grout mixtures. The database for training and testing this model contained 228 data points associated with 24 grout mixtures. The model and database have 6 input variables: the *w/b* ratio and the OPC, FA, SF, MK, and HRWRA dosages. The efflux time and spread flow of the TSC grouts constituted the experimental output parameters of the database. Hence, they also were the output predicted by the FL model I. **Figure 8.1** illustrates the general structure of the developed FL model I. The database was divided randomly into 188 data sets for training and 40 data sets for testing

the model, respectively. The properties of the training and testing data sets for model I are listed in **Table 8.4**.
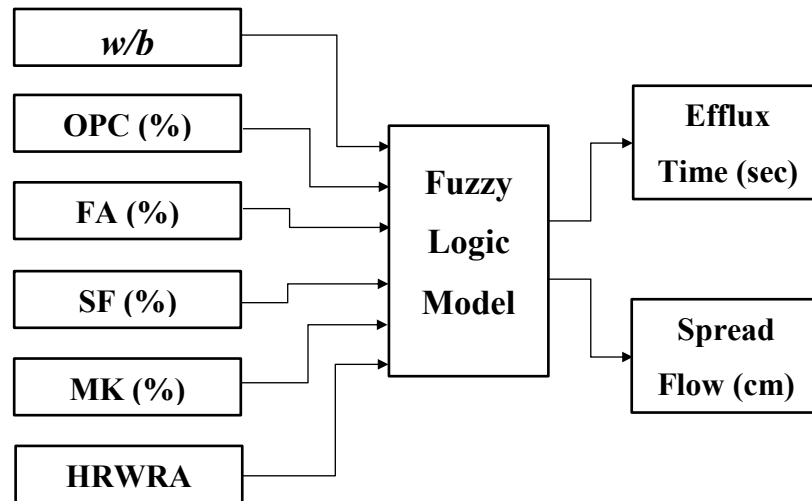
Figure 8.1 – General structure of the developed FL Model I.

Table 8.4 – Range of training and testing output variables for models I and II

FL Model/Property	Training Data			Testing Data		
	Min.	Max.	Avg.	Min.	Max.	Avg.
I/Grout efflux time (sec)	11.0	194.0	59.7	14.0	196.0	70.6
I/Grout spread flow (cm)	25.9	41.0	11.3	11.3	39.7	26.1
II/Grout compressive strength (MPa)	20.7	64.4	43.4	21.5	52.7	43.5
II/TSC compressive strength (MPa)	11.6	48.8	28.6	12.7	47.1	28.8
II/TSC tensile strength (MPa)	2.3	8.4	3.8	2.4	7.5	3.9

FL model II was then developed in order to predict the compressive and tensile strengths of a wide range of TSC mixtures. The database for training and testing this model contained 132 data points based on 19 TSC mixtures. The model and database have 7 input variables: the OPC, FA, SF, MK, short-steel fiber dosage, long-steel fiber dosage, and the age of the test specimen. The compressive and tensile strengths of the TSC mixtures constituted the experimental database parameters measured and were hence the output predicted by the FL model II. **Figure 8.2** illustrates the general structure of the developed FL model II. The

database was divided randomly into 116 data sets for training and 16 data sets for testing the model, respectively. The properties of the training and testing data sets for model II are listed in **Table 8.4**.
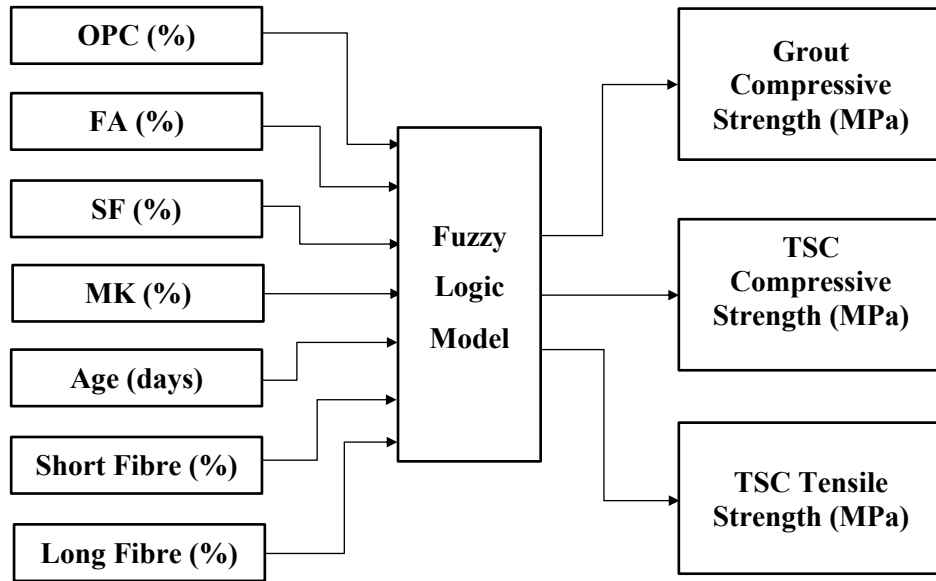
Figure 8.2 – General structure of the developed FL Model II.

8.4.2. Construction of Fuzzy Inference Systems

The FL models were created in a MATLAB environment. The Mamdani inference method was used to develop these models. Partial belonging to a set was described numerically using a membership function that assumes values between 0 and 1. Triangular membership functions were used for fuzzy modeling. The membership functions for the input parameters used for the fuzzy modeling are illustrated in **Figures 8.3** and **8.4**. After the membership functions were determined, rules were written based on the experimental results. The following are examples of the rules that were created:

For Model I: *IF w/b = 0.45 and OPC = 50% and FA = 40% and SF = 0% and MK = 10% and HRWRA = 0.2% THEN grout efflux time = 56 sec and grout spread flow is 17.5 cm.*

For Model II: *IF OPC = 100% and FA = 0% and SF = 0% and MK = 0% and short steel fibre= 0%, and long steel fiber = 0% and age of the test sample = 28 days THEN grout*

compressive strength = 50.4 MPa and TSC compressive strength = 35.9 MPa, and TSC tensile strength = 5.6 MPa.

In the final stage, the model results were obtained from the defuzzification monitor. The defuzzification was performed using the centroid of area method expressed in **Eq. 8.2**.
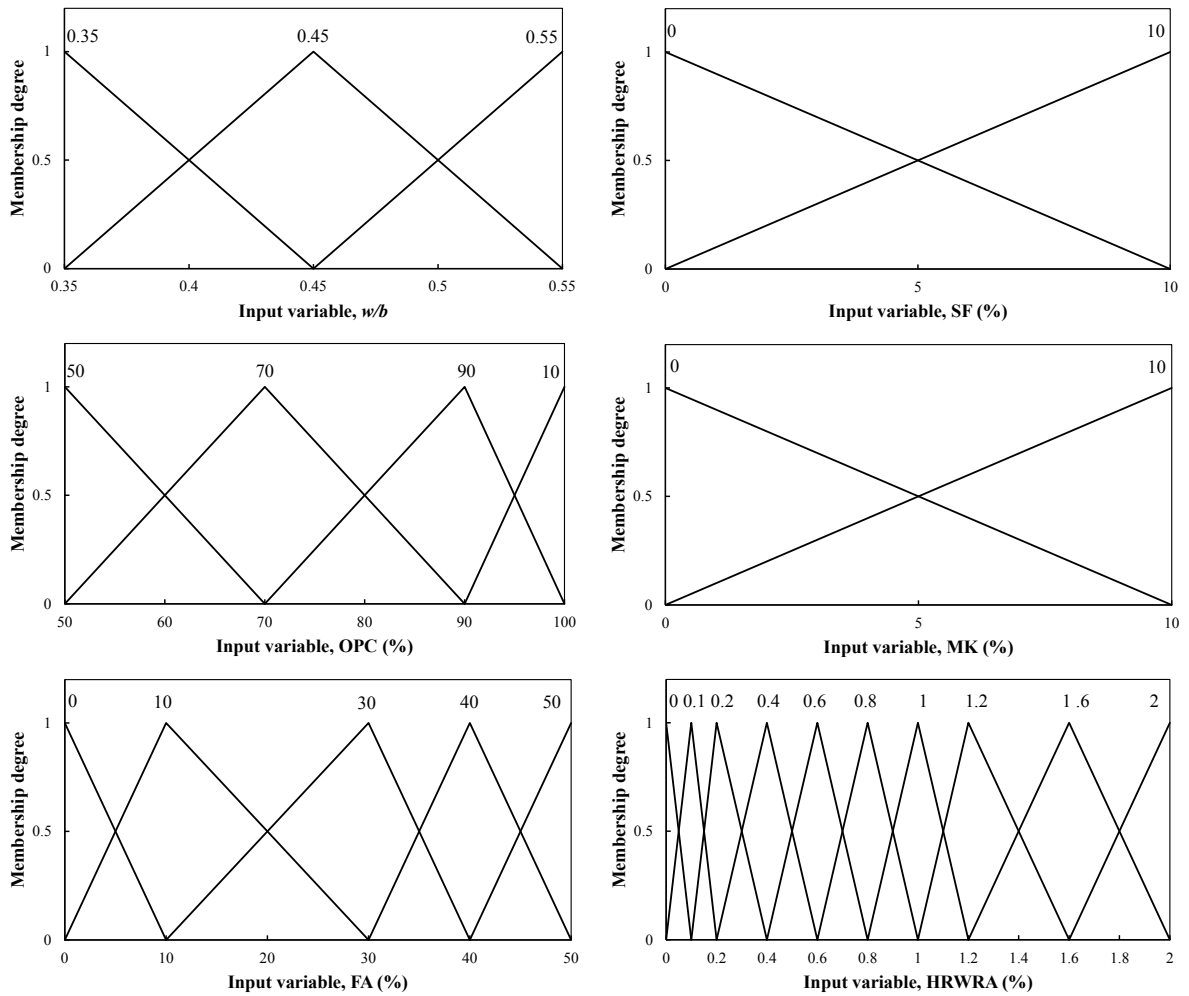
Figure 8.3 – Membership functions for input parameters of FL Model I.
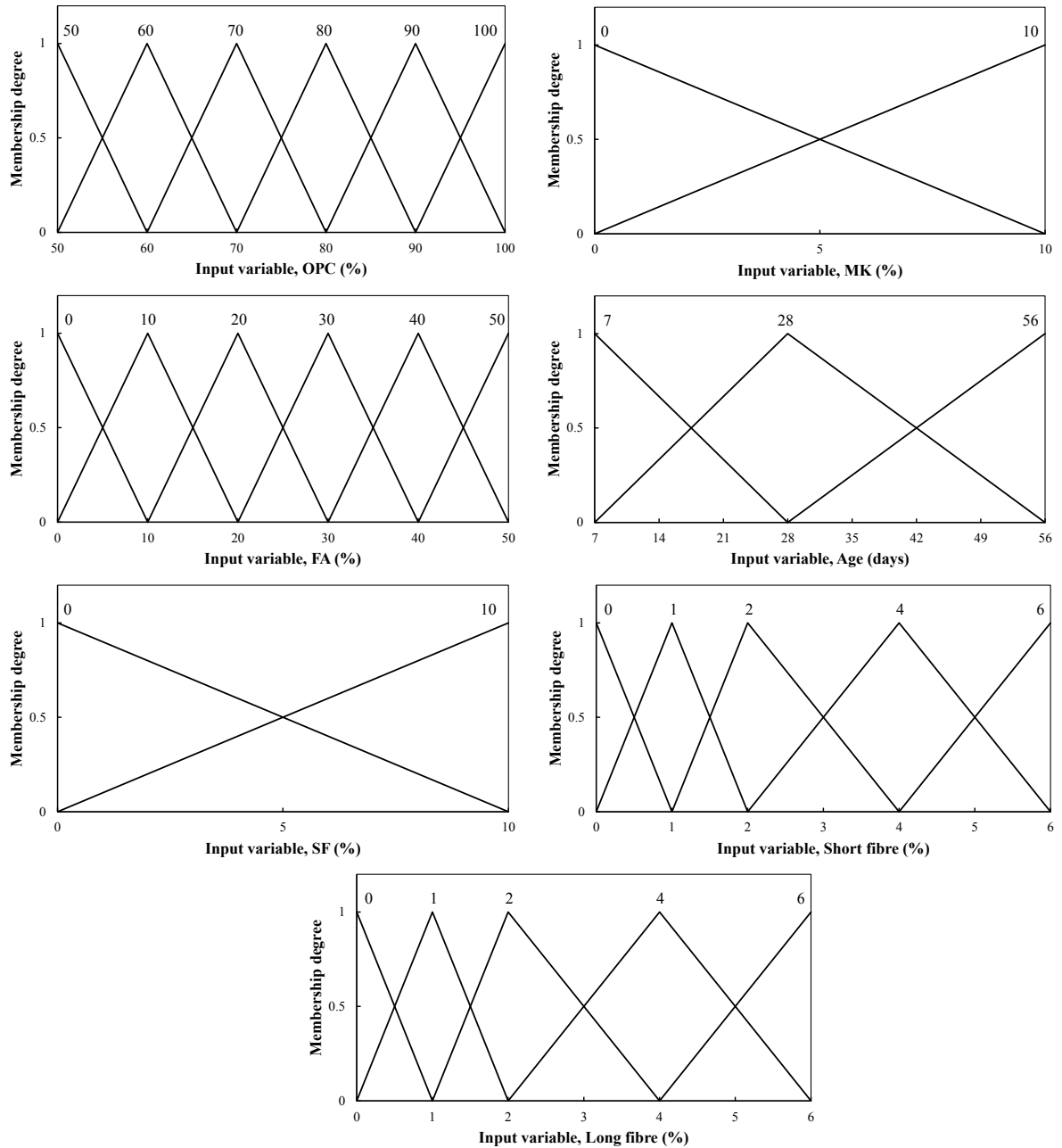
Figure 8.4 – Membership functions for input parameters of FL Model II.

8.5. ANALYSIS, RESULTS AND DISCUSSION

8.5.1. Trained FL Models

To evaluate the accuracy of the predictions of the trained system, the training data were revisited as a means of checking the trained FL models. The training data values predicted by

the two FL models for the properties (i.e. grout efflux time, grout spread flow, grout compressive strength, TSC compressive strength, and TSC tensile strength) are shown in **Figure 8.5**. It can be observed that the FL models have captured the input-output relations as the points located mostly on or slightly under/above the equity line between the experimental and predicted values. The performance of model I with respect to predicting the grout efflux time and the grout spread flow is also satisfactory. These results are confirmed by the results of a statistical analysis of the training data with respect to the ratio of the experimental-to-predicted values for each property (P_{exp}/P_{pre}), as portrayed in **Table 8.5**. For example, the average, the standard deviation, and the coefficient of variation (COV) for the (P_{exp}/P_{pre}) of the grout spread flow training data were 1.00, 0.05, and 4.99%, respectively. These findings indicate that the performance of model I with respect to predicting the spread flow is satisfactory and that the model exhibits good prediction accuracy.

Table 8.5 – Statistical analysis based on the ratio of experiential-to-predicted property

FL Model/Property	Training Data			Testing Data		
	Avg.	STDEV	COV (%)	Avg.	STDEV	COV (%)
I/Grout efflux time (sec)	1.00	0.06	5.79	1.02	0.07	7.35
I/Grout spread flow (cm)	1.00	0.05	4.99	0.97	0.06	5.84
II/Grout compressive strength (MPa)	1.02	0.04	4.30	1.03	0.05	5.15
II/TSC compressive strength (MPa)	1.01	0.04	3.49	1.03	0.03	3.14
II/TSC tensile strength (MPa)	1.01	0.04	3.77	1.03	0.05	4.57
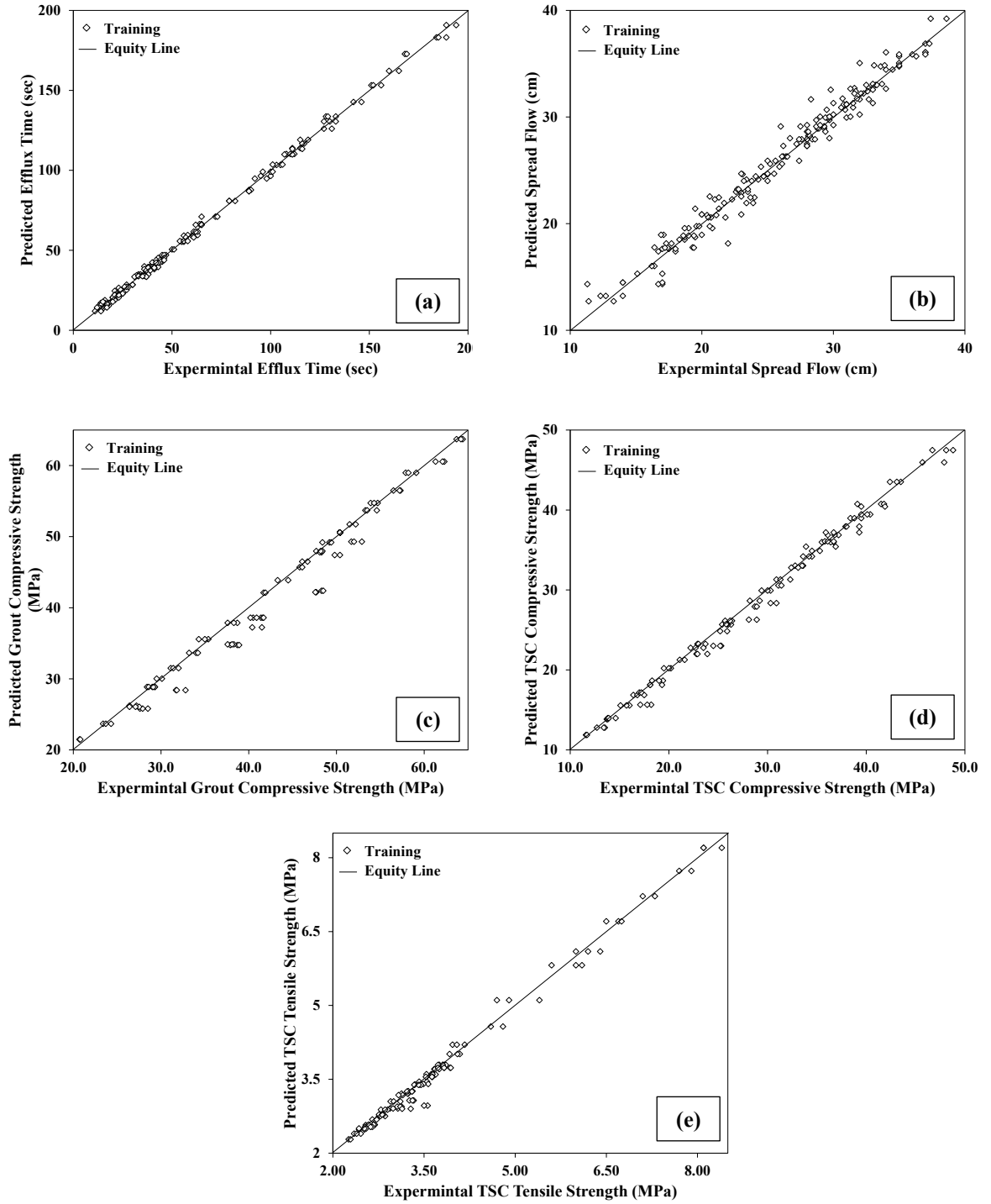
Figure 8.5 – Performance of FL models using training data in predicting: (a) grout efflux time, (b) grout spread flow, (c) grout compressive strength, (d) TSC compressive strength and (e) TSC tensile strength.

8.5.2. Testing Predictive Capability of FL Models

To examine the capacity of the FL model I and model II with respect to generalization, they were tested on 40 sets and 16 sets of test data, respectively. The values predicted by the two FL models for the properties of the test data (i.e. grout efflux time, grout spread flow, grout compressive strength, TSC compressive strength, and TSC tensile strength) are exhibited in **Figure 8.6**. Similar to the case involving the training data points, FL models I and II produced reasonable predictions relative to the actual corresponding values measured experimentally. It can be observed in **Figure 8.6** that test data points were located mostly on or slightly deviating from the equity line.

Table 8.5 summarizes the statistical parameters pertaining to the responses of the FL models I and II with respect to the actual experimental test data. For example, the average, the standard deviation, and the coefficient of variation (COV) of the (P_{exp}/P_{pre}) values of the TSC compressive strength test data were 1.03, 0.03, and 3.14 %, respectively. Based on the statistical analysis of the (P_{exp}/P_{pre}) values for the test data, it can be concluded that FL models I and II are capable of effectively generalizing the relationships between the input variables and the output results and that the models yield reasonably accurate predictions.

Moreover, the performance of the FL model II was validated using data collected from the literature as reported in **Table 8.6**. It can be observed that the FL results were in agreement with the experimental results published by others. The slight variation between the experimental and FL results can be due to differences in the properties of the materials used in the various studies.

8.5.3. Error Analysis of FL Models

The performance of both FL models thus developed was assessed based on the root-mean-square error ($RMSE$), the absolute fraction of variation (R^2), and the mean absolute percentage error ($MAPE$), using the following equations.

$$RMSE = \sqrt{\frac{1}{n}\sum \left|P_{exp} - P_{pre}\right|^2}$$

Eq. 8.3

$$R^2 = 1 - \left(\frac{\sum (P_{exp} - P_{pre})^2}{\sum P_{pre}^2} \right) \qquad \text{Eq. 8.4}$$

$$MAPE = \frac{1}{n} \sum \frac{|P_{exp} - P_{pre}|}{P_{exp}} \times 100 \qquad \text{Eq. 8.5}$$

where (P_{exp}) and (P_{pre}) are the experimental and predicted values of the properties (i.e. grout efflux time, grout spread flow, grout compressive strength, TSC compressive strength, and TSC tensile strength), respectively, and (n) is the number of data points.

Table 8.6 – Comparison between experimental results collected from the literature and corresponding FL model II predictions

Ref.	OPC (%)	FA (%)	SF (%)	Steel dosage (%)	Age (days)	Grout compressive strength results (MPa)		
						Exp.	FL	COV (%)
(Abdul Awal, 1984)	100	0	0	0	28	41.0	47.4	7.2
(Abdelgader, 1999)	100	0	0	0	28	43.8	47.4	3.9
	OPC (%)	FA (%)	SF (%)	Steel dosage (%)	Age (days)	TSC compressive strength results (MPa)		
						Exp.	FL	COV (%)
(Abdul Awal, 1984)	100	0	0	0	28	29.0	30.6	2.7
(Abdelgader, 1999)	100	0	0	0	28	30.7	30.6	0.2
(Bayer, 2004)	50	50	0	0	28	10.6	13.9	13.5
(Abdelgader et al., 2016)	94	0	6	0	28	22.6	32.8	18.4
	OPC (%)	FA (%)	SF (%)	Steel dosage (%)	Age (days)	TSC tensile strength results (MPa)		
						Exp.	FL	COV (%)
(Abdul Awal, 1984)	100	0	0	0	28	3.1	3.6	7.5
(Abdelgader and Ben-Zeitun, 2005)	100	0	0	0	28	3.0	3.6	9.1
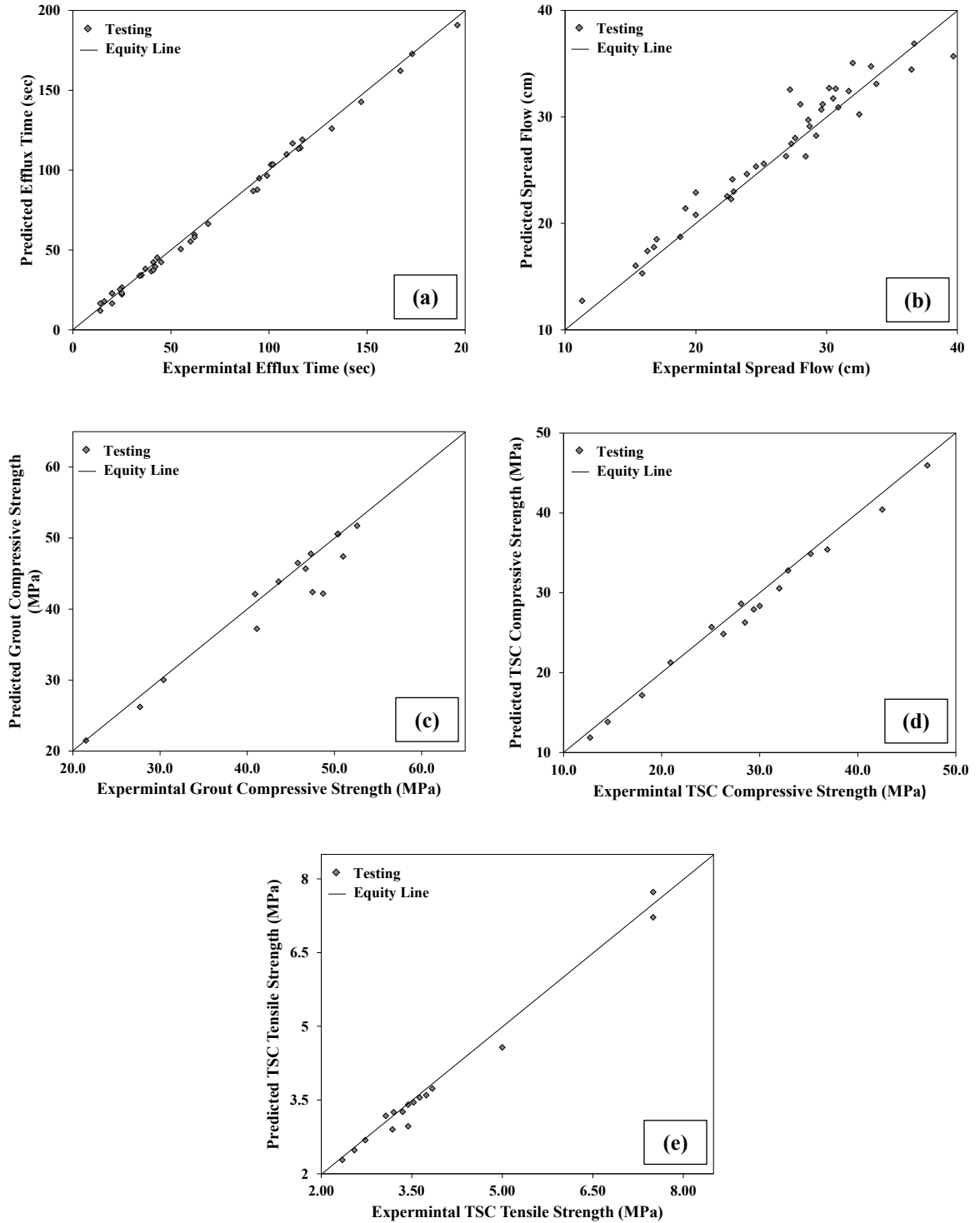
Figure 8.6 – Validation of FL models using testing data unfamiliar to the models in predicting: (a) grout efflux time, (b) grout spread flow, (c) grout compressive strength, (d) TSC compressive strength and (e) TSC tensile strength.

Table 8.7 presents the $RMSE$, R^2, and $MAPE$ values derived for the training and testing data sets in order to evaluate the performance of the FL models. It can be observed that the developed FL models provide a high degree of accuracy and that their predictions of flowability and mechanical properties are very close to the actual experiment results. For example, the $RMSE$, R^2, and $MAPE$ of the TSC tensile strength predicted by the FL model II using the test data were 0.209, 0.997, and 4.087, respectively.

Table 8.7 – Performance of the developed FL models I and II

FL Model/Property	Training Data			Testing Data		
	$RMSE$	R^2	$MAPE$ (%)	$RMSE$	R^2	$MAPE$ (%)
I/Grout efflux time (sec)	2.068	0.999	4.322	3.139	0.999	5.894
I/Grout spread flow (cm)	1.068	0.998	3.361	1.753	0.996	5.205
II/Grout compressive strength (MPa)	1.847	0.998	2.873	2.539	0.997	3.649
II/TSC compressive strength (MPa)	0.922	0.999	2.474	1.243	0.998	3.943
II/TSC tensile strength (MPa)	0.142	0.999	2.586	0.209	0.997	4.087

8.6. CONCLUSIONS

This chapter reports the development of fuzzy logic models for predicting the flowability and mechanical properties of two-stage concrete. Based on the results obtained in this study, the following conclusions can be drawn:

- The developed FL models offer simple and flexible tools for predicting the grout flowability and mechanical properties of TSC in which a variety of SCMs are incorporated. The properties predicted by the FL models were very close to the actual experimental results, providing evidence for the potential of these models as predictive tools.

- The models exhibit adequate capacity of generalization beyond the training stage, as verified by the fact that the predictions obtained for the new test data that is unfamiliar to the models were within a similar range of accuracy to those obtained for the training database.

- The proposed FL models represent reasonably accurate tools for designing TSC mixtures in which several types and dosages of SCMs are incorporated, and they can also save time as well as reduce wastage of materials and design costs.

- The FL models thus developed are flexible and can be easily updated and modified according to new findings and to accommodate data that might emerge in the future. Indeed, such models are adaptable and can encompass new parameters and new test data that becomes available in the future so that its predictive capability can be extended to include new materials, wider range of input parameters, or new test data such as durability.

8.7. REFERENCES

Abdelgader, H. S. and Elgalhud, A. A., (2008), "Effect of grout proportions on strength of two-stage concrete," *Structural Concrete*, Vol. 9, No. 3, pp. 163-170.

Abdelgader, H. S., (1999), "How to design concrete produced by a two-stage concreting method," *Cement and Concrete Research*, Vol. 29, No. 3, pp. 331-337.

Abdelgader, H. S., (1996), "Effect of quantity of sand on the compressive strength of two-stage concrete," *Magazine of Concrete Research*, Vol. 48, No. 177, pp. 353-360.

Abdul Awal, A. S., (1984), "Manufacture and properties of pre-packed aggregate concrete," *Master Thesis*, University of Melbourne, Australia, 121 p.

ACI 304.1, (2005), "Guide for the use of preplaced aggregate concrete for structural and mass concrete applications," *American Concrete Institute*, Farmington Hills, Michigan, USA, 19 p.

Anifowose, F., Labadin, J. and Abdulraheem, A., (2013), "A least-square-driven functional networks type-2 fuzzy logic hybrid model for efficient petroleum reservoir properties prediction," *Neural Computing and Applications*, Vol. 23, No. S1, pp. 179-190.

ASTM C938, (2010), "Standard practice for proportioning grout mixtures for preplaced-aggregate concrete," *American Society for Testing and Materials*, West Conshohocken, PA, USA, 3 p.

ASTM C 939, (2010), "Standard Test Method for Flow of Grout for Preplaced-Aggregate Concrete (Flow Cone Method)," *American Society for Testing and Materials*, West Conshohocken, PA, USA, 3 p.

ASTM C 942, (2010), "Standard Test Method for Compressive Strength of Grouts for Preplaced-Aggregate Concrete in the Laboratory," *American Society for Testing and Materials*, West Conshohocken, PA, USA, 2 p.

ASTM C496/C496M, (2011), "Standard test method for splitting tensile strength of cylindrical concrete specimens," A*merican Society for Testing and Materials*, West Conshohocken, PA, USA.

ASTM C943, (2010), "Standard practice for making test cylinders and prisms for determining strength and density of preplaced-aggregate concrete in the laboratory," A*merican Society for Testing and Materials*, West Conshohocken, PA, USA.

Bedirhanoglu, İ., (2014), "A practical neuro-fuzzy model for estimating modulus of elasticity of concrete," *Structural Engineering and Mechanics*, Techno Press, Vol. 51, No. 2.

Bassuoni, M. T. and Nehdi, M. L., (2008), "Neuro-fuzzy based prediction of the durability of self-consolidating concrete to various sodium sulfate exposure regimes," *Computers and Concrete*, Vol. 5, No. 6, pp. 573-597.

Coo, M. and Pheeraphan, T., (2015), "Effect of Sand, Fly Ash, and Coarse Aggregate Gradation on Preplaced Aggregate Concrete Studied Through Factorial Design," *Construction and Building Materials*, Vol. 93, pp. 812-821.

Da Silva, W. R. and Stemberk, P., (2013), "Optimized fuzzy logic model for predicting self-compacting concrete shrinkage," *Mechanika*, Vol. 19, No. 1, pp. 67-72.

Demir, F., (2005), "A new way of prediction elastic modulus of normal and high strength concrete-fuzzy logic," *Cement and Concrete Research*, Vol. 35, No. 8, pp. 1531-1538.

Feng, M. Q., Chung, L., and Park, T. W., (2009), "Neuro-fuzzy application for concrete strength prediction using combined non-destructive tests," *Magazine of Concrete Research*, Vol. 61, No. 4, pp. 245-256.

Hunger, M., and Brouwers, H. J. H., (2009), "Flow analysis of water–powder mixtures: application to specific surface area and shape factor," *Cement and Concrete Composites*, Vol. 31, No. 1, pp. 39–59.

Kute, S. Y., and Kale, R. S., (2013), "Five-layer fuzzy inference system to design a concrete," *ACI Materials Journal*, Vol. 110, No. 6, pp. 629-639.

Mamdani, E. H. and Assilian, S., (1975), "An experiment in linguistic synthesis with a fuzzy logic controller," *International Journal of Man-Machine Studies*, Vol. 7, No.1, pp. 1-13.

Najjar, M., Soliman, A. and Nehdi, M., (2014), "Critical Overview of Two Stage Concrete: Properties and Applications," *Construction and Building Materials*, Vol. 62, pp. 47-58.

Najjar, M., Soliman, A. and Nehdi, M., (2016), "Two-Stage Concrete Made With Single, Binary and Ternary Binders," *Materials and Structures*, Vol. 49, No. 1, pp. 317-327.

Nehdi, M. L and Bassuoni, M. T., (2009), "Fuzzy logic approach for estimating durability of concrete," *Proceedings of the Institution of Civil Engineers-Construction Materials*, Vol. 162, No. 2, pp. 81-92.

O'Malley, J. and Abdelgader, H., (2010), "Investigation into viability of using two stage (preplaced aggregate) concrete in an Irish setting," *Frontiers of Architecture and Civil Engineering in China*, Vol. 4, No. 1, pp. 127-132.

Ross, T. J., (2010), "Fuzzy logic with engineering applications," (3rd Edition), John Wiley & Sons Ltd, Chichester, West Sussex, United Kingdom.

Sivanandam, S.N., Sumathi, S. and Deepa, S.N., (2007), "Introduction to Fuzzy Logic using MATLAB," Springer, Springer-Verlag Berlin Heidelberg, New York, Berlin, 430 p.

Subaşı, S., Beycioğlu, A., Sancak, E. and Şahin, İ., (2013), "Rule-based mamdani type fuzzy logic model for the prediction of compressive strength of silica fume included concrete using non-destructive test results," *Neural Computing and Applications*, Vol. 22, No. 6, pp. 1133-1139.

Topçu, İ. B. and Sarıdemir, M., (2008), "Prediction of compressive strength of concrete containing fly ash using artificial neural networks and fuzzy logic," *Computational Materials Science*, Vol. 41, No. 3, pp. 305-311.

Tsai, P-W., Hayat, T., Ahmad, B., and Cheng-Wu Chen, C-W., (2015), "Structural system simulation and control via NN based fuzzy model," *Structural Engineering and Mechanics*, Techno Press, Vol. 56, No. 3.

Zadeh, L. A., (1965), "Fuzzy set," *Information and control*, Vol. 8, No. 3, pp. 338-353.

Zhang, Y., (2015), "A fuzzy residual strength based fatigue life prediction method," *Structural Engineering and Mechanics*, Techno Press, Vol. 56, No. 2, pp. 201-221.

Chapter 9

9. SUMMARY, CONCLUSIONS AND RECOMMENDATIONS

9.1. SUMMARY AND CONCLUSIONS

Two-stage concrete (TSC) has been used in the past primarily in repair, mass concrete, and underwater concreting. However, its applications are still limited despite major advancements in modern concrete technology. Therefore, the goal of this dissertation is to explore advancing the TSC technology through the development of a comprehensive database on the mechanical and durability performance of a wide scope of TSC types as well as discover new possibilities and applications for TSC through adjusting and improving its properties.

The initial component of this study, Chapter 2, provides a critical overview of the TSC technology, including its development history, material specifications, engineering properties and long-term performance. It was revealed that there is currently scarce data on the effects of adding new generation of chemical admixtures (e.g. high-range water-reducing admixtures (HRWRA)) and using supplementary cementitious materials (e.g. silica fume, metakaolin, and fly ash) on the TSC properties. Furthermore, mobilizing the TSC technology in other applications where it can provide particular advantages still needs dedicated research. Thus, to fill these knowledge gaps, this dissertation explores the effects of using different supplementary cementitious materials (SCMs) on the TSC grout flowability, and the mechanical properties and durability of TSC. Furthermore, this research contributes to producing new types and novel products of TSC, such as green TSC pavements.

In Chapter 3, the flowability of grouts made with single, binary and ternary binders incorporating various supplementary cementitious materials and having different *w/b* ratios was investigated using the flow cone method and the spread flow test. Results showed that grouts made with *w/b* = 0.45 and 0.55 can achieve the target flowability for TSC grouts specified in pertinent standards, while those made with *w/b* = 0.35 were too thick to use in

TSC production despite the use of HRWRA. It was concluded that the w/b = 0.45 can be perceived as optimum to produce grouts having an efflux time of 35-40 $\pm$ 2 sec as recommended by ACI 304.1 for successful TSC production. Therefore, in the remainder of this research, grout mixtures with w/b = 0.45 and an optimum HRWRA dosage were selected for further investigation.

Chapter 4 expanded on the finding of Chapter 3. The rheological and mechanical properties of two-stage concrete made with single, binary and ternary binders were explored. Results indicated that the partial replacement of OPC with FA improved the grout's flowability while reducing its resistance to bleeding. Partial replacement of OPC with SF or MK increased the grout's bleeding resistance and mechanical properties, while reducing its flowability. Also, an empirical equation for predicting the compressive strength of TSC based on the corresponding grout's compressive strength and considering the binder type was proposed. Moreover, it was found that there was no significant effect of the binder type on the relation between the compressive and tensile strengths of TSC. Finally, an empirical relationship between the modulus of elasticity of TSC and its compressive strength was proposed. The proposed empirical relationships between the properties of the grout and those of the corresponding TSC should offer potential tools for estimating TSC properties based on primary grout properties.

Chapter 5 presented novel data on the mechanical performance of two-stage steel fibre-reinforced concrete (TSSFRC), which so far has not been explored in the open literature. Results showed that the compressive and tensile strengths of TSSFRC increased with increasing steel fibre dosage. In particular, a high steel fiber dosage (6%) achieved significant improvement in TSSFRC compressive and tensile strengths. Moreover, the flexural strength and post-crack behaviour of TSSFRC were greatly enhanced by steel fibre addition. Higher steel fibre length also had significant influence on the flexural strength and post-crack behaviour. The addition of steel fibres greatly enhanced the flexural toughness and residual strength of TSSFRC. Highest values of toughness indices were obtained for TSSFRC specimens having 6% of steel fibre dosage. In conventional steel fibre-reinforced concrete, optimal mechanical performance is usually reached at a fibre dosage of around 2% since greater dosages tend to cause serious concrete consolidation problems emanating from

fibre intermingling and interaction. Conversely, TSSFRC can be produced with 6% of long steel fibres, thus allowing to achieve superior mechanical performance.

Chapter 6 induced the performance of TSC made with single, binary and ternary binders exposed to different environments conducive to physical and chemical sulfate attack. In both sulfate exposure regimes, the effects of using SCMs on TSC were investigated. Results showed that TSC specimens incorporating FA as partial replacement for OPC achieved adequate resistance to chemical sulfate attack. However, under physical sulfate exposure, such specimens exhibited significant surface scaling, while maintaining its compressive strength.

Under chemical sulfate exposure, using 10% SF as partial replacement for OPC caused severe damage in the TSC (S1) specimens as a result of thaumasite formation in the presence of limestone coarse aggregates. Moreover, S1 specimens were entirely destroyed after 6 months of physical sulfate exposure. The drying portion of S1 specimens was physically damaged by salt crystallization, while the immersed portion was chemically attacked through thaumasite formation. The unexpected severe thaumasite formation in TSC incorporating 10% SF in the presence of limestone aggregates requires further attention since silica fume is generally perceived as a performance enhancer with regards to the durability of concrete.

However, the TSC mixture incorporating 10% MK as partial replacement for OPC exhibited excellent resistance to both chemical and physical sulfate attacks. It also achieved compressive strength gain after chemical and physical sulfate exposures. Specimens from ternary binder TSC achieved adequate chemical sulfate resistance. Under physical sulfate exposure, the TSC specimens made with ternary binders (50% OPC-10% MK-40% FA) exhibited better resistance to surface scaling compared with that of the TSC specimens made with ternary binders (50% OPC-10% SF-40% FA). The apparently conflicting effects of SCMs on the resistance of TSC to chemical and physical attacks warrant concerted research effort to allow the designer striking a balance for concrete exposed to environments conducive to both damage mechanisms.

In Chapter 7, the performance of TSC mixtures incorporating recycled concrete aggregates, scrap tire granules, and tire steel wire fibers was explored along with grouts made with ternary binders incorporating high volume fly ash. This material is intended for creating

a novel eco-efficient construction technology of sidewalks and pavements, which requires minimal materials mixing and minimal placement effort.

TSC mixtures made with recycled concrete aggregates performed poorly under freeze-thaw cycles. Hence, it may not be suitable for pavement construction in cold climates. Results indicated that incorporating tire rubber particles significantly decreased the mechanical properties of TSC, while enhancing its toughness and resistance to freezing-thawing cycles. However, the addition of fibers made from recycled tire wire in TSC allowed overcoming the negative effects on the mechanical properties induced by tire rubber particles. Moreover, the toughness and freeze-thaw resistance were significantly enhanced by the inclusion of tire steel wire fibers. It was concluded that an eco-efficient technology for making durable, sustainable and more economical pavements and sidewalks seems to be possible using the proposed "green" TSC method.

In Chapter 8, an original approach based on fuzzy logic (FL) was proposed to predict the flowability and mechanical properties of a variety of TSC mixtures. It was found that the developed FL models have a strong potential as adaptable and flexible tools for predicting the grout flowability and mechanical properties of TSC in which a variety of SCMs are incorporated. The properties predicted by the FL models were very close to the experimental results, which is an evidence of the accuracy of these models. In fact, the proposed FL models represent accurate tools for designing TSC mixtures and they can also save time as well as reduce wastage of materials and design costs. Moreover, the developed FL models are flexible since they can be easily updated and modified according to new findings and data that might emerge in the future.

9.2. RECOMMENDATIONS FOR FUTURE RESEARCH

The current research revealed that some further studies on TSC may be needed as follows:

1) Extensive research is needed in order to investigate the effects of the coarse aggregate properties, including the size, shape, and the mineral composition of the particles, on the mechanical properties and durability of TSC.

2) The durability of TSC exposed to sulfate attack was experimentally evaluated in the current thesis. A detailed study on the chloride ions penetration properties of TSC is

required. Moreover, the sulfate resistance, the chloride ions penetration and corrosion potential of TSSFRC need to be studied. Consequently, models base on fuzzy logic may be developed for estimating the durability of a variety of TSC mixtures.

3) The mechanical properties and durability of two-stage fibre-reinforced concrete made with various shapes, sizes, aspect ratio and materials should be considered in the future investigations.

4) Further research is needed to refine TSC formulations for pavement construction, particularly with regards to using various binder combinations in the grout and developing various strength classes for structural pavement design requirements.

5) In the present thesis, a novel TSC technology for pavement and sidewalk construction is proposed. In order to pave the way for wider implementation of TSC in today's concrete industry, there is still need to discover other TSC products such as precast lightweight TSC housing panels.

6) Ultra high-strength concrete (UHSC) has recently attracted growing attention of researchers because of its unique mechanical properties and excellent durability. Since UHSC has an excellent flowability; a new type of TSC produced by pouring UHSC over coarse aggregates needs to be investigated.

APPENDIX

Table A.1 – Database used in the FL model I

w/b	OPC (%)	FA (%)	SF (%)	MK (%)	HRWRA (%)	Efflux Time (sec)	Spread flow (cm)
0.35	100	0	0	0	1.0	160	21.1
0.35	100	0	0	0	1.0	165	20.4
0.35	100	0	0	0	1.0	167	20.0
0.35	100	0	0	0	1.2	127	26.1
0.35	100	0	0	0	1.2	131	25.2
0.35	100	0	0	0	1.2	132	25.2
0.35	100	0	0	0	1.6	117	28.1
0.35	100	0	0	0	1.6	116	28.2
0.35	100	0	0	0	1.6	112	29.2
0.35	100	0	0	0	2.0	111	30.9
0.35	100	0	0	0	2.0	115	29.5
0.35	100	0	0	0	2.0	116	29.6
0.35	90	10	0	0	1.0	115	23.5
0.35	90	10	0	0	1.0	119	22.6
0.35	90	10	0	0	1.0	117	22.9
0.35	90	10	0	0	1.2	111	28.0
0.35	90	10	0	0	1.2	116	27.2
0.35	90	10	0	0	1.2	115	27.3
0.35	90	10	0	0	1.6	108	29.3
0.35	90	10	0	0	1.6	112	28.8
0.35	90	10	0	0	1.6	110	28.9
0.35	90	10	0	0	2.0	107	31.5
0.35	90	10	0	0	2.0	111	30.6
0.35	90	10	0	0	2.0	109	30.9
0.35	70	30	0	0	0.6	151	28.0
0.35	70	30	0	0	0.6	156	26.2
0.35	70	30	0	0	0.6	152	28.0
0.35	70	30	0	0	1.0	105	26.2
0.35	70	30	0	0	1.0	103	26.4
0.35	70	30	0	0	1.0	101	26.9
0.35	70	30	0	0	1.2	64	32.7
0.35	70	30	0	0	1.2	65	31.6

Table A.1 cont'd – Database used in the FL model I

w/b	OPC (%)	FA (%)	SF (%)	MK (%)	HRWRA (%)	Efflux Time (sec)	Spread flow (cm)
0.35	70	30	0	0	1.2	69	30.2
0.35	70	30	0	0	1.6	56	33.0
0.35	70	30	0	0	1.6	60	31.5
0.35	70	30	0	0	1.6	61	30.0
0.35	70	30	0	0	2.0	55	32.6
0.35	70	30	0	0	2.0	56	31.7
0.35	70	30	0	0	2.0	60	31.7
0.35	50	50	0	0	0.6	79	28.4
0.35	50	50	0	0	0.6	82	27.6
0.35	50	50	0	0	0.6	79	28.0
0.35	50	50	0	0	1.0	50	31.0
0.35	50	50	0	0	1.0	51	30.8
0.35	50	50	0	0	1.0	55	29.7
0.35	50	50	0	0	1.2	45	32.3
0.35	50	50	0	0	1.2	47	31.6
0.35	50	50	0	0	1.2	46	32.1
0.35	50	50	0	0	1.6	43	35.0
0.35	50	50	0	0	1.6	46	33.6
0.35	50	50	0	0	1.6	43	33.4
0.35	50	50	0	0	2.0	42	33.2
0.35	50	50	0	0	2.0	45	32.5
0.35	50	50	0	0	2.0	42	33.3
0.35	90	0	10	0	2.0	189	33.0
0.35	90	0	10	0	2.0	194	29.8
0.35	90	0	10	0	2.0	196	27.2
0.35	50	40	10	0	1.6	168	29.7
0.35	50	40	10	0	1.6	169	28.7
0.35	50	40	10	0	1.6	173	28.6
0.35	50	40	10	0	2.0	95	34.0
0.35	50	40	10	0	2.0	100	31.3
0.35	50	40	10	0	2.0	99	30.7
0.35	50	40	0	10	1.6	184	28.6
0.35	50	40	0	10	1.6	189	27.4

Table A.1 cont'd – Database used in the FL model I

w/b	OPC (%)	FA (%)	SF (%)	MK (%)	HRWRA (%)	Efflux Time (sec)	Spread flow (cm)
0.35	50	40	0	10	1.6	185	28.0
0.35	50	40	0	10	2.0	101	32.0
0.35	50	40	0	10	2.0	106	30.0
0.35	50	40	0	10	2.0	102	32.5
0.45	100	0	0	0	0.2	89	18.7
0.45	100	0	0	0	0.2	90	18.3
0.45	100	0	0	0	0.2	94	17.0
0.45	100	0	0	0	0.4	38	24.7
0.45	100	0	0	0	0.4	40	24.1
0.45	100	0	0	0	0.4	39	24.7
0.45	100	0	0	0	0.6	37	31.0
0.45	100	0	0	0	0.6	37	31.0
0.45	100	0	0	0	0.6	40	28.0
0.45	90	10	0	0	0.2	40	24.3
0.45	90	10	0	0	0.2	44	23.4
0.45	90	10	0	0	0.2	45	22.8
0.45	90	10	0	0	0.4	34	28.7
0.45	90	10	0	0	0.4	38	27.5
0.45	90	10	0	0	0.4	33	29.3
0.45	90	10	0	0	0.6	33	37.0
0.45	90	10	0	0	0.6	36	34.0
0.45	90	10	0	0	0.6	33	37.0
0.45	70	30	0	0	0.0	89	16.4
0.45	70	30	0	0	0.0	89	16.2
0.45	70	30	0	0	0.0	92	15.4
0.45	70	30	0	0	0.2	32	25.9
0.45	70	30	0	0	0.2	35	24.5
0.45	70	30	0	0	0.2	35	24.6
0.45	70	30	0	0	0.4	22	31.0
0.45	70	30	0	0	0.4	25	29.6
0.45	70	30	0	0	0.4	25	29.4
0.45	70	30	0	0	0.6	24	35.0
0.45	70	30	0	0	0.6	22	36.3

Table A.1 cont'd – Database used in the FL model I

w/b	OPC (%)	FA (%)	SF (%)	MK (%)	HRWRA (%)	Efflux Time (sec)	Spread flow (cm)
0.45	70	30	0	0	0.6	20	39.7
0.45	50	50	0	0	0.0	39	19.1
0.45	50	50	0	0	0.0	42	17.3
0.45	50	50	0	0	0.0	36	20.6
0.45	50	50	0	0	0.2	27	26.7
0.45	50	50	0	0	0.2	23	29.7
0.45	50	50	0	0	0.2	25	27.6
0.45	50	50	0	0	0.4	24	34.0
0.45	50	50	0	0	0.4	22	34.5
0.45	50	50	0	0	0.4	20	36.5
0.45	50	50	0	0	0.6	16	41.0
0.45	50	50	0	0	0.6	20	38.6
0.45	50	50	0	0	0.6	21	37.4
0.45	90	0	10	0	0.2	98	16.4
0.45	90	0	10	0	0.2	92	19.3
0.45	90	0	10	0	0.2	95	16.8
0.45	90	0	10	0	0.4	58	25.0
0.45	90	0	10	0	0.4	63	23.1
0.45	90	0	10	0	0.4	62	23.9
0.45	90	0	10	0	0.6	42	32.7
0.45	90	0	10	0	0.6	44	32.0
0.45	90	0	10	0	0.6	46	28.3
0.45	90	0	10	0	0.8	38	35.0
0.45	90	0	10	0	0.8	43	32.0
0.45	90	0	10	0	0.8	42	32.0
0.45	50	40	10	0	0.0	57	18.0
0.45	50	40	10	0	0.0	61	16.7
0.45	50	40	10	0	0.0	62	16.3
0.45	50	40	10	0	0.2	39	22.7
0.45	50	40	10	0	0.2	40	22.8
0.45	50	40	10	0	0.2	38	23.5
0.45	50	40	10	0	0.4	21	35
0.45	50	40	10	0	0.4	25	33.9

Table A.1 cont'd – Database used in the FL model I

w/b	OPC (%)	FA (%)	SF (%)	MK (%)	HRWRA (%)	Efflux Time (sec)	Spread flow (cm)
0.45	50	40	10	0	0.4	26	33.1
0.45	50	40	10	0	0.6	23	37.0
0.45	50	40	10	0	0.6	21	37.3
0.45	50	40	10	0	0.6	25	36.7
0.45	90	0	0	10	0.4	96	20.8
0.45	90	0	0	10	0.4	100	19.0
0.45	90	0	0	10	0.4	101	18.7
0.45	90	0	0	10	0.6	65	25.0
0.45	90	0	0	10	0.6	62	27.4
0.45	90	0	0	10	0.6	65	25.6
0.45	90	0	0	10	0.8	43	33.0
0.45	90	0	0	10	0.8	42	33.7
0.45	90	0	0	10	0.8	41	33.8
0.45	50	40	0	10	0.0	128	17.0
0.45	50	40	0	10	0.0	129	16.7
0.45	50	40	0	10	0.0	133	11.3
0.45	50	40	0	10	0.2	54	18.0
0.45	50	40	0	10	0.2	56	17.0
0.45	50	40	0	10	0.2	58	17.5
0.45	50	40	0	10	0.4	36	29.3
0.45	50	40	0	10	0.4	41	26.0
0.45	50	40	0	10	0.4	37	28.7
0.45	50	40	0	10	0.6	27	37.0
0.45	50	40	0	10	0.6	30	35.0
0.45	50	40	0	10	0.6	30	36.0
0.55	100	0	0	0	0.0	33	19.4
0.55	100	0	0	0	0.0	36	17.4
0.55	100	0	0	0	0.0	36	17.2
0.55	100	0	0	0	0.1	27	21.0
0.55	100	0	0	0	0.1	24	22.3
0.55	100	0	0	0	0.1	24	22.7
0.55	100	0	0	0	0.2	14	25.0
0.55	100	0	0	0	0.2	16	23.8

Table A.1 cont'd – Database used in the FL model I

w/b	OPC (%)	FA (%)	SF (%)	MK (%)	HRWRA (%)	Efflux Time (sec)	Spread flow (cm)
0.55	100	0	0	0	0.2	18	23.2
0.55	90	10	0	0	0.0	22	19.5
0.55	90	10	0	0	0.0	25	18.7
0.55	90	10	0	0	0.0	25	18.8
0.55	90	10	0	0	0.1	20	24.0
0.55	90	10	0	0	0.1	20	23.7
0.55	90	10	0	0	0.1	23	21.3
0.55	90	10	0	0	0.2	14	25.0
0.55	90	10	0	0	0.2	18	23.0
0.55	90	10	0	0	0.2	13	25.5
0.55	70	30	0	0	0.0	17	23.0
0.55	70	30	0	0	0.0	17	23.0
0.55	70	30	0	0	0.0	20	20.0
0.55	70	30	0	0	0.1	17	28.0
0.55	70	30	0	0	0.1	14	29.4
0.55	70	30	0	0	0.1	17	28.1
0.55	70	30	0	0	0.2	15	29.0
0.55	70	30	0	0	0.2	14	29.7
0.55	70	30	0	0	0.2	13	31.3
0.55	50	50	0	0	0.0	17	26.5
0.55	50	50	0	0	0.0	17	26.1
0.55	50	50	0	0	0.0	14	28.4
0.55	50	50	0	0	0.1	15	28.0
0.55	50	50	0	0	0.1	14	29.0
0.55	50	50	0	0	0.1	13	30.0
0.55	50	50	0	0	0.2	11	31.8
0.55	50	50	0	0	0.2	14	30.7
0.55	50	50	0	0	0.2	14	30.5
0.55	90	0	10	0	0.0	130	12.7
0.55	90	0	10	0	0.0	127	14.0
0.55	90	0	10	0	0.0	133	12.3
0.55	90	0	10	0	0.1	61	19.4
0.55	90	0	10	0	0.1	63	18.6

Table A.1 cont'd – Database used in the FL model I

w/b	OPC (%)	FA (%)	SF (%)	MK (%)	HRWRA (%)	Efflux Time (sec)	Spread flow (cm)
0.55	90	0	10	0	0.1	62	19.0
0.55	90	0	10	0	0.2	31	23.0
0.55	90	0	10	0	0.2	37	20.0
0.55	90	0	10	0	0.2	37	20.0
0.55	50	40	10	0	0.0	33	17.0
0.55	50	40	10	0	0.0	35	15.1
0.55	50	40	10	0	0.0	34	15.9
0.55	50	40	10	0	0.1	22	20.7
0.55	50	40	10	0	0.1	21	21.8
0.55	50	40	10	0	0.1	23	20.5
0.55	50	40	10	0	0.2	17	21.7
0.55	50	40	10	0	0.2	13	23.4
0.55	50	40	10	0	0.2	12	23.9
0.55	90	0	0	10	0.0	142	13.3
0.55	90	0	0	10	0.0	146	11.4
0.55	90	0	0	10	0.0	147	11.3
0.55	90	0	0	10	0.1	65	20.0
0.55	90	0	0	10	0.1	72	17.1
0.55	90	0	0	10	0.1	73	16.9
0.55	90	0	0	10	0.2	37	21.3
0.55	90	0	0	10	0.2	39	19.5
0.55	90	0	0	10	0.2	41	19.2
0.55	50	40	0	10	0.0	41	14.0
0.55	50	40	0	10	0.0	38	17.0
0.55	50	40	0	10	0.0	41	14.0
0.55	50	40	0	10	0.1	28	19.6
0.55	50	40	0	10	0.1	27	19.8
0.55	50	40	0	10	0.1	26	20.6
0.55	50	40	0	10	0.2	15	23.0
0.55	50	40	0	10	0.2	20	20.6
0.55	50	40	0	10	0.2	16	22.4

Table A.2 – Database used in the FL model II

OPC (%)	FA (%)	SF (%)	MK (%)	Age (days)	Short fibre dosage (%)	Long fibre dosage (%)	Compressive Strength of grout (MPa)	Compressive Strength of TSC (MPa)	Tensile Strength of TSC (MPa)
100	0	0	0	7	0	0	33.2	25.4	3.35
100	0	0	0	7	0	0	34.0	26.3	3.42
100	0	0	0	7	0	0	34.2	26.0	3.43
100	0	0	0	28	0	0	49.8	31.1	3.67
100	0	0	0	28	0	0	51.0	32.0	3.74
100	0	0	0	28	0	0	50.4	31.4	3.69
100	0	0	0	56	0	0	53.9	32.8	3.75
100	0	0	0	56	0	0	54.7	33.6	3.84
100	0	0	0	56	0	0	54.3	33.5	3.81
90	10	0	0	7	0	0	31.1	22.9	3.13
90	10	0	0	7	0	0	32.0	23.7	3.24
90	10	0	0	7	0	0	31.4	23.0	3.23
90	10	0	0	28	0	0	47.7	28.7	3.42
90	10	0	0	28	0	0	48.7	29.4	3.53
90	10	0	0	28	0	0	47.6	28.9	3.55
90	10	0	0	56	0	0	53.3	36.1	3.67
90	10	0	0	56	0	0	54.6	37.2	3.75
90	10	0	0	56	0	0	53.5	36.8	3.68
80	20	0	0	7	0	0	28.4	16.4	2.54
80	20	0	0	7	0	0	29.3	17.5	2.68
80	20	0	0	7	0	0	29.0	16.8	2.58
80	20	0	0	28	0	0	40.5	22.8	2.94
80	20	0	0	28	0	0	41.4	23.9	3.07
80	20	0	0	28	0	0	40.2	22.9	2.99
80	20	0	0	56	0	0	47.3	28.1	3.44
80	20	0	0	56	0	0	48.3	29.2	3.56
80	20	0	0	56	0	0	48.1	28.2	3.50
70	30	0	0	7	0	0	26.4	13.7	2.43
70	30	0	0	7	0	0	27.7	14.5	2.55
70	30	0	0	7	0	0	27.2	13.8	2.52
70	30	0	0	28	0	0	37.9	18.3	2.76
70	30	0	0	28	0	0	38.7	19.4	2.86
70	30	0	0	28	0	0	38.9	19.0	2.78

Table A.2 cont'd – Database used in the FL model II

OPC (%)	FA (%)	SF (%)	MK (%)	Age (days)	Short fibre dosage (%)	Long fibre dosage (%)	Compressive Strength of grout (MPa)	Compressive Strength of TSC (MPa)	Tensile Strength of TSC (MPa)
70	30	0	0	56	0	0	45.8	25.2	3.24
70	30	0	0	56	0	0	46.7	26.3	3.35
70	30	0	0	56	0	0	46.1	25.9	3.31
60	40	0	0	7	0	0	23.4	12.7	2.35
60	40	0	0	7	0	0	24.3	13.5	2.46
60	40	0	0	7	0	0	23.7	13.4	2.39
60	40	0	0	28	0	0	31.7	17.1	2.59
60	40	0	0	28	0	0	32.8	18.2	2.69
60	40	0	0	28	0	0	31.8	17.8	2.67
60	40	0	0	56	0	0	40.9	20.9	3.07
60	40	0	0	56	0	0	41.7	21.6	3.15
60	40	0	0	56	0	0	41.9	21.1	3.08
50	50	0	0	7	0	0	20.7	11.6	2.26
50	50	0	0	7	0	0	21.5	12.7	2.35
50	50	0	0	7	0	0	20.8	11.7	2.29
50	50	0	0	28	0	0	27.6	13.8	2.53
50	50	0	0	28	0	0	28.5	14.6	2.65
50	50	0	0	28	0	0	27.9	13.9	2.62
50	50	0	0	56	0	0	37.6	18.1	2.76
50	50	0	0	56	0	0	38.7	19.3	2.83
50	50	0	0	56	0	0	38.3	18.1	2.81
90	0	10	0	7	0	0	43.3	32.4	3.54
90	0	10	0	7	0	0	44.5	33.1	3.63
90	0	10	0	7	0	0	43.6	32.9	3.63
90	0	10	0	28	0	0	51.7	33.6	3.73
90	0	10	0	28	0	0	52.9	34.5	3.86
90	0	10	0	28	0	0	52.0	34.2	3.81
90	0	10	0	56	0	0	56.5	38.4	3.97
90	0	10	0	56	0	0	57.3	39.5	4.17
90	0	10	0	56	0	0	57.2	38.8	4.04
60	30	10	0	7	0	0	29.5	17.0	2.65
60	30	10	0	7	0	0	30.4	18.0	2.73
60	30	10	0	7	0	0	30.1	17.2	2.72

Table A.2 cont'd – Database used in the FL model II

OPC (%)	FA (%)	SF (%)	MK (%)	Age (days)	Short fibre dosage (%)	Long fibre dosage (%)	Compressive Strength of grout (MPa)	Compressive Strength of TSC (MPa)	Tensile Strength of TSC (MPa)
60	30	10	0	28	0	0	40.9	25.7	3.26
60	30	10	0	28	0	0	41.6	26.4	3.33
60	30	10	0	28	0	0	41.7	26.2	3.31
60	30	10	0	56	0	0	47.7	29.4	3.54
60	30	10	0	56	0	0	48.4	30.3	3.62
60	30	10	0	56	0	0	48.2	30.0	3.64
50	40	10	0	7	0	0	26.4	15.1	2.43
50	40	10	0	7	0	0	27.5	16.0	2.55
50	40	10	0	7	0	0	27.1	15.7	2.52
50	40	10	0	28	0	0	37.6	24.5	3.06
50	40	10	0	28	0	0	38.3	25.3	3.13
50	40	10	0	28	0	0	38.1	25.2	3.11
50	40	10	0	56	0	0	45.8	25.1	3.20
50	40	10	0	56	0	0	46.7	25.9	3.30
50	40	10	0	56	0	0	46.1	25.8	3.22
90	0	0	10	7	0	0	51.5	34.5	3.73
90	0	0	10	7	0	0	52.6	35.2	3.84
90	0	0	10	7	0	0	52.2	35.3	3.83
90	0	0	10	28	0	0	61.3	39.5	3.83
90	0	0	10	28	0	0	62.3	40.4	3.93
90	0	0	10	28	0	0	62.1	40.1	3.94
90	0	0	10	56	0	0	63.7	42.4	3.92
90	0	0	10	56	0	0	64.4	43.5	4.09
90	0	0	10	56	0	0	64.2	43.1	4.05
60	30	0	10	7	0	0	34.3	22.2	2.95
60	30	0	10	7	0	0	35.4	23.5	3.11
60	30	0	10	7	0	0	35.0	22.7	3.00
60	30	0	10	28	0	0	47.5	30.0	3.44
60	30	0	10	28	0	0	48.3	30.9	3.57
60	30	0	10	28	0	0	48.5	30.3	3.49
60	30	0	10	56	0	0	57.9	35.5	3.53
60	30	0	10	56	0	0	59.1	36.7	3.64
60	30	0	10	56	0	0	58.2	36.4	3.63

Table A.2 cont'd – Database used in the FL model II

OPC (%)	FA (%)	SF (%)	MK (%)	Age (days)	Short fibre dosage (%)	Long fibre dosage (%)	Compressive Strength of grout (MPa)	Compressive Strength of TSC (MPa)	Tensile Strength of TSC (MPa)
50	40	0	10	7	0	0	28.6	19.5	2.79
50	40	0	10	7	0	0	29.3	20.2	2.90
50	40	0	10	7	0	0	29.1	20.0	2.86
50	40	0	10	28	0	0	40.4	28.1	3.14
50	40	0	10	28	0	0	41.5	28.9	3.28
50	40	0	10	28	0	0	41.1	28.5	3.18
50	40	0	10	56	0	0	48.4	30.9	3.34
50	40	0	10	56	0	0	49.2	32.3	3.45
50	40	0	10	56	0	0	49.4	31.3	3.41
100	0	0	0	28	1	0	50.4	33.9	4.6
100	0	0	0	28	1	0	50.4	36.9	4.8
100	0	0	0	28	1	0	50.4	36.9	5.0
100	0	0	0	28	2	0	50.4	36.7	6.1
100	0	0	0	28	2	0	50.4	35.9	5.6
100	0	0	0	28	2	0	50.4	39.3	6.0
100	0	0	0	28	4	0	50.4	41.5	6.5
100	0	0	0	28	4	0	50.4	39.1	6.7
100	0	0	0	28	4	0	50.4	41.8	6.8
100	0	0	0	28	6	0	50.4	47.1	7.5
100	0	0	0	28	6	0	50.4	45.7	7.9
100	0	0	0	28	6	0	50.4	47.9	7.7
100	0	0	0	28	0	1	50.4	35.8	5.4
100	0	0	0	28	0	1	50.4	36.1	4.7
100	0	0	0	28	0	1	50.4	36.7	4.9
100	0	0	0	28	0	2	50.4	37.9	6.0
100	0	0	0	28	0	2	50.4	38.0	6.2
100	0	0	0	28	0	2	50.4	39.3	6.4
100	0	0	0	28	0	4	50.4	42.5	7.5
100	0	0	0	28	0	4	50.4	41.9	7.1
100	0	0	0	28	0	4	50.4	39.5	7.3
100	0	0	0	28	0	6	50.4	46.7	8.4
100	0	0	0	28	0	6	50.4	48.1	8.1
100	0	0	0	28	0	6	50.4	48.8	8.1

CURRICULUM VITAE

Name: Manal Najjar

**Post-secondary
Education and
Degrees:**

Doctor of Philosophy, 2011-2016
Department of Civil and Environmental Engineering
Faculty of Engineering
Western University
London, Ontario, Canada

Master of Science, 2005-2010
Department of Civil and Environmental Engineering
Faculty of Engineering
Tripoli University (Former; Al-Fateh University)
Tripoli, Libya

Bachelor of Civil Engineering, 1995-2000
Department of Civil and Environmental Engineering
Faculty of Engineering
Tripoli University (Former; Al-Fateh University)
Tripoli, Libya

**Honours and
Awards:**

Post Graduate External Scholarship, The Libyan Authority of
Higher Education. Libya, 2010-2016
Post Graduate Internal Scholarship, The Libyan Authority of
Higher Education. Libya, 2007-2010

**Academic
Appointments:**

Teaching Assistant, 2012-2015
Department of Civil and Environmental Engineering
Faculty of Engineering
Western University
London, Ontario, Canada

Teaching Assistant, 2004-2010
Department of Civil and Environmental Engineering
Faculty of Engineering
Tripoli University
Tripoli, Libya

**Professional
Appointments:**

Structural Engineer, 2001-2004
National Consulting Bureau
Tripoli, Libya

Publications:

Najjar, M.F, Soliman, A.M. and Nehdi, M.L., (2016) "Sustainable high-volume fly ash grouts for two-stage concrete," *Proceedings of the CSCE Annual Conference: Resilient Infrastructure*, London, Ontario, Canada.

Najjar, M.F, Soliman, A.M., Azabi, T.M. and Nehdi, M.L., (2016) "Green sidewalks using sustainable two-stage concrete," *Proceedings of the CSCE Annual Conference: Resilient Infrastructure*, London, Ontario, Canada.

Najjar, M., Soliman, A. and Nehdi, M., (2016), "Two-stage concrete made with single, binary and ternary binders," *Materials and Structures*, Vol. 49, No. 1, pp. 317-327.

Najjar, M., Soliman, A. and Nehdi, M., (2014), "Critical overview of two stage concrete: properties and applications," *Construction and Building Materials*, Vol. 62, pp. 47-58.

Abdelgader, H.S., **Najjar, M.F**. and Azabi, T.M., (2010) "Study of underwater concrete using two-stage (pre-placed aggregate) concrete in Libya," *Journal of Structural Concrete*, Vol. 11, No. 3, pp. 161-165.

Abdelgader, H.S., **Najjar, M.F**., El-Baden, A.S. and Azabi, T.M., (2010) "A study on underwater concreting by using two-stage (pre-placed aggregate) concrete in Libya," *Proceedings of the 6th International RILEM Symposium on Self-Compacting Concrete & 4th North American Conference on the Design and Use of SCC*, Sherbrooke. Canada.

Abdelgader, H. S. and **Najjar, M. F**., (2009), "Advances in concreting methods, ", *Proceedings of the 1st International Conference on sustainable Built Environment Infrastructures in Developing Countries*, Oran, Algeria, PP. 315-324.

Najjar, M.F. and Abdelgader, H.S., (2009), " Underwater concreting by using two-stage (pre-placed aggregate) concrete," *Proceedings of the 1st International Conference on Concrete Technology*, Tabriz, Iran, Paper Code No. CT0001.